Evolution of floral organisation and architecture in Boraginales and Geraniales

Dissertation

zur

Erlangung des Doktorgrades (Dr. rer. nat.)

der

Mathematisch-Naturwissenschaftlichen Fakultät

der

Rheinischen Friedrich-Wilhelms-Universität Bonn

vorgelegt von

Julius Jeiter

geboren in

Aachen, Deutschland

Bonn, 2019

To my family.

Angefertigt mit Genehmigung der Mathematisch-Naturwissenschaftlichen Fakultät der Rheinischen Friedrich-Wilhelms-Universität Bonn

Erstgutachter : Prof. Dr. Maximilian Weigend

Zweitgutachter: Prof. Dr. Erik F. Smets

Tag der Promotion: 3. Februar 2020

Erscheinungsjahr: 2020

Contents

Acknowledgements

First of all, I would like to thank my supervisor and mentor Maximilian Weigend, to whom I am not only grateful for supervising and guiding me through my time as doctoral student at the Nees-Institute. My very first contact with plant morphology was when I did an internship with him in Berlin in the Hilger working group back in 2009. At that time he also introduced me to the Geraniales and woke my interest in floral nectaries. Since then he helped me to improve my skills as a scientist and constantly supported me.

I would also like to thank Erik F. Smets for agreeing to be my second supervisor. Since I was introduced to him at the first *Impatiens* meeting in Bonn in 2015, we stayed in contact, connected through our common fascination for floral nectaries. He was always open to questions and he always gave valuable advice. The article on nectary development and floral architecture in Geraniaceae and Hypseocharitaceae (chapter 7), which he co-authored, is not only one of my favourite articles, but also turned out to be influential on how my thesis developed from this point onwards.

Another influential friend and colleague, I would like to thank here, is Federico Luebert. Working with him on several projects was always fun. His influence on my career did not stop there. If it was not for him, I would probably not have written my master thesis about flower and nectary morphology in Geraniales and would not have started my doctoral studies on flower morphology here in Bonn. He taught me a lot about evolution and phylogenetics, philosophical principles of science and his ideas about science in general. I will always keep the 'Tuesday Evening Meetings' with him, Juliana Chacón, Rafael Acuña and Norbert Holstein in good memory.

My time in Berlin in the Hilger working group was truly influential for my career. I would like to thank Hartmut H. Hilger for his support and the opportunities he gave me. I would like to thank Christoph Dietrich for his technical support.

Several co-authors contributed to chapters of this thesis. I would like to thank Fränze Danisch, Stella Langecker, Jürg Schönenberger, Yannick M. Staedler and Alexander Ziegler for their valuable contributions and their help in conducting these studies and I hope we will continue to collaborate in the future.

The published chapters underwent a peer-review process. I would like to thank all the editors and anonymous reviewers for critically reviewing and improving my manuscripts.

I would also like to thank the students who contributed to the datasets or helped out in the lab: Alina Gebauer, Helen Mika, Silvia Pappagallo, Carlotta Rixen, Jonathan Ruhm, Dora Straus and Maria-Anna Vasile.

Furthermore, I would like to thank all present and former members of the Nees-Institute: Stefan Abrahamczyk, Wilhelm Barthlott, Thomas Barton, Julia Bechteler, Tim Böhnert, Hans-Jürgen Ensikat, Bernadette Große-Veldmann, Elke Hedke, Jonathan Hense, Thomas Joßberger, Julian Kokott, Michael Krug, Marcus Lehnert, Matthias Mail, Karola Maul, Felix Merklinger, Andreas Mues, Adeel Mustafa, Jens Mutke, Jörg Nettekoven, Constantin Poretschkin, Dietmar Quandt, Annette Scheersoi, Nicole Schmandt, Birgit Sülzer, Amélie Tessartz, Philip Testroet and Lara Weiser. Many contributed to this thesis by critical discussions, collection of material, comments and corrections on the manuscript, through their help, by providing support and much more.

Most of the material used in this study was cultivated in the Bonn University Botanic Gardens and I want to express my gratitude to the staff and especially Michael Neumann, Klaus Bahr, Wolfram

Lobin, former scientific curator, and Cornelia Löhne, current scientific curator, for taking care of the collections and granting me access to them.

The high-resolution x-ray computed tomography was conducted at the University of Vienna. I would like to thank Susanne Pamperl and Susanne Sontag for their technical support, for providing access to the facilities and for an introduction to 3D-visualisation software.

Micro-computed tomography was conducted at the Institute of Evolutionary Biology and Ecology at the University of Bonn. I would like to thank Thomas Bartolomaeus for granting me access to the computer workstations and the facilities. Funding for the Skyscan 1272 μCT was provided by the Deutsche Forschungsgemeinschaft (INST 217/849-1 FUGG).

I am grateful to be a member of the Boraginales Working Group and for the valuable discussions on the 'Boraginales Meetings' in Bonn and Florence, Italy.

To a great extent, my doctoral studies and the research stay in Vienna, Austria, were made possible through a scholarship and funding by the Studienstiftung des deutschen Volkes.

Last but not least, I would like to express my gratitude to my family. My parents Kathrin and Karl-Heinz supported and encouraged me to pursue a scientific career. They were always there for me throughout my entire life and especially during my doctoral studies. My grandparents Mia† and Michael showed great interest in my research and their support allowed me to move to Bonn. My sister Clara and my brother Felix, his wife Marion and their children Mia, Anton and Rosa were always a welcome distraction from the everyday life at university.

Finally, I would like to thank my beloved wife Christina and our son Junus. They were always there for me, helped me to keep my feet on the ground and encouraged me to continue even when times were more difficult. Because of all their encouragement and support, I am dedicating this thesis to my family.

Chapter 1

General introduction

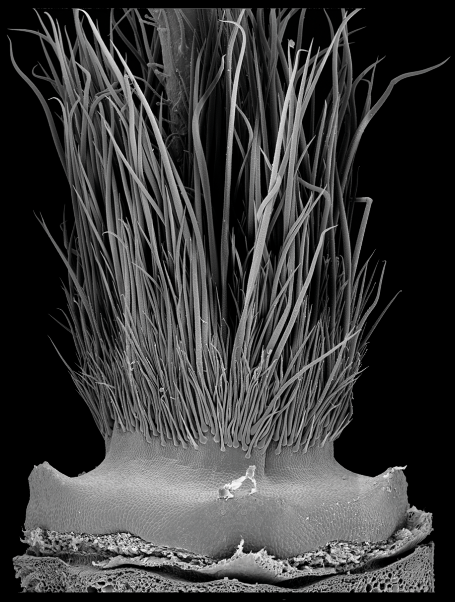

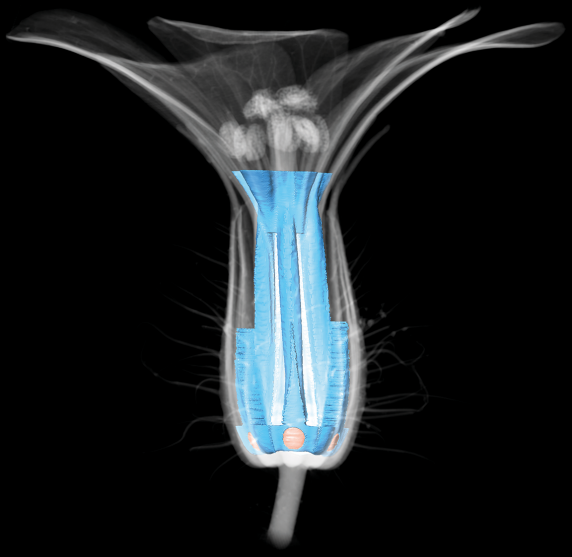

1 General introduction

1.1 Foreword

My fascination for floral morphology began with the study of floral nectaries in Geraniales. At first sight, this order is morphologically diverse, however, if carefully examined, a number of shared characters become apparent. The most diverse structure in the flowers of Geraniales is the nectary. In my first morphological and anatomical study (Jeiter *et al.*, 2017), I reinvestigated the evolution of floral nectaries in Geraniales in the context of the most recent phylogenetic understanding of this order (Palazzesi *et al.*, 2012). This approach of carefully studying morphological characters in the context of the recent phylogenetic understanding of a particular group is one of the threads connecting the majority of chapters of this thesis.

Chapter 2 is only connected through this thread. It is about gynoecium and fruit development in *Heliotropium* sect. *Heliothamnus*. The idea for this study arose from a redefined phylogenetic understanding and long-standing assumptions about gynoecium and fruit characters, that have not been critically checked in this context so far.

The second thread – integration of structures into floral architecture – developed gradually. With each new chapter on this topic, the ideas behind it were further elaborated. As laid out below, the thesis is structured logically and not chronologically. Thus, the development of the ideas of floral architecture applied in the individual chapters might vary.

Chapter 3 is the first study on flower and fruit development in monogeneric Codonaceae (Boraginales). In this study, an idea about floral architecture began to form, however, the concept of floral architecture was not clearly defined then.

A first definition of floral architecture (*sensu* Endress, 1994, 1996) was introduced in the study of floral nectaries in Geraniaceae and Hypseocharitaceae (Geraniales, chapter 7). The placement as chapter 7 is due to the taxonomic isolation of this study; apart from chapters 7 and 8 all other chapters focus on Boraginales.

The definition of floral architecture was further improved and extended in the study on stamen-corolla tube modifications in Hydrophyllaceae (chapter 5). The same definition was then employed in the second study on Hydrophyllaceae (chapter 6) and in the study of faucal and basal scales in Boraginaceae (chapter 4). Finally, based on the definition of floral architecture and compartmentalisation of flowers, the idea of visualisation of the air-filled spaces inside the flower arose (chapter 8).

This thesis contributes to the understanding of floral structure evolution. In the light of recent phylogenetic studies of the study groups Boraginales and Geraniales, morphological structures such as nectaries, stamen-corolla tube modifications and the gynoecium are investigated. These structures are integrated into a complex three-dimensional, functional unit, the flower.

1.2 Morphology and phylogeny

The first thread of this thesis is the study of floral structure in the light of recent phylogenies. Since the beginnings of plant systematics (Linnaeus, 1753), morphology and later anatomy, were the main sources of information classifications were built on. With the evolutionary theory being introduced

(Darwin, 1859), the goal shifted from simple classification on the basis of similarities, towards a natural, evolution-based system. The problems of a morphology-based natural system are *i*) morphological similarity of unrelated species due to convergence and analogy and *ii*) placement of morphologically aberrant species, without apparent similarity to any extant species. Several technology driven advances, such as micromorphology of pollen and chemical analyses, contributed to a more refined natural system of plants. However, the main issues remained and resulted in uncertainties in taxon placement and consequently in any down-stream analyses addressing character and trait evolution.

With the introduction of molecular phylogenetics and the first wide-scale molecular systematic studies of angiosperms (e.g., Chase *et al.*, 1993; Morgan & Soltis, 1993), new phylogenetic hypotheses were formulated. Advances in sequencing and computation technology, increasing simplicity of its application, coupled with decreasing prices contribute to this date to an increasingly well-resolved and robust phylogeny of the angiosperms. With the upsurge of molecular phylogenetics, the importance of classical systematic approaches, such as comparative morphology, declined. They became more of an accessory subject of plant systematics. With the decline in interest and a consequent decline in research in this field, studies on structural character evolution became dependent on already published literature, especially taxonomic and classification literature. This literature mining approach harbours several pitfalls for an understanding of structural evolution: *i*) older literature often lacks detailed visualisation of the phenomena described therein, *ii*) studies were conducted under the premise that the structures compared are homologous, *iii*) taxonomic studies emphasise differences more than similarities and *iv*) taxonomic studies are often focused on anthetic flowers and mature fruits, evidence from developmental studies is rarely reported or considered.

One thread of this study demonstrates how studies on floral structure evolution benefit from a phylogenetic framework. Two different approaches are applied: *i*) using recent phylogenies to understand the evolution of floral structure and *ii*) re-evaluating previously proposed evolutionary hypotheses on the basis of new phylogenetic evidence.

1.3 Floral architecture

The second thread of this thesis deals with the integration of floral parts into floral architecture. Floral structure describes all morphological aspects of a flower. It can be further subdivided into floral organisation, floral architecture and floral mode. Endress (1994, 1996) defined and coined these terms. Floral organisation is the number and insertion of floral organs. Floral architecture is the result of differential growth rates, synorganisation and organ fusion. As will be shown later, another category has been added to this list: modifications of basic floral organs. Floral mode takes ecological interactions into account. It roughly corresponds to pollination syndrome (Endress, 1994). These definitions have been applied in the majority of chapters of this thesis.

In figure 1.1, the difference between floral organisation and floral architecture is illustrated by comparing flowers of two boraginaceous species. Both species, *Borago officinalis* (Fig. 1.1A) and *Echium vulgare* (Fig. 1.1B) have an identical floral organisation, as illustrated by the numbers in the floral formulae, but differ in their floral architecture (e.g., actinomorphic vs. zygomorphic, faucal scales present vs. absent, short corolla tube vs. long corolla tube, anther cone vs. exserted, non-synorganised anthers).

Flowers with identical organisation can have different architectures, but flowers with different organisation cannot have identical architectures. Similar appearances in flowers with different organisations

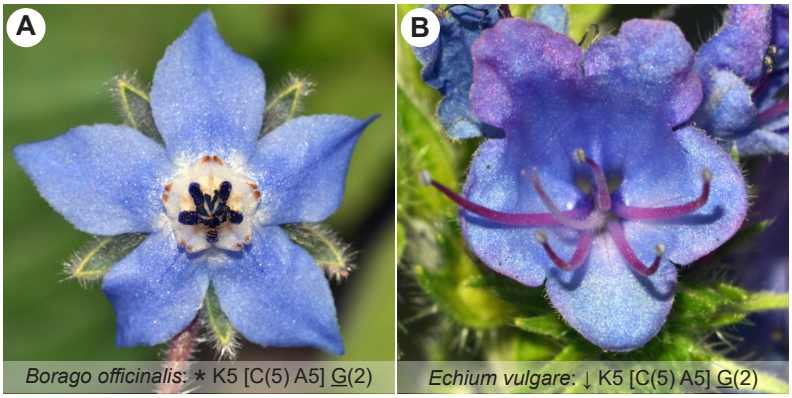

Figure 1.1: Illustration of the difference between floral organisation and floral architecture. Both flowers have the same floral organisation (numbers of floral organs per whorl as indicated in the floral formulae), but differ in floral architecture. A, *Borago officinalis*. B, *Echium vulgare*. Both species belong to Boraginaceae, Boraginales.

can be attributed to similar modes. Conversely, different architectures can result in different modes.

The relations of the different levels of floral structure are important to be kept in mind when studying floral evolution. On the one hand, the drivers of floral evolution are likely to act differently on the different levels. Changes in floral mode are likely to occur faster than changes in floral organisation, as indicated by several studies on pollinator shifts (e.g., Wasserthal, 1997; Whittall & Hodges, 2007; Cohen, 2012; Smith & Kriebel, 2018). Floral architecture, on the other hand, appears to be quite variable in its speed of evolutionary change. Especially, changes in length of stamen-corolla tubes, spurs and other tubular floral structures apparently happened independently in different time frames in several taxa (e.g., Hodges & Arnold, 1995; Whittall & Hodges, 2007; Cohen, 2012, 2016; Röschenbleck *et al.*, 2014).

Two features of floral architecture are in the focus of this thesis: *i*) floral nectaries and *ii*) modifications of basic floral organs, especially of the corolla and the stamen-corolla tube.

All species investigated in this thesis have floral nectaries. They are integrated into floral architecture and usually the primary reward producing structures. Due to their morphological and anatomical variability and importance in flower-pollinator interaction (Nicolson *et al.*, 2007), the study of nectaries is important to understand floral architecture, mode and function.

Modifications of the corolla and stamen-corolla tube are quite common in angiosperms (Endress & Matthews, 2006). However, the development of these structures and their integration into floral architecture is rarely addressed and thus poorly understood. Modifications are present in both study groups, as will be shown below.

One specific type of floral architecture is revolver architecture. In revolver flowers, the flower has separate compartments, each holding part of the full reward. A pollinator has to probe each compartment to collect the full reward of the flower. The resulting pollinator movement and the increased handling time, have been found to increase the likelihood of successful pollen transfer (Manetas & Petropoulou, 2000). Revolver architecture is quite common in angiosperms (Endress, 1994). The structures involved in its formation are quite diverse. They range from staminodes in *Nasa* (Weigend & Gottschling, 2006) and specialised nectar leaves in *Aquilegia* (Tucker & Hodges, 2005), to synorganised compartments formed by six different organs in *Geranium robertianum* (Endress, 2010).

The study of floral architecture is difficult due to the complex three-dimensional structure of flowers. The application of 3D-model based approaches, based on high-resolution x-ray computed tomography

(HRXCT) respectively micro-computed tomography (μCT) harbour new insight into floral architecture and its evolution.

1.4 Study groups

Both threads discussed above connect the studies made on two different study groups: Geraniales and Boraginales. Both orders are comprised in different clades of the angiosperms and differ in floral organisation. Below, brief overviews of both orders are given. Examples of their flowers are shown in figure 1.2.

Geraniales

The first taxon, the Geraniales, is a relatively small order in the rosids. It comprises about 890 species in approximately 14 genera and – according to a recent familial classification based on phylogenetic and morphological evidence – five families: Francoaceae, Geraniaceae, monogeneric Hypseocharitaceae, Melianthaceae and Vivianiaceae (Palazzesi *et al.*, 2012). Their taxonomic history was quite variable (summarised in Albers & van der Walt, 2007; Linder, 2007; Weigend, 2007) and only recently, molecular phylogenetic studies resulted in a refined understanding of the systematics of Geraniales (Morgan & Soltis, 1993; Price & Palmer, 1993; Palazzesi *et al.*, 2012). Several taxa within Geraniales have been studied using molecular phylogenies (e.g., Fiz *et al.*, 2006, 2008; Linder *et al.*, 2006; Touloumenidou *et al.*, 2007; Fiz-Palacios *et al.*, 2010; Röschenbleck *et al.*, 2014; Marcussen & Meseguer, 2017). For the majority of taxa floral developmental and morphological (e.g., Devi, 1991; Ronse Decraene & Smets, 1999; Aldasoro *et al.*, 2001; Ronse Decraene *et al.*, 2001; Klenter & Albers, 2004; Weigend, 2005; Endress, 2010), and taxonomic studies have been conducted (e.g., Verdcourt, 1950; Lefor, 1975; Aedo *et al.*, 2005a,b; Weigend, 2011; Röschenbleck *et al.*, 2014; Ferreira *et al.*, 2016).

One much-noticed feature of the flowers in the majority of Geraniales are the nectaries. Floral nectaries were studied in plenty of studies (e.g., Verdcourt, 1950; Eckert, 1966; Link, 1994, 1989; Vogel, 1998; Ronse Decraene & Smets, 1999; Ronse Decraene *et al.*, 2001; Weigend, 2005; Endress, 2010). In a recent overview article about nectary anatomy and morphology, similarities between the diverse nectaries across all Geraniales were described and an evolutionary series based on homology of the nectary glands was proposed (Jeiter *et al.*, 2017).

Apart from a few studies on nectary morphology and development in Geraniaceae (e.g., Payer, 1857; Japp, 1909; Eckert, 1966; Link, 1994, 1989; Endress, 2010), no systematic study on this family and related Hypseocharitaceae in the context of recent phylogenetic studies has been conducted. Especially, the formation of the 'spur' in *Pelargonium* is poorly understood (Japp, 1909; Labbe, 1964; Wetzstein & Armitage, 1983; Loehrlein & Craig, 2000). Even less is known about the integration of nectaries into floral architecture of Geraniaceae and enigmatic Hypseocharitaceae. The only study on floral architecture is on *Geranium robertianum* (Endress, 2010). In this study, development and morphology of the nectary glands and modifications of the petal bases were described. Both contribute to the formation of revolver architecture. Some examples of flowers of Hypseocharitaceae and Geraniaceae are shown in figure 1.2A–C.

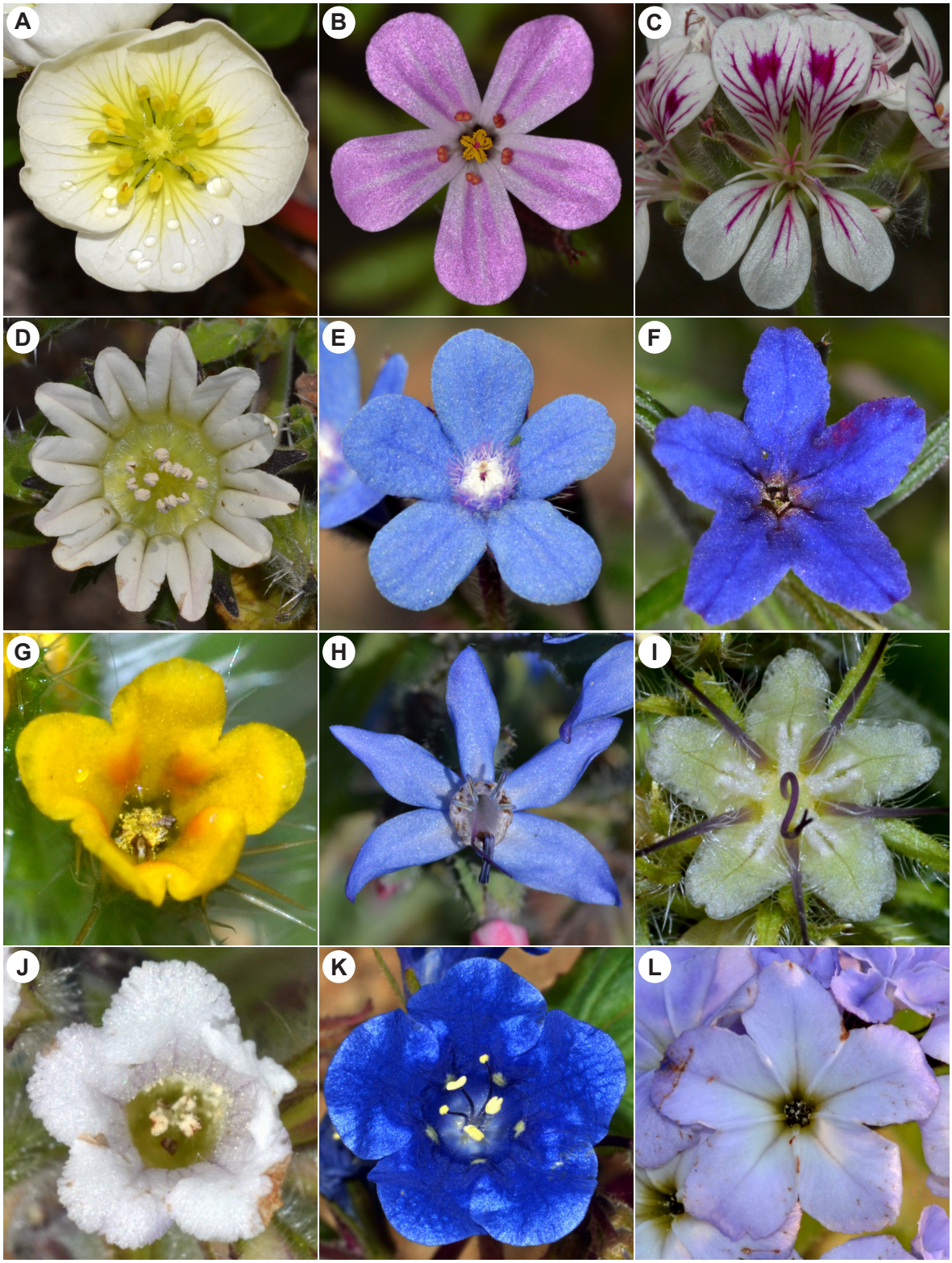

Figure 1.2: Flowers representing the taxonomic groups studied in this thesis. A–C, Geraniales. A, Hypseocharitaceae, *Hypseocharis bilobata*. B, C, Geraniaceae. B, *Geranium robertianum*. C, *Pelargonium australe* (Image by H. H. Hilger). D–L, Boraginales. D, Codonaceae, *Codon royenii*. E–H, Boraginaceae. E, *Anchusa azurea*. F, *Aegonychon purpurocaeruleum*. G, *Amsinckia spectabilis*. H, *Caccinia strigosa*. I–K, Hydrophyllaceae. I, *Hydrophyllum tenuipes*. J, *Draperia systyla*. K, *Phacelia campanularia*. L, Heliotropiaceae, *Heliotropium corymbosum*.

Boraginales

The second study taxon, Boraginales, is a medium sized order of about 2700 species in 125 genera nested within the lamiids clade of the asterids (Luebert *et al.*, 2016). Luebert *et al.* (2016) recently proposed a new familial classification of Boraginales, dividing them into eleven families in two phylogenetically well-supported clades (Boraginales I and Boraginales II; Weigend *et al.*, 2014). Boraginales I comprise monogeneric Codonaceae, monogeneric Wellstediaceae and Boraginaceae, by far the largest family with 1600 to 1700 species (Chacón *et al.*, 2016; Luebert *et al.*, 2016). Boraginales II comprise eight families: monotypic Coldeniaceae, Cordiaceae, Ehretiaceae, Heliotropiaceae, monogeneric Hoplestigmataceae, Hydrophyllaceae, Lennoaceae and Namaceae (Luebert *et al.*, 2016). Flowers of some Boraginales species studied in this thesis are shown in figure 1.2D–L.

The phylogeny of Boraginales is relatively well-resolved (Gottschling *et al.*, 2001; Weigend *et al.*, 2014; Refulio-Rodriguez & Olmstead, 2014; Stull *et al.*, 2015). Only within Boraginales II, the relations between Hydrophyllaceae, Namaceae and the clade comprising the remaining families of Boraginales II is not resolved and chloroplast marker phylogenies (e.g., Stull *et al.*, 2015) differ from nuclear marker phylogenies (e.g., Gottschling *et al.*, 2001).

The phylogenetic resolution within families differs. Numerous studies have focussed on Boraginaceae and subordinate taxa (e.g., Weigend *et al.*, 2009, 2013; Cohen, 2012, 2014, 2016; Chacón *et al.*, 2016, 2017, 2019). Other families are moderately to poorly known (e.g. Heliotropiaceae, Diane *et al.*, 2002; Hilger & Diane, 2003; Luebert *et al.*, 2011; Hydrophyllaceae, Ferguson, 1999; Walden *et al.*, 2014; Namaceae, Taylor, 2012; Cordiaceae, Gottschling *et al.*, 2005; Ehretiaceae, Gottschling *et al.*, 2014a; Holstein & Gottschling, 2018b).

There are numerous studies on floral and fruit structure in Boraginales focussing either on individual species, sections, genera, tribes or families (e.g., Uhlarz & Weberling, 1977; Hilger, 1984, 1987, 1992, 2014; Di Fulvio, 1989; Di Fulvio *et al.*, 1999, 1997; Di Fulvio, 1991; Hofmann, 1999; Gottschling, 2004; Gottschling *et al.*, 2014b; Holstein & Gottschling, 2018a). Despite plenty of studies, several taxa have not received as much attention as others and overall structural evolution between Boraginales families remains poorly understood.

In this thesis, two aspects of structural evolution in Boraginales are addressed: *i*) fruit evolution, and *ii*) evolution of stamen-corolla tube modifications.

Phylogenetic studies revealed some interesting patterns in fruit evolution within Boraginales (Weigend *et al.*, 2014). Boraginales I and Boraginales II both comprise few- to many-seeded capsule and single-seeded nutlet bearing families. In Boraginales I, Boraginaceae have four single seeded nutlets (eremocarps; Weigend *et al.*, 2016), their consecutive sister taxa, Wellstediaceae and Codonaceae, have few- and many-seeded capsules, respectively (Hilger & Weigend, 2016; Weigend & Hilger, 2016). Within Boraginales II, four single-seeded nutlets or drupes with four seeds are found in Coldeniaceae, Cordiaceae, Ehretiaceae, Heliotropiaceae and Hoplestigmataceae (Diane *et al.*, 2016; Gottschling *et al.*, 2016). The consecutive sister taxa of these Boraginales II families, Namaceae and Hydrophallceae, have four- to many-seeded capsules (Hofmann *et al.*, 2016). Only Lennoaceae, derived desert parasites, deviate from this pattern in having fruits falling into several single-seeded pyrenes (Bittrich, 2016). Despite the general knowledge about fruits in Boraginales, little is known about fruit development in the majority of taxa.

In Heliotropiaceae, there is a long standing observation, that the fruits in *Heliotropium* sect. *Heliothmanus*, sister to the remaining *Heliotropium* species, share some similarities with the fruits of

Boraginaceae. Especially, the presence of a columella, a structure between the nutlets at the base of the style had been suggested (Hilger, 1992). Since recent phylogenetic evidence indicates that Heliotropiaceae and Boraginaceae are not sister to each other, but that both are sister to capsule bearing taxa (Weigend *et al.*, 2014), homology (*sensu* Stevens, 1984; de Pinna, 1991; Scotland, 2011) of the fruit can be rejected *a priori*. However, the question of whether fruits in both taxa are structurally correspondent (*sensu* Scotland, 2011) remains unanswered.

Codonaceae are poorly studied. No floral developmental studies have been conducted and not much is known about their flower and fruit morphology (Gess, 1999; Weigend & Hilger, 2010). Since they are the sister to all remaining Boraginales I, an understanding of their gynoecium and fruit morphology contributes to the reconstruction of fruit evolution in this clade.

Several families of the Boraginales have modifications of the stamen-corolla tube. The most prominent example are faucal and basal scales in Boraginaceae (Weigend *et al.*, 2016). Despite their prominence only a few studies on their development and morphology were conducted (Payer, 1857; Arber, 1939; Schaefer, 1942). Modifications in other Boraginales taxa have been reported: the 'false bottom' in Codonaceae (Gess, 1999), various corolla scales in Hydrophyllaceae (Walden & Patterson, 2012; Hofmann *et al.*, 2016), winged filament bases in some Namaceae (Hitchcock, 1933b,a; Di Fulvio *et al.*, 1997; Hofmann *et al.*, 2016), scales in Wellstediaceae (Hunt, 1969; Thulin & Johansson, 1996; Hilger & Weigend, 2016) and some sparse observations from other families (Diane *et al.*, 2016; Gottschling *et al.*, 2016). Although they are named differently, they share similarities so that homology for some of these stamen-corolla tube modifications has been assumed (Brand, 1913) and proposed (Weigend *et al.*, 2016). Little is known about development and morphology of these modifications, even less is known about their integration into floral architecture. In this thesis, stamen-corolla tube modification development and morphology are studied systematically in Codonaceae, Boraginaceae and Hydrophyllaceae to understand their evolution, integration into floral architecture and function.

This thesis seeks to contribute to the understanding of the evolution of floral architectures. The application of developmental and morphological approaches, coupled with 3D-visualisation approaches shed new light on evolution and integration of these structures into floral architecture. Similarly, a developmental approach might further contribute to the understanding of gynoecium evolution in the Boraginales. Some of the knowledge gaps about floral structure in Boraginales and Geraniales will be filled.

1.5 Hypotheses

The hypotheses of this thesis are based on the two main threads: structural evolution in the context of recent phylogenetic reconstructions (*i*, *ii*) and integration of structures into floral architecture (*iii*–*viii*). Not always both topics are addressed in each individual chapter of this thesis. *i*) Detailed investigations of development and morphology of parts and entire flowers in the context of recent phylogenies allow the reconstruction of the evolution of the focal structures. *ii*) Revisiting long-standing claims about structural evolution in the light of recent phylogenies sheds new light on the focal structures and contributes to a refined understanding of structural evolution. *iii*) Floral architecture in a defined group of taxa is more variable than floral organisation within the same group of taxa. *iv*) Most changes in floral architecture, nectaries and modifications of floral organs appear in late stages of floral ontogeny. *v*) Modifications have a great influence on floral architecture. *vi*) In the Boraginales, the modifications of the basal part of the corolla tube and all modifications associated

with the filament bases evolved from one common ancestor. *vii*) Spaces enclosed by the flower are a crucial part of floral architecture. Compartmentalisation and compartment configuration influence floral function. *viii*) Floral architecture is more than structure. Nectar properties such as volume and viscosity also play a role.

1.6 Goals

Research questions

The following general research questions have arisen and are going to be dealt with in this thesis:

1. Are gynoecium and fruit of *Heliotropium* sect. *Heliothamnus* structurally correspondent to those of the Boraginaceae?
2. How does the flower of *Codon* develop?
3. How do the stamen-corolla tube modifications of the Boraginaceae develop, how are they integrated into floral architecture and is there a phylogenetic pattern?
4. How do the stamen-corolla tube modifications of the Hydrophyllaceae develop, how are they integrated into floral architecture and is there a phylogenetic pattern underlying these structures?
5. How are the internal floral spaces, enclosed by stamen-corolla tube modifications, in the Hydrophyllaceae configured and how are the modifications contributing to the floral architecture?
6. What is the relationship between floral nectaries and floral architecture in Geraniaceae and Hypseocharitaceae?
7. What is the internal floral space and how does it contribute to our understanding of floral ecology and evolution?
8. Can the various stamen-corolla tube modifications found in different Boraginales families be homologised and if so, is it possible to propose an evolutionary series?

Specific objectives

1. Describe the development of gynoecium and fruit of *Heliotropium* sect. *Heliothamnus* and compare it to the Boraginaceae.
2. Describe morphology and development of flower and fruit in *Codon*.
3. Describe morphology and development of the stamen-corolla tube modifications in Boraginaceae, assess their integration into floral architecture and check for possible phylogenetic patterns.
4. Describe morphology and development of stamen-corolla tube modifications and floral nectaries of Hydrophyllaceae.
5. Assess how stamen-corolla tube modifications are integrated into floral architecture, what kind of spaces they enclose, if there is a difference in nectar presentation and if there is a phylogenetic pattern in floral architecture and stamen-corolla tube modifications in Hydrophyllaceae.

6. Describe the morphology and development of the nectaries in Geraniaceae and Hypseocharitaceae and assess how they relate to floral architecture.

7. Propose the internal floral space as a new feature of floral structure and as a useful tool in a variety of floral evolutionary and ecological studies.

8. Homologise the various stamen-corolla tube modifications found in the Boraginales and propose an evolutionary series for these structures.

To achieve these objectives, several methods have been employed, including scanning electron microscopy and light microscopy, high-resolution x-ray computed tomography respectively micro-computed tomography, followed by the segmentation of entire flowers or internal floral spaces, 3D-landmarking and 3D-geometric morphometrics, and molecular phylogenetics, followed by character mapping and testing for phylogenetic signal. Most commonly an ontogentic approach was chosen to understand the evolution of the focal structures.

1.7 Overview of the dissertation

This thesis is a cumulative work of manuscripts, either published, submitted or in preparation to be submitted. Chapters 2, 3, 5 and 7 are included in the form as provided by the respective journals. Chapters 4, 6 and 8 are included as manuscripts. Each chapter includes separate introduction-, material and methods-, results- and discussion-sections. The structure of the chapters might vary, depending on the article type and journal style. References are cited separately for each chapter. The appendix of chapter 6 is provided immediately after the references of this chapter.

Chapter 2[a] is a study on the morphology and development of the gynoecium and fruit in *Heliotropium* sect. *Heliothamnus* (Heliotropiaceae, Boraginales). Morphology and anatomy of one species of this sister clade to the remaining *Heliotropium* species has previously been studied and certain similarities to the gynoecium of the Boraginaceae have been proposed. However, due to recent phylogenetic reconstructions, homology of the fruits could be rejected *a priori*. On the basis of a comparative approach using scanning electron microscopy, light microscopy and high-resolution x-ray computed tomography, it is shown that gynoecium and fruit of *Heliotropium* sect. *Heliothamnus* develop differently compared to the Boraginaceae. Especially, the central disrupting tissue of the ovary differs from the columella of the Boraginaceae. Thus, it can be concluded that both structures are not structurally correspondent.

Chapter 3[b] is about the flower development and morphology of two species of *Codon* from monogeneric Codonaceae (Boraginales). The study uses scanning electron microscopy and light microscopy. Striking features of *Codon* are the polymerous perianth and androecium, as well as the formation of septa between filament bases and corolla tube. The ontogenetic part of the study reveals that sepals and stamens each arise in two separate phases. At first, five to six organs arise in a spiral order, whereas in the second phase of development the remaining organs arise subsimultaneously. The septa arise late in flower development. They divide the corolla tube into separate compartments, contributing to a revolver architecture of the flower. Homology to the corolla scales of the Hydrophyllaceae is suggested.

[a] **Jeiter J**, Staedler YM, Schönenberger J, Weigend M, Luebert F. 2018. Gynoecium and fruit development in *Heliotropium* sect. *Heliothamnus* (Heliotropiaceae). *International Journal of Plant Sciences* 179: 275–286.

[b] **Jeiter J**, Danisch F, Hilger HH. 2016. Polymery and nectary chambers in *Codon* (Codonaceae) – flower and fruit development in a small, capsule-bearing family of Boraginales. *Flora* 220: 94–102.

Chapter 4[c] is the first family wide developmental and morphological study of faucal and basal scales of the boraginaceous flower. In this study, scanning electron microscopy is used to describe the development and the morphology of the scales. Furthermore, it is investigated how these modifications are integrated into floral architecture. For this purpose, micro-computed tomography is used and virtual cross-sections and high-resolution surface renderings are visualised. Both floral architectural characters, and the presence and absence of faucal and basal scales were mapped onto a recent phylogeny of the Boraginaceae. Both types of scales are inserted in late flower development, indicating, that they might be peramorphoses. The analysis of the floral architecture showed that faucal scales play a role in constricting the entrance of the flower or in contributing to the formation of an anther cone. Basal scales on the other hand cover either the disc nectary or the entire ovary. Character mapping revealed no phylogenetic pattern.

In **chapter 5**[d], morphology and development of stamen-corolla tube modifications and floral nectaries in Hydrophyllaceae are studied using scanning electron microscopy. The modifications are present in all species studied. They arise in a similar pattern in late floral ontogeny and their development is correlated with the elongation of the corolla tube. Each filament base is associated with two adjacent modifications. The modifications compartmentalise the flower and result in a revolver architecture in the majority of species. An evolutionary series is proposed.

Based on the observations of the variable configurations of stamen-corolla tube modifications in Hydrophyllaceae, in **chapter 6**[e] floral architecture and integration of the modifications and nectaries are studied. This study uses high-resolution x-ray computed tomography and molecular phylogenetics. On the basis of the 3D-models, 3D-landmarking based 3D-geometric morphometrics are employed and the results are mapped onto the phylogeny. Furthermore, the spaces enclosed by the modifications and other floral organs are visualised and three types of independent spaces (completely, incompletely, non-compartmentalised) are described. To check their function in the proposed revolver architecture, nectar measurements were conducted, showing that in completely compartmentalised flowers, all separate compartments behave similarly. In incompletely compartmentalised flowers, the patterns of the nectar removal experiment are more variable, indicating that factors such as nectar amount and nectar concentration play a role in floral function. This represents a different route towards revolver architecture.

In **chapter 7**[f], nectary development and floral architecture in Geraniaceae and Hypseocharitaceae are studied using scanning electron microscopy and light microscopy. The receptacular nectaries develop in late floral ontogeny. In several species, their development is correlated with an elongation of the receptacle, resulting in the formation of a short anthophore. In *Pelargonium* the entire flower is lifted by receptacular growth leaving only the single nectary gland in place, which leads to the formation of a receptacular cavity. The formation of stamen triplets, through broadened filaments or a dédoublement in one of the stamen whorls, and modifications of the petals in some species result in elaborate or lax revolver architecture. An evolutionary series of the evolution of floral architecture in Geraniaceae and Hypseocharitaceae is proposed.

[c] **Jeiter J**, Langecker S, Weigend M. Towards an integrative understanding of stamen-corolla tube modifications and floral architecture in Boraginaceae (Boraginales). *Botanical Journal of the Linnean Society*. Submitted 16.08.2019.

[d] **Jeiter J**, Weigend M. 2018. Simple scales make complex compartments – ontogeny and morphology of stamen-corolla tube modifications in Hydrophyllaceae (Boraginales). *Biological Journal of the Linnean Society* 125: 802-820.

[e] **Jeiter J**, Staedler YM, Schönenberger J, Luebert F, Weigend M. Three levels of floral architecture in the waterleaf family (Hydrophyllaceae). To be submitted.

[f] **Jeiter J**, Hilger HH, Smets EF, Weigend M. 2017. The relation between nectaries and floral architecture: a case study in Geraniaceae and Hypseocharitaceae. *Annals of Botany* 120: 791–803.

In **chapter 8**[g], the concept of the internal floral space is introduced. The internal floral space is the entirety of air-filled spaces enclosed by a flower. It can be reconstructed from 3D-models as outcome of 3D-scanning methods such as micro-computed tomography. The internal floral space has so far rarely been considered, although it might harbour new insights into flower evolution and ecology. Potential applications of the segmentation of the internal floral space are volumetric approaches, comparative morphology and 3D-visualisation of complex spatial arrangements.

Chapter 9 is the general conclusion of the thesis. Floral architecture and nectaries, as well as the interpretation of structural observation in the context of recent phylogenetic studies are discussed. Furthermore, an evolutionary transformation series for the stamen-corolla tube modifications of the Boraginales is proposed. Finally, an outlook for further research questions in relation to this thesis is given.

1.8 Contributions to chapters

Chapter 2: **Jeiter J**, Staedler YM, Schönenberger J, Weigend M, Luebert F. 2018. Gynoecium and fruit development in *Heliotropium* sect. *Heliothamnus* (Heliotropiaceae). *International Journal of Plant Sciences* 179: 275–286. https://doi.org/10.1086/696219

> Own contributions: Designed work (together with F. Luebert), collected material (with F. Luebert), prepared samples, performed SEM, processed and visualised HRXCT-data, analysed the data, processed images and wrote the manuscript (together with F. Luebert and M. Weigend).

Chapter 3: **Jeiter J**, Danisch F, Hilger HH. 2016. Polymery and nectary chambers in *Codon* (Codonaceae) – flower and fruit development in a small, capsule-bearing family of Boraginales. *Flora* 220: 94–102. https://doi.org/10.1016/j.flora.2016.02.010

> Own contributions: Designed work (together with H.H. Hilger), collected plant material (together with H.H. Hilger and F. Danisch), prepared samples for SEM (together with F. Danisch), collected the data (together with F. Danisch), analysed the data (together with H.H. Hilger) and wrote the manuscript (together with H.H. Hilger).

Chapter 4: **Jeiter J**, Langecker S, Weigend M. Towards an integrative understanding of stamen-corolla tube modifications and floral architecture in Boraginaceae (Boraginales). *Botanical Journal of the Linnean Society*. Submitted 16.08.2019.

> Own contributions: Designed work (together with M. Weigend), collected the plant material, prepared the samples for SEM and µCT, collected the data, performed image and data processing (all together with S. Langecker), processed and visualised the µCT-data, analysed the data and wrote the manuscript (together with M. Weigend).

Chapter 5: **Jeiter J**, Weigend M. 2018. Simple scales make complex compartments – ontogeny and morphology of stamen-corolla tube modifications in Hydrophyllaceae (Boraginales). *Biological Journal of the Linnean Society* 125: 802–820. https://doi.org/10.1093/biolinnean/bly167

> Own contributions: Designed work (together with M. Weigend), collected the plant material, prepared samples for SEM, collected, processed and analysed the data and wrote the manuscript (together with M. Weigend).

[g] **Jeiter J**, Ziegler A, Weigend M. Internal floral spaces provide three-dimensional insights into angiosperm ecology and evolution. To be submitted.

Chapter 6: **Jeiter J**, Staedler YM, Schönenberger J, Luebert F, Weigend M. Three levels of floral architecture in the waterleaf family (Hydrophyllaceae). To be submitted.

> Own contributions: Designed work (together with M. Weigend and Y.M. Staedler), collected plant material, prepared samples for HRXCT, processed and visualised the HRXCT-data, conducted the 3D-landmarking for the geometric morphometric analyses, analysed the data and wrote the manuscript (together with M. Weigend).

Chapter 7: **Jeiter J**, Hilger HH, Smets EF, Weigend M. 2017. The relationship between nectaries and floral architecture: a case study in Geraniaceae and Hypseocharitaceae. *Annals of Botany* 120: 791–803. https://doi.org/10.1093/aob/mcx101

> Own contributions: Designed work (together with E.F. Smets and M. Weigend), collected material (together with H.H. Hilger), processed the samples for SEM and light microscopy, collected and analysed the data and wrote the manuscript (together with H. H. Hilger, E.F. Smets and M. Weigend).

Chapter 8: **Jeiter J**, Ziegler A, Weigend M. Internal floral spaces provide three-dimensional insights into angiosperm ecology and evolution. To be submitted.

> Own contributions: Designed work (together with M. Weigend and A. Ziegler), collected plant material, prepared samples for μCT, visualised, processed and analysed the data and wrote the manuscript (together with M. Weigend and A. Ziegler).

1.9 References

Aedo, C., Fiz, O., Alarcón, M.L., Navarro, C. & Aldasoro, J.J. (2005a) Taxonomic revision of *Geranium* sect. *Dissecta* (Geraniaceae). *Systematic Botany* **30**, 533–338.

Aedo, C., Navarro, C. & Alarcón, M.L. (2005b) Taxonomic revision of *Geranium* sections *Andina* and *Chilensia* (Geraniaceae). *Botanical Journal of the Linnean Society* **149**, 1–68.

Albers, F. & van der Walt, J.J.A. (2007) Geraniaceae. *The Families and Genera of Vascular Plants* (ed. K. Kubitzki), vol. 9, pp. 157–167, Springer, Heidelberg.

Aldasoro, J.J., Navarro, C., Vargas, P. & Aedo, C. (2001) Anatomy, morphology, and cladistic analysis of *Monsonia* L. (Geraniaceae). *Anales del Jardín Botánico de Madrid* **59**, 75–100.

Arber, A. (1939) Studies in flower structure: V. On the interpretation of the petal and 'corona' in *Lychnis*. *Annals of Botany* **3**, 337–346.

Bittrich, V. (2016) Lennoaceae. *Families and Genera of Vascular Plants* (eds. K. Kubitzki, J.W. Kadereit & V. Bittrich), vol. 14, pp. 257–261, Springer, Heidelberg.

Brand, A. (1913) *Hydrophyllaceae In: Engler, Das Pflanzenreich [Heft 59] IV. 251*, vol. 59 of *Das Pflanzenreich*. Wilhelm Engelmann, Leipzig.

Chacón, J., Luebert, F., Hilger, H.H., Ovchinnikova, S., Selvi, F., Cecchi, L., Guilliams, C.M., Hasenstab-Lehman, K., Sutorý, K., Simpson, M.G. & Weigend, M. (2016) The borage family (Boraginaceae s.str.): A revised infrafamilial classification based on new phylogenetic evidence, with emphasis on the placement of some enigmatic genera. *Taxon* **65**, 523–546.

Chacón, J., Luebert, F., Selvi, F., Cecchi, L. & Weigend, M. (2019) Phylogeny and historical biogeography of Lithospermeae (Boraginaceae): Disentangling the possible causes of Miocene diversifications. *Molecular Phylogenetics and Evolution* p. 106626.

Chacón, J., Luebert, F. & Weigend, M. (2017) Biogeographic events are not correlated with diaspore dispersal modes in Boraginaceae. *Frontiers in Ecology and Evolution* **5**, 1–14.

Chase, M.W., Soltis, D.E., Olmstead, R.G., Morgan, D., Les, D.H., Mishler, B.D., Duvall, M.R., Price, R.A., Hills, H.G., Qiu, Y.L., Kron, K.A., Rettig, J.H., Conti, E., Palmer, J.D., Manhart, J.R., Sytsma, K.J., Michaels, H.J., Kress, W.J., Karol, K.G., Clark, W.D., Hedren, M., Brandon S. Gaut, Jansen, R.K., Kim, K.J., Wimpee, C.F., Smith, J.F., Furnier, G.R., Strauss, S.H., Xiang, Q.Y., Plunkett, G.M., Soltis, P.S., Swensen, S.M., Williams, S.E., Gadek, P.A., Quinn, C.J., Eguiarte, L.E., Golenberg, E., Learn, Jr., G.H., Graham, S.W., Barrett, S.C.H., Dayanandan, S. & Albert, V.A. (1993) Phylogenetics of seed plants: An analysis of nucleotide sequences from the plastid gene rbcL. *Annals of the Missouri Botanical Garden* **80**, 528–580.

Cohen, J.I. (2012) Continuous characters in phylogenetic analyses: Patterns of corolla tube length evolution in *Lithospermum* L. (Boraginaceae): Evolution of corolla tube length. *Biological Journal of the Linnean Society* **107**, 442–457.

Cohen, J.I. (2014) A phylogenetic analysis of morphological and molecular characters of Boraginaceae: Evolutionary relationships, taxonomy, and patterns of character evolution. *Cladistics* **30**, 139–169.

Cohen, J.I. (2016) Floral evolution in *Lithospermum* (Boraginaceae): Independent origins of similar flower types. *Botanical Journal of the Linnean Society* **180**, 213–228.

Darwin, C. (1859) *On the Origin of Species by Means of Natural Selection, or, The Preservation of Favoured Races in the Struggle for Life*. John Murray, London.

de Pinna, M.G.G. (1991) Concepts and tests of homology in the cladistic paradigm. *Cladistics* **7**, 367–394.

Devi, D.R. (1991) Floral anatomy of *Hypseocharis* (Oxalidaceae) with a discussion on its systematic position. *Plant Systematics and Evolution* **177**, 161–164.

Di Fulvio, T.E. (1989) Embriologia de *Nama jamaicense* (Phacelieae, Hydrophyllaceae). *Kurtziana* **20**, 9–31.

Di Fulvio, T.E. (1991) Morfología y vascularización floral de *Lemmonia californica* y *Nama jamaicense* (Hydrophyllaceae). *Kurtziana* **21**, 23–38.

Di Fulvio, T.E., Cosa, M.T. & Dottori, N. (1997) Morfologia y vascularizacion floral en *Turricula*, *Eriodictyon* y *Wigandia* (Phacelieae; Hydrophyllaceae) con relacion a la taxonomia. *Kurtziana* **25**, 47–66.

Di Fulvio, T.E., Cosa, M.T. & Dottori, N. (1999) Morfología y vascularización floral de *Draperia*, *Emmenanthe*, *Hesperochiron*, *Romanzoffia* y *Tricardia* (Phacelieae, Hydrophyllaceae). *Kurtziana* **27**, 187–209.

Diane, N., Förther, H. & Hilger, H.H. (2002) A systematic analysis of *Heliotropium*, *Tournefortia*, and allied taxa of the Heliotropiaceae (Boraginales) based on ITS1 sequences and morphological data. *American Journal of Botany* **89**, 287–295.

Diane, N., Hilger, H.H., Förther, H., Weigend, M. & Luebert, F. (2016) Heliotropiaceae. *Families and Genera of Vascular Plants* (eds. K. Kubitzki, J.W. Kadereit & V. Bittrich), vol. 14, pp. 203–211, Springer, Heidelberg.

Eckert, G. (1966) Entwicklungsgeschichtliche und blütenanatomische Untersuchungen zum Problem der Obdiplostemonie. *Botanische Jahrbücher für Systematik* **85**, 523–604.

Endress, P.K. (1994) *Diversity and Evolutionary Biology of Tropical Flowers*. Cambridge Tropical Biology Series, Cambridge University Press, Cambridge.

Endress, P.K. (1996) Homoplasy in angiosperm flowers. *Homoplasy - The Recurrence of Similarity in Evolution* (eds. M.J. Sanderson & L. Hufford), pp. 303–325, Academic Press, San Diego, California, United States.

Endress, P.K. (2010) Synorganisation without organ fusion in the flowers of *Geranium robertianum* (Geraniaceae) and its not so trivial obdiplostemony. *Annals of Botany* **106**, 687–695.

Endress, P.K. & Matthews, M.L. (2006) Elaborate petals and staminodes in eudicots: Diversity, function, and evolution. *Organisms Diversity & Evolution* **6**, 257–293.

Ferguson, D.M. (1999) Phylogenetic analysis and relationships in Hydrophyllaceae based on ndhF sequence data. *Systematic Botany* **23**, 253–268.

Ferreira, J.P.R., Hassemer, G., Campestrini, S., Weigend, M. & Trevisan, R. (2016) A revision of the extra-Andean Vivianiaceae. *Phytotaxa* **246**, 23.

Fiz, O., Vargas, P., Alarcón, M., Aedo, C., Garcia, J.L. & Aldasoro, J.J. (2008) Phylogeny and historical biogeography of Geraniaceae in relation to climate changes and pollination ecology. *Systematic Botany* **33**, 326–342.

Fiz, O., Vargas, P., Alarcón, M. & Aldasoro, J.J. (2006) Phylogenetic relationships and evolution in *Erodium* (Geraniaceae) based on trnL-trnF sequences. *Systematic Botany* **31**, 739–763.

Fiz-Palacios, O., Vargas, P., Vila, R., Papadopulos, A.S.T. & Aldasoro, J.J. (2010) The uneven phylogeny and biogeography of *Erodium* (Geraniaceae): Radiations in the Mediterranean and recent recurrent intercontinental colonization. *Annals of Botany* **106**, 871–884.

Gess, S.K. (1999) *Codon* flowers, chalices of hidden nectar. *Veld & Flora* **85**, 30–31.

Gottschling, M. (2004) Floral ontogeny in *Bourreria* (Ehretiaceae, Boraginales). *Flora* **199**, 409–423.

Gottschling, M., Hilger, H.H., Wolf, M. & Diane, N. (2001) Secondary structure of the ITS1 transcript and its application in a reconstruction of the phylogeny of Boraginales. *Plant Biology* **3**, 629–636.

Gottschling, M., Luebert, F., Hilger, H.H. & Miller, J.S. (2014a) Molecular delimitations in the Ehretiaceae (Boraginales). *Molecular Phylogenetics and Evolution* **72**, 1–6.

Gottschling, M., Miller, J.S., Weigend, M. & Hilger, H.H. (2005) Congruence of a phylogeny of Cordiaceae (Boraginales) inferred from ITS1 sequence data with morphology, ecology, and biogeography. *Annals of the Missouri Botanical Garden* **92**, 425–437.

Gottschling, M., Nagelmüller, S. & Hilger, H.H. (2014b) Generative ontogeny in *Tiquilia* (Ehretiaceae: Boraginales) and phylogenetic implications. *Biological Journal of the Linnean Society* **112**, 520–534.

Gottschling, M., Weigend, M. & Hilger, H.H. (2016) Ehretiaceae. *Families and Genera of Vascular Plants* (eds. K. Kubitzki, J.W. Kadereit & V. Bittrich), vol. 14, pp. 165–178, Springer, Heidelberg.

Hilger, H.H. (1984) Wachstum und Ausbildungsformen des Gynoeceums von *Rochelia* (Boraginaceae). *Plant Systematics and Evolution* **146**, 123–139.

Hilger, H.H. (1987) Flower and fruit development in *Wigandia caracasana* (Hydrophyllaceae). *American Journal of Botany* **74**, 250–259.

Hilger, H.H. (1992) Morphology of *Heliotropium* (Boraginaceae) dispersal units. *Botanica Acta* **105**, 387–393.

Hilger, H.H. (2014) Ontogeny, morphology, and systematic significance of glochidiate and winged fruits of Cynoglosseae and Eritrichieae (Boraginaceae). *Plant Diversity and Evolution* **131**, 167–214.

Hilger, H.H. & Diane, N. (2003) A systematic analysis of Heliotropiaceae (Boraginales) based on trnL and ITS1 sequence data. *Botanische Jahrbücher* **125**, 19–51.

Hilger, H.H. & Weigend, M. (2016) Wellstediaceae. *Families and Genera of Vascular Plants* (eds. K. Kubitzki, J.W. Kadereit & V. Bittrich), vol. 14, pp. 403–406, Springer, Heidelberg.

Hitchcock, C.L. (1933a) A taxonomic study of the genus *Nama*. I. *American Journal of Botany* **20**, 415–430.

Hitchcock, C.L. (1933b) A taxonomic study of the genus *Nama*. II. *American Journal of Botany* **20**, 518–534.

Hodges, S.A. & Arnold, M.L. (1995) Spurring plant diversification: Are floral nectar spurs a key innovation? *Proceedings of the Royal Society B-Biological Sciences* **262**, 343–348.

Hofmann, M. (1999) Flower and fruit development in the genus *Phacelia* (Phacelieae, Hydrophyllaceae): Characters of systematic value. *Systematics and Geography of Plants* **68**, 203–212.

Hofmann, M., Walden, G.K., Hilger, H.H. & Weigend, M. (2016) Hydrophyllaceae. *Families and Genera of Vascular Plants* (eds. K. Kubitzki, J.W. Kadereit & V. Bittrich), vol. 14, pp. 221–238, Springer, Heidelberg.

Holstein, N. & Gottschling, M. (2018a) Flowers of *Halgania* (Ehretiaceae, Boraginales) are set up for being buzzed and the role of intertwining anther trichomes. *Flora* **240**, 7–15.

Holstein, N. & Gottschling, M. (2018b) Waking sleeping beauties: A molecular phylogeny and nomenclator of *Halgania* (Ehretiaceae, Boraginales). *Australian Systematic Botany* **31**, 107.

Hunt, D.R. (1969) *Wellstedia*. *Hooker´s Icones Plantarum* **37**, 3665–3667.

Japp, G. (1909) über die morphologische Wertigkeit des Nektariums der Blüten des *Pelargonium zonale*. *Verhandlungen des Naturforschenden Vereines Brünn* **47**, 201–216.

Jeiter, J., Weigend, M. & Hilger, H.H. (2017) Geraniales flowers revisited: Evolutionary trends in floral nectaries. *Annals of Botany* **119**, 395–408.

Klenter, T. & Albers, F. (2004) Comparative studies of the androecium of *Monsonia* species from the sections *Olopetalum* and *Sarcocaulon* (Geraniaceae). *Schumannia* **4**, 87–92.

Labbe, A. (1964) On the spur of the flower of *Pelargonium*. *Bulletin de la Société Botanique de France* **8**, 321–324.

Lefor, M.W.M. (1975) A taxonomic revision of the Vivianiaceae. *University of Connecticut Occasional Papers, Biological Science Series* **2**, 225–255.

Linder, H.P. (2007) Melianthaceae. *The Families and Genera of Vascular Plants* (ed. K. Kubitzki), vol. 9, pp. 250–259, Springer, Heidelberg.

Linder, H.P., Dlamini, T., Henning, J. & Verboom, G.A. (2006) The evolutionary history of *Melianthus* (Melianthaceae). *American Journal of Botany* **93**, 1052–1064.

Link, D.A. (1989) *Die Nektarien Der Geraniales - Morphologie, Anatomie, Histologie, Blütenökologische Bedeutung Und Konsequenzen Für Die Systematik*. Ph.D. thesis, Johannes Gutenberg Universität Mainz, Mainz.

Link, D.A. (1994) The nectaries of Geraniaceae. *Proceedings of the International Geraniaceae Symposium* (ed. P. Vorster), pp. 215–225, Stellenbosch University, South Africa.

Linnaeus, C. (1753) *Species Plantarum, Exhibentes Plantas Rite Cognitas, Ad Genera Relatas, Cum, Differentiis Specificis, Nominibus Trivialibus, Synonymis Selecti, Locis Natalibus, Secundum Systema Sexuale Digestas*, vol. 1. Impensis Laurentii salvii, Holmiae [Stockholm].

Loehrlein, M. & Craig, R. (2000) Floral Ontogeny of *Pelargonium* x *domesticum*. *Journal of the American Society of Horticultural Science* **125**, 36–40.

Luebert, F., Brokamp, G., Wen, J., Weigend, M. & Hilger, H.H. (2011) Phylogenetic relationships and morphological diversity in Neotropical *Heliotropium* (Heliotropiaceae). *Taxon* **60**, 663–680.

Luebert, F., Cecchi, L., Frohlich, M.W., Gottschling, M., Guilliams, C.M., Hasenstab-Lehman, K.E., Hilger, H.H., Miller, J.S., Mittelbach, M., Nazaire, M., Nepi, M., Nocentini, D., Ober, D., Olmstead, R.G., Selvi, F., Simpson, M.G., Sutorý, K., Valdés, B., Walden, G.K. & Weigend, M. (2016) Familial classification of the Boraginales. *Taxon* **65**, 502–522.

Manetas, Y. & Petropoulou, Y. (2000) Nectar amount, pollinator visit duration and pollination success in the mediterranean shrub *Cistus creticus*. *Annals of Botany* **86**, 815–820.

Marcussen, T. & Meseguer, A.S. (2017) Species-level phylogeny, fruit evolution and diversification history of *Geranium* (Geraniaceae). *Molecular Phylogenetics and Evolution* **110**, 134–149.

Morgan, D.R. & Soltis, D.E. (1993) Phylogenetic relationships among members of Saxifragaceae *sensu lato* based on rbcL sequence data. *Annals of the Missouri Botanical Garden* **80**, 631–660.

Nicolson, S.W., Nepi, M. & Pacini, E. (eds.) (2007) *Nectaries and Nectar*. Springer, Dordrecht.

Palazzesi, L., Gottschling, M., Barreda, V. & Weigend, M. (2012) First Miocene fossils of Vivianiaceae shed new light on phylogeny, divergence times, and historical biogeography of Geraniales. *Biological Journal of the Linnean Society* **107**, 67–85.

Payer, J.B. (1857) *Traité d'organogénie Comparée de La Fleur*. V. Masson, Paris.

Price, R.A. & Palmer, J.D. (1993) Phylogenetic relationships of the Geraniaceae and Geraniales from rbcL sequence comparisons. *Annals of the Missouri Botanical Garden* **80**, 661–671.

Refulio-Rodriguez, N.F. & Olmstead, R.G. (2014) Phylogeny of Lamiidae. *American Journal of Botany* **101**, 287–299.

Ronse Decraene, L.P., Linder, H.P., Dlamini, T. & Smets, E.F. (2001) Evolution and development of floral diversity of Melianthaceae, an enigmatic southern African family. *International Journal of Plant Sciences* **162**, 59–82.

Ronse Decraene, L.P. & Smets, E.F. (1999) Similarities in floral ontogeny and anatomy between the genera *Francoa* (Francoaceae) and *Greyia* (Greyiaceae). *International Journal of Plant Sciences* **160**, 377–393.

Röschenbleck, J., Albers, F., Müller, K., Weinl, S. & Kudla, J. (2014) Phylogenetics, character evolution and a subgeneric revision of the genus *Pelargonium* (Geraniaceae). *Phytotaxa* **159**, 31–76.

Schaefer, H. (1942) Die Hohlschuppen der Boraginaceen. *Botanische Jahrbücher für Systematik, Pflanzengeschichte und Pflanzengeographie* **72**, 304–346.

Scotland, R.W. (2011) What is parallelism? *Evolution & Development* **13**, 214–227.

Smith, S.D. & Kriebel, R. (2018) Convergent evolution of floral shape tied to pollinator shifts in Iochrominae (Solanaceae). *Evolution* **72**, 688–697.

Stevens, P.F. (1984) Homology and Phylogeny: Morphology and Systematics. *Systematic Botany* **9**, 395–409.

Stull, G.W., de Stefano, R.D., Soltis, D.E. & Soltis, P.S. (2015) Resolving basal lamiid phylogeny and the circumscription of Icacinaceae with a plastome-scale data set. *American Journal of Botany* **102**, 1794–1813.

Taylor, S.E. (2012) *Molecular Systematics and the Origins of Gypsophily in* Nama *L. (Boraginaceae).* Thesis.

Thulin, M. & Johansson, N.B. (1996) Taxonomy and biogeography of the anomalous genus *Wellstedia*. *The Biodiversity of African Plants* (eds. L.J.G. van der Maesen, X.M. van der Burgt & J.M. van Madenbach de Rooy), pp. 73–86, Kluwer Academic Publishers, Dordrecht.

Touloumenidou, T., Bakker, F.T. & Albers, F. (2007) The phylogeny of *Monsonia* L. (Geraniaceae). *Plan Systematics and Evolution* **264**, 1–14.

Tucker, S.C. & Hodges, S.A. (2005) Floral ontogeny of *Aquilegia*, *Semiaquilegia*, and *Enemion* (Ranunculaceae). *International Journal of Plant Sciences* **166**, 557–574.

Uhlarz, H. & Weberling, F. (1977) Ontogenetische Untersuchungen an *Cordia verbenacea* DC. (Boraginaceae), ein Beitrag zur Kenntnis der Syndesmien. *Berichte der Deutschen Botanischen Gesellschaft* **90**, 127–134.

Verdcourt, B. (1950) Notes on the Genus *Bersama* in Africa. *Kew Bulletin* **5**, 233–244.

Vogel, S. (1998) Remarkable nectaries: Structure, ecology, organophyletic perspectives IV. Miscellaneous cases. *Flora* **193**, 225–248.

Walden, G.K., Garrison, L.M., Spicer, G.S., Cipriano, F.W. & Patterson, R. (2014) Phylogenies and chromosome evolution of *Phacelia* (Boraginaceae: Hydrophylloideae) inferred from nuclear ribosomal and chloroplast sequence data. *Madroño* **61**, 16–47.

Walden, G.K. & Patterson, R. (2012) Nomenclature of subdivisions within *Phacelia* (Boraginaceae: Hydrophylloideae). *Madroño* **59**, 211–222.

Wasserthal, L.T. (1997) The pollinators of the malagasy star orchids *Angraecum sesquipedale*, *A. sororium* and *A. compactum* and the evolution of extremely long spurs by pollinator shift. *Botanica Acta* **110**, 343–359.

Weigend, M. (2005) Notes on the floral morphology in Vivianiaceae (Geraniales). *Plant Systematics and Evolution* **253**, 125–131.

Weigend, M. (2007) Ledocarpaceae. *The Families and Genera of Vascular Plants* (ed. K. Kubitzki), vol. 9, pp. 213–220, Springer, Heidelberg.

Weigend, M. (2011) The genus *Balbisia* (Vivianiaceae, Geraniales) in Peru, Bolivia and northern Chile. *Phytotaxa* **22**, 47–56.

Weigend, M. & Gottschling, M. (2006) Evolution of funnel-revolver flowers and ornithophily in *Nasa* (Loasaceae). *Plant Biology* **8**, 120–142.

Weigend, M., Gottschling, M., Selvi, F. & Hilger, H.H. (2009) Marbleseeds are gromwells – Systematics and evolution of *Lithospermum* and allies (Boraginaceae tribe Lithospermeae) based on molecular and morphological data. *Molecular Phylogenetics and Evolution* **52**, 755–768.

Weigend, M. & Hilger, H.H. (2010) Codonaceae - a newly required name in Boraginales. *Phytotaxa* **10**, 26–30.

Weigend, M. & Hilger, H.H. (2016) Codonaceae. *Families and Genera of Vascular Plants* (eds. K. Kubitzki, J.W. Kadereit & V. Bittrich), vol. 14, pp. 137–141, Springer, Heidelberg.

Weigend, M., Luebert, F., Gottschling, M., Couvreur, T.L., Hilger, H.H. & Miller, J.S. (2014) From capsules to nutlets – phylogenetic relationships in the Boraginales. *Cladistics* **30**, 508–518.

Weigend, M., Luebert, F., Selvi, F., Brokamp, G. & Hilger, H.H. (2013) Multiple origins for Hound's tongues (*Cynoglossum* L.) and Navel seeds (*Omphalodes* Mill.) – The phylogeny of the borage family (Boraginaceae s.str.). *Molecular Phylogenetics and Evolution* **68**, 604–618.

Weigend, M., Selvi, F., Thomas, D.C. & Hilger, H.H. (2016) Boraginaceae. *Families and Genera of Vascular Plants* (eds. K. Kubitzki, J.W. Kadereit & V. Bittrich), vol. 14, pp. 41–102, Springer, Heidelberg.

Wetzstein, H.Y. & Armitage, A. (1983) Inflorescence and floral development in *Pelargonium* x *hortorum*. *Journal of the American Society of Horticultural Science* **108**, 595–600.

Whittall, J.B. & Hodges, S.A. (2007) Pollinator shifts drive increasingly long nectar spurs in columbine flowers. *Nature* **447**, 706–709.

Chapter 2

Gynoecium and fruit development in *Heliotropium* sect. *Heliothamnus* (Heliotropiaceae)

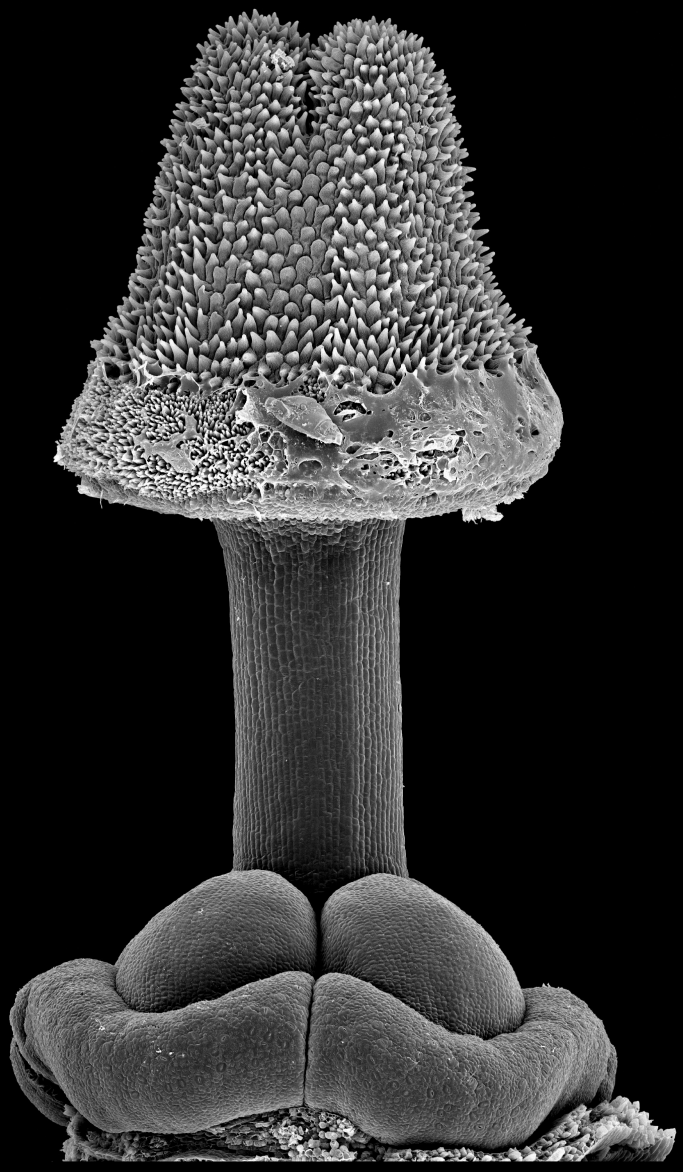

Jeiter J, Staedler YM, Schönenberger J, Weigend M, Luebert F. 2018. Gynoecium and fruit development in *Heliotropium* sect. *Heliothamnus* (Heliotropiaceae). *International Journal of Plant Sciences* 179: 275–286. https://doi.org/10.1086/696219

Int. J. Plant Sci. 179(4):275–286. 2018.

1058-5893/2018/17904-0002$15.00 DOI: 10.1086/696219

GYNOECIUM AND FRUIT DEVELOPMENT IN *HELIOTROPIUM* SECT. *HELIOTHAMNUS* (HELIOTROPIACEAE)

Julius Jeiter,[1,*] Yannick M. Staedler,† Jürg Schönenberger,† Maximilian Weigend,* and Federico Luebert*,‡

*Nees-Institute for Biodiversity of Plants, University of Bonn, Meckenheimer Allee 170, 53115 Bonn, Germany; †Department of Botany and Biodiversity Research, University of Vienna, Rennweg 14, 1030 Vienna, Austria; and ‡Departmento de Silvicultura y Conservacíon de la Naturaleza, Universidad de Chile, 9206 Santiago, Chile

Editor: Gerhard Prenner

Premise of research. Heliotropiaceae (Boraginales) are morphologically readily defined by their peculiar floral morphology, especially their conspicuous stigmatic heads. *Heliotropium* L. is the largest genus of the family, and within this genus, *Heliotropium* sect. *Heliothamnus* I.M. Johnst. is the sister clade to the remaining *Heliotropium* species. Earlier studies have pointed out a series of gynoecium morphological features of *H*. sect. *Heliothamnus* (e.g., a seemingly persisting columella and a gynobasic style) that are not present in the remainder of the genus but are paralleled in the closely related family Boraginaceae *s. str*. However, a detailed, ontogenetic understanding of the gynoecium and fruit morphology of *H*. sect. *Heliothamnus* has not been achieved.

Methodology. Here we describe the development of the gynoecium and fruit of *H*. sect. *Heliothamnus* using SEM, light microscopy, and high-resolution X-ray computed tomography.

Pivotal results. The two-carpellate, syncarpous gynoecium is characterized by four functional subunits: a nectary, an ovary with four mericarpids, a style, and a stigmatic head. All four subunits differentiate simultaneously. At first, the stigmatic head is formed, followed by the style and the gynoecial nectary disc, which is then followed by the onset of the development of mericarpids. After anthesis, the size of the mericarpids increases and their surface sculpturing differentiates. All four mericarpids are laterally attached to each other around the central tissue of the ovary, which disintegrates during fruit development. The ovary is lobed and divided through septa between and within the carpels. After detachment, the contact areas between the mericarpids leave scars, which resemble the cicatrix of the Boraginaceae *s. str*. In contrast to the Boraginaceae *s. str*., the whole gynoecium is dispersed.

Conclusions. Mericarpid development in *Heliotropium* sect. *Heliothamnus* follows a different developmental trajectory than in Boraginaceae *s. str*. Individual nutlets separate in two steps and not simultaneously. A tissue in the center of the ovary is present in immature fruits of *H*. sect. *Heliothamnus*, but it disintegrates during maturation and is absent in mature fruits. It is not structurally equivalent to the persisting columella characterizing the fruit of Boraginaceae *s. str*. The style is not gynobasic but rather distally attached to the mericarpids. The schizocarpic mericarpids in *Heliotropium* sect. *Heliothamnus* are thus not structurally correspondent to the eremocarps of the Boraginaceae *s. str*., as previously suggested.

Keywords: morphology, ontogeny, Boraginaceae, Boraginales, flower.

Introduction

The order Boraginales consists of two major clades, Boraginales I and II, each comprising a basal grade of two small to medium-sized families with capsular fruits (Boraginales I: Codonaceae, Wellstediaceae; Boraginales II: Hydrophyllaceae, Namaceae). The remaining families of both clades possess fruits with four mericarpids (nutlets), which originated independently during the evolution of the order (Luebert et al. 2016). Mericarpids (see glossary) of Boraginales I and II differ in their ontogeny. In Boraginales I, represented by Boraginaceae *s. str*., nutlets are of eremocarpic origin (see glossary). They emerge as four ab initio independent mericarpids, separated by apical and lateral growth from the very earliest stages of gynoecium development onward (Hilger 1984, 2014). Their mericarpids develop—clearly separated from each other—around a central structure, the columella (see glossary). The columella is the base of the style, which thus originates between the mericarpids. The style is therefore gynobasic (see glossary). Both the apical part of the style and columella are persistent, that is, they are still present at fruit maturity. In Boraginales II, represented by Coldeniaceae, Cordiaceae, Ehretiaceae, Heliotropiaceae, and Hoplestigmataceae, if nutlets are present, they are of schizocarpic origin. They remain attached to each other during most of fruit

[1] Author for correspondence; e-mail: jjeiter@uni-bonn.de.

Manuscript received July 2017; revised manuscript received October 2017; electronically published February 1, 2018.

Box 1

Glossary

Cicatrix: abscission scar on the side of the mericarpid (Hilger 2014).

Columella: basal part of a gynobasic style, to which the mericarpids are attached (Hilger 2014).

Eremocarp: usually one-seeded nutlet derived from a syncarpous ovary via ab initio separate development (Hilger 2014; Luebert et al. 2016).

Gynobase: style and basal part of the gynoecium where the mericarpids are attached (columella) and that remains on the mother plant at fruit dispersal (Hilger 2014).

Gynoecial cone: early stage in gynoecium development, where fused carpel primordia form a cone-shaped structure (Hilger 2014).

Mericarpid: dispersal unit of schizocarpic or eremocarpic fruits formed by a part of a carpel (Hilger 2014).

Rhexigenous: holes or cavities in tissue formed through rupturing cells caused by dilatational growth of the surrounding tissue (Wagenitz 2008, p. 276).

Schizogenous: holes or cavities forming in tissue through a dissolving middle lamella (Wagenitz 2008, p. 287).

Stigmatic head: structure formed by the stigma consisting of an upper sterile part and a basal ring of receptive tissue (Diane et al. 2016).

development and separate only at fruit maturity. As a consequence, the style is not gynobasic but apical, and no gynoecial columella is present (Gottschling et al. 2014).

Heliotropiaceae belong to Boraginales II and are the second-largest family in the Boraginales after Boraginaceae *s. str.* They comprise ~450 species in four genera (Diane et al. 2016; Luebert et al. 2016). The genus *Heliotropium* L. makes up two-thirds of the species currently included in the Heliotropiaceae.

Heliotropiaceae differ from other families of Boraginales in the presence of a conical stigmatic head (see glossary), with the receptive tissue located around the base of it (the typical morphology of a *Heliotropium* gynoecium is shown in fig. 1). Both stigmatic head and style vary between species in relative and absolute length (Johnston 1928; Förther 1998). The style is inserted apically on the ovary, the latter being a feature shared by all nutlet-producing families of Boraginales except Boraginaceae *s. str.*, where the style is gynobasic (Luebert et al. 2016).

Heliotropium shows surprising diversity in fruit morphology, ranging from four-seeded drupes to schizocarps separating into either two two-seeded or four single-seeded mericarpids, or sometimes reduced to one single-seeded mericarpid (Hilger 1992). *Heliotropium* was subdivided into 19 sections by Förther (1998), who based his classification on morphological and anatomical evidence. Recent molecular phylogenetic studies (Diane et al. 2002; Hilger and Diane 2003; Luebert et al. 2011) changed our understanding of the relationships within the genus *Heliotropium* and provided the basis for new generic delimitations in Heliotropiaceae (Diane et al. 2016). The largely South American section *Heliothamnus* I.M. Johnst. is a well-supported clade and the sister group to all remaining *Heliotropium* species (Hilger and Diane 2003; Luebert et al. 2011). This clade is well characterized by its leaf (Diane et al. 2003), flower, and fruit morphology (Johnston 1928).

Fruits of *Heliotropium* sect. *Heliothamnus* separate into four mericarpids (nutlets; fig. 1) at fruit maturity, which is also found in other sections of *Heliotropium*. However, in contrast to the other species of *Heliotropium* showing this fruit type, the fruit of *H.* sect. *Heliothamnus* appears to have a central gynoecial columella and each mericarpid a cicatrix (see glossary) similar

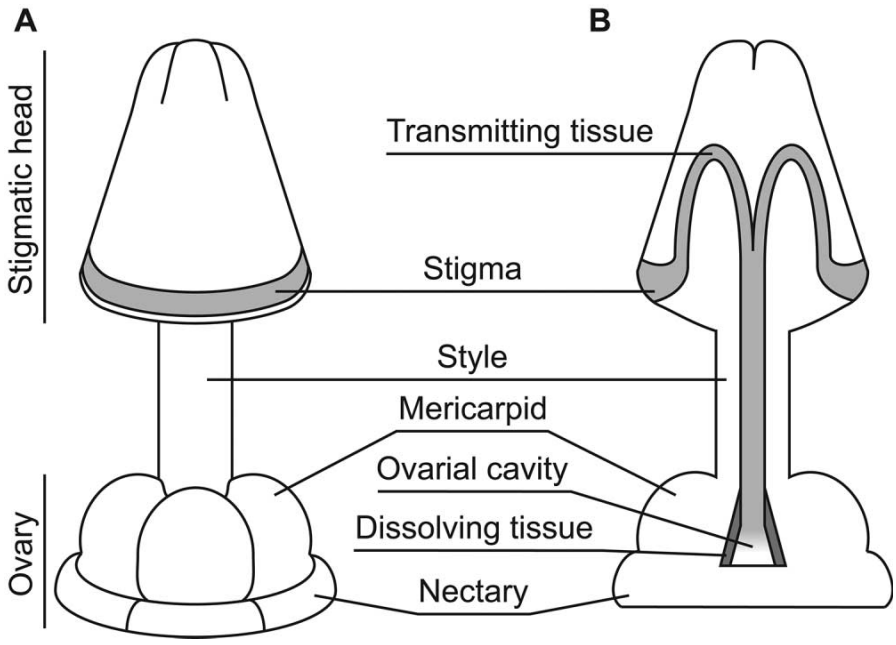

Fig. 1 Schematic drawing and terminology of the anthetic gynoecium of *Heliotropium* sect. *Heliothamnus*. *A*, Gynoecium in lateral view. *B*, Longitudinal section through the gynoecium and two mericarpids.

to those in the fruits of Boraginaceae *s. str.* and, in particular, in the fruits of the boraginaceous tribe Eritrichieae (Hilger 1992). The latter suggests that the fruits of *Heliotropium* sect. *Heliothamnus* and Boraginaceae *s. str.* may be structurally correspondent (sensu Scotland 2011). Since Boraginaceae *s. str.* and Heliotropiaceae belong to separate, nonsister clades of Boraginales, the presence of a persisting gynoecial columella in both taxa (so far only documented for Boraginaceae *s. str.*) would be the result of convergence. This is at odds with current explanations about the origin of fruit characters in Boraginales that a persisting columella is present only in Boraginaceae *s. str.* (Luebert et al. 2016). Given our previous knowledge about the phylogenetic relationships of Boraginales (see above), homology as understood by Stevens (1984), de Pinna (1991), and Scotland (2011) can be rejected a priori.

Gynoecium and fruit ontogeny of Boraginaceae *s. str.* is relatively well known (Payer 1857; Hilger 1984, 2014; Hofmann 1994). Conversely, only few studies have addressed the gynoecium development in Heliotropiaceae (Hilger 1987, 1989, 1992), and we are not aware of any such study with focus on *Heliotropium* sect. *Heliothamnus*. Furthermore, the sequence of developmental stages in the ontogeny of the gynoecium in general has so far been poorly documented in *Heliotropium*. The latter is essential to understand whether a persisting gynoecial columella is present and, if so, whether it is structurally correspondent to that of Boraginaceae *s. str.*

This study focuses on two questions: (1) How do the gynoecium and fruit develop in *Heliotropium* sect. *Heliothamnus*? (2) What are the similarities and differences between the fruits of this section compared to other sections of *Heliotropium* and, especially, compared to the fruits found in various taxa of Boraginaceae *s. str.*?

Material and Methods

Fresh flowers for comparative developmental and morphological studies were either collected from plants in cultivation or from the wild. In addition, mature fruits were removed from air-dried herbarium specimens (table 1).

Plants were fixed in formaldehyde-acetic acid-ethanol (FAA; formaldehyde 2%, acetic acid 2%, ethanol 70%) for at least 1 wk and afterward stored either in FAA or ethanol (70%).

SEM

The material was transferred into ethanol (70%) and dissected under a stereo microscope. Afterward, it was transferred back into FAA for at least 1 h, then dehydrated using formaldehyde dimethyl acetal (FDA; 99.0%, Sigmar-Aldrich Chemie, Munich, Germany), and finally stored in acetone (modified from Gerstberger and Leins 1978). The dehydrated material was dried in a critical-point dryer (CPD 020, Balzers Union, Liechtenstein) following standard protocol. Dried specimens were mounted on aluminium stubs using conductive carbon cement (Leit-C, PLANO, Wetzlar, Germany). Mounted specimens were further dissected and subsequently sputter-coated with palladium in a sputter-coater (SCD 040, Balzers Union, Liechtenstein) for 1.5 to up to 3 min (depending on the complexity of the specimen) at ~30 mA. Finally, images were obtained using a Stereoscan 200 electron microscope (Cambridge, England) at 10 or 15 kV. Contrast and brightness of the images were partially improved using standard image-editing software.

Light Microscopy

The samples for light microscopy were prepared following standard protocol. Sections were made using a rotary microtome (Rotationsmikrotom 1515, Leitz, Wetzlar, Germany). Afterward, the sections were stained and documented using a light microscope (Axio Scope.A1, Carl Zeiss Microscopy, Jena, Germany) with a digital camera (AxioCam ERc5s, Carl Zeiss Microscopy, Jena, Germany). Contrast and brightness were improved and individual images were combined using standard image-editing software. The detailed procedure is described elsewhere (Jeiter et al. 2016).

High-Resolution X-Ray Computed Tomography

For high-resolution X-ray computed tomography (HRXCT), the FAA-fixed samples were transferred into an infiltration me-

Table 1

Studied Species and Vouchers

Species	Material[a]	Voucher	Herbarium
Heliotropium arborescens L. 'alba'	SEM (development), µCT	xx-0-BONN-24925	BONN
H. corymbosum Ruiz & Pav.	SEM (mature fruit)	Weigend et al. 8288	BONN
H. corymbosum Ruiz & Pav.	SEM (development), µCT	PE-0-BONN-33458	BONN
H. corymbosum Ruiz & Pav.	µCT	PE-0-BONN-33455	BONN
H. corymbosum Ruiz & Pav.	SEM (mature fruit)	PE-0-BONN-36610	BONN
H. pamparomasense Luebert & Weigend	SEM (flower and fruit)	Weigend & Skrabal 5890	BSB(B)
H. pamparomasense Luebert & Weigend	LM	Henning et al. 27	BSB(B)
H. rufipilum (Benth.) I. M. Johnst.	SEM (flower and fruit)	Förther et al. 10252	BSB(B)
H. rufipilum (Benth.) I. M. Johnst.	SEM (mature fruit)	Brokamp & Mittelbach 2011–01	BSB(B)
H. rufipilum (Benth.) I. M. Johnst.	SEM (mature fruit)	Brokamp & Mittelbach 2011–08	BSB(B)

[a] Complete development of the gynoecium using formaldehyde-acetic acid-ethanol (FAA)–fixed material using SEM (development), mature, air-dried fruits removed from herbarium specimens observed with the SEM (mature fruit), FAA-fixed, anthetic flowers and (almost) mature fruits using SEM (flower and fruit), FAA-fixed and phosphotungstic acid–infiltrated flowers and fruits for high-resolution X-ray computed tomography (µCT), FAA-fixed flowers and fruits dehydrated and Paraplast embedded for light microscopy (LM).

Table 2

High-Resolution X-Ray Computed Tomography Scan Settings

Species, sample	Acceleration voltage (kV)	Source current (μA)	Exposure time (s)	Pictures per sample	Camera binning	Optical magnification (×)	Pixel size (μm)
Heliotropium arborescens:							
Flower	30	200	20	728	1	10	1.018
Fruit	35	200	20	728	1	10	1.059
H. corymbosum:							
Flower	35	200	3	728	2	10	1.824
Fruit	30	200	6	728	1	4	2.361

dium (1% phosphotungstic acid [PTA] in 70% ethanol) and infiltrated for at least 2 wk to increase their contrast (Staedler et al. 2013). The contrasting solution was exchanged five times. The samples were dehydrated using increasing concentrations of ethanol plus 1% PTA and, finally, acetone plus 1% PTA. The dehydrated samples were critical-point dried (Autosamdri–3 15, Series A, Rockville, MD) and individually mounted on aluminium poles with epoxy glue (UHU PLUS Sofortfest, UHU, Bühl, Germany). The scans were performed on a MicroXCT-200 imaging system (Xradia, Pleasanton, CA) with a L9421-02 90kV Microfocus X-ray source (Hamamatsu Photonics, Iwata City, Japan). The HRXCT scan settings are given in table 2. A 3-D reconstruction from the scanning data was performed using the XMReconstructor 8.1.6599 (XRadia, Pleasanton, CA). Scans were visualized using the AMIRA 5.4.1 (FEI Visualization Sciences, Bordeaux, France).

Results

Preanthetic to Anthetic Gynoecium Development

The results of this section are divided into several paragraphs, each of which covers the development of a particular part of the gynoecium. The corresponding SEM images in figures 2 and 3 are arranged by species to clearly illustrate the complete development of the gynoecium.

Stigmatic head. The ontogeny of the gynoecium was studied in *Heliotropium arborescens* and *H. corymbosum* (table 1) and is similar in both species. During early developmental stages, the abaxial carpel is slightly larger than the adaxial one. It starts with the development of the abaxial carpel primordium, which is subsequently followed by the adaxial one. The difference in initiation time is noticeable in a minor size difference between the two young carpels and the apical parts of the stigmatic head in older developmental stages. Both undifferentiated and fused carpel primordia form the gynoecial cone (see glossary; figs. 2*A*, 2*B*, 3*A*). The apical part of the cone develops into a ring (fig. 3*B*). Already in early ontogenetic stages, the ring develops into a stigmatic head (figs. 2*C*, 3*C*). The constriction below the ring forms the style (figs. 2*C*, 3*C*). The basal part of the stigmatic head covers most of the short, young style. The stigmatic head elongates throughout the development of the flower. It appears to elongate through continuous apical cell-division and growth, followed by an increase of cell volume toward anthesis (figs. 2*D*–2*F*, 3*D*–3*F*, 4*A*, 4*F*). The papillate epidermis of the nonreceptive part of the stigmatic head (see fig. 1) forms at intermediate developmental stages (figs. 2*E*, 3*E*). In contrast to the nonreceptive epidermis cells, which appear at an early stage and are relatively large and pointed, the receptive stigmatic cells are formed later, are smaller in size, and have a rounded tip (not shown). The stigmatic surface is apparently covered with a mucilage-like substance already during preanthetic stages (figs. 2*G*–2*I*, 3*G*–3*I*, 4*A*, 4*F*).

Nectary. After formation of a gynoecial cone (figs. 2*A*, 2*B*, 3*A*), the radial growth of the ovary exceeds the apical growth. The ovary appears flat, with only the young stigmatic head emerging above it (fig. 3*B*). After formation of the stigmatic head, the nectary disc emerges from the base of the ovary (figs. 2*D*, 3*C*, 3*D*). At the onset of nectary development, all four mericarpids are already discernible as individual bulges. In both species, the nectary forms a ring around the base of the ovary, which is regularly divided into four equal parts. The nectary disc is homogeneously covered with nectarostomata in both species (not shown). However, nectary development differs slightly between the two species studied: in *H. arborescens*, the margin of the ovary develops into a massive nectary ringlike structure surrounding the base of the ovary (figs. 2*D*, 2*I*, 4*A*). It is clearly divided into two parts corresponding to the sectors of the two carpels already during early developmental stages, but the division between the two mericarpids of each carpel forms only during intermediate stages of gynoecium development, along with mericarpid formation. In the anthetic flower of *H. corymbosum*, the nectary is equally massive as in *H. arborescens* but less distinctly segregated from the mericarpids (figs. 3*D*–3*I*, 4*F*). In *H. corymbosum*, the development of the nectary appears to be slightly delayed and less pronounced compared to *H. arborescens* (fig. 3*D*–3*I*).

Ovary. During early developmental stages, a shallow depression on the ovary surface indicates the fusion zone between the two carpels (figs. 2*D*, 3*C*). Subsequently, the four mericarpids are formed, which first appear as low mounds on the ovary (figs. 2*D*, 4*D*, 4*E*). They enlarge, become increasingly convex, finally filling all the spaces between the base of the elongating style and the developing nectary disc. Even in the youngest stages, they are clearly separated from each other but remain connected through the central tissue of the ovary. The central tissue of the ovary is formed by septal tissue and contains the ovarial cavity, which is partially filled with transmitting tissue (fig. 4*A*, 4*B*, 4*F*, 4*G*). The growth of the central tissue of the ovary is exceeded by that of the nutlets, so that it is finally almost completely enclosed and hidden (figs. 2*F*–2*I*, 3*E*–3*I*). The resulting septa between and within the carpels are short, leading to a lobed ovary. The septa between the carpels are relatively longer than the septa

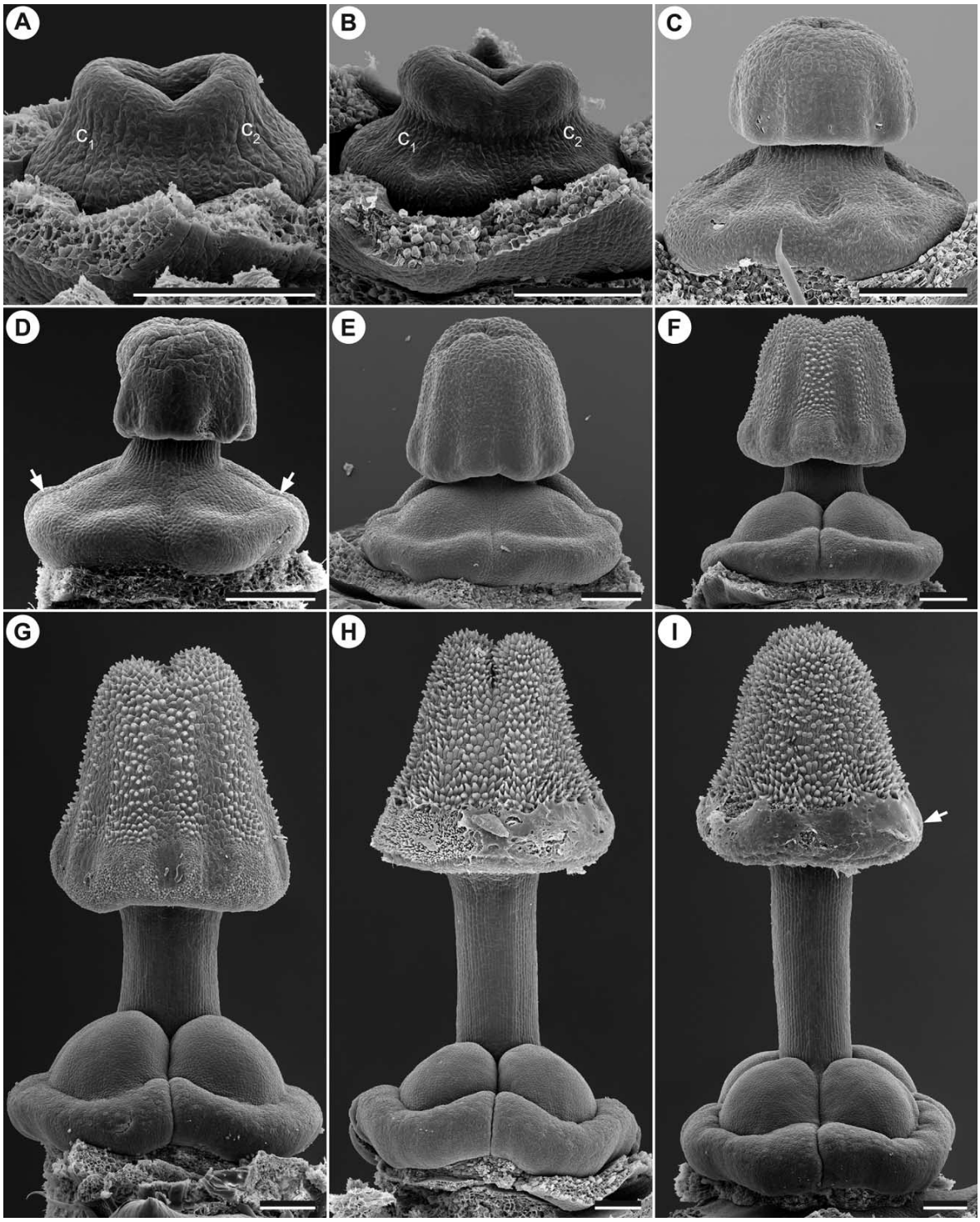

Fig. 2 Gynoecium development in *Heliotropium arborescens*. *A*, Gynoecial cone; lateral view. *B*, Gynoecial cone with onset of stigmatic head formation; lateral view. *C*, Young stigmatic head on a short style and flattened ovary; adaxial view. *D*, Onset of nectary and mericarpid development, with intercarpellary cleft visible (arrows); adaxial view. *E*, Stage with elongated stigmatic head, developing nectary, and young mericarpids; adaxial view. *F*, Slightly older stage than *E*; abaxial view. *G, H*, Style elongation and formation of papillae on stigmatic head, with mucilage forming on the receptive part of stigmatic head and mericarpids clearly divided; both lateral views. *I*, Gynoecium at anthesis, with arrow pointing at receptive tissue of the stigmatic head; adaxial view. c = carpel, c_1 = abaxial carpel, c_2 = adaxial carpel. Scale bars = 100 μm.

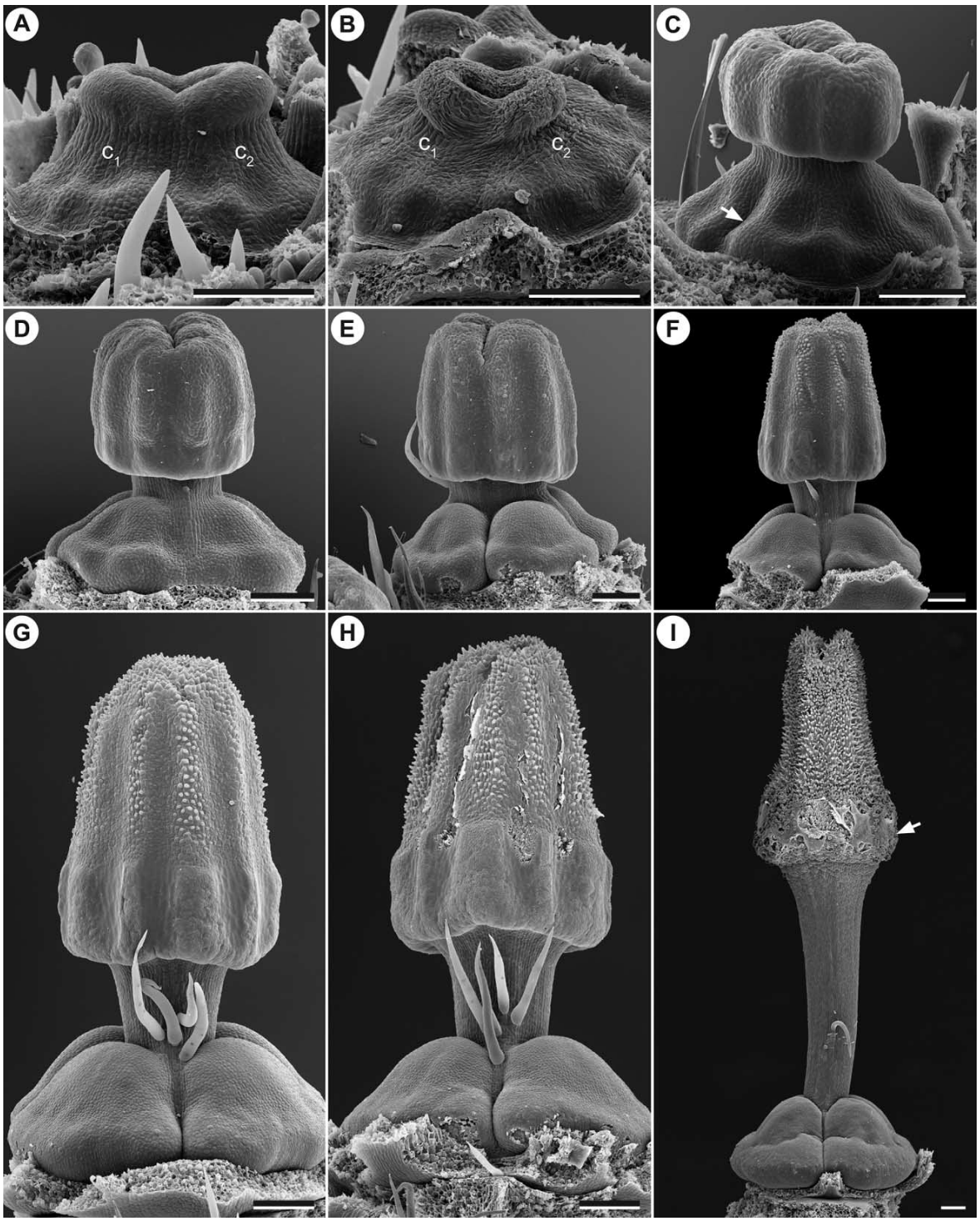

Fig. 3 Gynoecium development in *Heliotropium corymbosum*. *A*, Gynoecial cone; lateral view. *B*, Flattened gynoecial cone with onset of stigmatic head formation; lateral view. *C*, Young stigmatic head on a short style, with intercarpellary cleft visible (arrow); adaxial view. *D*, Onset of nectary and mericarpid development; adaxial view. *E*, Stage with elongated stigmatic head, developing nectary and young mericarpids; lateral view. *F*, Slightly older stage than *E*, with cleft between mericarpids beginning to form; abaxial view. *G*, *H*, Style and stigmatic head elongation and formation of papillae on the distal, sterile part of the stigmatic head, with mucilage forming on receptive part of stigmatic head and mericarpids clearly divided; both adaxial views. *I*, Gynoecium at anthesis. Arrow points to receptive tissue of the stigmatic head; adaxial view. c = carpel, c_1 = abaxial carpel, c_2 = adaxial carpel. Scale bars = 100 μm.

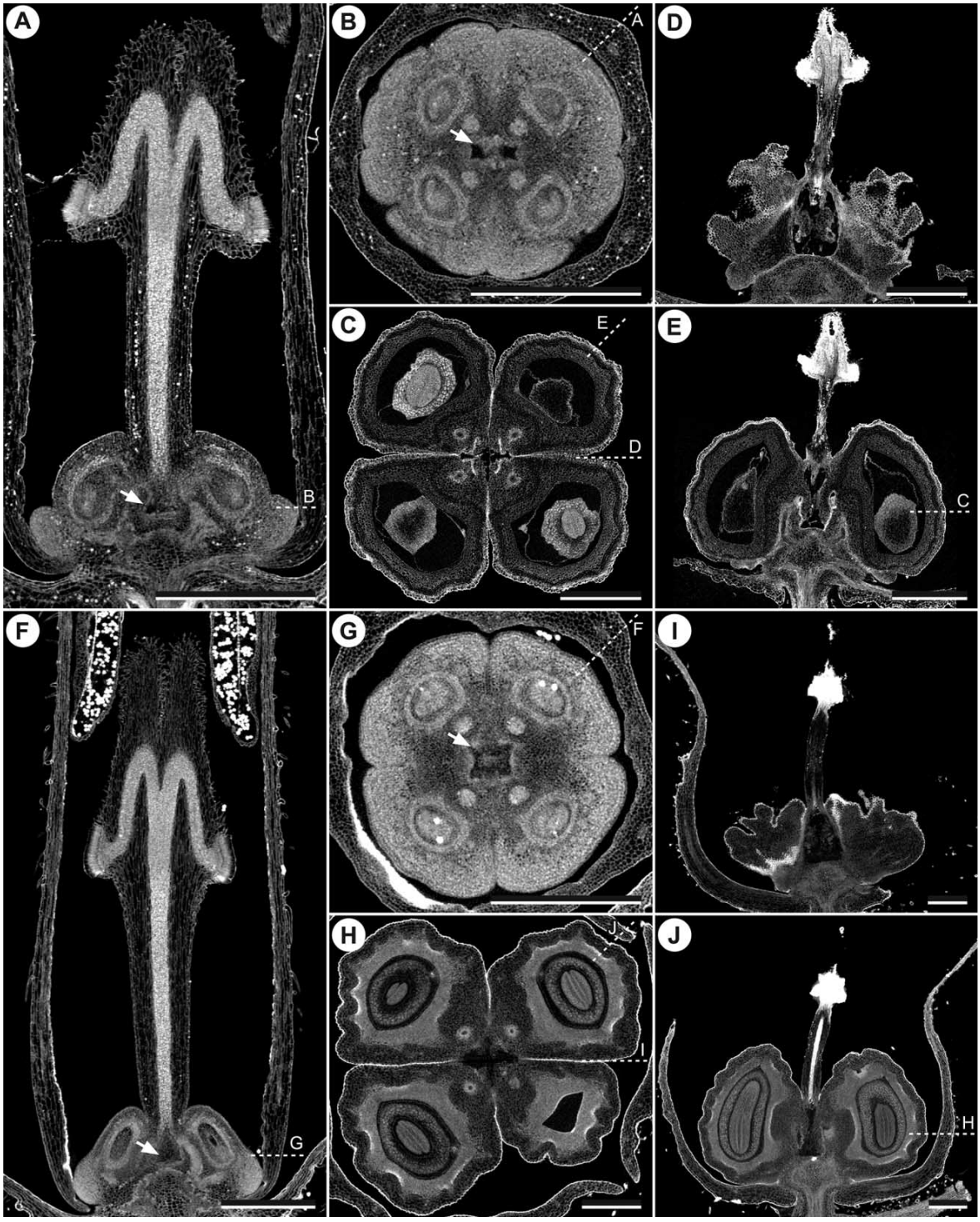

Fig. 4 Sections reconstructed from high-resolution X-ray computed tomography (HRXCT) scans of anthetic flowers and fruits of *Heliotropium arborescens* and *H. corymbosum*. *A–E*, *Heliotropium arborescens*; dashed white lines with letters indicate the corresponding reconstructed sections in other panels of this figure. *A*, *B*, Anthetic flower. *A*, Longitudinal section; arrow points to the ovarial cavity. *B*, Cross section through the ovary at the level of the nectary; arrow points to the ovarial cavity. *C–E*, Fruit. *C*, Median cross section through the fruit. *D*, Longitudinal section through the fruit in between the carpels. *E*, Longitudinal section through the fruit through two mericarpids. *F–J*, *Heliotropium corymbosum*; dashed white lines with letters indicate the corresponding reconstructed sections in other figures. *F*, *G*, Anthetic flower. *F*, Longitudinal section; arrow indicates the ovarial cavity. *G*, Cross section through the ovary at the level of the nectary. Arrow points to the ovarial cavity. *H–J*, Fruit. *H*, Median cross section through the fruit. *I*, Longitudinal section through the fruit in between the carpels. *J*, Longitudinal section through the fruit through two mericarpids. Scale bars = 500 μm.

within the carpels (figs. 4*C*, 4*H*, 5*A*, 5*B*, 6). The base of the style is hidden between the elongating mericarpid tips.

Fruit Development from Anthesis to Mature Fruit

Development of the mericarpids. Postanthetic fruits were studied in *H. arborescens*, *H. corymbosum*, *H. pamparomasense*, and *H. rufipilum* (table 1). After anthesis, the mericarpids continue to grow. The basal parts enlarge and extend beyond the nectary disc (figs. 4*E*, 5*A*, 5*D*, 5*G*). The apical parts surround a portion of the style. The upper part of the style and the stigmatic head shrink and get easily detached. The part of the style attached to the developing mericarpids remains connected to the ventral parts of the mericarpids (fig. 5*A*, 5*B*, 5*D*, 5*E*). The cells of this lower part do not collapse as in the upper part of the style (fig. 5*A*, 5*B*, 5*D*). Simultaneously to the growth of the mericarpids, their surface structure diversifies. It remains smooth but irregularly reticulate in *H. arborescens* and *H. corymbosum* (figs. 5*C*, 5*F*, 7*A*), densely covered with stalked glandular trichomes in *H. pamparomasense* and a combination of pro-

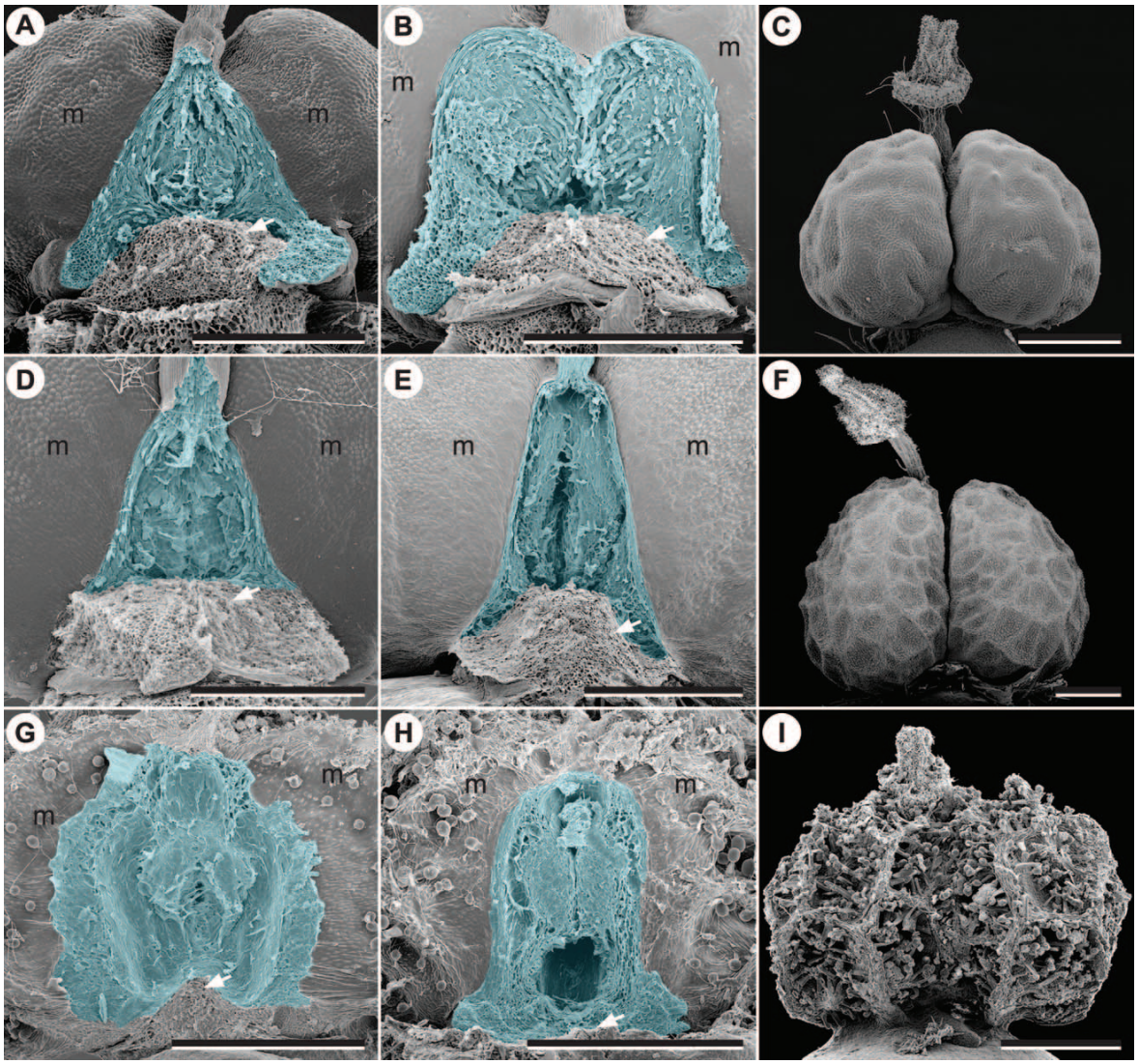

Fig. 5 Mature fruit and disintegration of the central tissue of the ovary. *A–C*, *Heliotropium arborescens*. *A*, Advanced stage of disintegration of the central tissue of the ovary. *B*, Central cavity at fruit maturity. *C*, Mature fruit. *D–E*, *Heliotropium corymbosum*. *D*, Advanced stage of disintegration of the central tissue of the ovary. *E*, Central cavity at fruit maturity. *F*, Mature fruit. *G–I*, *Heliotropium rufipilum*. *G*, Advanced stage of disintegration of the central tissue of the ovary. *H*, Central cavity at fruit maturity. *I*, Mature fruit. *A, B, D, E, G, H*, Two mericarpids originating from one carpel have been removed; the area of the central tissue of the ovary/cavity and attachment scars between the mericarpids are in turquoise. m = mericarpids. Arrows point to the scars left from detachment from the receptacle. Scale bars = 500 μm.

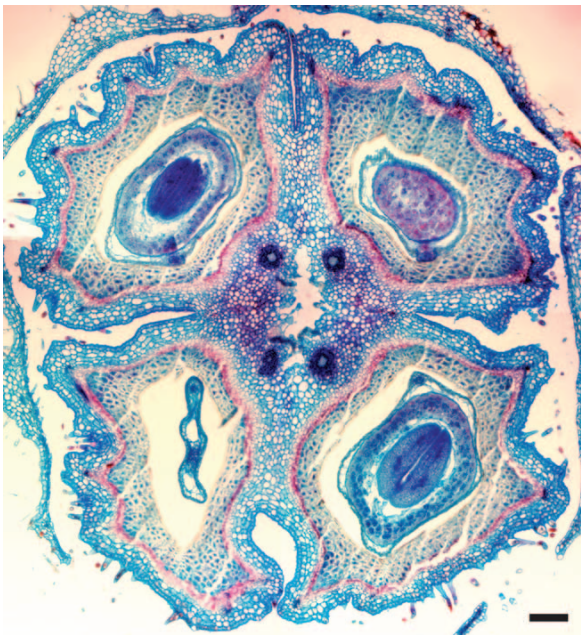

Fig. 6 Microtome cross section through a young fruit of *Heliotropium pamparomasense*. Scale bar = 100 μm.

nounced reticulation and sessile or stalked glandular trichomes in *H. rufipilum* (figs. 5*I*, 7*B*). Furthermore, there are shape differences in the mature fruits and mericarpids and in the length of the common septa between and within the carpels. In *H. arborescens* and *H. corymbosum*, the ovary is lobed, that is, the part where the mericarpids are joined is short (figs. 4*C*, 4*H*, 6, 7*A*). In *H. pamparomasense* and *H. rufipilum*, the overall shape of the fruit is round and the common septa between the mericarpids are longer than those of the aforementioned species, which results in an overall triangular shape with a rounded outer part (fig. 7*B*).

Central tissue and cavity formation. As described above, the mericarpids develop around the central tissue of the ovary, which tapers into the style. It consists of simple parenchymatic cells and encloses the ovarial cavity, which at anthesis is partially filled with transmitting tissue (figs. 4*A*, 4*B*, 4*F*, 4*G*, 6). The central tissue of the ovary is the product of the fused septa of the carpels. It is visible in younger stages of development and becomes hidden by the enlarging mericarpids. Additionally, the style becomes hidden by the tips of the enlarging mericarpids.

During fruit maturation, the rounded and unmodified parenchymatic cells are separated from each other or are ruptured through elongation and dilatational growth of the mericarpids (figs. 5*A*, 5*D*, 5*G*, 6). The same happens to the massive transmitting tissue. In mature fruits, the cavity in the center between the mericarpids enlarges through disintegration of the transmitting tissue and the surrounding parenchyma (figs. 5*B*, 5*E*, 5*H*, 6). The resulting cavity is irregular and cross- or rhombus-shaped in cross section (figs. 4*C*, 4*H*, 6). The largest expansion of the forming cavity takes place between the carpels (fig. 4*D*, 4*I*). The style originates from the morphological apex of the syncarpous ovary, in between the apical parts of the mericarpids (figs. 4*D*, 4*E*, 4*I*, 4*J*, 5*A*–5*I*). It is attached to the mericarpids and is not lost as the central tissue of the ovary dissolves and ruptures in between the mericarpids below. The attachment is rather fragile. As a result of the fragile connection between style and mericarpids, the style detaches easily.

Dispersed mericarpids show an angled scar on their ventral side (fig. 7*A*, 7*B*). The upper part corresponds to the position of the dissolved central tissue of the ovary. The lower part is the attachment scar. It finds its counterpart on the receptacle of the flower (fig. 5*A*, 5*B*, 5*D*, 5*E*, 5*G*, 5*H*).

The development of different gynoecial parts described above takes place simultaneously. Figure 8 summarizes the relative timing of the major events in gynoecium and fruit ontogeny of *Heliotropium* sect. *Heliothamnus*.

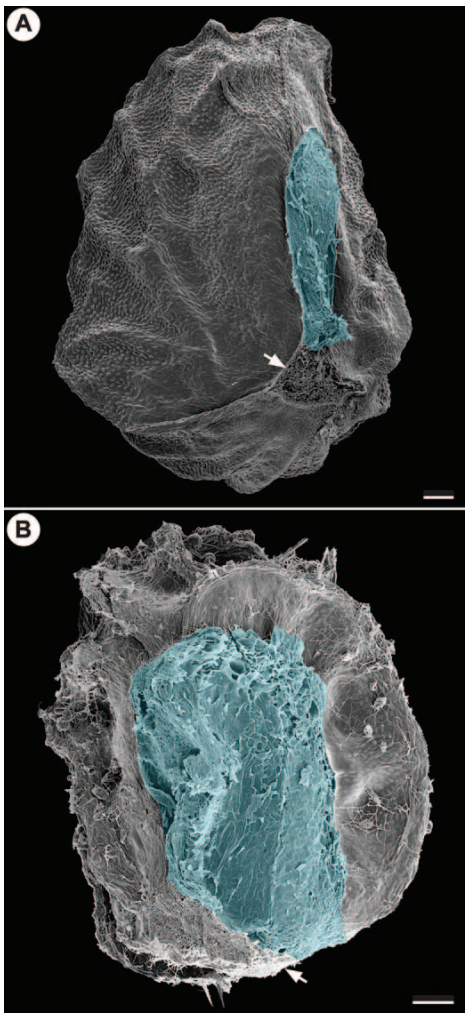

Fig. 7 Mature nutlets of *Heliotropium corymbosum* and *H. rufipilum*. *A*, Individual mericarpid of *H. corymbosum*, with the attachment scar to the receptacle (arrow) and cicatrix-like structure above (turquoise). *B*, Individual mericarpid of *H. rufipilum*, with the attachment scar to the receptacle (arrow) and cicatrix-like structure above (turquoise). The background of the images has been removed. Scale bars = 100 μm.

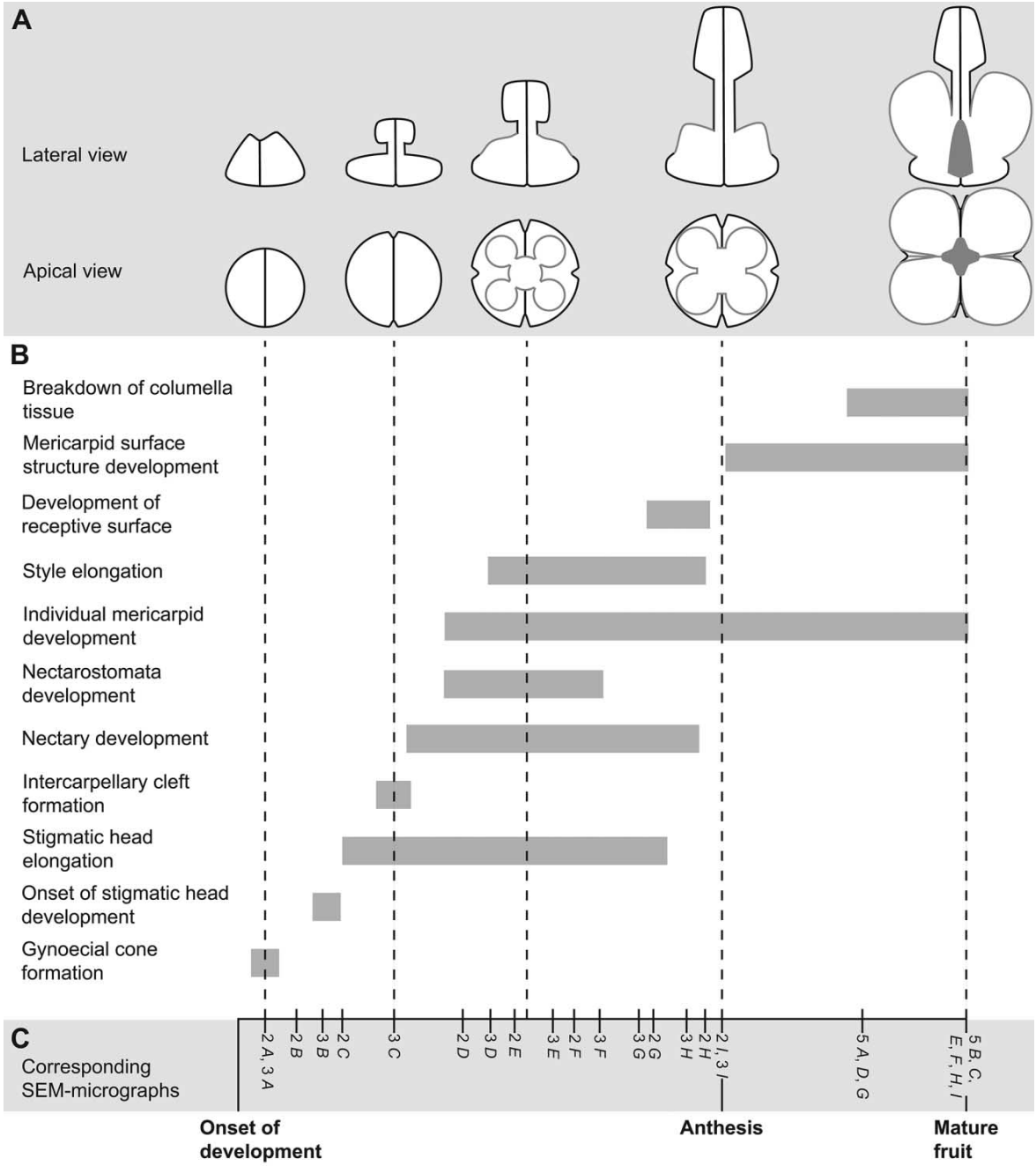

Fig. 8 Summary of gynoecium and fruit development in *Heliotropium* sect. *Heliothamnus*. Schematic representations of five stages of the gynoecium development (*A*), illustrating the chronology of the development (*B*) and linking to the corresponding SEM micrographs in figures 2, 3, and 5 (*C*). *A*, Illustration of five steps of gynoecium development in lateral and apical view. Relative sizes are not according to actual sizes. The black central lines indicate the individual carpels. Nutlet outlines and columella are in dark gray. *B*, Chronology of general gynoecium development. Gray bars indicate an approximation of the relative time a certain process takes. Vertical dashed lines indicate where to find stages corresponding to the schematic representations of *A*. The chronology of the development spans between onset of development and the mature fruit, with anthesis as a fixed point in development. Duration of development is relative, not absolute.

Discussion

The development of the gynoecium and fruit in *Heliotropium* sect. *Heliothamnus* varies only weakly between the different species studied. Variations mainly occur in the relation between the length of the stigmatic head and the style and the relative size of the gynoecial nectary and the mericarpids. Both sets of characters might be related to ecological factors (e.g., pollination) and seem to be correlated with flower size. Especially the relation between stigmatic head and style has been found to be taxonomically informative (Johnston 1928; Förther 1998; Luebert et al. 2010; Luebert and Weigend 2012).

The gynoecium and fruit development in the species of *Heliotropium* sect. *Heliothamnus* studied here (fig. 8) is similar to the development observed in other *Heliotropium* species (Hilger 1987, 1989, 1992). The presence of a structure similar to a cicatrix on the ventral side of the nutlets indicated the presence of a persisting columella (Hilger 1992). We found the cicatrix-like structure on mature nutlets (fig. 7) but did not find any persisting columella. The central tissue of the ovary is in the same position as the persisting columella of the Boraginaceae *s. str.* but disintegrates during development. The remaining scars in *Heliotropium* sect. *Heliothamnus* reflect the common septa. They resemble the cicatrix present in Boraginaceae *s. str.* However, the cicatrix in Boraginaceae *s. str.* reflect the contact surface between mericarpids and persisting columella. The attachment scar in *Heliotropium* sect. *Heliothamnus* is located at the base of the mericarpids, where they detach from the receptacle. The formation of cavities in the median portions of the ventral sides of the mericarpids during fruit maturing is a common phenomenon in several different *Heliotropium* species (Hilger 1987, 1989, 1992). However, the rhexigenous and schizogenous (see glossary) disintegration of a specific tissue has so far not been described.

We also confirm that the style in *H.* sect. *Heliothamnus* is inserted on the ventral side of the individual mericarpids and does not form a persisting columella as in Boraginaceae *s. str.* (Weigend et al. 2016). The point of insertion of the style in *H.* sect. *Heliothamnus* is overtopped by the growth of the distal portions of the mericarpids, but the connection to the ventral side of the individual mericarpids is maintained. The tendency toward bulged ovaries (Endress 2011) and apical septa (Hartl 1962) has been described for several groups in the angiosperms (Endress 2011). The bulging of the ovary in *H.* sect. *Heliothamnus* is minor compared to the bulging of the ovary in Boraginaceae *s. str.* but is the result of the same evolutionary trend. While the apical position of the style is maintained in *H.* sect. *Heliothamnus*, in Boraginaceae *s. str.*, the apex of the ovary touches its base, which represents the extreme of a bulged ovary (Endress 2011). Further studies on the ontogeny and internal structure of gynoecium and fruit of other boraginalean species are necessary for a clearer understanding of their fruit evolution.

The formation of nutlets was used as a criterion to include *Heliotropium* into Boraginaceae (classification history summarized in Luebert et al. 2016). Phylogenetic studies using molecular markers show that the evolution of fruits consisting of four mericarpids occurred at least twice in the Boraginales (Weigend et al. 2014). Although superficially similar, the nutlets of the Boraginaceae *s. str.* emerge as four separate mericarpids, which are distinct from the very earliest developmental stage (eremocarps; Hilger 2014; Weigend et al. 2016), while in the Heliotropiaceae, they are of schizocarpic origin (Diane et al. 2016). Our study of *H.* sect. *Heliothamnus* demonstrates that the mericarpid formation in Boraginaceae and *Heliotropium* differs in both process and result, contradicting Hilger's (1992) suggestion. The formation of four nutlets is homoplastic (convergent), and the mode of formation is different between both families. This indicates that the fruit types of both families are not fully structurally correspondent.

Acknowledgments

We thank S. Langecker for helping with sample preparation, the Bonn University Botanic Gardens for providing the fresh material used in this study, and T. Joßberger for vouchering the collections. We are also grateful to S. Pamperl for help with the HRXCT scanning and data analysis and to S. Sontag for help with the sample preparation for the HRXCT. We are grateful for the valuable comments made by two anonymous reviewers. J. Jeiter receives a scholarship for his doctoral thesis from the Studienstiftung des deutschen Volkes.

Literature Cited

Diane N, H Förther, HH Hilger 2002 A systematic analysis of *Heliotropium*, *Tournefortia*, and allied taxa of the Heliotropiaceae (Boraginales) based on ITS1 sequences and morphological data. Am J Bot 89:287–295.

Diane N, HH Hilger, H Förther, M Weigend, F Luebert 2016 Heliotropiaceae. Pages 203–211 *in* JW Kadereit, V Bittrich, eds. Families and genera of vascular plants. Vol. 14. Springer, Heidelberg.

Diane N, C Jacob, HH Hilger 2003 Leaf anatomy and foliar trichomes in Heliotropiaceae and their systematic relevance. Flora 198:468–485.

Endress PK 2011 Evolutionary diversification of the flowers in angiosperms. Am J Bot 98:370–396.

Förther H 1998 Die infragenerische Gliederung der Gattung *Heliotropium* L. und ihre Stellung innerhalb der subfam. Heliotropioideae (Schrad.) Arn. (Boraginaceae). Sendtnera 5:35–241.

Gerstberger P, P Leins 1978 Rasterelektronenmikroskopische Untersuchungen an Blütenknospen von *Physalis philadelphica* (Solanaceae)—Anwendung einer neuen Präparationsmethode. Ber Deutsch Bot Ges 91:381–387.

Gottschling M, S Nagelmüller, HH Hilger 2014 Generative ontogeny in *Tiquilia* (Ehretiaceae: Boraginales) and phylogenetic implications. Biol J Linn Soc 112:520–534.

Hartl D 1962 Die morphologische Natur und die Verbreitung des Apikalseptums. Analyse einer bisher unbekannten Gestaltungsmöglichkeit des Gynoeceums. Beitr Biol Pflanzen 37:241–330.

Hilger HH 1984 Wachstum und Ausbildungsformen des Gynoeceums von *Rochelia* (Boraginaceae). Plant Syst Evol 146:123–139.

——— 1987 Fruchtbiologische Untersuchungen an Heliotropioideae (Boraginaceae). I. Die Ontogenie der monospermen Früchte von *Heliotropium supinum* L. Flora 179:291–303.

——— 1989 Flower and fruit development in the Macaronesian endemic *Ceballosia fruticosa* (syn. *Messerschmidia fruticosa*, Boraginaceae, Heliotropioideae). Plant Syst Evol 166:119–129.

——— 1992 Morphology of *Heliotropium* (Boraginaceae) dispersal units. Bot Acta 105:387–393.

——— 2014 Ontogeny, morphology, and systematic significance of glochidiate and winged fruits of Cynoglosseae and Eritrichieae (Boraginaceae). Plant Divers Evol 131:167–214.

Hilger HH, N Diane 2003 A systematic analysis of Heliotropiaceae (Boraginales) based on trnL and ITS1 sequence data. Bot Jahrb Syst Pflanzengesch Pflanzengeogr 125:19–51.

Hofmann M 1994 Untersuchungen zur Gynoecealentwicklung in der Tribus Eritrichieae (Boraginaceae-Boraginoideae). PhD thesis. Freie Universität Berlin, Berlin.

Jeiter J, F Danisch, HH Hilger 2016 Polymery and nectary chambers in *Codon* (Codonaceae)—flower and fruit development in a small, capsule-bearing family of Boraginales. Flora 220:94–102.

Johnston IM 1928 Studies in the Boraginaceae VII.1. The South American species of *Heliotropium*. Contrib Gray Herb Harv Univ 81:3–73.

Luebert F, G Brokamp, J Wen, M Weigend, HH Hilger 2011 Phylogenetic relationships and morphological diversity in Neotropical *Heliotropium* (Heliotropiaceae). Taxon 60:663–680.

Luebert F, L Cecchi, MW Frohlich, M Gottschling, CM Guilliams, KE Hasenstab-Lehman, HH Hilger, et al. 2016 Familial classification of the Boraginales. Taxon 65:502–522.

Luebert F, M Weigend 2012 Three new species of *Heliotropium* sect. *Heliothamnus* (Heliotropiaceae) from Peru. Phytotaxa 49:35–44.

Luebert F, M Weigend, HH Hilger 2010 Epitypification of *Heliotropium arborescens* L. (Heliotropiaceae). Taxon 59:1263–1266.

Payer J-B 1857 Traité d'organogénie comparée de la fleur. V. Masson, Paris.

de Pinna MGG 1991 Concepts and tests of homology in the cladistic paradigm. Cladistics 7:367–394.

Scotland RW 2011 What is parallelism? Evol Dev 13:214–227.

Staedler YM, D Masson, J Schönenberger 2013 Plant tissues in 3D via X-ray tomography: simple contrasting methods allow high resolution imaging. PLoS ONE 8:e75295.

Stevens PF 1984 Homology and phylogeny: morphology and systematics. Syst Bot 9:395–409.

Wagenitz G 2008 Wörterbuch der Botanik: Morphologie, Anatomie, Taxonomie, Evolution. 2nd ed. Nikol, Hamburg.

Weigend M, F Luebert, M Gottschling, TLP Couvreur, HH Hilger, JS Miller 2014 From capsules to nutlets—phylogenetic relationships in the Boraginales. Cladistics 30:508–518.

Weigend M, F Selvi, DC Thomas, HH Hilger 2016 Boraginaceae. Pages 41–102 *in* JW Kadereit, V Bittrich, eds. Families and genera of vascular plants. Vol. 14. Springer, Heidelberg.

Chapter 3

Polymery and nectary chambers in *Codon* (Codonaceae) – flower and fruit development in a small, capsule-bearing family of Boraginales

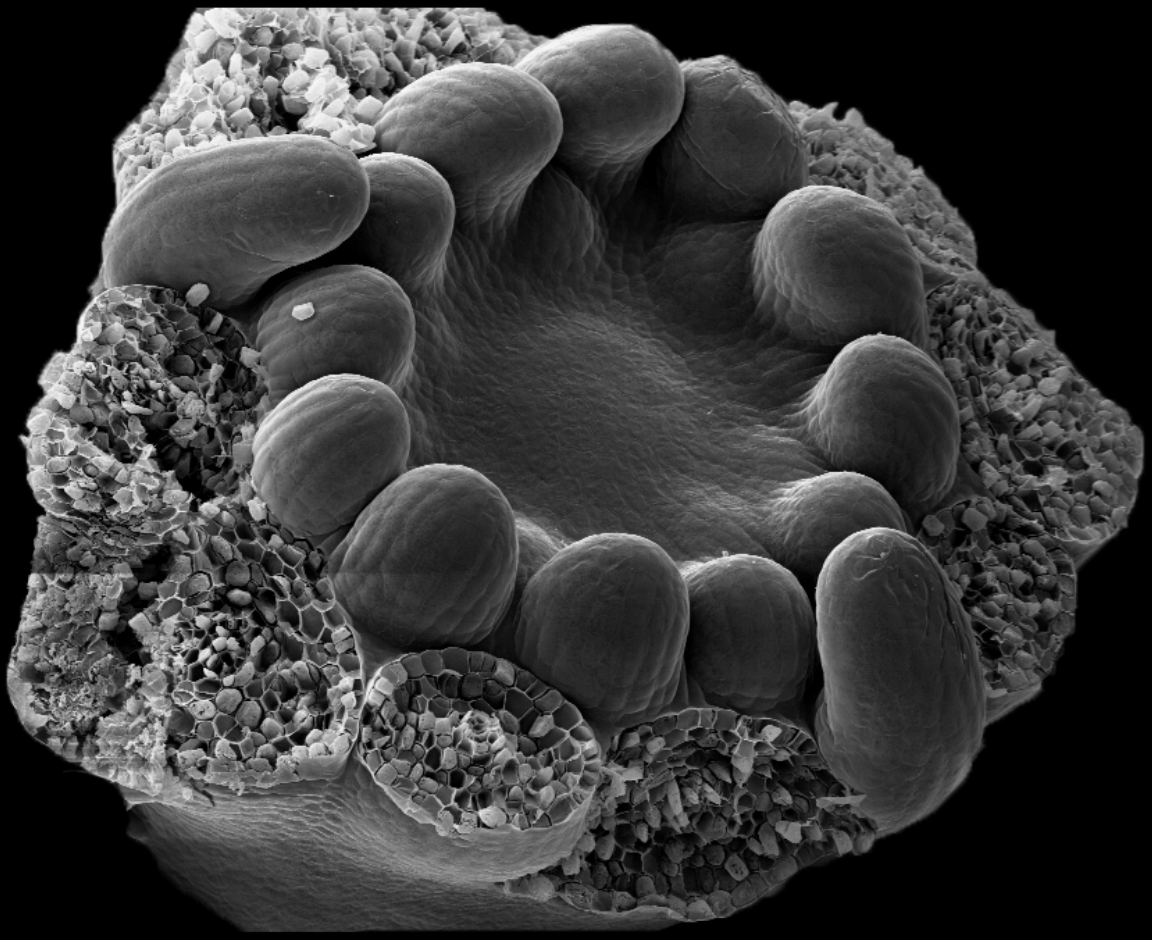

Jeiter J, Danisch F, Hilger HH. 2016. Polymery and nectary chambers in *Codon* (Codonaceae) – flower and fruit development in a small, capsule-bearing family of Boraginales. *Flora* 220: 94–102. https://doi.org/10.1016/j.flora.2016.02.010

Flora 220 (2016) 94–102

Contents lists available at ScienceDirect

Flora

journal homepage: www.elsevier.com/locate/flora

Polymery and nectary chambers in *Codon* (Codonaceae): Flower and fruit development in a small, capsule-bearing family of Boraginales

Julius Jeiter*, Fränze Danisch, Hartmut H. Hilger

Freie Universität Berlin, Biologie–Botanik, Altensteinstraße 6, D-14195 Berlin, Germany

ARTICLE INFO

Article history:
Received 2 December 2015
Received in revised form 15 February 2016
Accepted 19 February 2016
Edited by Shahin Zarre
Available online 24 February 2016

Keywords:
Codon schenckii
Codon royenii
Floral ontogeny
Nectary compartments
Floral morphology
Floral anatomy

ABSTRACT

Flower and fruit ontogeny in both species of *Codon* D. Royen (Codonaceae) has been investigated. Morphological differences and similarities between the Hydrophyllaceae I and II (Nameae) (*Wigandia* Kunth), as well as the Boraginaceae *s.str.* and Wellstediaceae are discussed. Flowers and fruits representing different ontogenetic stages were collected from culture and observed by scanning electron microscopy and light microscopy. The polymerous calyx, corolla and androecium develop acropetally. Sepals and stamens arise in two steps: after initiation of the first half in a 2/5-spiral, the second half arises subsimultaneously. Petals and stamens arrange later on in zigzag order to form two pseudowhorls and usually differ in size. In the mature stage, the gynoecium is nearly completely superior and symmetrical. Nectar compartments are formed by partitioning septa developing between filaments and corolla tube. They are covered by trichomes and laterally broadened filaments and present nectar from a nectary at the base of the gynoecium. This nectary formation leading to a revolver flower is unique in Boraginales. Our results indicate that Codonaceae share similarities with Wellstediaceae (Boraginales I) and Hydrophyllaceae I and II (Boraginales II). They are similar in gynoecium and fruit ontogeny and morphology, but differ dramatically in flower morphology. Especially polymery and the formation of nectary chambers are unique to these plants within the Boraginales and support their treatment as a separate family.

1. Introduction

Codon is a South African genus consisting of two species. Their habit as annual to perennial herbs (to shrublets) armed with stiff-erect spines, flowers with 10–12 perianth and stamen members and large nectary chambers at the base of the floral tube make it unique in the order Boraginales (e.g. Weigend and Hilger, 2016).

Codon royenii was originally described by D. Royen (in Linnaeus, 1767) as a member of the *Decandria Monogynia—flores monopetali aequales*. De Candolle (1845: 565) placed the genus in the family Hydrophyllaceae and a second species – *Codon schenckii* – was added by Schinz in 1888 (see Brand, 1913; for a classification history of the genus). Retief and van Wyk (2005) transferred *Codon* to Boraginaceae – based on the phylogeny of Hydrophyllaceae of Ferguson (1999) – and placed it into a separate subfamily Codonoideae Retief & A.E. van Wyk. Morphologically, *Codon* differs from Hydrophyllaceae by its inflorescence morphology and the floral features mentioned above. The nectar production is so copious in *Codon royenii* that its vernacular name is "honeybush" (Retief et al., 2005). As an Old-World genus it is geographically isolated from New World Hydrophyllaceae. Weigend and Hilger (2010) transferred the genus into its own monogeneric family Codonaceae (Retief & A.E. van Wyk) Weigend & Hilger based on the profound morphological differences in respect to both *Wellstedia* Balf.f. (Wellstediaceae) and Boraginaceae *s.str.* Additional justification for this decision came from a fairly comprehensive phylogeny of Boraginales, retrieving *Codon* as the first branch of the Boraginales I-clade as sister to Wellstediaceae + Boraginaceae *s.str.* (Weigend et al., 2014). This is somewhat unexpected, since the many-seeded capsules of *Codon* are morphologically very similar to those of Hydrophyllaceae, while they are quite different in *Wellstedia* (Thulin and Johansson, 1996) and Boraginaceae *s.str.* (Weigend et al., 2014). Furthermore, the flower and fruit morphology of *Codon* differ markedly from both Boraginales I-clades: in *Wellstedia* the perianth and androecium are tetramerous, and capsules are laterally flattened and one- (to two-) seeded, while in Boraginaceae *s.str.* perianth and androecium are pentamerous, and the fruit breaks down into eremocarps (="Klausen", "nutlets").

Flower and fruit development in Hydrophyllaceae have been described in detail by Hilger (1987) for *Wigandia caracasana* Kunth (Nameae, Hydrophyllaceae II), by Hofmann (1999) for *Phacelia* Juss.,

* Corresponding author. Present address: Nees-Institut für Biodiversität der Pflanzen, Rheinische Friedrich-Wilhelms-Universität Bonn, Meckenheimer Allee 170, D-53115 Bonn, Germany.
E-mail address: jjeiter@uni-bonn.de (J. Jeiter).

http://dx.doi.org/10.1016/j.flora.2016.02.010
0367-2530/

and by Hilger (2014) for Boraginaceae *s.str.* Comparative ontogenetical studies of *Codon* and *Wellstedia* are lacking.

Royen (in Linnaeus, 1767) and Brand (1913) already mentioned the nectary of *C. royenii*, but apparently nothing is known about its ontogeny or details of flower and fruit morphology and development. The aim of this paper is to investigate the ontogeny of the flower and fruit of *Codon* to understand the origin of its peculiar polymery and nectary.

2. Material and methods

Flower and fruit material of *C. schenckii* Schinz (Namibia, Kaokoveld, *M. Weigend 9460*, BONN) and *C. royenii* D. Royen (*M. Weigend s.n.*, BONN and *A.W. Mues 5*, BONN) was collected from cultivated plants at the Institut für Biologie—Systematische Botanik und Pflanzengeographie, Freie Universität Berlin resp. Botanische Gärten der Universität Bonn.

For scanning electron microscopy (SEM), the material was dissected under a dissecting stereo microscope, fixed in formaldehyde-acetic acid-ethanol (FAA) for at least one week, dehydrated with formaldehyde-dimethyl-acetal (FDA) and finally stored in the fridge in pure acetone (Gerstberger and Leins, 1978). Flowers representing different ontogenetic stages were critical point dried with CO_2 (Critical point dryer CPD 020, Balzers, Liechtenstein), sputter coated with gold (ca. 30 nm) (SCD 040 Sputter-Coater, Balzers, Liechtenstein), and the SEM micrographs were taken with a LEO 430 (Zeiss, Oberkochen, Germany) in Berlin and a LEO 1450 (Zeiss, Oberkochen, Germany) in Bonn.

Flowers of various developmental stages were prepared for light microscopy (LM) and anatomical studies. After fixation, the material was dehydrated using slow dehydration in a graded tertiary butanol/isopropanol series and finally embedded in Paraplast®. The specimens were serially sectioned with a Leitz 1515 rotary microtome (at 10 or 12 μm), stained with astra blue and safranin and documented with a Leitz Diaplan and Olympus CX 41 microscope. Photographs were taken with a Leica DC 300 digital camera (V 2.0).

3. Results

3.1. Inflorescence morphology, floral morphology and merosity

Flowers are arranged in frondose-bracteose monochasia, which are initially scorpioid and straighten out post-anthetically (Fig. 1E). Monochasia are rarely reduced to single flowers.

Overall flower morphology and merosity are similar in *C. schenckii* and *C. royenii*, but they differ in perianth shape and colour. The corolla of *C. schenckii* is yellow and saucer-shaped from a short, tubular base (Fig. 1A and B), while the flowers of *C. royenii* are whitish and campanulate (Fig. 1C and D). Flowers are tetracyclic and 12-merous, but merosity is fairly plastic, ranging from 10- up to 20-merous with slightly different combinations in three whorls (calyx, corolla and androecium), often varying within a single inflorescence. The organs of the different whorls alternate. Each whorl is shifted by approximately 15° relative to the preceding whorl (in perfectly 12-merous flowers). The resulting typical floral formula is *K (10-12-20) [C (10-12-20) A 10-12-20] G (2), the floral diagram is provided in Fig. 1F.

The calyx typically consists of six larger sepals alternating with six smaller sepals (Fig. 1D and E). Aestivation is apert. The calyx, like the whole plant, is densely covered with spines, simple trichomes and stalked glandular trichomes. The large sepals differ between both species. In *C. schenckii* they only differ in size from the small sepals (Fig. 1B), whereas they are distally widened and elliptical to ovoid in the upper half, contrasting with the linear and smaller sepals in *C. royenii* (Fig. 1D and E). At anthesis the distal half of the sepals are recurved and they are overtopped by the corolla, anthers and stigmas. The corolla is fused, in *C. schenckii* for approximately half of its length, in *C. royenii* for up to three quarters. The free lobes of the corolla are oblong to ovate. Petal aestivation is best described as imbricate (quincuncial): five to six petal lobes are visible from the outside completely enclosing the remaining seven to six petal lobes. The filaments are fused with the basal corolla forming a stamen-corolla tube (Figs. 1A; 2G; 3D and I). Each filament arises from the top of a septum on the stamen-corolla tube (Fig. 3E; this septum not to be confused with ovary-partitioning septa). The septa thus proximally subdivide the tube into separate compartments. The septa are adpressed to the gynoecium, sealing each compartment adaxially. The closure is completed by simple, single-celled trichomes arising from the proximal side of the septa (Fig. 3C–F, I, J). The distal pole of each compartment is closed by the same type of trichomes (Figs. 1 A and C; 3F, J, K). The structural modifications of the septa differ between both species (as will be described below).

Six long filaments are alternating with six shorter filaments at anthesis (Fig. 1A, B, D). Anthers are exserted, dorsifixed and introrse and apically twisted by 90° to 180°. The syncarpous gynoecium is bicarpellate (Figs. 2F, 4B and D) with an ovoid to spherical ovary tapering into a style which then divides into two stigmatic branches (Fig. 3C). The stigmas are punctiform. The ovary is nearly bilocular with a short synascidiate zone partly immersed into the receptacle. Placentae are T-shaped on two long gynoecial septa in cross-section, mutually adpressed with their adaxial surfaces and covered by numerous ovules (Fig. 4B and C). Ovules are unitegmic and anatropous (Fig. 4A and G). The dry stigmatic surface consists of papillose epidermal cells at the very tips of the stigmatic branches (Fig. 4E). Each branch shows a distinct groove on the adaxial side containing the transmitting tissue. The transmitting tissue of both branches unites into a "*compitum*" in the style. The placentae are covered with papillose cells, resembling those of the stigmatic surface. Gynoecium and corolla are covered with lentil-shaped hollow protuberances in their upper halves (Figs. 3I, 4D and F). A disc nectary (Fig. 3E) at the base of the gynoecium secretes nectar in each of the twelve compartments (Fig. 3J) through modified stomata.

3.2. Flower ontogeny

Floral organs develop centripetally (Fig. 2C–E), both calyx and androecium develop in two discrete steps. In a first step, the set of members develops (e.g. 6 of the 12 sepals), then the second set is initiated. The first set originates spirally, the second half is distinguished by a subsimultaneous initiation, and these organs also remain smaller at anthesis. In the corolla, no such pattern could be identified. The two carpels develop simultaneously.

3.3. Calyx

Calyx primordia are initially hemispherical, then conical and finally start to flatten out (Fig. 2C). First they are circular to obovate in shape. Formation of the apical part, which differs between both species, is followed by an elongation of the sepals. In later stages the sepals are connate at the very base forming a short, but distinct tube around the developing floral apex (Fig. 2E). At anthesis, the spiral sequence of initiation becomes obvious by the different size of the larger sepals in *C. royenii* (Fig. 1D and E). Five sepals are distinctly larger than the remaining (usually) seven sepals. Aestivation is valvate. Their early function as protective organs around the developing floral apex is reinforced by large, incrusted trichomes on multicellular bases. This, together with the presence of stalked glandular trichomes, leads to a partial capillinection of the sepals.

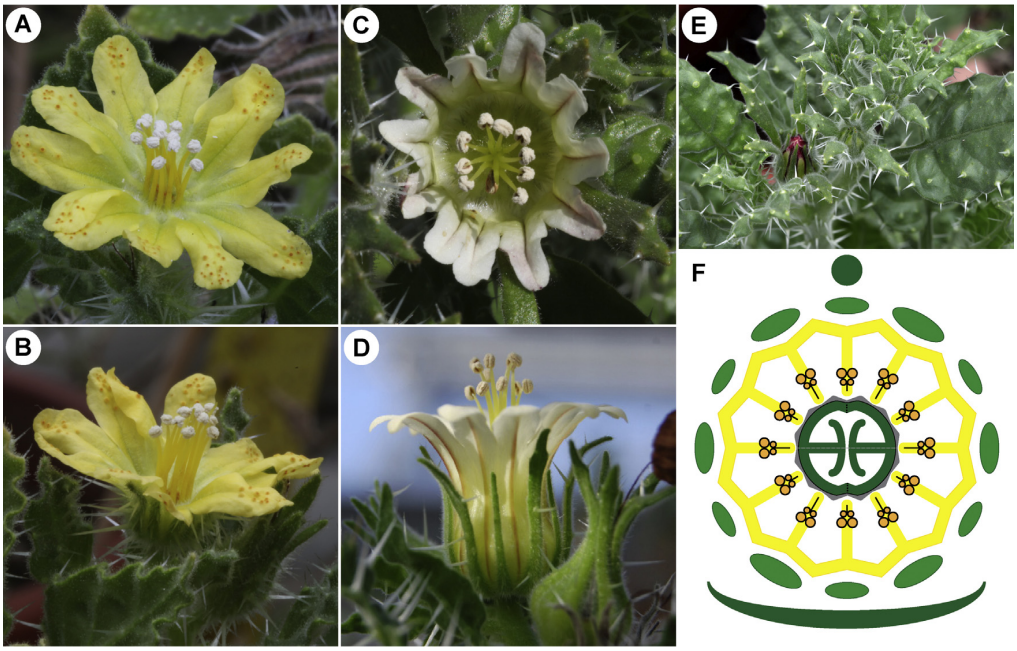

Fig. 1. (A, B) *Codon schenckii*. (A) Top view of flower. (B) Side view of flower. (C–E) *Codon royenii*. (C) Top view of flower. (D) Side view of flower showing different length of outer and inner stamens. (E) Inflorescence. (F) General floral diagram of *Codon* (green: sepals, yellow: corolla plus septa, light brown: stamens, grey: nectary, dark green: gynoecium) with carpels oriented in median position. (For interpretation of the references to colour in this figure legend, the reader is referred to the web version of this article.)

3.4. Corolla

Petal aestivation is imbricate, alternating with the sepals. Petal primordia are hemispherical and slightly laterally broadened (Fig. 2C and D). Petals are initiated subsimultaneously or in a tight spiral. All primordia grow to almost the same size in early stages of development. The lateral growth of the primordia leads to an outward (distal) displacement of six petal primordia, while the other six petal primordia retain a proximal position (Fig. 2D). All 12 primordia are free at the early stages of development and later raised by a connecting rim (late sympetaly, Fig. 2E and G).

3.5. Androecium and stamen-corolla tube

Stamens are inserted as hemispherical primordia in a regular ring on the flat or slightly bowl-shaped floral apex (Fig. 2D). The androecium develops in two stages. At first six staminal primordia arise between every second pair of petals. Soon after, the remaining six stamens, alternating with the first ones, are initiated. Both groups form two pseudowhorls. The filaments of the outer stamens are shorter than those of the inner ones (Fig. 2G and H) forming the shorter stamens at anthesis (Fig. 1D).

From the early stages of development, the staminal primordia are associated with the developing corolla (Fig. 2A and B). The staminal primordia are close to the young corolla, although there is plenty of space on the flat floral apex. Apparently they originate from a common meristematic base. Soon after initiation of all twelve stamen primordia their base is shifted from the flat receptacle towards the fusing corolla base. After this, the stamens are not lifted significantly further until the anthers are fully developed. Then the corolla and the stamens are lifted by the rapid growth of the common tube (congenital growth, Fig. 2G and I).

3.6. Nectar compartments and nectary

The growth of the stamen-corolla tube proceeds in three directions: (i) it lifts the corolla and the androecium upwards, whereby the filament bases are raised by the developing septa (Fig. 3I); (ii) at the point of filament insertion a “bridge” tissue is initiated as common base in radial direction (Fig. 3A: arrow) and lifts their bases; (iii) by intercalary growth in radial and vertical direction the filament base is “separated” from the corolla tube, and a connecting radial wall is formed (Fig. 3E).

The walls grow upward, pushing the filaments towards the gynoecium, and the stamen-corolla tube increases in diameter ultimately constrained by the calyx (Fig. 3E, F, I). Finally, the tissue of the tube between the radial walls expands tangentially, resulting in a bulging of the compartments towards the calyx. The parts of the walls which are pressed against the gynoecium are flat or slightly concave in *C. schenckii*. In *C. royenii*, which bears much more nectar than *C. schenckii*, they form a deep invagination which is filled and covered with simple trichomes. They now are septa which separate the usually 10 or 12 nectary chambers.

Also the shape of the nectary septa differs in the two species. In *C. schenckii* the apical rim is steeply sinoidal in the beginning and becomes increasingly flat towards anthesis (Fig. 3D–F, I). In *C. royenii* the nectary septa show an apical bulging towards the stamens. The nectary septa consist of two different sections. Basally they are formed by a thin layer of cells (Fig. 3E). This tissue apically abruptly changes into a lateral part, which is densely covered with simple trichomes, developing in early stages (Fig. 3A). The bulge is small in *C. schenckii*, while in *C. royenii* it is broader and almost completely closes the compartment. Viewed from above, the bulges look like basally broadened filaments (Fig. 3K). The entrance to the compartment is abaxially shifted towards the stamen-corolla tube, which is tightly adpressed to the calyx. The apical bulges in *C. royenii* fuse postgenitally through capillinection of the simple trichomes

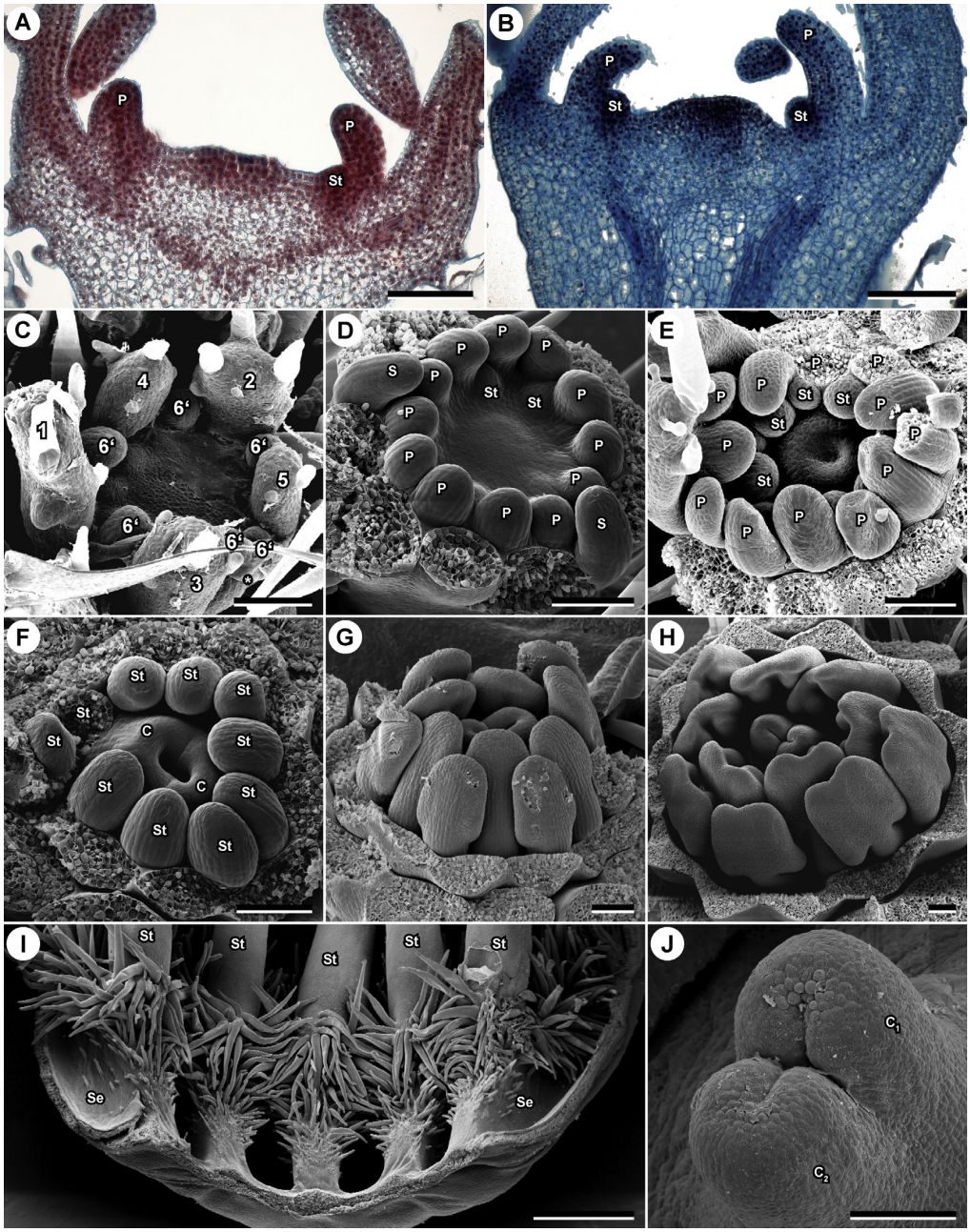

Fig. 2. Floral development of *Codon schenckii*. (A, B) LM, longitudinal sections through the developing floral apex, (B) slightly older than (A) stamen primordia closely associated with petals. (C) Spiral inception of the first five sepals (1–5), note that one sepal is absent (asterisk), subsimultaneous inception of the following six sepals (6′). (D) Inception of petals and stamens (alternating to every second petal). The floral apex is slightly rounded. (E) Six petals centrifugally shifted. Six smaller stamens, simultaneously arisen, are present as smaller primordia alternating with six larger stamen primordia. Young gynoecium visible as central ring. (F) Horseshoe-shaped carpels. (G) Stamens arranging in two pseudowhorls, congruence with their final size difference. (H) Anthers almost fully developed, gynoecial cleft closed. (I) Fully developed stamen-corolla tube showing the septa with dense coverage of simple trichomes. (J) Slight size-difference between the carpel apices. The stigmatic surface is formed. Abbreviations: P = petal, S = sepal, Se = septum, St = stamen, C = carpel. Scale bars: A–H, J = 100 μm, I = 1 mm.

(Fig. 3C), which also run up to tube and filament bases. After anthesis, at the beginning of fruit development, corolla and androecium are pushed upwards by the inflating ovary and are shed.

In *C. schenckii* the septa are shorter and the trichomes are more inflated than in *C. royenii*. These differences coincide with the overall floral architecture and lead to an increased volume of the resulting compartments in *C. royenii*.

The gynoecial nectary is inserted in a late developmental stage, apparently just before anthesis and develops as a small disc from the basal part of the ovary (Fig. 3D and E). In circumference it is not

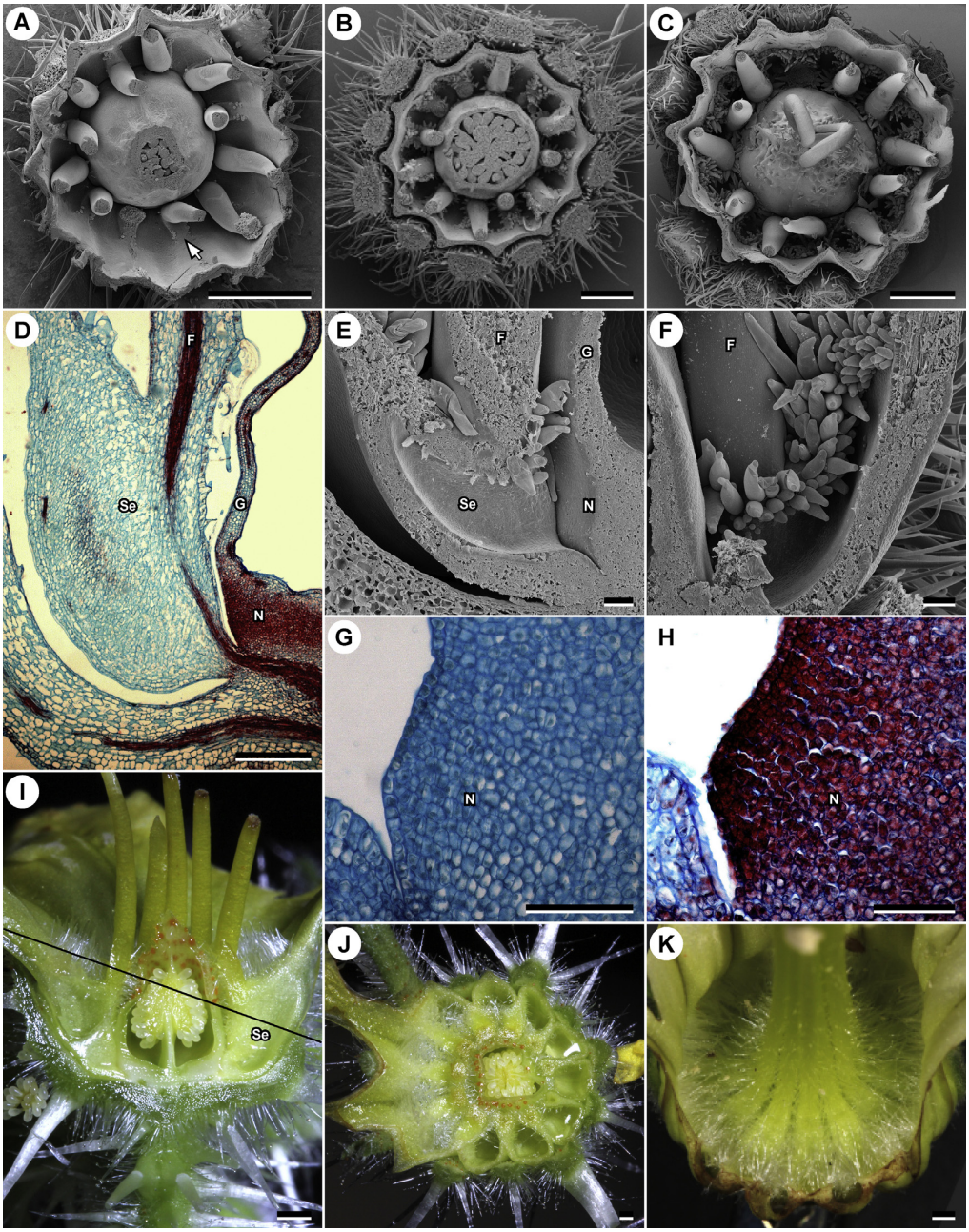

Fig. 3. (A–J) *Codon schenckii*. (A–C) Nectary chamber development, apical view. Septa arise between corolla tube and stamen base (A, arrow). (B, C) Closure by trichomes. (D) Longitudinal section through septum and nectary at gynoecium base. (E) Side view on septum pressed against gynoecium with nectary. (F) Side view of the septum with simple trichomes. (G, H) Longitudinal sections showing the development of the nectary gland. (G) Young cells densely packed. (H) active nectary, secreting cells are disintegrating. (I) Longitudinal section through a flower. Black line indicates section plane in (J). (J) Top view on nectary chambers of a mature flower. (K) *Codon royenii*. View on broad septum bulges and gradually narrowing filaments, nectary chambers closed by trichomes. Abbreviations: F = filament, G = gynoecial wall, N = nectary, Se = septum. Scale bars: A–C, I–K = 1 mm, D = 0.5 mm, E–H = 100 μm.

round, but more or less divided into twelve portions which slightly bulge into the compartments formed by the septa.

Fig. 3G and H shows the shift of cellular contents and the disintegration of cell walls from the juvenile parenchymatous (astra blue staining prevailing) to the functional (safranin staining prevailing) nectary tissue. Nectar is secreted through nectar-modified stomata. The number of stomata per compartment is relatively low and their size is around 20 μm in diameter.

3.7. Gynoecium

Prior to gynoecium formation, the receptacle is flat or plate-like (Fig. 2A–C). It is surrounded by the emerging, still unfused petals which form a shallow wall around it. On this flat receptacle a shallow bulge is formed (Fig. 2D). This is the inception of the short inferior part of the ovary, visible also by the intensely staining meristematic tissue (Fig. 2A, also Fig. 5E–G). The bulge

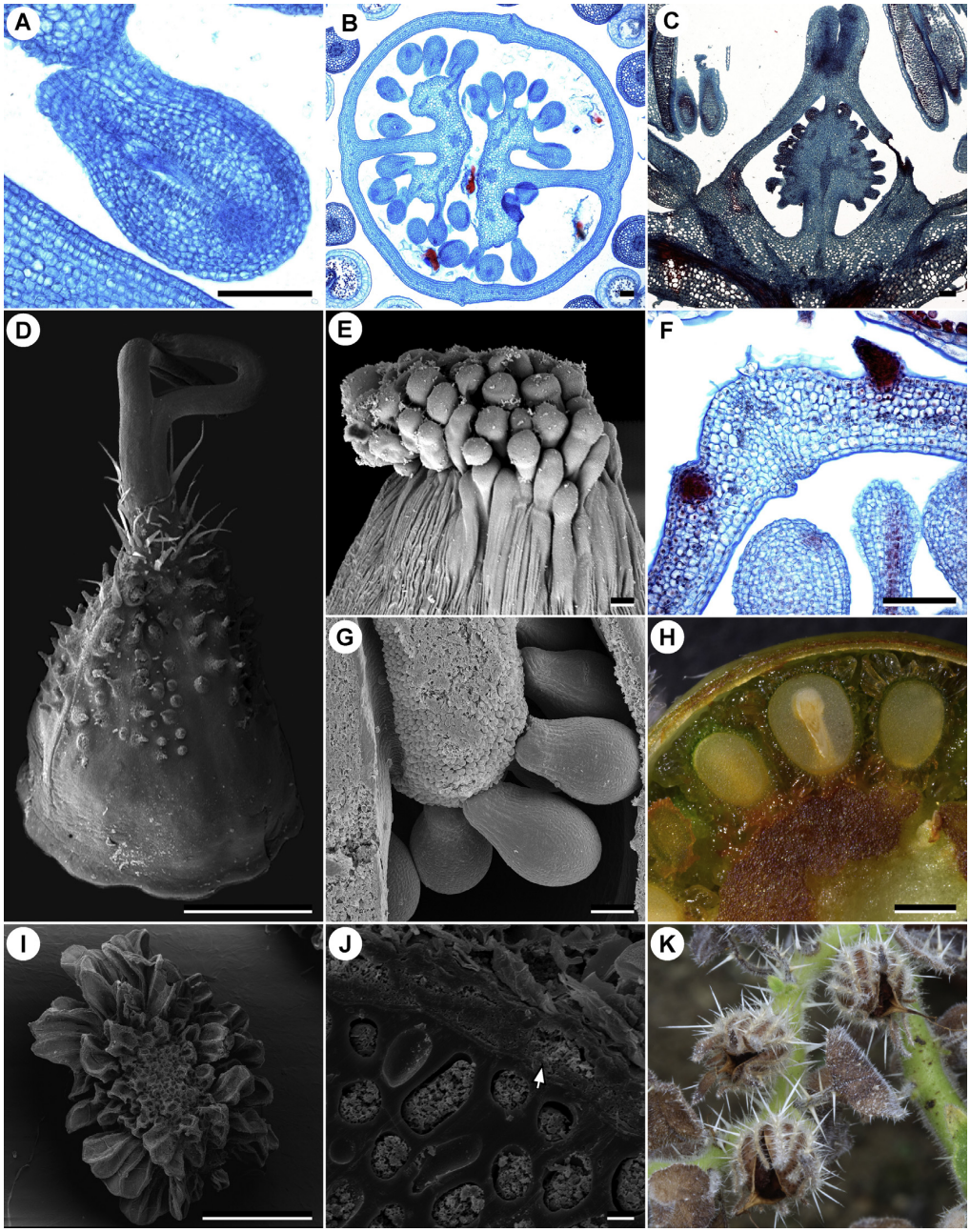

Fig. 4. Gynoecial and fruit characters in *Codon schenckii*. (A) Longitudinal section through ovule. (B) Cross-section through the ovary depicting the T-shaped, axile placentation. (C) Developing gynoecium. Note that the ovary is slightly sunken into the receptacle and surrounded by the developing nectary disc. (D) Fully developed gynoecium with apical trichomes and hollow protuberances. The lobed nectary disc is visible at the base. (E) Papillate dry stigma. (F) Cross-section through the pericarp showing the dorsal vascular bundle with developing dehiscence tissue. (G) Placenta with papillate surface and numerous ovules. Note the micropyle is in close contact with the placenta surface. (H) Longitudinal section through capsule. Testa still translucent and the cells are filled with liquid. (I) Mature seed. Testa dried, irregular shape of the cell-wall thickenings. (J) Transfer cells (arrow) in inner testa layer. (K) Dehisced capsules. Scale bars: A–C, G = 100 μm, D, H, J = 1 mm, E, F = 10 μm.

continues its growth on two sides, while the centre stops developing (Fig. 2E). From this ring of tissue two poles arise, which develop faster than the tissue in between them (Fig. 2F). They are the tips of the developing carpels. Both carpels continue to grow apically while a gap forms between them. Seen from above, both young carpels are shaped like horseshoes (Fig. 2F). In all specimens observed, one carpel is slightly larger than the other one (Fig. 2G). This may indicate that they are sequentially inserted, but with a very short plastochron.

The conical ovary increases its diameter while it continues to grow apically to reach its final, ovoid shape. At the end of development before anthesis, the style grows out. The stigma formation starts with the development of a papillate tissue at the apices of the horseshoe-shaped carpels (Figs. 2J; 4E). Both carpel apices elongate

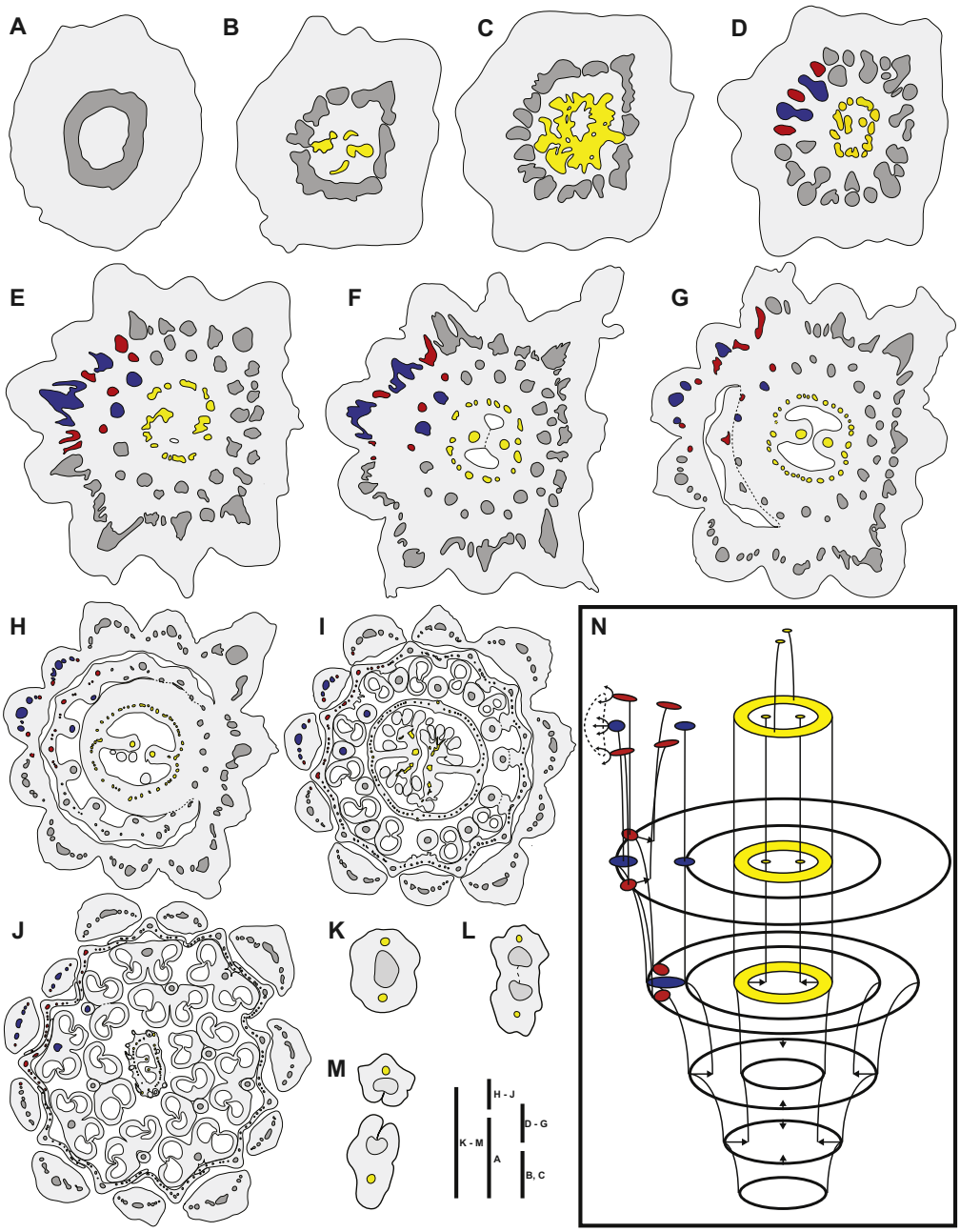

Fig. 5. Vascularisation of *Codon schenckii* flower, cross sections. (A) Petiole. (B) Separation of the gynoecial traces. (C) Gynoecial traces forming a vascular ring. (D) Staminal traces emerge from the sepal midrib traces and alternate with the joint petal and sepal lateral traces. (E) Orientation of androecial bundles to the inner part. Basal cavity of first gynoecial locule, formation of gynoecial septa, transition from synascidiate to symplicate. (F, G) Bundle arrangement in floral organs. (H–J) final bundle arrangement. (K–M) Vascular traces in style and stigmatic branches (transmitting tissue dark grey). (N) Schematic path of vascular bundles running from petiole to floral organs. Arrows indicate division of traces. Gynoecial traces (yellow), stamens + sepal medians (blue), petals + sepal laterals (red). Scale bars: 0.5 mm. (For interpretation of the references to colour in this figure legend, the reader is referred to the web version of this article.)

and form two branches. The branches spread in a 60° angle. Finally, both branches are lifted by the style which extends from the tip of the ovary (Fig. 4C and D). Both stigmatic branches keep an adaxial indentation containing the transmitting tissue merging in the style, thus forming a *compitum* (Fig. 4C, dark staining tissue).

3.8. Fruit and seed development, transfer cells

The mature fruit is an ovoidal capsule (Fig. 4D) with apical-loculicidal dehiscence (Fig. 4F, dehiscence tissue). While the androecium and corolla are shed, the calyx persists under the developing ovary and the sepals are pressed against the ovary. When

the developing capsule inflates, the sepals are pushed apart. They start wilting at a stage where the capsule is still green and closed. Capsules (Fig. 4K) of *C. schenckii* are smaller (ca. 2 cm long, 1 cm in diameter, up to 80 seeds) than those of *C. royenii* (ca. 2.5 cm long, 1.5 cm in diameter, up to 120 seeds). Exo- and endocarp are single-layered, the mesocarp consists of approximately ten cell layers (Fig. 4F). The numerous seeds are irregularly shaped, flattened globular, elliptical, ovoid or conical (Fig. 4I).

The integument develops into a multi-layered testa. At capsule dehiscence the thin outer walls collapse, resulting in irregularly shaped seeds with a large surface area. Between the massive starch containing endosperm, a single cell layer with cell wall protuberances (=transfer cells) originates from the inner testa layer (Fig. 4J).

3.9. Vascularisation of the flower

The flower is supplied by a continuous vascular ring (Fig. 5A). From it bundles are released into its interior, (Fig. 5B, yellow) which then form a ring and supply the gynoecium (Fig. 5C). The outer ring splits regularly. First, the traces supplying the stamens detach (Fig. 5D and E), then the traces for the petals follow. The bundles alternatingly run either to the inside or to the outside, forming two discontinuous rings (Fig. 5F–G). The inner bundles alternatingly supply the petals (red) and the stamens (blue, Fig. 5D–J). The outer bundles either form: (a) the median sepal bundles (which subsequently trifurcate, Fig. 5E–G), or (b) the lateral bundles of adjacent sepals (Fig. 5G and H).

From the gynoecial ring two traces separate to the inside (Fig. 5D–F). These two traces are the "fused lateral" carpellary traces supplying the placentae. The remaining ring of tissue divides into several smaller traces. With more than 30 traces per carpel they are arranged in a regular pattern in the mesocarp (Fig. 5F–H). At the level of the placenta several traces emerge from the common ventral bundles (Fig. 5L). These traces divide into smaller traces and fan out into the funicules to supply the ovules. The peripheral traces in the mesocarp disappear before the ovary tapers into the style (Fig. 5M). The style is supplied by the carpel medians (Fig. 5M and N). Both bundles remain independent and bend out into the stigmatic branches (Fig. 5J–M). The complete vascularisation is shown in Fig. 5N.

4. Discussion

A polymerous perianth as described for *Codon* has no equivalent in any Boraginales family except the woody *Hoplestigma* Pierre and few *Cordia* L. species (e.g. C. *decandra* Hook. & Arn., *C. dodecandra* DC.). The inception of petals and stamens in *Hoplestigma* are described cursorily as originating from three or four whorls (Gilg, 1908; Goldberg, 1986; Stevens, 2001), but without further ontogenetic investigation in both groups this remains highly uncertain. Both taxa, *Hoplestigma* and *Cordia* are phylogenetically very distant from the Hydrophyllaceae and Codonaceae. Thus, the polymery in *Codon* flowers has to be considered as a unique, autapomorphic character.

The shift, however, from a primarily circular ontogeny to a rearrangement of perianth and androecium in two whorls each corresponds to Fig. 6 depicted by Ronse De Craene (in press). This is also true for *Codon*. These pseudowhorl formations are linked to spatial restrictions. Lateral broadening of the primordia forces the subsequently set of arising primordia on another, alternating whorl (also described for Sapotaceae; Kümpers et al., 2016). Furthermore, our results are in line with the mechanisms involved in meristic changes in flowers proposed by Ronse De Craene (in press) and expressed as "anisomerous" for *Codon* (Ronse De Craene, in press, Table 2). The combination of a large floral meristem with relatively small perianth members and androecial organs are also clearly visible in *Codon*.

4.1. Gynoecium and fruit morphology

The bicarpellate and bilocular gynoecium of *Codon* with its axile placentation shows considerable similarities to the gynoecium of *Phacelia* (Hofmann, 1999) and *W. caracasana* (Hilger, 1987). However, both carpels arise subsimultaneously in *Codon*, while arising sequentially in the former taxa. Style and stigma are similarly organised in *Codon* and *Phacelia* (Hofmann, 1999), but differ from *W. caracasana*, where the stylodia are free and stigmas are capitate.

As in many other asterids, the nectary develops late in ontogeny and is apparently part of the basal portion of the ovary. Compared with *Wigandia* (Hilger, 1987) the nectary is axially elongated and not flat. Most probably the assumption of a receptacular origin in *Wigandia* expressed by Hilger should be reconsidered.

"False septa" in the form of weakly elevated bulges are present in *Codon* and *W. caracasana*. These structures lining the dorsal sutures of the carpels were discussed as the evolutionary starting point of the formation of eremocarp fruits in Boraginaceae. In the Boraginaceae, gynoecium formation diverges dramatically from this pattern (basistylous with its four locules of the ovary developing into eremocarps and style gynobasic and free), not permitting a direct comparison. Ontogenetic studies on the formation of eremocarps revealed that each eremocarp is formed individually by growing out of the gynobase and not by invagination of false septa (Hilger, 2014). Thus the fruit of *Codon* closely resembles that of *W. caracasana* (Hilger, 1987) and *Phacelia* (Hofmann, 1999). Capsules of *Wellstedia* differ from those of *Codon* in their general shape, but share apical-loculicidal dehiscence (Hunt, 1969; Thulin and Johansson, 1996).

4.2. Seed and transfer cells

The seeds of *Codon* with their sunken outer tangential cell walls and partial cell-wall thickenings are similar to those of the Hydrophyllaceae II (sensu Weigend et al., 2014), especially of the *Nama*-group (e.g. *Nama* L., Chance and Bacon, 1984; *W. caracasana*, Hilger, 1987). Another similarity between *Nama* (*N. johnstonii* C.L. Hitchc.) and *Codon* is the occurrence of the above mentioned cell-wall thickenings on the equatorial plain of the flattened seeds. We can now also add the presence of transfer cells in the inner testa layer to the features which are shared by Hydrophyllaceae and Codonaceae.

4.3. Differences in nectar compartments

The compartments differ markedly between both species. While they are open and only covered by trichomes in *C. schenckii*, they are covered by scale-like structures in *C. royenii*, further narrowing down the entrance to the nectar stock and shifting it towards the wall of the stamen-corolla tube. The function of the trichome and scale cover of the nectar compartments remains ambiguous. Weigend and Hilger (2016) discuss two possible functions: on the one hand, it may select potential pollinators and protect from nectar parasites. On the other hand, it could prevent nectar from evaporating, which may be necessary for plants of semiarid and arid habitats such as *Codon*. The flowers of *C. schenckii* are bowl-shaped and more openly organised (Fig. 1A and B) and also show less densely covered nectar compartments. The campanulate flowers of *C. royenii* show scale-shaped modifications of the septa (Figs. 1C and D; 3K). A more complex floral architecture may indicate a more elaborate flower-pollinator interaction. Most likely both factors may have influenced the cover of the nectar compartments.

Differences in the septa of both *Codon* species may also be explained by differences in nectar production.

Both *Codon* species differ significantly in the amount of nectar produced. While *C. royenii* ("honeybush") produces copious nectar, which can be seen with the naked eye as glistering droplets on the hairs in the corolla, we found only dry nectar compartments in *C. schenckii*. Maybe that – together with the whitish flower colour – allows *C. schenckii* to attract nightly pollinators, but even then remains of the nectar should have been found when investigating plants in the morning hours and in excluding any other flower visitors. Pollination of *C. royenii* seems to predominantly occur by carpenter bees (e.g. *Xylocopa lugubris*, Apidae: Xylocopinae, Gess, 1999; Gess and Gess, 2004), but apparently nothing is known for the case of *C. schenckii*. In other Boraginales, especially Boraginaceae, the nectaries are often covered by basal scales, if present. They may form a more or less complete ring or be dispersed to hairs or hair tufts. In the related family Wellstediaceae, basal scales are present in the NE African species only, but not in the South African *W. dinteri* Pilg. Their interpretation remains uncertain since a distinct nectary disc seems to be absent (Hunt, 1969).

Brand (1913) extensively described "scales" in Hydrophyllaceae (including *Codon*), which show an enormous diversity from small scales to tube-like structures. SEM pictures of basal scales are found in Hofmann (1999). In contrast to Boraginaceae, all the scales ("squamae") in Hydrophyllaceae are inserted longitudinally along the filament base, rather than between the filaments and the corolla tube.

The septa in *Codon* leading to a "revolver architecture" of the flower (Fig. 3I and J; comparable to those of Loasaceae; Weigend and Gottschling, 2006) may have a function in plant-pollinator interaction.

Congenital growth ("fusion") of the filaments with the corolla tube, either basally or over the complete length and insertion alternating with the corolla lobes is a characteristic of all Boraginales, but the formation of septa and nectary chambers has so far not been described in this order.

5. Conclusions

The Codonaceae are morphologically aberrant in the Boraginales. In habit, floral morphology and indumentum the species differ markedly from others. Nevertheless, *Codon* and Hydrophyllaceae *s.l.* (clades I and II, Nameae, Boraginales II) share the many-seeded conical capsular fruit type. In the poorly known Wellstediaceae (Boraginales I) the capsules are flat and the seeds are reduced to four or two. The occurrence of capsules in basal clades of both Boraginales I- and II-clades points to this as being a plesiomorphic character within this order.

On the other hand, pentamerous floral morphology with a stamen-corolla-tube and a gynoecium composed of two carpels is more or less uniform (except of the polymerous flowers in *Hoplestigma* and some *Cordia* species). There is, however, one similarity in the floral morphology of these groups and also in the Boraginales: the stamen-corolla tubes show various modifications (e.g. basal scales or hair tufts). Radial nectary septa, as present in *Codon*, are not known for any other species. The interpretation of these modifications as being homologous remains ambiguous. Since only little is known about the function and development of these structures in most clades of Boraginales, the interpretation as homologous is mainly based on their position within the flowers. From the results of this study it is not possible to provide a final answer to this question. Thus, this will remain an issue for further research and shall be addressed elsewhere. The same applies in regard to the evolution of fruits in Boraginales.

Acknowledgements

This work is partly based on the MEd thesis of F.D. We thank R. Lintermann (Berlin) for excellent field work, Chr. Dietrich (Berlin) for help with the preparation of the SEM and light microscopy specimens and H.-J. Ensikat (Bonn) for help and support with SEM. Theodor C. H. Cole (Heidelberg) kindly improved the English text. We thank M. Weigend (Bonn) for access to technical facilities and providing material support. We are grateful to M. Weigend, F. Selvi (Florence) and E. Smets (Leiden) for useful advice on the manuscript. One anonymous reviewer gave valuable hints for improvement.

References

Brand, A., 1913. Hydrophyllaceae. In: Engler, Das Pflanzenreich (Eds.) [Heft 59] IV. 251. Wilhelm Engelmann, Leipzig. http://biodiversitylibrary.org/page/22042393.

Chance, G.D., Bacon, J.D., 1984. Systematic implications of seed coat morphology in *Nama* (Hydrophyllaceae). Am. J. Bot. 71, 829–842.

De Candolle, A.P., 1845. Prodromus systematis naturalis regni vegetabilis, 9 Treuttel et Würtz, Paris. http://biodiversitylibrary.org/page/162364.

Ferguson, D.M., 1999. Phylogenetic analysis and relationships in Hydrophyllaceae based on *ndhF* sequence data. Syst. Bot. 23, 253–268.

Gerstberger, P., Leins, P., 1978. Rasterelektronenmikroskopische Untersuchungen an Blütenknospen von *Physalis philadelphica* (Solanaceae) Anwendung einer neuen Präparationsmethode. Ber. Deutsch. Bot. Ges. 91, 381–387, http://dx.doi.org/10.1111/j.1438-8677.1978.tb03660.x.

Gess, S.K., 1999. *Codon* flowers, chalices of hidden nectar. Veld Flora 85, 30–31.

Gess, S.K., Gess, F.W., 2004. Distributions of flower associations of pollen wasps (Vespidae: Masarinae) in southern Africa. J. Arid Environ. 57, 17–44, http://dx.doi.org/10.1016/S0140-1963(03)00093-4.

Gilg, E.F., 1908. Die systematische Stellung der Gattung *Hoplestigma* und einiger anderer zweifelhafter Gattungen. Ber. Zusammenk. Freien Vereinigung Syst. Bot. 5, 76–84.

Goldberg, A., 1986. Classification, evolution, and phylogeny of the families of Dicotyledons. In: Smithsonian Contributions to Botany. Smithsonian Institution Press, Washington.

Hilger, H.H., 2014. Ontogeny, morphology, and systematic significance of glochidiate and winged fruits of Cynoglosseae and Eritrichieae (Boraginaceae). Plant Divers. Evol. 131, 167–214, http://dx.doi.org/10.1127/1869-6155/2014/0131-0080.

Hilger, H.H., 1987. Flower and fruit development in *Wigandia caracasana* (Hydrophyllaceae). Am. J. Bot. 74, 250–259, http://dx.doi.org/10.2307/2444027.

Hofmann, M., 1999. Flower and fruit development in the genus *Phacelia* (Phacelieae, Hydrophyllaceae): characters of systematic value. Syst. Geogr. Plants 68, 203–212, http://dx.doi.org/10.2307/3668601.

Hunt, D.R., 1969. *Wellstedia*, Hooker's Icon. Pl. 37, 3665–3667.

Kümpers, B.M.C., Richardson, J.E., Anderberg, A.A., Wilkie, P., Ronse De Craene, L.P., 2016. The significance of meristic changes in the flowers of Sapotaceae. Bot. J. Linn. Soc. 180, 161–192, http://dx.doi.org/10.1111/boj.12363.

Linnaeus, C., 1767. Systema Naturae per Regna Tria Naturae: Secundum Classes, Ordines, Genera, Species, Cum Characteribus, Differentiis, Synonymis, Locis, 12th ed. Holmiae, Stockholm.

Retief, E., van Wyk, A.E., 2005. [Boraginaceae] Codonoideae, a new subfamily based on *Codon*. Bothalia 35, 78–80.

Retief, E., van Wyk, A.E., Condy, G., 2005. *Codon royenii*. Flower. Plants Afr. 59, 114–121.

Ronse De Craene, L.P., 2015. Meristic changes in flowering plants: how flowers play with numbers. Flora, http://dx.doi.org/10.1016/j.flora.2015.08.005 (in press).

Stevens, P.F., 2001. Angiosperm Phylogeny Website [WWW Document]. URL: http://www.mobot.org/MOBOT/research/APweb/ (accessed 09.17.15).

Thulin, M., Johansson, N.B., 1996. Taxonomy and biogeography of the anomalous genus *Wellstedia*. In: van der Maesen, L.J.G., van der Burgt, X.M., van Madenbach de Rooy, J.M. (Eds.), The Biodiversity of African Plants. Kluwer Academic Publishers, Dordrecht, pp. 73–86.

Weigend, M., Gottschling, M., 2006. Evolution of funnel-revolver flowers and ornithophily in *Nasa* (Loasaceae). Plant Biol. 8, 120–142, http://dx.doi.org/10.1055/s-2005-873034.

Weigend, M., Hilger, H.H., 2010. Codonaceae—a newly required name in Boraginales. Phytotaxa 10, 26–30, http://dx.doi.org/10.11646/phytotaxa.10.1.3.

Weigend, M., Hilger, H.H., 2016. Codonaceae. In: Kubitzki, K. (Ed.), Families and Genera of Vascular Plants, vol. 14. Springer, Heidelberg.

Weigend, M., Luebert, F., Gottschling, M., Couvreur, T.L.P., Hilger, H.H., Miller, J.S., 2014. From capsules to nutlets—phylogenetic relationships in the Boraginales. Cladistics 30, 508–518.

Chapter 4

Towards an integrative understanding of stamen-corolla tube modifications and floral architecture in Boraginaceae (Boraginales)

Jeiter J, Langecker S, Weigend M. Towards an integrative understanding of stamen-corolla tube modifications and floral architecture in Boraginaceae (Boraginales). *Botanical Journal of the Linnean Society*. Submitted 16.08.2019.

Towards an integrative understanding of stamen-corolla tube modifications and floral architecture in Boraginaceae (Boraginales)

Julius Jeiter*, Stella Langecker, Maximilian Weigend

Nees-Institute for Biodiversity of Plants, University of Bonn,
Meckenheimer Allee 170, 53115 Bonn, Germany

*Corresponding author: jjeiter@uni-bonn.de

Abstract

Morphological studies rarely address floral organ modifications and their integration into floral architecture and floral function. Boraginaceae show two prominent types of stamen-corolla tube modifications: faucal and basal scales. Both types, especially faucal scales, are widely used in classification. Here, the ontogeny and morphology of faucal and basal scales are studied in 29 species from eight tribes and all three subfamilies of Boraginaceae using scanning electron microscopy. Integration into floral architecture is visualised with micro-computed tomography (μCT). Faucal and basal scales are present in 18 respectively 27 species. Both types of scales develop late in flower ontogeny, but with variable timing. Faucal scales are morphologically much more variable than basal scales. Faucal scales are topologically associated with the anthers and sometimes involved in anther cone formation. Basal scales cover either the gynoecial disc nectary or the entire ovary. The different scale morphologies here identified enclose complex internal spaces, but show no obvious phylogenetic patterns. This likely indicates strong functional constraints and adaptive pressures. This is a first in-depth study of the morphology and development of stamen-corolla tube modification in Boraginaceae, demonstrating that *in situ* three-dimensional visualisation of floral architecture with μCT permits unprecedented insights into the evolution and functional integration of stamen-corolla tube modifications in Boraginales.

Keywords: Flower – morphology – floral structure – floral organisation – evolution – faucal scales – basal scales – micro-computed tomography

4.1 Introduction

One of the most fascinating aspects of angiosperms are their flowers. The diversity of shapes, sizes and functions in their ecological interactions are enormous and our knowledge of this diversity increases constantly. At the very basis of an understanding of floral evolution is the detailed observation and description of the structure (i.e. development, morphology and anatomy) of the flower and its parts. Overall, there are still many plant groups for which a detailed and comparative understanding of flower structure is missing, despite the fact that individual features of flower morphology may be widely used in taxonomy and classification. Taxonomic studies often describe floral organisation and some aspects of floral architecture, but they focus on differential characters for taxon delimitation and

Figure 4.1: Diversity of flowers and floral architectures in Boraginaceae. A–C, Boraginoideae, Boragineae. A, *Anchusa officinalis*. B, *Borago officinalis*. C, *Symphytum tuberosum*. D–G, Boraginoideae, Lithospermeae. D, *Podonosma orientalis*. E, *Cerinthe major*. F, *Aegonychon purpurocaeruleum*. G, *Echium vulgare*. H–L, Cynoglossoideae. H–I, Trichodesmeae. H, *Caccinia strigosa*. I, *Trichodesma indicum*. J, *Omphalodes cappadocica* (Omphalodeae). K–L, Cynoglosseae. K, *Rindera lanata*. L, *Amsinckia spectabilis*.

rarely study the integration of flower parts or structural details that may be difficult to observe or of little classificatory value. This is especially true for floral architecture, which does not provide simple characters for classification: Floral structure can be broken down into floral organisation and floral architecture (Endress, 1996). Floral organisation describes merosity of the different organ whorls and their arrangement and is widely used in classification, as is the size of different organs. Conversely, floral architecture describes the flower as the outcome of synorganisation and fusion, differential growth rates (Endress, 1996), and the modification of floral organs (Jeiter *et al.*, 2017; Jeiter & Weigend, 2018). Modifications of specific organs are quite common in angiosperm flowers, but detailed studies of these structures are limited. Modifications may be found on any part of the flower, but various types of scales and appendages on the corolla are particularly common. A summary of modifications of petals ('elaborate petals') is presented by Endress & Matthews (2006). Examples for detailed studies on the structure of modifications can be found for *Spermacoce* L. (Rubiaceae, Vaes *et al.*, 2006), *Lychnis* L. (Caryophyllaceae, Arber, 1939) and Hydrophyllaceae (Boraginales, Jeiter & Weigend, 2018). The modifications in *Spermacoce* likely function as barriers preventing self-pollination and protect the anthers from biotic and abiotic pollen loss (Vaes *et al.*, 2006). The corona-scales in *Lychnis* (Arber, 1939) and related Caryophylloideae (Bittrich, 1993) probably function as optical and mechanical nectar guides and reinforce the architecture of the flower (Endress & Matthews, 2006). In Hydrophyllaceae, ten scales, spatially related to the filament bases, fully or partially separate the internal floral space into compartments which partition the nectar and likely increase pollinator handling time (Jeiter & Weigend, 2018). All cited studies have in common that the function of the modifications is inferred from anecdotal evidence. An exception is a study of filament appendages in some arid-adapted Zygophyllaceae (Naghiloo *et al.*, 2018). In that study, development and ecological consequences of the appendages were described and experimentally tested. Naghiloo *et al.* (2018) found that the appendages prevented nectar from evaporation under dry and windy conditions. However, this kind of study linking detailed morphological descriptions and experiments are rare.

Boraginaceae with their sympetalous corollas have two distinct types of stamen-corolla tube modifications: the so-called faucal scales and the basal scales. The faucal scales are strikingly obvious in many groups of Boraginaceae and may play a crucial role in floral display (Fig. 4.1A, J) and floral function, e.g., by stabilizing the anther cone (Fig. 4.1B, C). The presence, absence and shape of faucal scales are often used for classification (Chacón *et al.*, 2016; Weigend *et al.*, 2016). Basal scales are deeply hidden in the tube and thus much less conspicuous. Accordingly, they have received little attention in the literature. The main differences widely used in taxonomy and classification are their presence and absence, whether an annulus is formed and whether trichomes are present, absent or replace the entire basal scales (Weigend *et al.*, 2016). Their association with the nectary disc (Weigend *et al.*, 2016) led to the misconception of the basal scales being the nectar secreting structure (addressed by Schaefer, 1942). Detailed floral architectural studies, however, combining the above-mentioned architectural characters with detailed observations of faucal and basal scales, are wanting. In general, there are very few comparative studies on either faucal or basal scales. The most recent studies date from the early 20th century (Arber, 1939; Schaefer, 1942) and their development has not been studied in recent decades (Payer, 1857; Schaefer, 1942). It is therefore not surprising that the integration of these structures into floral architecture is poorly understood and that we have virtually no knowledge about their function beyond anecdotal inferences (e.g., summarised in Weigend *et al.*, 2016).

The Boraginaceae are the largest family of the Boraginales. They comprise ca. 1700 species in approximately 90 genera and are subcosmopolitan in distribution (Luebert *et al.*, 2016; Weigend *et al.*, 2016). Various phylogenetic (e.g., Böhle *et al.*, 1996; Weigend *et al.*, 2009, 2013; Cohen, 2011, 2014; Chacón *et al.*, 2017) and structural (e.g., Hilger, 1984, 2014; Bigazzi & Selvi, 2000) aspects

have been addressed in previous studies, culminating in a revised infrafamilial classification for the family (Chacón *et al.*, 2016). This recent classification subdivides the family into three subfamilies (Echiochiloideae, Boraginoideae and Cynoglossoideae) and eleven tribes.

Like many notoriously florally diverse families such as Orchidaceae (Ronse De Craene, 2010), Balsaminaceae (Fischer, 2004) or Apocynaceae (Endress, 1994, 1996; Ronse De Craene, 2010), the Boraginaceae (and indeed Boraginales) show highly conserved floral organisation, which contrasts spectacularly with an outstanding diversity of floral architecture. An overview of some flowers used in this study is shown in figure 4.1. Flowers of Boraginaceae are tetracyclic, imperfect pentamerous with five sepals, five petals, five stamens, two carpels and a nectary disc at the base of the ovary. They are predominantly actinomorphic, rarely more or less zygomorphic (e.g., *Echium* L., *Caccinia* Savi, Weigend *et al.*, 2016). The petals are fused and, together with the stamens, form a stamen-corolla tube. The corolla tube is subdivided into a basal part from the base of the tube to the insertion points of the filaments and an apical part, ranging from the insertion points of the filaments to the sinuses of the corolla lobes (compare Jeiter & Weigend, 2018). The ovary consists of (usually) four separate mericarps and a gynobasic style arising between the mericarps. The nectary disc is part of the gynobase (Weigend *et al.*, 2016). Major conspicuous differences in floral architecture arise from overall corolla shape, orientation an shape of the corolla limb, the position of the filaments and the anthers relative to the corolla tube and their synorganisation, and presence, absence, shape and size of faucal (and basal) scales.

Overall corolla shape is commonly infundibuliform and hypocrateriform, but a wide variety of other shapes such as campanulate, cylindrical, urceolate to subrotate corollas may be found. The anthers are either included or partially or completely exserted from the corolla tube. Several species have connivent anthers, in extreme cases modified into an anther cone. The combination of a hypocrateriform or subrotate corolla with connivent anthers or an anther cone is sometimes described as 'solanoid flower' (Fægri & van der Pijl, 1979) or, due to the presence of nectar and introrse loculicidal anther dehiscence (e.g., in *Borago officinalis* L.), as '*Borago* type flower' (Fægri, 1986; Dukas & Dafni, 1990). Presence and absence of faucal and basal scales has rarely been addressed in a phylogenetic context (but see Cohen, 2014) and their integration into floral architecture has only been studied in the very specific context of anther cones and buzz-pollination (e.g., Teppner, 2011).

Generally, the morphology and structural integration of faucal and basal scales into floral architecture is very poorly understood. We therefore address this topic in the present study based on material from 29 species representing all three subfamilies and eight (of eleven) tribes of the Boraginaceae. We aim at describing the development and morphology of the faucal and basal scales and the morphology of the nectary disc using scanning electron microscopy (SEM) and we evaluate the integration of these structures into floral architecture using micro-computed tomography (μCT).

This study aims at clarifying the following specific questions: *i*) How do faucal and basal scales develop? *ii*) What is the localization and structure of the disc nectary? *iii*) How are faucal and basal scales integrated into floral architecture? *iv*) Are there phylogenetic patterns in faucal and basal scales, and their integration into floral architecture?

4.2 Material and methods

Inflorescences with flowers of different developmental stages – from onset of stamen-corolla tube development to anthetic flowers – were collected as fresh material from the living collection at the Bonn University Botanic Gardens. All collected specimens were prepared for scanning electron microscopy

(SEM) and a subset of samples prepared for micro computed tomography (µCT). Sampled species and applied methods are shown in table 4.1.

Scanning electron microscopy

Two different scanning electron microscopy (SEM) procedures were applied, requiring different methods of sample fixation and preparation. Part of the freshly collected material was directly processed for cryo-SEM, the remaining material was fixed in formaldehyde-acetic acid-ethanol (FAA; formaldehyde 2%, acetic acid 2%, ethanol 70%) for further examination using standard SEM techniques. Cryo-SEM massively reduces the number of artefacts which may result from the fragility of the stamen-corolla tube.

Cryo-SEM. The stamen-corolla-tubes of freshly collected flowers were carefully removed from the receptacle under a stereomicroscope, cut open on one side and placed onto conductive carbon tape (Leit-Tap, PLANO GmbH, Wetzlar, Germany). The spread corolla tube was additionally held in place by droplets of conductive carbon cement (Leit-C, PLANO GmbH, Wetzlar, Germany). The mounted samples were sputter coated with gold or palladium at 0.1 mbar and 30 mA for 20 seconds in a sputter coater (SCD 040, Balzers Union, Liechtenstein). The coated sample attached to the conductive carbon tape was mounted onto a 'cryo-holder'. The cryo-holder is a modified block of aluminium attached to a piece of hard plastic for thermal insulation and two aluminium frames, enclosing the coated sample. The sample was covered with a copper lid to prevent formation of ice crystals on the surface of the samples. The mount was submerged in liquid nitrogen until its temperature stabilised (1 – 1.5 mins) and subsequently placed in the vacuum chamber of the SEM (Stereoscan 200, Cambridge, UK). After evacuation and prior to studying the sample in the SEM, the copper lid was removed by tilting the mount. Samples were viewed at temperatures between -100° and -70° C at 5 to 15 kV.

Standard-SEM. Samples not suitable for the cryo-SEM technique – gynoecia and stamen-corolla tube development – were prepared for SEM following standard methods: the samples were fixed in FAA, rinsed with ethanol (70%) and dissected under a stereomicroscope. Prior to dehydration, they were transferred into acetic acid-ethanol (acetic acid 2%, ethanol 70%) for at least one hour, which was subsequently replaced with formaldehyde dimethyl acetal (FDA; 99%, Sigmar-Aldrich Chemie GmbH, Munich, Germany) and finally stored in acetone (protocol modified after Gerstberger & Leins, 1978). Critical point drying (CPD 020, Balzers Union, Liechtenstein) followed the standard protocol. Dried specimens were mounted on aluminium stubs using conductive carbon tape and conductive carbon cement followed by the final sample preparation. The mounted specimens were coated with gold or palladium in a sputter coater (SCD 040, Balzers Union, Liechtenstein) for 1.5 up to 3 min at 30 mA. Images were taken with a Stereoscan 200 SEM at 10 to 15 kV. Contrast and brightness of the images were partially adjusted using standard image editing software.

Micro-computed tomography

Preparation of the material for µCT-scanning was based on Staedler *et al.* (2013). Fixed anthetic flowers were transferred for infiltration into a solution of phosphotuncstic acid (PTA; 1%) dissolved in ethanol (70%). The samples were infiltrated for at least two weeks and the infiltration medium was exchanged every second day. After infiltration the samples were dehydrated in PTA (1%) dissolved in

Table 4.1: Studied species, IPEN-numbers and voucher placement.

Species	Tribe	Subfamily	Material	Methods	IPEN-number
Ogastemma pussillum (Coss. & Durieu ex Bonnet & Barratte) Brummitt	Echiochileae	Echiochiloideae	development, anthetic, gynoecium	SEM	IL-0-BONN-38381
Anchusa officinalis L.	Boragineae	Boraginoideae	development, anthetic, gynoecium	(cryo-)SEM, µCT	GR-0-MB-1983/294
Anchusa azurea Mill.			gynoecium	SEM	TJ-0-BONN-37005
Nonea lutea DC.			development, anthetic, gynoecium	SEM	xx-0-BONN-3851
Borago officinalis L.			development, anthetic, gynoecium	(cryo-)SEM, µCT	xx-0-BONN-7868
Borago pygmaea (DC.) Chater & Greuter			anthetic, gynoecium	(cryo-)SEM	IT-0-BONN-37020
Symphytum officinale L.			anthetic	(cryo-)SEM	DE-0-BONN-13533
Symphytum tuberosum L.			anthetic, gynoecium	SEM, µCT	AT-0-BONN-6371
Podonosma orientalis (L.) Feinbrun	Lithospermeae		development, anthetic, gynoecium	(cryo-)SEM, µCT	IL-0-BONN-37891
Alkanna graeca Boiss. & Spruner			development, anthetic, gynoecium	(cryo-)SEM	xx-0-BONN-28715
Huynhia pulchra (Willd. ex Roemer & Schultes) Greuter & Burdet			development, anthetic, gynoecium	SEM	RU-0-IB-007641
Cerinthe major L.			development, anthetic, gynoecium	(cryo-)SEM	xx-0-BONN-3859
Moltkia aurea Boiss.			development, anthetic, gynoecium	SEM	xx-0-BONN-36925
Lithospermum officinale L.			development, anthetic, gynoecium	(cryo-)SEM	GE-0-BONN-35815
Glandora oleifolia (Lapeyr.) D.C.Thomas			development, anthetic, gynoecium	SEM	xx-0-BONN-15184
Aegonychon purpurocaeruleum (L.) Holub			development, anthetic, gynoecium	(cryo-)SEM	DE-0-MB-1970/1149
Onosma alborosea Fisch. & C.A.Mey.			anthetic, gynoecium	SEM, µCT	TR-0-BONN-38567
Echium vulgare L.			gynoecium	SEM	DE-0-OSN-2006-123
Echium wildpretii H.Pearson ex Hook.f.			development, anthetic, gynoecium	(cryo-)SEM, µCT	xx-0-BONN-34155
Echium webbii Coincy			gynoecium	SEM	xx-0-BONN-25323
Caccinia strigosa Boiss.	Trichodesmeae	Cynoglossoideae	development, anthetic, gynoecium	SEM, µCT	xx-0-BONN-3837
Trichodesma indicum (L.) Lehm.			development, anthetic, gynoecium	SEM, µCT	PK-0-BONN-39165
Trichodesma scottii Balf.f.			anthetic	µCT	YE-0-BONN-14450
Lappula sessiliflora (Boiss.) Gürke	Rochelieae		gynoecium	SEM	JO-0-BONN-37173
Omphaldes cappadocica DC.	Omphalodeae		development, anthetic, gynoecium	SEM	RU-0-BONN-22714
Myosotis sylvatica Hoffm.	Myosotideae		development, anthetic, gynoecium	SEM, µCT	xx-0-ULM-2005-F-69
Amsinckia spectabilis Fisch. & C.A.Mey.	Cynoglosseae		development, anthetic, gynoecium	SEM, µCT	US-0-BONN-37350
Rindera lanata Bunge			development, anthetic, gynoecium	SEM, µCT	IR-0-BONN-37887
Cynoglossum australe R.Br.			development, anthetic, gynoecium	SEM, µCT	AU-0-BONN-37351

an ascending ethanol series (70%, 85%, 96%, 99%) and finally transferred into PTA (1%) in acetone (100%). Dehydrated samples were critical point dried from acetone and stored in an exsiccator.

Table 4.2: Skyscan 1272 µCT scan settings.

Species	**Acceleration voltage [kV]**	**Source current [µA]**	**Exposure time [s] (frame average)**	**Pictures per sample**	**Camera binning**	**Image pixel size [µm]**
Amsinckia spectabilis	50	200	0.305 (4x)	1800	2	5
Anchusa officinalis	50	200	0.305 (4x)	1800	2	6.5
Borago officinalis	50	200	0.305 (4x)	1800	2	8.5
Caccinia strigosa	50	200	0.305 (4x)	1800	2	8.6
Cynoglossum australe	50	200	0.569 (4x)	1800	2	4
Echium wildpretii	50	200	0.305 (8x)	1800	2	7
Myosotis sylvatica	50	200	0.305 (4x)	1800	2	4.5
Onosma alborosea	50	200	0.569 (4x)	1800	2	9
Podonosma oriantalis	50	200	0.305 (6x)	1800	2	7
Rindera lanata	50	200	0.305 (4x)	1800	2	7
Symphytum tuberosum	50	200	0.305 (4x)	1800	2	6
Trichodesma indicum	50	200	0.305 (6x)	1800	2	8.5
Trichodesma scottii	50	200	0.877 (4x)	1800	2	8.6

The dried samples were mounted on aluminium rods (6 mm Ø x 30 mm) with two-component epoxy resin (UHU PLUS Sofortfest, UHU, Bühl, Germany). Scans were performed in a SkyScan 1272 (Bruker Co, Billerica, MA, US) equipped with a HAMAMATSU L11871 20 source (Hamamatsu, Japan) and a Ximea xiRAY16 camera (Ximea GmbH, Münster, Germany). Scan settings are shown in table 4.2.

3D reconstruction from the scanning data was performed in InstaRecon Engine v2 (InstaRecon, Champaign, IL, USA). Processing and adjusting of the resulting image stacks was done in Fiji (ImageJ 1.52a; Schindelin *et al.*, 2012). Scans were visualised in AMIRA 6.5.0 (FEI Visualization Sciences Group, Bordeaux, France). Longitudinal sections through the 3D-flower models were created using the slice function. Slices were manually adjusted. The surface of the flower was rendered based on labelling of the entire flower. Labelling was done semiautomatically in the segmentation module of AMIRA in the histogram option. The histogram was manually adjusted between ∼3500 – ∼10000 and 65536 at 16-bit and 15 – 25 and 256 at 8-bit, respectively. The selection was smoothed and 'remove islands' set to 50 pixels was applied to the segmented volume. Surfaces were rendered with the surface generation tool (compactify enabled; constrained smoothing of the surface set to 5).

4.3 Results

Faucal scales

Development. In total, 18 of the 29 species in our sampling have faucal scales and for twelve of these 18 species we studied their development.

Faucal scale development, in general, is initiated in late stages of flower development and correlates with the elongation of the (apical part of the) corolla tube. Faucal scales are always localised above or at the level of the insertion points of the filaments in antepetalous position. *Rindera lanata* is the only exception, where the faucal scales are inserted below the filaments. The speed of their development and their development in relation to the apical part of the corolla tube varies between the species. Rapid faucal scale development is present in *Borago officinalis* where the scales are initiated close to anthesis and rapidly reach their final morphology and size. The position of the faucal scales in relation to the sinuses of the corolla lobes and the insertion points of the filaments often changes throughout their development. Either the part of the tube beneath the faucal scales and above the points of filament insertion or the part between faucal scales and corolla lobe sinuses elongates, or both elongate differentially.

Faucal scale development often coincides with simple and glandular trichomes and papillae in the same position. In most species trichomes are initiated during faucal scale development, but in some species (e.g., *Lithospermum officinale*, *Aegonychon purpurocaeruleum*) scale development is preceded by trichome development. In some species, bands of trichomes or papillae bridge the space between neighbouring faucal scales (e.g., *Omphalodes cappadocica*). These bands form early in faucal scale development.

In the following, four species as examples from the Echiochiloideae, Boraginoideae – Boragineae and Lithospermeae – and Cynoglossoideae are used to describe the development of faucal scales in the Boraginaceae (Fig. 4.2).

In *Ogastemma pusillum* (Echiochiloideae, Fig. 4.2A–C), the faucal scales are initiated in late flower development. They start off as simple bulges above and between the tips of the anthers and close to the sinuses of the corolla lobes. Their relative position to the anthers changes towards anthesis, as the apical part of the corolla tube elongates between stamens and faucal scales. At anthesis, the faucal scales are glabrous invaginations.

In *Anchusa officinalis* (Boraginoideae, Boragineae, Fig. 4.2D–F), faucal scales are inserted as sharp-edged protuberances at the end of elongate ridges which protrude down to the base of the corolla tube. The protuberances fit between the neighbouring anthers. Shortly after, broad, triangulate invaginations form at the positions of the protuberances and elongate acroscopically. The bulges are dorsally restricted by the corolla tube wall and ventrally by the anthers. They are inserted at the level of the corolla lobe sinuses and with some distance to the insertion points of the filaments. After onset of invagination, first trichomes and papillae on the faucal scales are initiated. At anthesis, faucal scales are elongate triangulate, margins and the dorsal surface are covered with papillae and short trichomes. The tips of the faucal scales are blunt and have slightly longer, straight trichomes pointing towards the centre of the flower. The position of the faucal scales relative to the insertion points of the filaments does not change during development, but the apical part of the corolla tube elongates above the faucal scales.

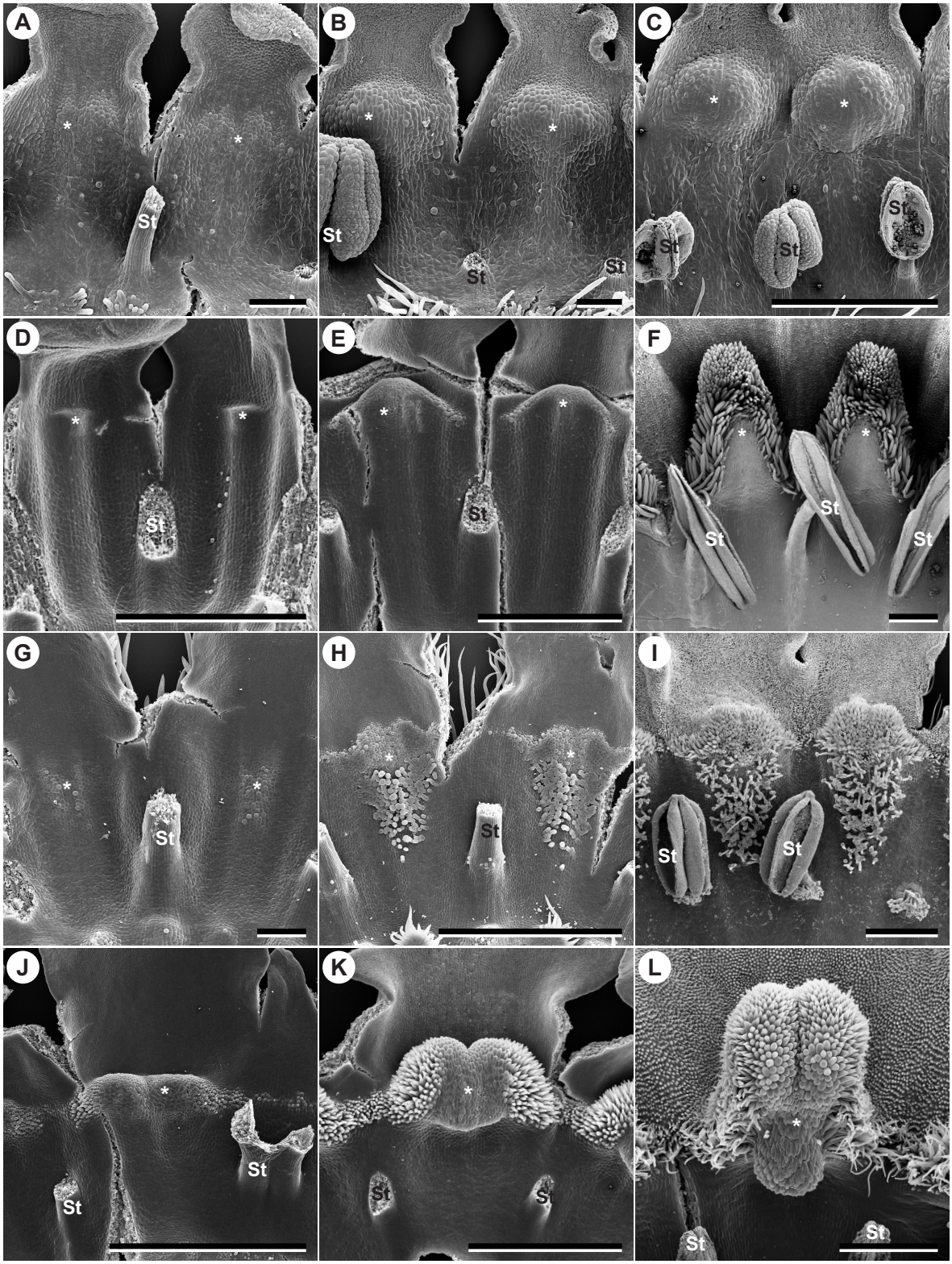

Figure 4.2: Faucal scale development. Development of the faucal scales in four species representing all three subfamilies and the two major clades of the Boraginaceae. A–C, *Ogastemma pusillum* (Echiochiloideae). A, onset of faucal scale development. B, intermediate state of faucal scale development. C, faucal scales at anthesis. D–I, Boraginoideae. D-F, *Anchusa officinalis* (Boragineae, Boraginoideae). D, onset of faucal scale development as protuberances of the corolla tube. E, intermediate state of faucal scale development. F, faucal scales at anthesis. G–I, *Lithospermum officinale* (Lithospermeae, Boraginoideae). G, onset of faucal scale development. H, intermediate stage of faucal scale development. I, faucal scales at anthesis. J–L, *Omphalodes cappadocica* (Omphalodeae, Cynoglossoideae). J, young stage of faucal scale development as a slightly bilobed invagination with the onset of papillae development on its margins. K, intermediate state of faucal scale development. L, faucal scale at anthesis. Asterisks (*) denote (the position of) the faucal scales. St = stamen. In several stages, anthers needed to be removed. Scale bars: A, B, G = 100 µm, C–F, H–L = 500 µm

In *Lithospermum officinale* (Lithospermeae, Boraginoideae, Fig. 4.2G–I), onset of faucal scale development is preceded by the initiation of glandular trichomes in antepetalous position on the distal part of the corolla tube. Trichome development is followed by the onset of invagination of the tube in these positions, which is accompanied by an increase in glandular trichome number at the bases and papillae on the apical parts of the slightly bilobed faucal scales. At anthesis, the scales only slightly overlap the corolla tube. Apart from patches of glandular trichomes below the actual faucal scales, the enclosed part of the corolla tube is glabrous. Faucal scales, apical part of the corolla tube and corolla lobes are covered with papillae. The position of the faucal scales shifts during their development. They are inserted closer to the insertion points of the filaments than to the sinuses of the corolla lobes. Their relative position to the corolla lobes remains constant, while the relative distance between faucal scales and insertion points of the filaments increases until anthesis.

In *Omphalodes cappadocica* (Cynoglossoideae, Fig. 4.2J–L), faucal scale development starts with slightly bilobed invaginations of the corolla tube. The onset of scale development is accompanied by the onset of papillae formation on the lateral margins and between neighbouring scales. During development of the scales, they become increasingly deeply bilobed and the development of papillae proceeds along their lateral margins. Shortly before anthesis, the basal part of the faucal scales invaginates, forming one hollow appendage on the base of each faucal scale. At anthesis, the notably bilobed faucal scales are covered with papillae of various lengths and neighbouring scales are interconnected by a band of elongate papillae or simple trichomes.

Morphological diversity. In all species studied, faucal scales are antepetalous (Fig. 4.3). Only in *Trichodesma indicum* (Fig. 4.3H), modifications of the apical part of the corolla tube are localised in an antesepalous position. Faucal scales are usually localised above the insertion points of the filaments, with *Rindera lanata* (Fig. 4.3L) as the only exception. Faucal scales are always hollow invaginations of the corolla tube.

The appearance of the faucal scales is quite variable. It ranges from simple, shallow invaginations accompanied by differentiated epidermis (*Borago pygmaea*, Fig. 4.3B, *Amsinckia spectabilis*, Fig. 4.3J) to elaborate structures (e.g., *Borago officinalis*, Fig. 4.3C, *Omphalodes cappadocica*, Fig. 4.2J–L). Less elaborate scales usually do not overlap the corolla tube. They invaginate from the corolla tube, but taper either gradually or abruptly into the surrounding corolla tube. Examples for less elaborate faucal scales are *Ogastemma pusillum* (Fig. 4.2A–C), *Alkanna graeca* (Fig. 4.3E) and *Aegonychon purpurocaeruleum* (Fig. 4.3F). Elaborate scales are present in a variety of shapes. Elongate triangular scales are present in *Symphytum officinale* and *S. tuberosum* (Fig. 4.3D), triangulate, but blunt scales are present in *Anchusa azurea* and *A. officinalis* (Fig. 4.2D–F). Partially bilobed faucal scales are present in *Nonea lutea* (Fig. 4.3A), *Borago officinalis* (Fig. 4.3C), *Lithospermum officinale* (Fig. 4.2G–I), *Omphalodes cappadocica* (Fig. 4.2J–L), *Myosotis sylvatica* (Fig. 4.3I), *Cynoglossum australe* (Fig. 4.3K) and *Rindera lanata* (Fig. 4.3L).

The epidermis of the faucal scales is variously differentiated. Glabrous scales are present in *Ogastemma pusillum* (Fig. 4.2A–C), *Alkanna graeca* (Fig. 4.3E) and *Caccinia strigosa* (Fig. 4.3G). The epidermis of the scales in *Alkanna graeca* (Fig. 4.3E) and *Caccinia strigosa* (Fig. 4.3G) is rough and irregular compared to the smooth epidermis of the corolla lobes and tube. Quite common are papillae, simple trichomes and transitions from papillae to simple trichomes growing on and between the faucal scales (e.g., *Symphytum officinale*, *S. tuberosum*, Fig. 4.3D, *Myosotis sylvatica*, Fig. 4.3I). Less common are glandular trichomes (e.g., *Lithospermum officinale*, Fig. 4.2G–I, *Aegonychon purpurocaeruleum*, Fig.

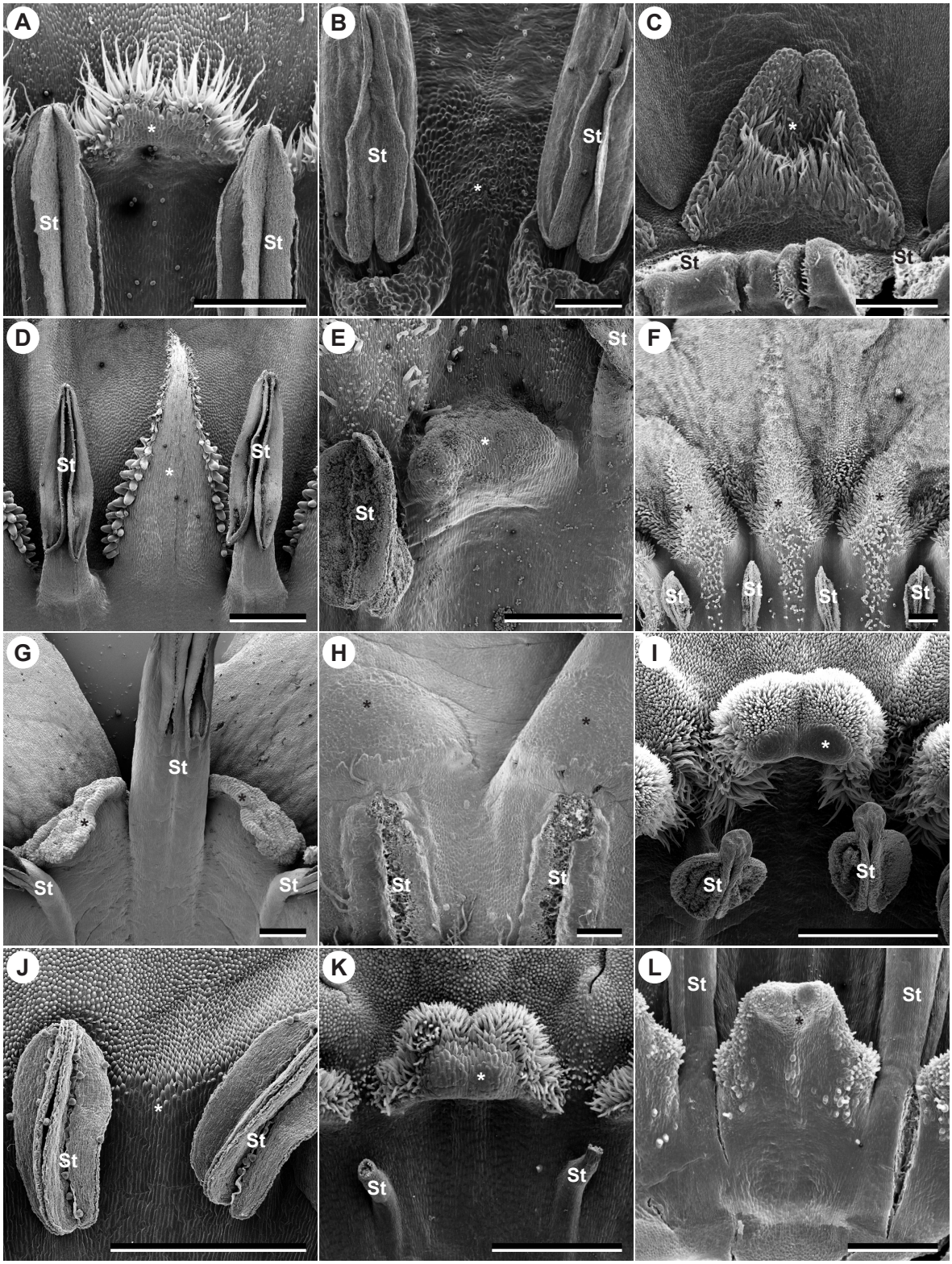

Figure 4.3: Diversity of faucal scales. A–D, Boragineae, Boraginoideae. A, *Nonea lutea*. B, *Borago pygmaea*. C, *Borago officinalis*. D, *Symphytum tuberosum*. E, F, Lithospermeae, Boraginoideae. E, *Alkanna graeca*. F, *Aegonychon purpurocaeruleum*. G–L, Cynoglossoideae. G, H, Trichodesmeae. G, *Caccinia strigosa*. H, *Trichodesma indicum*. I, *Myosotis sylvatica* (Myosotideae). J–L, Cynoglosseae. J, *Amsinckia spectabilis*. K, *Cynoglossum australe*. L, *Rindera lanata*. Asterisks (*) denote (the position of) the faucal scales. St = stamen. In several species, anthers needed to be removed. Scale bars: A–L = 500 µm

4.3F), which are usually located not directly on the faucal scales, but beneath them inside the corolla tube.

Basal scales

Development. Basal scales are discernible in 27 of the 29 species in our sampling. For 20 species, the development of the basal scales was investigated.

Basal scales are protuberances of the basal part of the corolla tube. They are initiated in late flower development and develop during the elongation of the basal part of the corolla tube. There are usually ten basal scales per flower: five scales in antepetalous and five in antesepalous position. The scales in antesepalous position are inserted on the bulges of the adnate parts of the filaments. The antepetalous set of scales in inserted between the bulges of the filaments, either as clearly separated structures, or on a common, shallow ring above the very base of the corolla (e.g., *Anchusa officinalis*, Fig. 4.4D–F). The sequence of development of both sets of scales varies between the species. Either the antesepalous or the antepetalous scales are initiated first, or both sets of scales arise subsimultaneously. The insertion of the basal scales is always beneath the anthers and at the level of the upper half of the nectary disc. The position of the basal scales relative to the insertion points of the filaments changes shortly before anthesis when the basal part of the corolla tube elongates, increasing the distance between scales and level of filament insertion. In some species (e.g., *Borago officinalis*, Fig. 4.5A, *Podonosma orientalis*, Fig. 4.5C, *Myosotis sylvatica*, Fig. 4.5J), the tube below the basal scales elongates slightly. This elongation is correlated with an increase in ovary and nectar disc diameter. In anthetic flowers, basal scales are either present or absent, in the latter case this is generally due to secondary reduction: In *Rindera lanata* (Fig. 4.5L) basal scales are initiated in late development, but their development stagnates during corolla tube elongation, so that they are present only as shallow bulges in anthetic flowers.

Trichomes and papillae growing on the basal scales are initiated either before, subsequently or after onset of scale development. The development of the typical indumenta of basal scales is subsimultaneous for all 10 scales (e.g., *Omphalodes cappadocica*, Fig. 4.4K). It may also be disjunct between both sets of scales with trichomes developing first on either the antesepalous (e.g., *Anchusa officinalis*, Fig. 4.4E) or the antepetalous scales (e.g., *Lithospermum officinale*, Fig. 4.4H). In some species, basal scales arise from a common ring (annulus). This annulus develops later in basal scale ontogeny (e.g., *Podonosma orientalis*, Fig. 4.5C). This pattern of late development can be observed for all types of basal scale elaborations (e.g., basal scale triplets in *Borago officinalis*, Fig. 4.5A)

Four species from the Echiochiloideae, Boraginoideae – Boragineae and Lithospermeae – and Cynoglossoideae are exemplarily used to describe the development of basal scales in the Boraginaceae in the following:

In *Ogastemma pusillum* (Echiochiloideae, Fig. 4.4A–C), basal scale development is preceded by patches of simple trichomes developing in antepetalous and antesepalous positions. Trichomes in antepetalous position appear earlier in development. Throughout development, the trichomes are the most prominent feature of the basal scales. Close to anthesis, the corolla tube in position of the trichome patches bulges and forms the actual basal scales. The trichomes are on the proximal or basal surface of the scales. The basal part of the corolla tube between scales and points of filament insertion slightly elongates until anthesis. The scales in antepetalous position are slightly larger than those in antesepalous position. The actual size and shape of the scales is influenced by their relative position

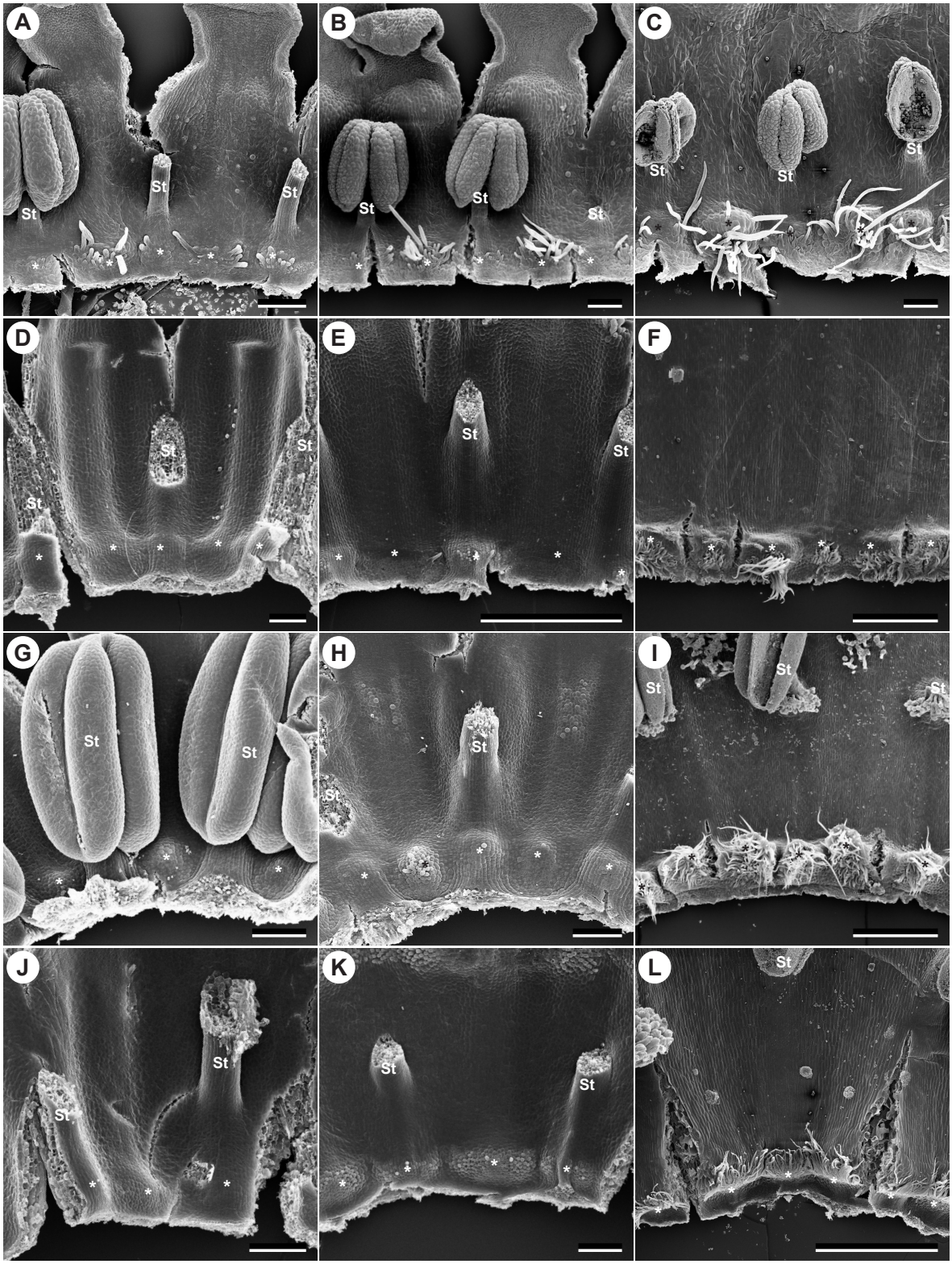

Figure 4.4: Basal scale development. Development of the basal scales in four species representing all three subfamilies and the two major clades of the Boraginaceae. A–C, *Ogastemma pusillum* (Echiochiloideae). A, young developmental stage of the basal scales. B, intermediate developmental stage. C, basal scales at anthesis. D–F, *Anchusa officinalis* (Borageineae, Boraginoideae). D, onset of basal scale development. E, intermediate developmental stage. F, basal scales at anthesis. G–I, *Lithospermum officinale* (Lithospermeae, Boraginoideae). G, onset of basal scale development. H, intermediate developmental stage. I, basal scales at anthesis. J–L, *Omphalodes cappadocica* (Omphalodeae, Cynoglossoideae). J, onset of basal scale development. K, intermediate developmental stage. L, basal scales at anthesis. Asterisks (*) denote (the position of) the basal scales. St = stamen. In several stages, anthers needed to be removed. Scale bars: A–D, G, H, J, K = 100 µm, E, F, I, L = 500 µm

to the mericarps. Scales at the position between two neighbouring mericarps are more pronounced and often slightly asymmetrical (Fig. 4.4C).

In *Anchusa officinalis* (Boraginoideae, Boragineae, Fig. 4.4D–F), the basal scales are inserted on a common, shallow ring. The adnate parts of the filaments emerge over the basal part of the corolla tube and bulge in the position of the antesepalous basal scales. The antesepalous basal scales develop before the scales in antepetalous positions are initiated. Bulges of tissue can be observed before trichomes on the scales are initiated during intermediate developmental stages. In late development, the scales and trichomes in antepetalous position are initiated. The basal part of the corolla tube elongates throughout development. Antepetalous scales are slightly larger than those in antesepalous position at anthesis. Trichomes are predominantly located on the basal side of the scales. The actual shape of the scales is influenced by their relative position to the mericarps (Fig. 4.4F).

In *Lithospermum officinale* (Lithospermeae, Boraginoideae, Fig. 4.4G–I), at first the basal scales in antepetalous position are initiated as conical bulges between the adnate filaments. They are followed by the scales in antesepalous position, but only after the basal part of the corolla tube elongates noticeably. Trichomes are initiated simultaneously on the scales in antepetalous position. The basal part of the corolla elongates throughout scale development. Antepetalous basal scales are slightly larger than antesepalous scales at anthesis. Simple trichomes are located on the basal surfaces of the glands, their apical surface is glabrous. There are only narrow gaps between the individual scales. There is a short section of the basal part of the corolla tube below the basal scales (Fig. 4.4I).

In *Omphalodes cappadocica* (Cynoglossoideae, Fig. 4.4J–L), basal scales are initiated subsimultaneously. At the onset of development, the scales in antesepalous position correspond in their width to the width of the adnate parts of the filaments. The scales in antepetalous position are approximately twice as wide. Trichome development is initiated in intermediate developmental stages and takes place simultaneously on both sets of basal scales. During development, the width of the basal scales in antesepalous position increases. Throughout basal scale development, the basal part of the corolla tube elongates. At anthesis, the actual scales are rather inconspicuous. Most prominent are the simple trichomes on the scales, which form a ring around the base of the corolla tube. A short elongation of the basal part of the corolla tube beneath the basal scales is formed shortly before anthesis (Fig. 4.4L).

Morphological diversity. The majority of the species here studied have basal scales. The usual number of basal scales is ten. Only in *Trichodesma indicum* just five modifications of the basal part of the corolla tube in antesepalous positions are present. Similarly, in *Trichodesma scottii* there are five modifications in antesepalous positions, but also a shallow annulus close to the base of the corolla tube. In *Cerinthe major*, basal scales form an annulus from the onset of their development and no individual scales are differentiated (Fig. 4.5D). An annulus with distinguishable scales is formed in *Borago officinalis* (Fig. 4.5A), *Podonosma orientalis* (Fig. 4.5C) and *Aegonychon purpurocaeruleum* (Fig. 4.5H). There is a gradual transition between separate scales and an annulus with noticeable scales. In *Omphalodes cappadocica* (Fig. 4.4J–L), the trichome-covered scales form a seemingly uninterrupted ring, while remaining separate. In some species basal scales are only rudimentary but differentiated throughout development (e.g., *Glandora oleifolia*, Fig. 4.5G), *Rindera lanata*, Fig. 4.5L) or replaced by trichome patches at anthesis (e.g., *Caccinia strigosa*, Fig. 5I). Basal scales are absent in only two species in our sampling (*Moltkia aurea*, *Amsinckia spectabilis*).

Size relations between antesepalous and antepetalous scales vary between species. Size differences between the scales can be minute and several species appear to have similarly sized basal scales (e.g. *Anchusa officinalis*, Fig. 4.4F). Most common are larger antepetalous and smaller antesepalous scales

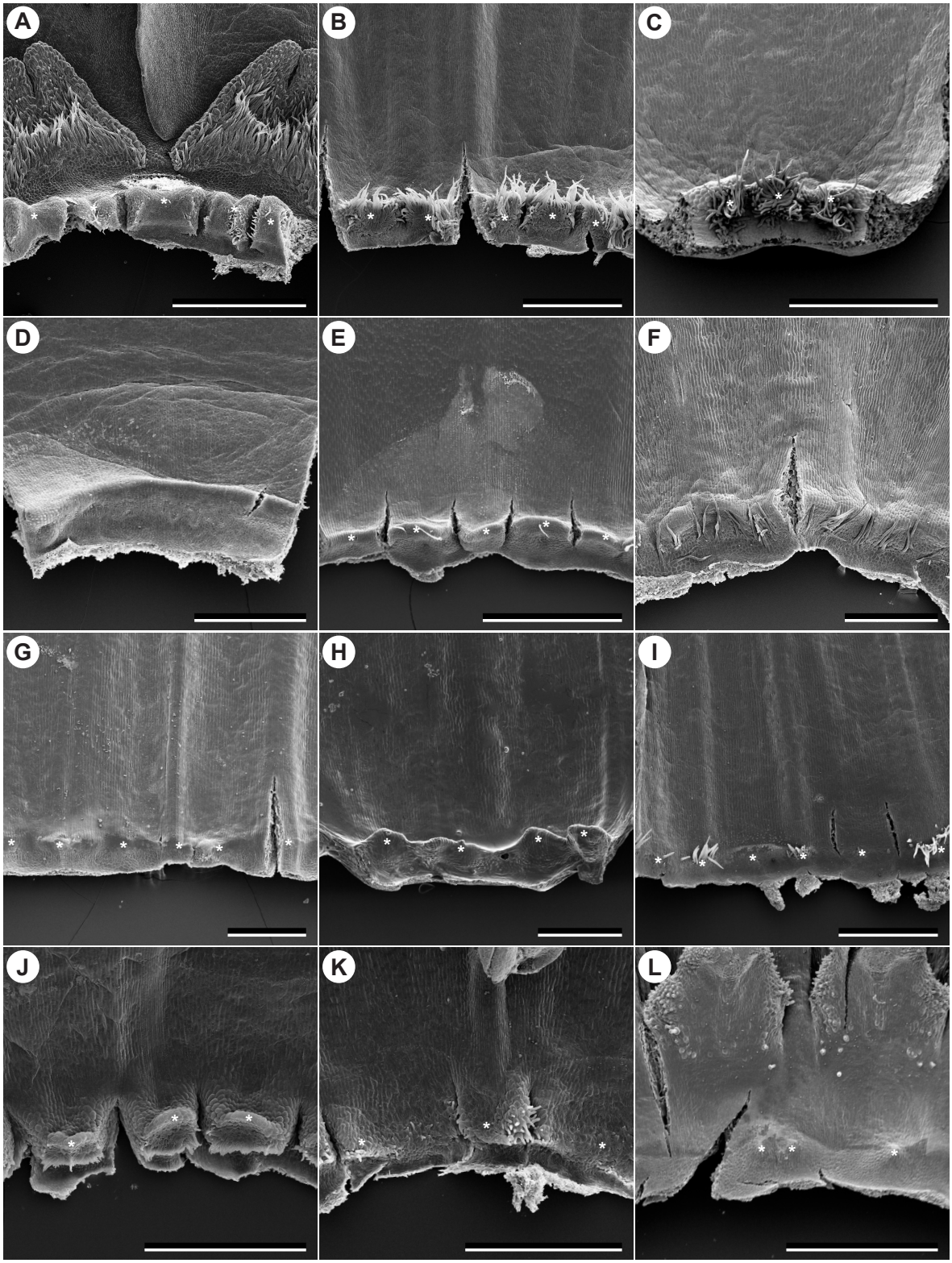

Figure 4.5: Diversity of basal scales. A, B, Boragineae, Boraginoideae. A, *Borago officinalis*. B, *Symphytum officinale*. C–H, Lithospermeae, Boraginoideae. C, *Podonosma orientalis*. D, *Cerinthe major*. E, *Onosma alborosea*. F, *Echium wildpretii*. G, *Glandora oleifolia*. H, *Aegonychon purpurocaeruleum*. I-L, Cynoglossoideae. I, *Caccinia strigosa* (Trichodesmeae). J, *Myosotis sylvatica* (Myosotideae). K, L, Cynoglosseae. K, *Cynoglossum australe*. L, *Rindera lanata*. Asterisks (*) denote the basal scales. Scale bars: A–C, E, I, L = 1 mm, D, F–H, J, K = 500 µm

(e.g., *Omphalodes cappadocica*, Fig. 4.4L). The actual size and shape of the scales, however, varies with their position in relation to the four mericarps of the gynoecium. Scales fully or partially facing a gap between the mericarps are usually larger and longer than those directly facing a mericarp. In some cases scales facing the ovary are asymmetric or shifted towards the gap (e.g., *Borago officinalis*, Fig. 4.5A, *Cynoglossum australe*, Fig. 4.5K) or almost completely reduced (e.g. *Ogastemma pusillum*, Fig. 4.4C, *Anchusa officinalis*, Fig. 4.4F). In *Borago officinalis*, basal scales are bilobed (Fig. 4.5A). Half of each of the broader and shallower antesepalous scales form groups with the narrower, but larger antepetalous scales. These groups appear as five triplets of basal scales in the anthetic flower.

The position of the basal scale at the base of the corolla tube is rather conserved. In some species, however, there is a short tube beneath the location of the scales (e.g. *Borago officinalis*, Fig. 4.5A, *Echium wildpretii*, Fig. 4.5F, *Myosotis sylvatica*, Fig. 4.5J).

Trichomes growing on the basal scales are quite common. In most species, the trichomes grow from the downwards facing side of the scales and often protrude apically (e.g., *Symphytum officinale*, Fig. 4.5B). In *Borago officinalis* (Fig. 5A) and *Cynoglossum australe* (Fig. 4.5K), short, simple trichomes grow in the gaps between the scales. In *Onosma alborosea*, only a few trichomes appear randomly on the scales (Fig. 4.5E). In *Trichodesma indicum* long trichomes grow laterally from the basal scales right below the insertion points of the filaments and form a layer inside the corolla tube. Glabrous scales are present in a number of species (e.g, *Cerinthe major*, Fig. 4.5D, *Aegonychon purpurocaeruleum*, Fig. 4.5H, *Rindera lanata*, Fig. 4.5L).

Comparison of faucal and basal scale development

Both types of scales develop in late stages of flower ontogeny which coincides with the onset of stamen-corolla tube elongation. The development of the faucal and basal scales correlates to the differential elongation of the basal and apical parts of the corolla tube, respectively.

Onset of faucal scale development shows no clear correlation to the onset of basal scale development. Faucal and basal scales develop either subsimultaneously, (e.g. *Ogastemma pusillum*, Figs 4.2A–C, 4.4A–C), or one type of scale precedes the other. Basal scales developing before faucal scales are found in *Borago officinalis*, *Lithospermum officinale* (Figs 4.2G–I, 4.4G–I), *Alkanna graeca* and *Omphalodes cappadocica* (Figs 4.2J–L, 4.4J–L). Faucal scales develope before basal scales are found in *Anchusa officinalis* (Figs 4.2D–F, 4.4D–F) and *Caccinia strigosa*.

Nectary disc

All species in the sampling of this study have a nectary disc at the base of the ovary. The nectary disc differs from the upper part of the ovary by its larger epidermis cells with prominent outer cell walls and by the presence of nectarostomata.

The nectary disc is either entire or deeply incised between the mericarps. In some species with an entire nectary disc a bulge of the disc develops between the mericarps belonging to the same carpel (e.g., *Cynoglossum australe*, Fig. 4.6K, L, *Mertensia paniculata*, *Rindera lanata*). Entire nectary discs are present for example in *Ogastemma pusillum* (Fig. 4.6A, B), most Lithospermeae (e.g., *Podonosma orientalis*, Fig. 4.6E, F), and all Cynoglossoideae (Fig. 4.6G–L). Within the Boragineae, the nectary disc of *Borago pygmeae* is more or less entire. Within the Lithospermeae, *Cerinthe major* shows a different morphology, as the mericarps of one carpel remain attached to each other and additionally

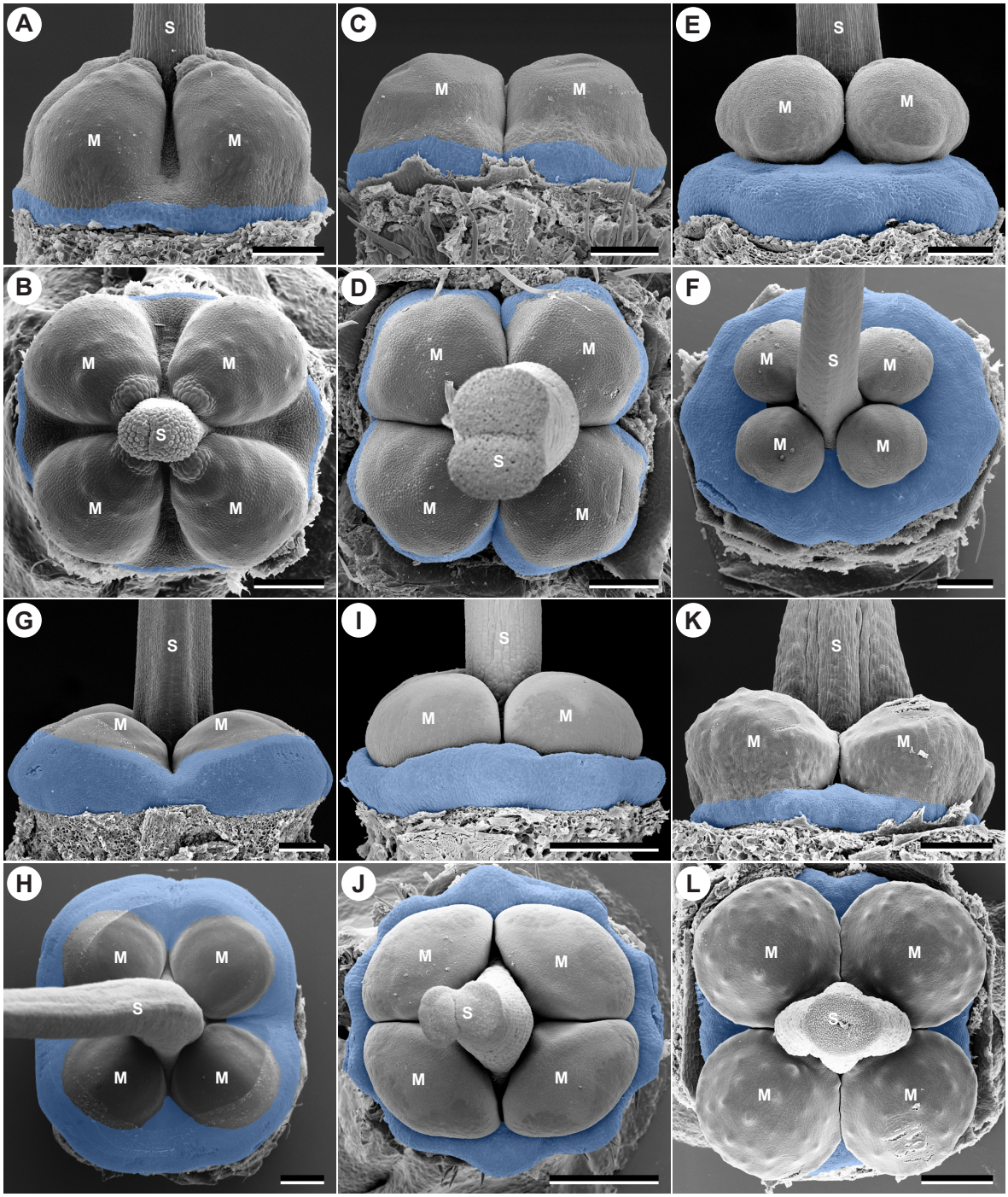

Figure 4.6: Ovary and nectary disc at anthesis. The nectary disc, defined as the part which is covered with nectarostomata, is highlighted in blue. A, B, *Ogastemma pusillum* (Echiochiloideae). C–F, Boraginoideae. C, D, *Anchusa officinalis* (Boragineae). E, F, *Podonosma orientalis* (Lithospermeae). G–K, Cynoglossoideae. G, H, *Caccinia strigosa* (Trichodesmeae). I, J, *Myosotis sylvatica* (Myosotideae). K, L, *Cynoglossum australe* (Cynoglosseae). M = mericarp, S = style and stigma. Scale bars: A, B = 100 µm, C–L= 200 µm

the nectary disc between the carpels is reduced. A deeply incised nectary disc is present only in Boragineae (e.g., *Anchusa officinalis*, Fig. 4.6C, D). The nectary disc either exceeds or equals the width of the mericarps at their widest circumference, or the disc is largely hidden beneath the mericarps and visible from above only between the mericarps. In some species, the nectary disc develops into a prominent, distinct ring at the base of the mericarps. This is the case in some Cynoglossoideae species (e.g., *Mertensia paniculata*, *Lappula sessiliflora*, *Myosotis sylvatica*, Fig. 4.6I, J). The nectary

disc is regularly lobed in some species (e.g. *Podonosma orientalis*, Fig. 4.6E, F, *Myosotis sylvatica*, Fig. 4.6I, J). Nectarostomata on the nectary disc are present in all species. Their location, density and distribution on the disc is slightly variable between the species studied. Typical conditions are as follows: In *Ogastemma pusillum* (Fig. 4.6A, B), nectarostomata are located on the basal part of the disc in a relatively high density compared to other species in our sampling. In *Anchusa officinalis* (Fig. 4.6C, D), nectarostomata are located on the downwards facing part of the disc and are relatively sparse. The massive nectary disc of Podonosma orientalis is regularly covered with nectarostomata on its entire apical facing surface (Fig. 4.6E, F). In *Caccinia strigosa* (Fig. 4.6G, H), nectarostomata in low density are located on the basal surface of the disc. In *Myosotis sylvatica* (Fig. 4.6I, J), the entire surface of the disc is covered with nectarostomata. In *Cynoglossum australe* (Fig. 4.6K, L), nectarostomata in intermediate density are located on the lateral and downward facing parts of the nectary disc.

Floral architecture

Stamen-corolla tube shape. A common architectural feature of all flowers here studied is the formation of a distinct stamen-corolla tube. The length of the corolla tube in relation to the corolla lobes varies between the species. *Borago officinalis* (Fig. 4.1B) has a short corolla tube and large, spreading corolla lobes. A long corolla tube versus reduced corolla lobes is found, e.g., in *Cerinthe major* (Fig.4.1E). The basal part of the corolla tube varies mainly in its relative length compared to the overall corolla tube. The apical part of the corolla tube shows some more variation between the species. If faucal scales are present, the lower portion of the tube is usually cylindrical, while the apical portion can be erect, spreading or nearly absent. Apart from the size variation in the corolla lobes and their relative length compared to the corolla tube, the way they spread, are recurved or erect contribute to overall flower shape. Spreading corolla lobes are most common. The flower shape of *Borago officinalis* is dominated by spreading corolla lobes (Fig. 4.1B). It is the only species in our sampling with a subrotate corolla. The most common combination found across all subfamilies is a cylindrical corolla tube and spreading corolla lobes resulting in a hypocrateriform flower (e.g. *Anchusa officinalis*, Fig. 4.1A, and *A. azurea*, *Caccinia strigosa*, Fig. 4.1H, *Omphalodes cappadocica*, Fig. 4.1J, *Myosotis sylvatica*, *Cynoglossum australe*). Most common are infundibuliform corollas (e.g., *Aegonychon purpurocaeruleum*, Fig. 4.1F, *Echium vulgare*, Fig. 4.1G, *Amsinckia spectabilis*, Fig. 4.1L). Less common are campanulate corollas (*Borago pygmaea*, *Trichodesma scottii*) and tubular (*Symphytum tuberosum*, Fig. 4.1C, *S. officinalis*) to urceolate corollas (e.g., *Podonosma orientalis*, Fig. 4.1D, *Rindera lanata*, Fig. 4.1K).

Faucal scales and floral architecture. Faucal scales are located on the apical part of the corolla tube. Their presence or absence and shape and position in relation to the corolla tube appears to be independent of overall corolla shape. In hypocrateriform and infundibuliform flowers, faucal scales are either absent (*Echium wildpretii*, *E. webbii*, *E. vulgare*, Fig. 4.1G), present at the transition between the tubular and the spreading part of the corolla (e.g., *Anchusa officinalis*, Figs 4.1A, 4.2F, 4.7G, H, *A. azurea*, *Myosotis sylvatica*, Figs 4.3I, 4.7I, J, *Cynoglossum australe*, Fig. 4.7K, L) or hidden inside the corolla tube (e.g., *Alkanna graeca*, Fig. 4.3E). In *Borago officinalis* (Figs 4.1B, 4.3C, 4.7C, D), with a subrotate corolla, the faucal scales are openly presented close to the sinuses of the corolla lobes. In both species with campanulate flowers, *Borago pygmaea* and *Trichodesma scottii*, faucal scales are reduced, respectively. In species with tubular corollas, faucal scales are either present and

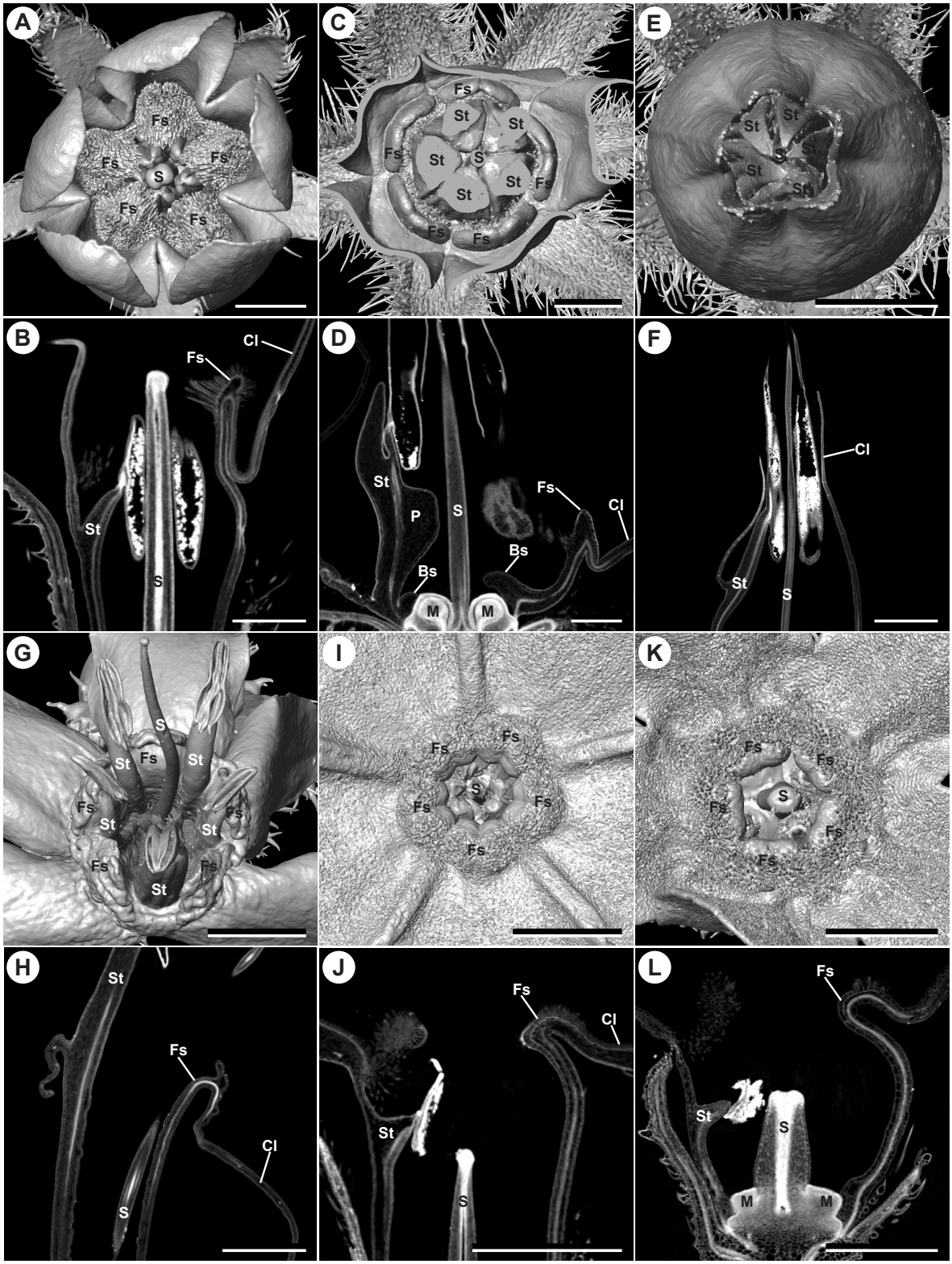

Figure 4.7: Faucal scales and their integration into floral architecture. Displayed are surface renderings and virtual longitudinal sections through the same digital model for six species. A–F, Boraginoideae. A–D, Boragineae. A, B, *Anchusa officinalis*. A, surface rendering of the flower viewed from apical. B, virtual longitudinal section. C, D, *Borago officinalis*. C, surface rendering of the flower viewed from apical. Anthers, style and most of the corolla lobes have been removed digitally. D, virtual longitudinal section. Note the modifications of the filament. E, F, *Podonosma orientalis* (Lithospermeae). E, surface rendering of the flower viewed from apical. At this stage the corolla lobes are erect. F, virtual longitudinal section. G–L, Cynoglossoideae. G, H, *Caccinia strigosa* (Trichodesmeae). G, surface rendering of the flower viewed from apical. H, virtual longitudinal section. I, J, *Myosotis sylvatica* (Myosotideae). I, surface rendering of the flower viewed from apical. J, virtual longitudinal section. K, L, *Cynoglossum australe* (Cynoglosseae). K, surface rendering of the flower viewed from apical. L, virtual longitudinal section. Cl = corolla lobe, Bs = basal scale, Fs = faucal scale, M = mericarp, P = pedestal, S = stigma, St = stamen. Scale bars: A, B, G–L = 1 mm, C–F = 2 mm

hidden inside the tube (*Symphytum officinale*, *S. tuberosum*, Fig. 4.1C, *Rindera lanata*, Fig. 4.1K), or absent (*Onosma alborosea*, *Podonosma orientalis*, Figs 4.1D, 4.7E, F, *Cerinthe major*, Fig. 4.1E). The majority of flowers in our sampling are actinomorphic. Species with zygomorphic flowers are *Echium wildpretii*, *E. webbii*, *E. vulgare* (Fig. 4.1G) and *Caccinia strigosa* (Figs 4.1H, 4.7G, H). Faucal scales are absent in *Echium*, but present in *Caccinia strigosa* (Figs 4.1H, 4.3G, 4.7G, H).

The position of the faucal scales – usually above the insertion points of the filaments – is in spatial relation to the anthers. Anthers are either fully exserted, partially exserted or included in the corolla tube. Fully exserted anthers are present in *Borago officinalis* (Figs 4.1B, 4.7D), *Moltkia aurea*, *Echium wildpretii*, *E. webbii*, *E. vulgare* (Fig. 4.1G) and *Caccinia strigosa* (Figs 4.1H, 4.7G, H). Faucal scales are present in *Borago officinalis* and *Caccinia strigosa*. In *Borago officinalis*, the faucal scales form a ring around the enlarged filament bases (Figs 4.1B, 4.7C). In *Caccinia strigosa*, they form a reinforced entrance to the corolla tube (Figs 4.1H, 4.7G). Partially exserted anthers are present in three species: *Podonosma orientalis* (Figs 4.1D, 4.7E, F), *Trichodesma indicum* (Fig. 4.1I), and *Rindera lanata* (Fig. 4.1K). Faucal scales are absent in *Trichodesma indicum* and *Podonosma orientalis*, while fully developed in *Rindera lanata*. Anthers are partially exserted from the tube but hidden between the erect and connivent corolla lobes. In the remaining species, the anthers are included in the corolla tube, independent of the presence of faucal scales. Anther inclusion differs between species. In *Ogastemma pusillum*, *Lithospermum officinale*, *Aegonychon purpurocaeruleum* (Fig. 4.1F), *Myosotis sylvatica*, *Omphalodes cappadocica* and *Cynoglossum australe* they are hidden deep inside the corolla tube, below the faucal scales. In all Boragineae (except *Borago officinalis*, Fig. 4.1B), anthers and faucal scales are at least partially at the same level. The same is true for *Alkanna graeca* and *Amsinckia spectabilis* (Fig. 4.1L). Included anthers in flowers without faucal scales are present in *Huynhia pulchra*, *Cerinthe major* (Fig. 4.1E), *Glandora oleifolia*, *Onosma alborosea* and *Trichodesma scottii*. In most sampled species, the corolla tube above the faucal scales or the insertion points of the filaments is widened compared to the corolla tube below (e.g., *Symphytum tuberosum*, Fig. 4.1C). This leads to the anthers being hidden, but still accessible inside the corolla tube.

Anther position in relation to corolla tube and faucal scales is only one floral architectural aspect, another one is synorganisation between the anthers. The anthers are either free and independent, connivent or modified. Connivent and modified anthers form anther cones. Modified anthers are held together (additionally) through hooks at the base of the thecae (*Cerinthe major*), adhesive interlocking at the base of the thecae (*Onosma alborosea*) or a combination of twisted, connective appendages and intertwined connective trichomes (*Trichodesma indicum* (Fig. 4.1I), *T. scottii*). In species with modified anthers faucal scales are absent. Connivent anthers are held together through architectural constraints. Connivent anthers are present in all Boragineae (except *Nonea lutea*) and associated with faucal scales (except *Borago pygmaea*). These anther cones are reinforced by the faucal scales formed through centripetally orientated filaments (*Anchusa officinalis*, Figs 4.1A, 4.7A, B, *A. azurea*, *Symphytum tuberosum*, Fig. 4.1C, *S. officinale*). In *Borago officinalis* (Fig. 4.7C, D) and *B. pygmaea* (Fig. 4.3B), filament bases are enlarged forming pedestals. In *Borago officinalis*, the pressure of the ring of faucal scales on the pedestals leads to the formation of the anther cone (Figs 4.1B, 4.7C, D). In *Borago pygmaea*, the narrow corolla tube is directly pressed against the pedestals. In species without faucal scales such as *Podonosma orientalis* and *Glandora oleifolia*, the anther cone is formed only through the orientation of the filaments and the shape of the corolla tube. In *Podonosma orientalis*, the anther cone is initially reinforced through erect corolla lobes, which recurve later in anthesis (Figs 4.1D, 4.7E, F). In *Rindera lanata*, faucal scales do not contribute to anther cone formation, instead it is stabilized by the specific filament orientation, the apically narrowing corolla tube and the erect

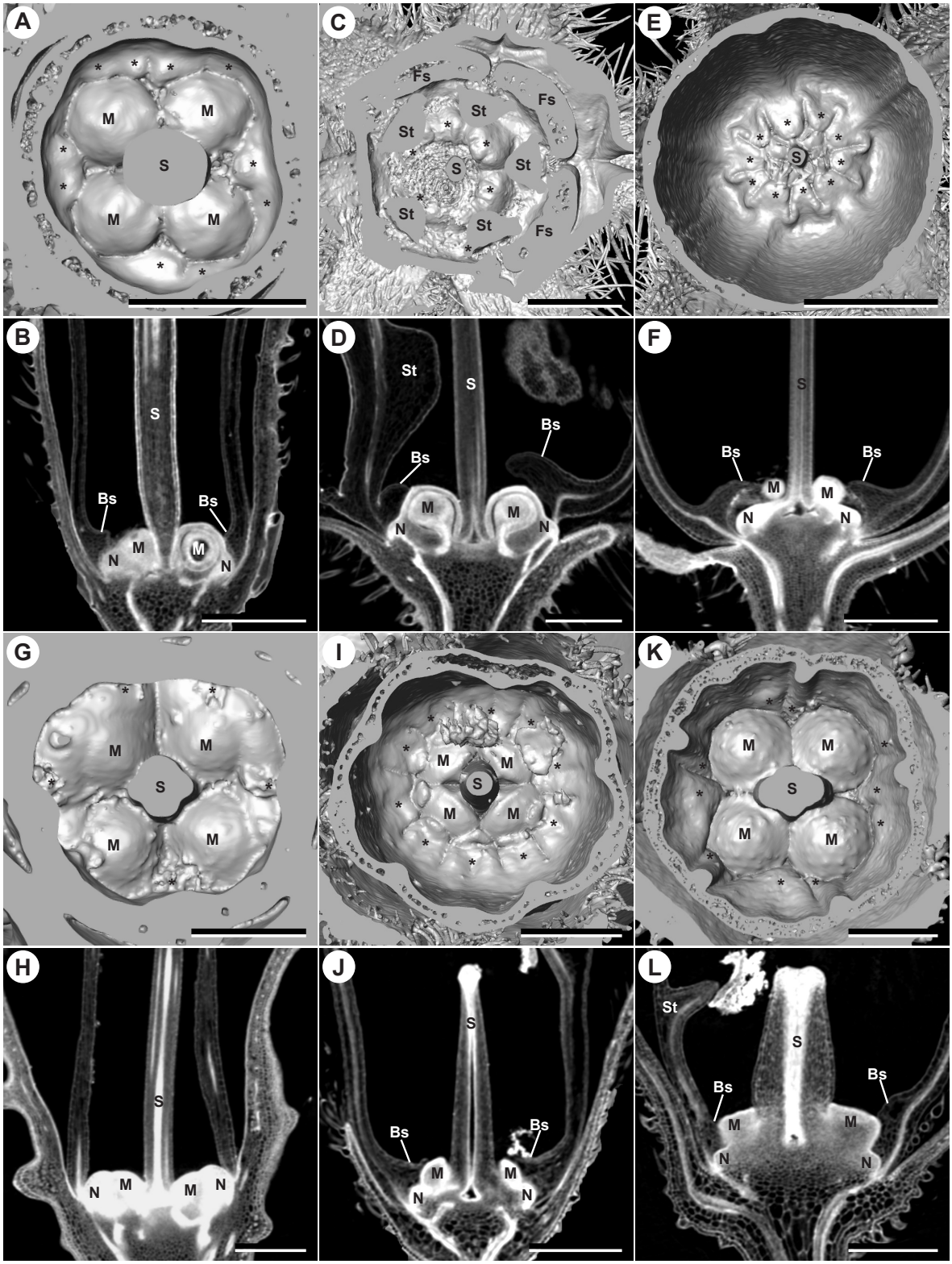

Figure 4.8: Basal scales and their integration into floral architecture. Displayed are surface renderings and virtual longitudinal sections through the same digital model for six species. A–F, Boraginoideae. A–D, Boragineae. A, B, *Anchusa officinalis*. A, surface rendering of the basal part of the flower. B, virtual longitudinal section. C, D, *Borago officinalis*. C, surface rendering of the basal part of the flower. Most of the stamens and faucal scales were digitally removed. Note that some of the basal scales are covered by ring artefacts resulting from µCT scanning. D, virtual longitudinal section. E, F, *Podonosma orientalis* (Lithospermeae). E, surface rendering of the basal part of the flower. F, virtual longitudinal section. G–L, Cynoglossoideae. G, H, *Caccinia strigosa* (Trichodesmeae). G, surface rendering of the basal part of the flower. H, virtual longitudinal section. I, J, *Myosotis sylvatica* (Myosotideae). I, surface rendering of the basal part of the flower. J, virtual longitudinal section. K, L, *Cynoglossum australe* (Cynoglosseae). K, surface rendering of the basal part of the flower. L, virtual longitudinal section. Bs = basal scale, M = mericarp, N = nectary disc, S = stigma, St = stamen. Asterisks (*) denote basal scales in the surface renderings. Scale bars: A, B, D, F–H = 1 mm, C, E = 2 mm, I–L = 500 µm

corolla lobes (Fig. 4.1K). Free and independent anthers can be arranged in relative proximity (e.g., *Ogastemma pusillum*, *Alkanna graeca*, *Myosotis sylvatica*, Fig. 4.7I, J, *Amsinckia spectabilis*, Fig. 4.1L, *Cynoglossum australe*, Fig. 4.7K, L) or distantly from each other (e.g. *Moltkia aurea*, *Echium wildpretii*, *E. webbii*, *E. vulgare*, Fig. 4.1G, *Caccinia strigosa*, Figs 4.1H, 4.7G, H).

Faucal scales in general constrict the entrance of the corolla tube. In *Borago officinalis* and *B. pygmaea*, this is additionally achieved by pedestals at the bases of the filaments (Fig. 4.7D). Additional to faucal scales, corolla tube constriction can be achieved through erect corolla lobes (e.g., *Podonosma orientalis*, Fig. 4.7E, F, *Rindera lanata*, Fig. 4.1K). Another floral architectural feature independent of faucal scales is the formation of grooves towards the base of the flower. These are present in *Echium wildpretii*, *E. webbii*, *E. vulgare* (Fig. 4.1G), *Trichodesma indicum* (Fig. 4.1I) and *T. scottii*. In *Echium*, plications of the corolla tube in the position of the filaments lead to the formation of differentially sized channels. In *Trichodesma*, the reduced filaments with their enlarged filament bases and connectives result in the formation of five channels converging into a chamber above the ovary. This chamber is sealed by simple, intertwining trichomes inserted on the filament bases in *Trichodesma indicum*.

Basal scales and floral architecture. Basal scales are present in most species and their position at the base of the corolla tube is largely conserved. Independent of their size, shape and of whether they form an annulus, they always cover either all of or part of the nectary disc (Fig. 4.8). In some species they even partially cover the mericarps (e.g., *Borago officinalis*, Fig. 4.8C, D, *Podonosma orientalis*, Fig. 4.8E, F, *Myosotis sylvatica*, Fig. 4.8I, J). The irregular shape of the basal scales, resulting from their position relative to the gaps between the mericarps, is a direct result of their synorganisation with the nectary disc (Fig. 4.8A, E, I, K). Only in *Trichodesma indicum* and *T. scottii*, the basal scales are lifted above the level of the nectary disc and closer to the insertion points of the filaments. On the other hand, an annulus at the level of the nectary disc is present in *T. scottii*.

The diameter and height of the nectary disc determines whether a section of the basal part of the corolla tube is formed below the basal scales (e.g., *Borago officinalis*, Fig. 4.8D, *Podonosma orientalis*, Fig. 4.8F, *Myosotis sylvatica*, Fig. 4.8J).

4.4 Discussion

The present study is the first systematic survey of the stamen-corolla tube modifications in the Boraginaceae. And it is the first study to combine ontogenetic, morphological and three-dimensional data to understand development and morphology of the faucal and basal scales, and their integration into floral architecture. A summary of presence, absence and the basic morphology of faucal and basal scales in relation to basic stamen-corolla tube features is shown in figure 4.9. This is in contrast to previous studies, which largely restricted their discussion on faucal scales (Arber, 1939; Schaefer, 1942; Cohen, 2014). The major results from the developmental part of this study are the late onset of faucal and basal scale development and their ontogeny in relation to the anthers and the disc nectary, respectively. Both types of modifications are initiated late in flower ontogeny and can be considered as peramorphoses. Flower development in (some) Boraginaceae is distinctly two-phased (studied in *Amsickia* Lehm., Li & Johnston, 2010). While most of the structures are initiated and elaborated in the constricted space of a small bud in the first phase, the stamen-corolla tube (the filaments and faucal scales) elongate rapidly in the second phase, providing space for the development of the final configuration. One consequence of this two-phased floral development is that all structures have to be

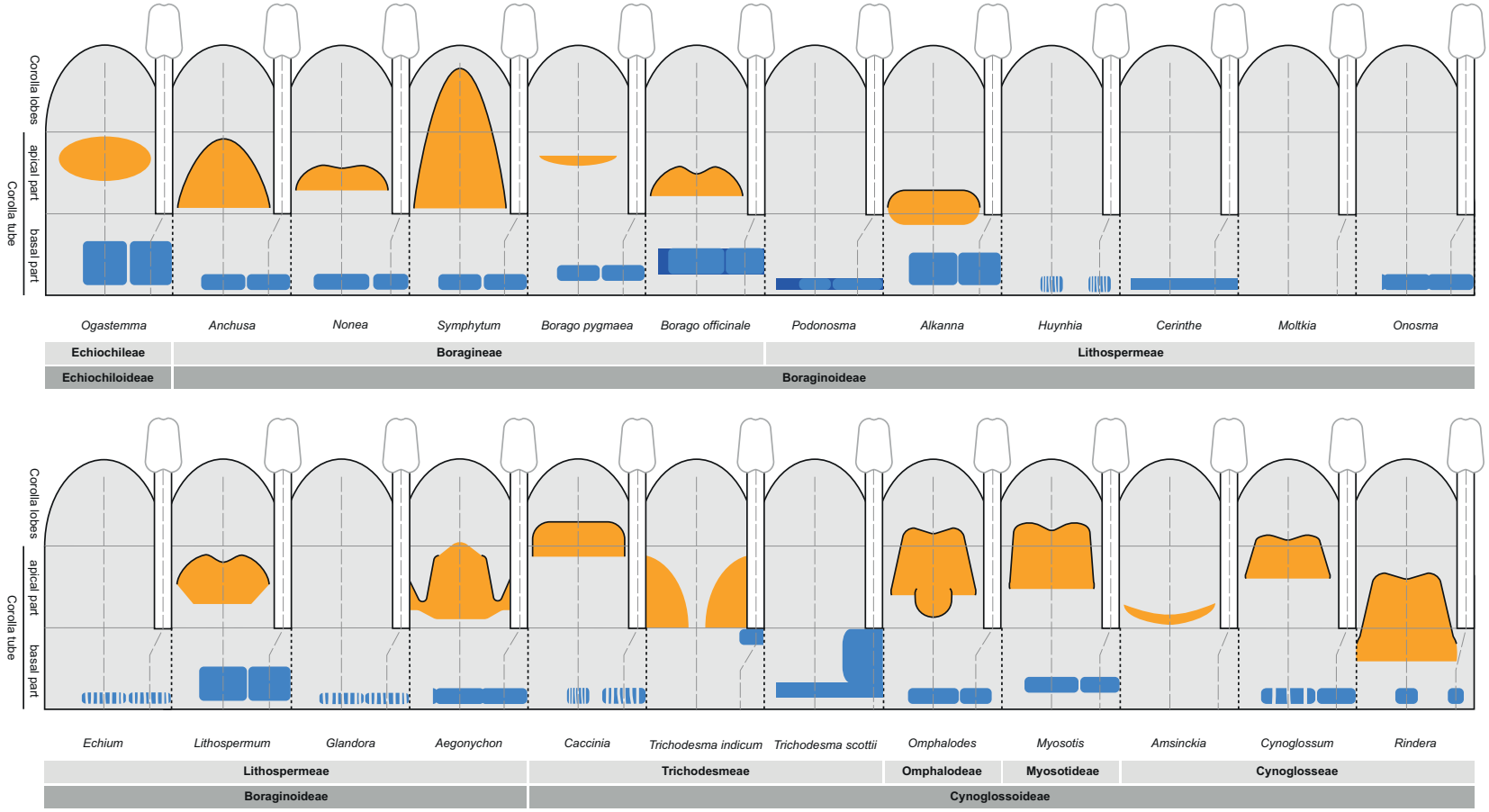

Figure 4.9: Schematic drawings of all studied genera. The positions in relation to basic features of the stamen-corolla tube (insertion points of the filaments, basal and apical part of the corolla tube, corolla lobes) are indicated. Faucal scales = orange, basal scales = blue. Solid black lines around the faucal scales indicate elaborate, overlapping scales. Dark blue rectangles overlain by lighter blue ones indicate an annulus with partially separate scales. Light grey dashed lines indicate the petal median and stamen vascular bundles.

packed inside a relatively small floral bud in an already advanced developmental stage. The positions and numbers of faucal and basal scales might thus be partially explained by architectural constraints. Throughout development, each faucal scale is situated between the upper halves of two adjacent stamens. Development of the faucal scale essentially takes place in this narrowly confined space until final corolla expansion takes place. The disc is initiated relatively early in flower development before any type of scale is initiated and the basal scales develop in the narrow space between the five anthers and the disc nectary.

Some morphological features of faucal and basal scales are conserved. Faucal scales are always antepetalous invaginations of the corolla tube (see also Arber, 1939; Schaefer, 1942; Weigend *et al.*, 2016). Basal scales are always protuberances at the base of the corolla tube. Scale numbers are relatively constant. However, there is more variation in the number of basal scales (ten, five, undifferentiated annulus, absent), compared to the faucal scales (five or absent). Both types of scales show morphological variation in terms of their shape and position in relation to other floral organs. Faucal scale morphology especially ranges from simple invaginations to elaborate scales.

The broad sampling of all three subfamilies based on the classification of the family presented by Chacón *et al.* (2016) allows a discussion of the observations in the context of recent phylogenetic studies (Weigend *et al.*, 2009, 2013; Cohen, 2014; Chacón *et al.*, 2016). The added use of developmental data and critical, direct observations eliminates the errors of data taken from the taxonomic literature since these are often based on macroscopic observations of anthetic flowers and focus on differences, not common features. Especially the basal scales are only mentioned when relatively prominent. Also, in some cases they have been described as 'absent' in taxa such as *Rindera lanata*, where basal scales are indeed present in early developmental stages but later virtually invisible, thus obscuring common ontogenetic trajectories. The observational data obtained in the present study was manually mapped onto the phylogeny. There seems to be no strong phylogenetic pattern (Fig. 4.10), but some character combinations are more common than others: Hypocrateriform corollas tend to have well-developed faucal scales and faucal scales are usually found where there are connivent anthers (many Boragineae) – unless corollas are narrowly tubular (*Podonosma orientalis*, *Cerinthe major*). Similarly, faucal scales are absent where there are genuine anther cones (i.e., modified anthers). Faucal scales are present in flowers with anthers included and free, but absent in flowers with exserted anthers. Thus, there appears to be considerable functional integration especially between corolla shape, anthers and faucal scales. In other words – shape, size and position of the faucal scales strongly influence overall floral architecture. Elongation of different parts of the corolla tube – above and below the faucal scales and above and below the insertion points of the filaments – lead to changes in floral architecture and the relation of the faucal scales to other parts of the flower. Anthers, faucal scales and corolla variously determine both, the internal space included in the flower and the access to this internal space for the flower visitor, by partly or completely closing the corolla throat. Endress & Matthews (2006) list a variety of possible functions of 'elaborate petals' (including stamen-corolla tube modifications of this study). They propose the following functions: *i*) optical and mechanical nectar guides, especially in flowers with differentially coloured faucal scales, *ii*) structures for pollinators to interact with, e.g., by providing additional grip or a landing platform, *iii*) protecting nectar and pollen from illegitimate flower visitors, by hiding nectar and anthers, and *iv*) reinforce floral architecture, e.g., by surrounding and/or reinforcing an anther cone. All these functions are likely realized individually or in different combinations by faucal scales in Boraginaceae, largely explaining their morphological diversity.

Basal scales are hidden inside the corolla tube. Endress & Matthews (2006) proposed the following functions for these structures: *i*) protection and presentation of nectar, and *ii*) protection of the

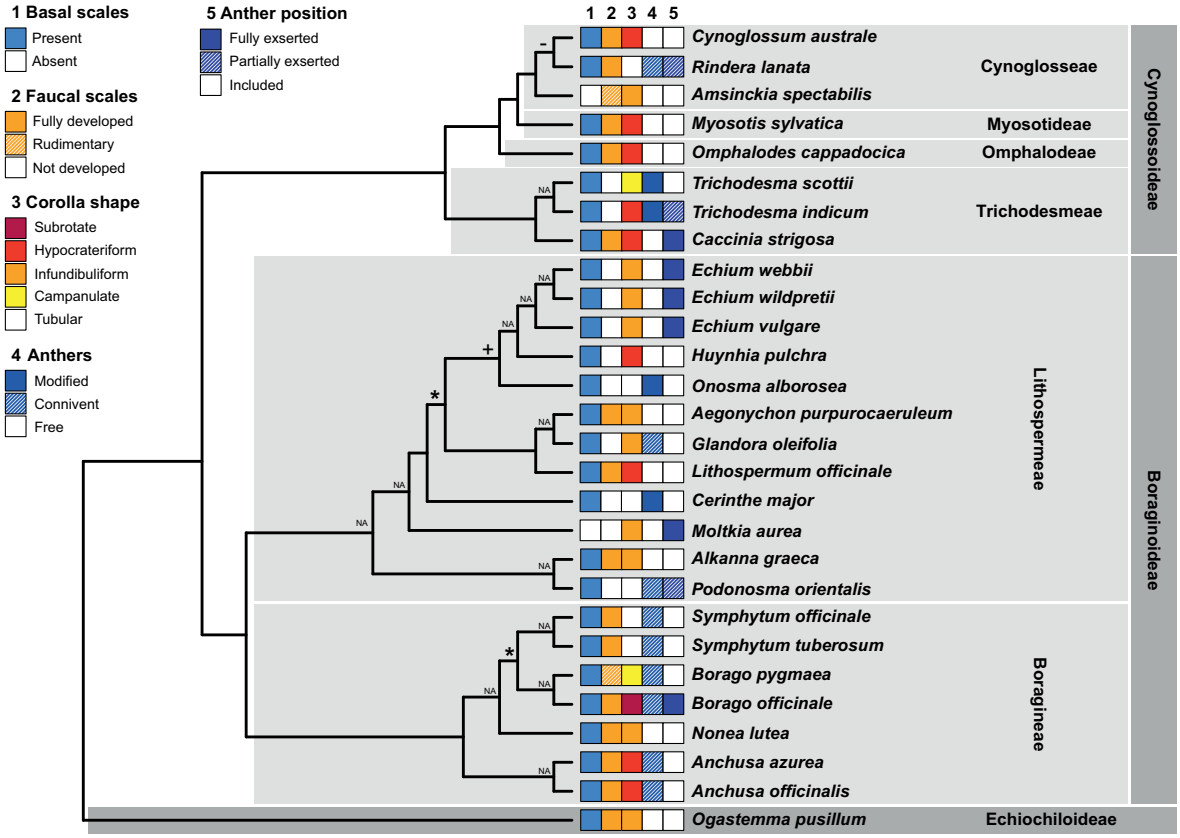

Figure 4.10: Character mapping of faucal and basal scales, and related floral architectural characters on a compilation of recent phylogenetic trees. The phylogenetic tree is based on Weigend et al. (2009, 2013), Cohen (2014) and Chacón et al. (2016). Support values (Bootstrap support [BS] and posterior probability [PP]) are taken from Chacón et al. (2016). High support values (BS > 70, PP > 0.95) are not shown. Asterisk (*) = BS < 70 and > 50, PP > 0.95. Plus (+) = BS < 70 and > 50, PP < 0.95 and > 0.9. Minus (-) = BS < 50, PP < 0.9. NAs indicate that the genera, but not the exact species were present in the studies. Subfamilial classification follows Chacón et al. (2016).

nectary disc or the entire ovary from mechanical damage. Our observations show that there is a distinct spatial relation between basal scales and disc nectary. In *Trichodesma indicum* (and *T. scottii*) the position of modifications of the basal part of the corolla tube is closer to the filament bases than to the nectary disc, thus enclosing a larger space – possibly to accommodate the notably higher nectar amounts in these species and thus creating some kind of 'nectar space' inside the corolla tube. Similar scales had previously only been described for *Lobostemon* Lehm., where five scales at the filament bases have been homologised with basal scales (Weigend *et al.*, 2016) and which – as a bird-pollinated species – also produces considerable amounts of nectar.

The evolution of basal scales in Boraginaceae has so far not been addressed in a phylogenetic context. Cohen (2014) conducted an ancestral state reconstruction for faucal scales, mainly based on observations made on herbarium specimens and literature mining. He concluded that faucal scales evolved several times independently within the Boraginaceae (Cohen, 2014). The observations made in the present study confirm a variable pattern of presence and absence of faucal scales across the family (Figs 4.9, 4.10). However, the observed patterns of faucal scale development, their shape and integration are highly variable and no obvious phylogenetic pattern was observed (Fig. 4.10). Based on the present data, there is no conclusive evidence for either several independent origins or several independent losses of faucal scales. Faucal scales might also be symplesimorphic for Boraginaceae and several reductions and reversals towards faucal scales are conceivable.

Faucal and basal scales of the Boraginaceae are modifications of the stamen-corolla tube. Similar stamen-corolla tube modifications can be found in related plant families of the order Boraginales. The families Wellstediaceae and Codonaceae are consecutive sisters to Boraginaceae in the clade Boraginales I (Luebert *et al.*, 2016). Wellstediaceae are poorly known with regards to their floral morphology, but some modifications of the basal part of the corolla tube have been observed (Pilger, 1911; Hunt, 1969; Thulin & Johansson, 1996; Thulin, 1998; Hilger & Weigend, 2016). These may or may not be homologous to the basal scales of Boraginaceae – detailed morphological and ontogenetic studies would be clearly desirable. Such studies are available for Codonaceae: Polymerous *Codon* D.Royen has apically broadened septa between the bases of the filaments and the corolla tube. These septa are distally widened and enclose up to 12 (to 20) distinct nectar chambers between the ovary and the corolla and its outgrowths (Jeiter *et al.*, 2016). As in Boraginaceae, these stamen-corolla tube modifications arise late in ontogeny. Thus, across Boraginales I – Boraginaceae, Codonaceae and Wellstediaceae – there seem to be protuberances of the basal part of the corolla tube in some way spatially related to the points of filament insertion and in a direct spatial relationship to the nectary tissue. They appear to enclose a 'nectar space' in Codonaceae and Wellstediaceae, while this function is complemented in Boraginaceae by the narrow corolla tube and/or the faucal scales, reducing the basal scales to one of several protective structures around nectary disc and ovary.

The clade Boraginales I is sister to Boraginales II (Luebert *et al.*, 2016). Boraginales II comprise eight families: Hydrophyllaceae, Namaceae, Heliotropiaceae, Ehretiaceae, Lennoaceae, Coldeniaceae, Hoplestigmataceae and Cordiaceae, but only the basally branching families are noteworthy for their stamen corolla-tube modifications: Hydrophyllaceae and Namaceae (Hitchcock, 1933b,a; Hofmann *et al.*, 2016). Both families share paired modifications at the bases of the filaments and corolla tube (Hofmann, 1999; Jeiter & Weigend, 2018). These modifiactions might be homologous to the apically broadened septa in *Codon*, the scales in *Wellstedia* Balf.f. and the basal scales in Boraginaceae. The question on homology of the structures in Boraginales I and II will need to be addressed in future research projects based on a broader sampling of Boraginales II families.

Three-dimensional imaging techniques, such as µCT, are a powerful tool for the study of floral architecture. They allow the *in situ* (as applied here) or even *in vivo* visualisation of anthetic flowers. Three-dimensional visualisation of complex morphological structures, such as flowers, is technically also possible with standard embedding and microtome sectioning, but this approach is seriously size-limited and prone to preparation artefacts. With the use of µCT in the present study we are able to visualise faucal and basal scale integration in situ and display this as virtual sections and high resolution surface renderings (both applied in Figs 4.7 and 4.8). The integration of faucal and basal scales into floral architecture was already known and especially the macroscopical integration of faucal scales into floral architecture has been described (Gürke, 1897; Weigend *et al.*, 2016), but a detailed spatial understanding and visual representation of the architectural detail was impossible. We can here show that the relation between ovary and basal scales is rather conserved and consequently modifications largely seem to follow evolutionary changes in the disc nectary and mericarp size and configuration. Conversely, faucal scales are shown to be highly variable in their spatial integration with other floral organs, indicating the possibility that they play a whole range of different roles in floral function and biology.

4.5 Conclusions

This is the first study of floral architecture in Boraginaceae with a special emphasis on faucal and basal scales, using morphological, developmental and three-dimensional data. Based on the data presented

here and elsewhere the basal scales of Boraginaceae are likely homologous to stamen-corolla tube modifications found in the sister family of Wellstediaceae and consecutive sister Codonaceae. Faucal scales, on the other hand, either evolved several times independently within the Boraginaceae which is indicated by their variable initiation patterns, by differences in shape and elaboration, or were several times independently lost due to changes in floral function, or a combination of independent gain and loss of faucal scales contributed to the pattern observed. Both basal and faucal scales are integrated into floral architecture. Basal scales are always related to the gynoecial disc nectary, while faucal scales show a high degree of synorganisation with the overall corolla shape, corolla throat, and shape, position and orientation of the anthers. However, no absolute correlation between certain floral architectural features and presence and absence of faucal scales has been found. Faucal scales likely play a range of different roles in flower-pollinator interactions and appear to play a crucial role in floral diversification in Boraginaceae.

As argued above, detailed structural and developmental studies are fundamental to studying flower evolution and cannot be replaced by literature mining. Classical methods in combination with increasingly powerful three-dimensional imaging techniques allow in situ studies of floral architecture that can easily be recruited for morphological and functional studies. This is the first study of stamen-corolla tube modifications in the Boraginaceae demonstrating the usefulness of this broad morphological and developmental approach for understanding floral function. Most importantly, it departs from the two-dimensional view of flowers towards an understanding of the three-dimensional integration of floral organs as functional spaces. It thus provides the basis for further studies on functional morphology and floral architecture, which should be complemented with morphometric and experimental approaches.

4.6 Acknowledgements

Plant material kindly was supplied for this study by the Israel Plant Gene Bank (*Podonosma orientalis*, *Ogastemma pusillum*), the Botanical Gardens of Iran (*Rindera lanata*) and the Botanic Gardens of Adelaide (*Cynoglossum australe*). We are grateful to A. Ziegler for the support on the µCT and for helpful suggestions regarding µCT-data analysis. We would like to thank F. Luebert who gave valuable input during different phases of this project. We are also grateful for the technical support by H.-J. Ensikat, T. Joßberger and J. Nettekoven. All plant material used in this study was cultivated at the University of Bonn Botanic Gardens. In that regard, we would like to express our gratitude to C. Löhne and the staff of the Gardens for maintaining the collections. J.J. received a scholarship by the Studienstiftung des deutschen Volkes for his doctoral thesis. Funding for the Skyscan 1272 µCT was provided by the Deutsche Forschungsgemeinschaft (INST 217/849-1 FUGG).

4.7 References

Arber, A. (1939) Studies in flower structure: V. On the interpretation of the petal and 'corona' in *Lychnis*. *Annals of Botany* **3**, 337–346.

Bigazzi, M. & Selvi, F. (2000) Stigma form and surface in the tribe Boragineae (Boraginaceae): Micromorphological diversity, relationships with pollen, and systematic relevance. *Canadian Journal of Botany* **78**, 388–408.

Bittrich, V. (1993) Caryophyllaceae. *Families and Genera of Vascular Plants* (eds. K. Kubitzki, J. Rohwer & V. Bittrich), vol. 2, pp. 206–236, Springer, Heidelberg.

Böhle, U.R., Hilger, H.H. & Martin, W.F. (1996) Island colonization and evolution of the insular woody habit in *Echium* L. (Boraginaceae). *Proceedings of the National Academy of Sciences* **93**, 11740–11745.

Chacón, J., Luebert, F., Hilger, H.H., Ovchinnikova, S., Selvi, F., Cecchi, L., Guilliams, C.M., Hasenstab-Lehman, K., Sutorý, K., Simpson, M.G. & Weigend, M. (2016) The borage family (Boraginaceae s.str.): A revised infrafamilial classification based on new phylogenetic evidence, with emphasis on the placement of some enigmatic genera. *Taxon* **65**, 523–546.

Chacón, J., Luebert, F. & Weigend, M. (2017) Biogeographic events are not correlated with diaspore dispersal modes in Boraginaceae. *Frontiers in Ecology and Evolution* **5**, 1–14.

Cohen, J.I. (2011) A phylogenetic analysis of morphological and molecular characters of *Lithospermum* L. (Boraginaceae) and related taxa: Evolutionary relationships and character evolution. *Cladistics* **27**, 559–580.

Cohen, J.I. (2014) A phylogenetic analysis of morphological and molecular characters of Boraginaceae: Evolutionary relationships, taxonomy, and patterns of character evolution. *Cladistics* **30**, 139–169.

Dukas, R. & Dafni, A. (1990) Buzz-pollination in three nectariferous Boraginaceae and possible evolution of buzz-pollinated flowers. *Plant Systematics and Evolution* **169**, 65–68.

Endress, P.K. (1994) *Diversity and Evolutionary Biology of Tropical Flowers*. Cambridge Tropical Biology Series, Cambridge University Press, Cambridge.

Endress, P.K. (1996) Homoplasy in angiosperm flowers. *Homoplasy - The Recurrence of Similarity in Evolution* (eds. M.J. Sanderson & L. Hufford), pp. 303–325, Academic Press, San Diego, California, United States.

Endress, P.K. & Matthews, M.L. (2006) Elaborate petals and staminodes in eudicots: Diversity, function, and evolution. *Organisms Diversity & Evolution* **6**, 257–293.

Fægri, K. (1986) The solanoid flower. *Transactions of the Botanical Society of Edinburgh* **45**, 51–59.

Fægri, K. & van der Pijl, L. (1979) *The Principles of Pollination Ecology*. Pergamon International Library of Science, Technology, Engineering, and Social Studies, Pergamon Press, Oxford, New York, third edn.

Fischer, E. (2004) Balsaminaceae. *Families and Genera of Vascular Plants* (ed. K. Kubitzki), vol. 6, pp. 20–25, Springer, Heidelberg.

Gerstberger, P. & Leins, P. (1978) Rasterelektronenmikroskopische Untersuchungen an Blütenknospen von *Physalis philadelphica* (Solanaceae) - Anwendung einer neuen Präparationsmethode. *Berichte der Deutschen Botanischen Gesellschaft* **91**, 381–387.

Gürke, M. (1897) Borraginaceae. *Die Natürlichen Pfanzenfamilien* (eds. A. Engler & K. Prantl), vol. 3a, pp. 71–131, W. Engelmann, Leipzig.

Hilger, H.H. (1984) Wachstum und Ausbildungsformen des Gynoeceums von *Rochelia* (Boraginaceae). *Plant Systematics and Evolution* **146**, 123–139.

Hilger, H.H. (2014) Ontogeny, morphology, and systematic significance of glochidiate and winged fruits of Cynoglosseae and Eritrichieae (Boraginaceae). *Plant Diversity and Evolution* **131**, 167–214.

Hilger, H.H. & Weigend, M. (2016) Wellstediaceae. *Families and Genera of Vascular Plants* (eds. K. Kubitzki, J.W. Kadereit & V. Bittrich), vol. 14, pp. 403–406, Springer, Heidelberg.

Hitchcock, C.L. (1933a) A taxonomic study of the genus *Nama*. I. *American Journal of Botany* **20**, 415–430.

Hitchcock, C.L. (1933b) A taxonomic study of the genus *Nama*. II. *American Journal of Botany* **20**, 518–534.

Hofmann, M. (1999) Flower and fruit development in the genus *Phacelia* (Phacelieae, Hydrophyllaceae): Characters of systematic value. *Systematics and Geography of Plants* **68**, 203–212.

Hofmann, M., Walden, G.K., Hilger, H.H. & Weigend, M. (2016) Hydrophyllaceae. *Families and Genera of Vascular Plants* (eds. K. Kubitzki, J.W. Kadereit & V. Bittrich), vol. 14, pp. 221–238, Springer, Heidelberg.

Hunt, D.R. (1969) *Wellstedia*. *Hooker´s Icones Plantarum* **37**, 3665–3667.

Jeiter, J., Danisch, F. & Hilger, H.H. (2016) Polymery and nectary chambers in *Codon* (Codonaceae) – flower and fruit development in a small, capsule-bearing family of Boraginales. *Flora* **220**, 94–102.

Jeiter, J., Hilger, H.H., Smets, E.F. & Weigend, M. (2017) The relationship between nectaries and floral architecture: A case study in Geraniaceae and Hypseocharitaceae. *Annals of Botany* **120**, 791–803.

Jeiter, J. & Weigend, M. (2018) Simple scales make complex compartments – ontogeny and morphology of stamen-corolla tube modifications in Hydrophyllaceae (Boraginales). *Biological Journal of the Linnean Society* **125**, 802–820.

Li, P. & Johnston, M.O. (2010) Flower development and the evolution of self-fertilization in *Amsinckia*: The role of heterochrony. *Evolutionary Biology* **37**, 143–168.

Luebert, F., Cecchi, L., Frohlich, M.W., Gottschling, M., Guilliams, C.M., Hasenstab-Lehman, K.E., Hilger, H.H., Miller, J.S., Mittelbach, M., Nazaire, M., Nepi, M., Nocentini, D., Ober, D., Olmstead, R.G., Selvi, F., Simpson, M.G., Sutorý, K., Valdés, B., Walden, G.K. & Weigend, M. (2016) Familial classification of the Boraginales. *Taxon* **65**, 502–522.

Naghiloo, S., Bellstedt, D.U. & Claßen-Bockhoff, R. (2018) Nectar protection in arid-adapted flowers of Zygophyllaceae-Zygophylloideae. *Perspectives in Plant Ecology, Evolution and Systematics* **34**, 37–50.

Payer, J.B. (1857) *Traité d'organogénie Comparée de La Fleur*. V. Masson, Paris.

Pilger, R. (1911) Die Gattung *Wellstedia* in Südwestafrika. *Botanische Jahrbücher für Systematik, Pflanzengeschichte und Pflanzengeographie* **46**, 558–561.

Ronse De Craene, L.P. (2010) *Floral Diagrams: An Aid to Understanding Flower Morphology and Evolution*. Cambridge University Press, Cambridge ; New York.

Schaefer, H. (1942) Die Hohlschuppen der Boraginaceen. *Botanische Jahrbücher für Systematik, Pflanzengeschichte und Pflanzengeographie* **72**, 304–346.

Schindelin, J., Arganda-Carreras, I., Frise, E., Kaynig, V., Longair, M., Pietzsch, T., Preibisch, S., Rueden, C., Saalfeld, S., Schmid, B., Tinevez, J.Y., White, D.J., Hartenstein, V., Eliceiri, K., Tomancak, P. & Cardona, A. (2012) Fiji: An open-source platform for biological-image analysis. *Nature Methods* **9**, 676–682.

Staedler, Y.M., Masson, D. & Schönenberger, J. (2013) Plant tissues in 3D via X-ray tomography: Simple contrasting methods allow high resolution imaging. *PLOS ONE* **8**, e75295.

Teppner, H. (2011) Flowers of Boraginaceae (*Symphytum*, *Onosma*, *Cerinthe*) and *Andrena symphyti* (Hymenoptera-Andrenidae) – Morphology, pollen portioning, vibratory pollen collection, nectar robbing. *Phyton (Horn, Austria)* **50**, 145–328.

Thulin, M. (1998) A new species of *Wellstedia* (Boraginaceae) from Somalia. *Nordic Journal of Botany* **18**, 663–665.

Thulin, M. & Johansson, N.B. (1996) Taxonomy and biogeography of the anomalous genus *Wellstedia*. *The Biodiversity of African Plants* (eds. L.J.G. van der Maesen, X.M. van der Burgt & J.M. van Madenbach de Rooy), pp. 73–86, Kluwer Academic Publishers, Dordrecht.

Vaes, E., Vrijdaghs, A., Smets, E.F. & Dessein, S. (2006) Elaborate petals in Australian *Spermacoce* (Rubiaceae) species: Morphology, ontogeny and function. *Annals of Botany* **98**, 1167–1178.

Weigend, M., Gottschling, M., Selvi, F. & Hilger, H.H. (2009) Marbleseeds are gromwells – Systematics and evolution of *Lithospermum* and allies (Boraginaceae tribe Lithospermeae) based on molecular and morphological data. *Molecular Phylogenetics and Evolution* **52**, 755–768.

Weigend, M., Luebert, F., Selvi, F., Brokamp, G. & Hilger, H.H. (2013) Multiple origins for Hound's tongues (*Cynoglossum* L.) and Navel seeds (*Omphalodes* Mill.) – The phylogeny of the borage family (Boraginaceae s.str.). *Molecular Phylogenetics and Evolution* **68**, 604–618.

Weigend, M., Selvi, F., Thomas, D.C. & Hilger, H.H. (2016) Boraginaceae. *Families and Genera of Vascular Plants* (eds. K. Kubitzki, J.W. Kadereit & V. Bittrich), vol. 14, pp. 41–102, Springer, Heidelberg.

Chapter 5

Simple scales make complex compartments – ontogeny and morphology of stamen-corolla tube modifications in Hydrophyllaceae (Boraginales)

Jeiter J, Weigend M. 2018. Simple scales make complex compartments – ontogeny and morphology of stamen-corolla tube modifications in Hydrophyllaceae (Boraginales). *Biological Journal of the Linnean Society* 125: 802–820. https://doi.org/10.1093/biolinnean/bly167

Biological Journal of the Linnean Society, 2018, **125**, 802–820. With 9 figures.

Simple scales make complex compartments: ontogeny and morphology of stamen–corolla tube modifications in Hydrophyllaceae (Boraginales)

JULIUS JEITER*, and MAXIMILIAN WEIGEND

Nees-Institute for Biodiversity of Plants, University of Bonn, Meckenheimer Allee 170, 53115 Bonn, Germany

Received 17 July 2018; revised 28 September 2018; accepted for publication 28 September 2018

Small structures such as scales together with outgrowth of other floral organs modify floral architecture and function. Here, the Hydrophyllaceae, a medium-sized family in the order Boraginales, are studied. The simple tetracyclic, pentamerous flowers have a stamen–corolla tube with typically ten scale-like appendices (modifications) on the inside. The morphology and development of these modifications and the morphology of the spatially associated nectaries are studied using standard and cryo-scanning electron microscopy. There are always ten modifications in antepetalous position, even in species previously described as lacking modifications. Modifications develop late in floral ontogeny and follow similar developmental trajectories. The size and shape of these modifications are correlated with elongation of the filaments and the corolla tube. They divide the overall internal space of the flower into separate compartments. The nectaries are five-lobed or arranged in five glands, each in antepetalous position and juxtaposed to the modifications. Nectaries and modifications are spatially and functionally integrated – producing, presenting and protecting the nectar. A function in plant–pollinator interactions is inferred, but observational and experimental data are lacking. An evolutionary series for the stamen–corolla tube modifications in Hydrophyllaceae is proposed. Similar, possibly homologous types of modifications can be found in related taxa from the Boraginales, but a detailed comparative study has yet to be provided.

ADDITIONAL KEYWORDS: compartmentalization – floral architecture – floral organization – flower morphology – revolver architecture.

INTRODUCTION

Flower morphology is one of the major drivers of angiosperm evolution and diversification. A broad variety of different morphologies and morphological phenomena have been addressed over the last centuries of morphological research. There are, however, still considerable gaps in our understanding of some phenomena. One poorly studied complex of structures are appendages, scales, invaginations and protrusions arising in different positions inside the flowers of various taxonomic groups of angiosperms. Examples of such structures are the coronas of several Caryophyllaceae (e.g. *Lychnis*: Arber, 1939), faucal and basal scales of the Boraginaceae (Weigend *et al.*, 2016) and petal appendages in *Spermococe* (Rubiaceae: Vaes *et al.*, 2006). The independent origin of these – often prominent – structures in various plant groups and their presumed function make them an interesting study object in an evolutionary and developmental context.

One plant group with known diversity of these structures are the Hydrophyllaceae. There are typically ten scale-like outgrowths of the stamen–corolla tube present, which are poorly understood, both in development and in function. Here we study these structures and their development in detail and describe how they integrate into the general floral architecture.

As functional units, flowers are composed of organs directly and/or indirectly involved in sexual reproduction. The gynoecium and the androecium are, of course, directly involved in pollination, while the attraction and rewarding of pollinators, pollinator selection and exclusion and protection of floral organs is taken over by the perianth, sometimes in combination with other organs. The arrangement and number of organs in

*Corresponding author. E-mail: jjeiter@uni-bonn.de

a flower is called floral organization (*sensu* Endress, 1996). Synorganization, fusion, differential growth rates and modification of floral organs lead to the functional diversification between organizationally similar flowers (Jeiter *et al.*, 2017a, b) and these different appearances are termed 'floral architectures' (Endress, 1996). Apart from the developmental and morphological factors influencing floral architecture, it is influenced by various environmental and evolutionary factors including pollinator behaviour, climatic conditions, and genetic and developmental constraints.

Synorganization describes the specific spatial correlation between organs of the same or different whorls into structures of higher order (Ronse De Craene, 2010). Synorganization can be the result of organ fusion (e.g. Jeiter *et al.*, 2016) or spatial integration in choripetalous flowers (e.g. Weigend & Gottschling, 2006; Endress, 2010; Jeiter *et al.*, 2017a). Differential growth rates here can result in changes in floral function. Examples are the differences in spur length driven by pollinator shifts (Whittall & Hodges, 2007) and the differentiation of the shape and length of the corolla tube in relation to pollination (Smith & Kriebel, 2018). Modifications (i.e. shifts in shape, proportions or the development of outgrowths) in floral organs are manifold. They are especially common – but not limited to – petals and stamen–corolla tubes (Endress & Matthews, 2006; Vaes *et al.*, 2006). 'Modifications' as used here refers to various elaborations of stamen–corolla tubes, such as scales, appendages, protrusions or invaginations.

In this study, we investigate the diversity and development of stamen–corolla tube modifications in the Hydrophyllaceae. The Hydrophyllaceae are a family of the Boraginales with approximately 250 species in 12 genera across the Americas (Luebert *et al.*, 2016). An overview of the general floral appearance for nine of the 11 species studied here is given in Figure 1. Most species show some type of modifications of the stamen–corolla tube (Hofmann *et al.*, 2016). Numerous different terms have been used for the stamen–corolla tube modifications of Hydrophyllaceae. Some are more descriptive (e.g. fornices, plicae, scales, squamae, appendages, lamellae; Brand, 1913) and others indicate an organ identity and homology (e.g. corolla scales, corolla plicae, filament appendages) or simply describe their position (interstaminal scales; Walden & Patterson, 2012; Hofmann *et al.*, 2016). Their presence or absence, shape and position are important diagnostic characters in differentiating taxa (Gray, 1875; within *Phacelia*, Walden & Patterson, 2012). The overall morphology of these modifications in the stamen–corolla tube has been previously described (Brand, 1913), but developmental studies of either these modifications or overall Hydrophyllaceae are largely wanting. The only exception is the genus *Phacelia*, four species of which have been studied (Hofmann, 1999). This latter study outlines the development of these modifications and characterizes them as outgrowths of the corolla. Nectary discs have also been studied only superficially and detailed morphological descriptions, especially at the microscopic level, are lacking (Walden & Patterson, 2012; Hofmann *et al.*, 2016). Studies in some Hydrophyllaceae species indicate spatial and functional integration of the nectary disc and modifications (Merritt, 1897; Brand, 1913). However, the consequence of this integration for floral architecture has so far not been examined.

Our study aims to fill these knowledge gaps in Hydrophyllaceae. What is the detailed morphology of the stamen–corolla tube modifications and nectaries? How do the stamen–corolla tube modifications develop? Can the function of these modifications in relation to the nectaries be inferred?

MATERIAL AND METHODS

Inflorescences with flowers of different developmental stages – from onset of stamen–corolla tube development to anthetic flowers – were collected as fresh material from the living collection at the Bonn University Botanic Gardens. Species used in this study, vouchers and applied methods are summarized in Table 1.

Two different scanning electron microscopy (SEM) procedures were applied, requiring different methods of sample fixation and preparation. Some of the freshly collected material was directly processed with the 'cryo-SEM technique', while the remaining material was fixed in formaldehyde–acetic acid–ethanol (FAA; formaldehyde 2%, acetic acid 2%, ethanol 70%) for further examination using standard SEM techniques. Cryo-SEM massively reduced the number of introduced preparation artefacts that result from the fragility of the stamen–corolla tube. It also allowed the visualization of nectar inside the corolla tube as frozen liquid.

Cryo-SEM technique

The stamen–corolla tubes of freshly collected flowers were carefully removed under a stereomicroscope, cut open on one side and placed onto conductive carbon tape (Leit-Tap, PLANO GmbH, Wetzlar, Germany). The spread corolla tube was additionally held in place by two droplets of conductive carbon cement (Leit-C, PLANO GmbH). The mounted samples were sputter coated with gold or palladium at 0.1 mbar and 30 mA for 20 s in a sputter coater (SCD 040, Balzers Union, Liechtenstein). The coated sample attached to the conductive carbon tape was mounted onto a 'cryo-holder'. The cryo-holder is a modified block of aluminium attached to a piece of hard plastic for thermal insulation and two aluminium frames, enclosing the coated

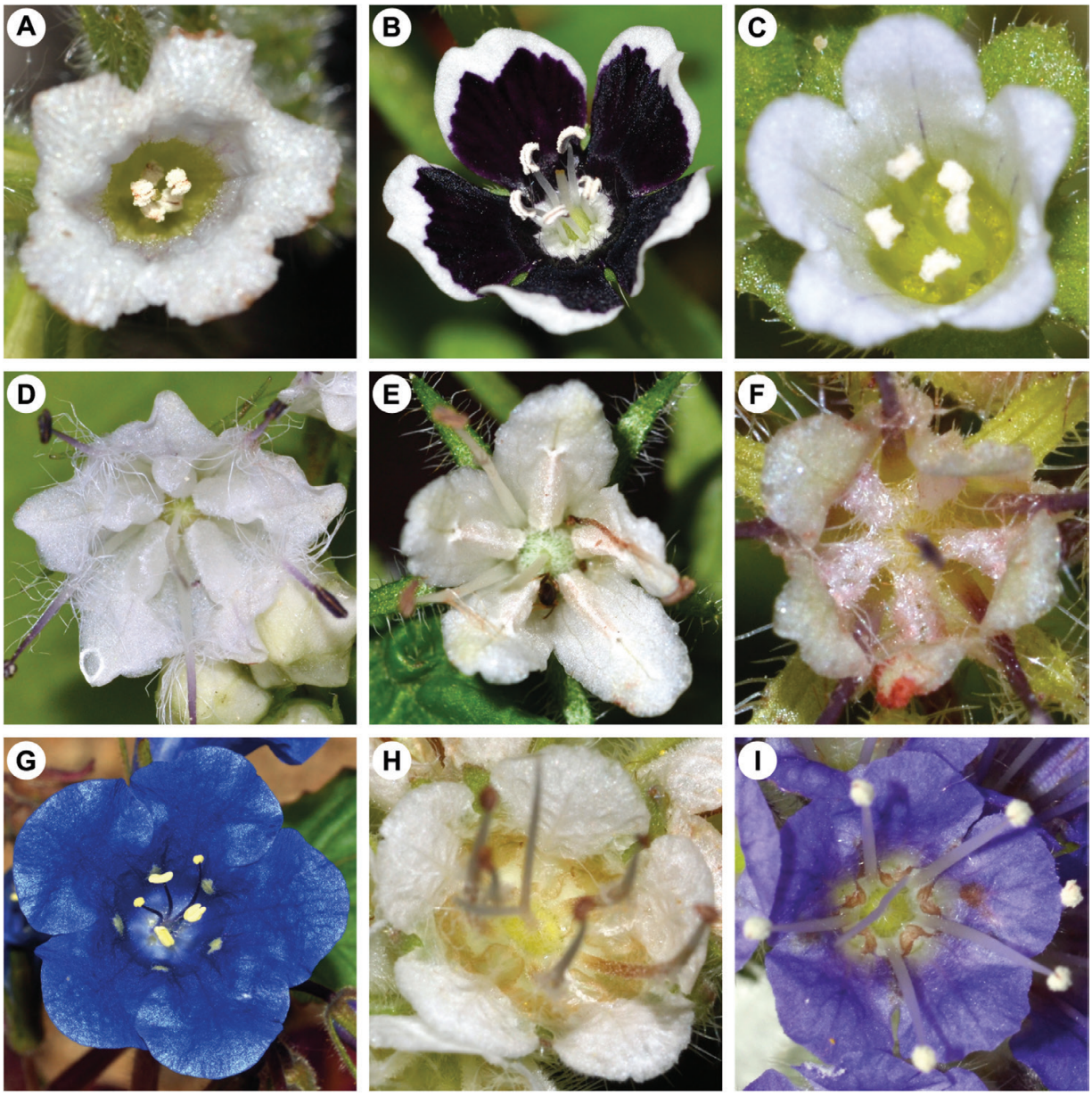

Figure 1. Flower diversity in the Hydrophyllaceae. A, *Draperia systyla*. B, *Nemophila menziesii*. C, *Eucrypta chrysanthemifolia*. D, *Hydrophyllum canadense*. E, *Hydrophyllum fendleri*. F, *Hydrophyllum tenuipes*. G, *Phacelia campanularia*. H, *Phacelia malvifolia*. I, *Phacelia secunda*. Images are focused at the level of stamen–corolla tube modifications.

sample. The sample was covered with a copper lid. The lid prevents the formation of ice crystals on the surface of the samples. The holder with the mounted sample was submerged in liquid nitrogen until its temperature stabilized (1–1.5 min). It was then placed in the vacuum chamber of the scanning electron microscope (Stereoscan 200, Cambridge, UK). After evacuation and prior to studying the sample by SEM, the copper lid was removed by tilting the holder. Samples were observed at temperatures between –100 and –70 °C at 5–15 kV. Most of the samples were stable for up to 1 h at high vacuum, whereas others were too fragile for this method (Table 1).

Standard SEM

Samples not suitable for the cryo-SEM technique – gynoecia and most early developmental stages – were

Table 1. Plant material and vouchers; all vouchers are placed in the Herbarium of the Nees-Institute for Biodiversity of Plants of the University of Bonn (BONN)

Species	Method	Examined flower stages*	IPEN number
Draperia systyla Torr.	Cryo- and standard SEM	Development	US-0-BONN-33089
Eucrypta chrysanthemifolia Greene	Standard SEM	Development	US-0-BONN-36929
Hydrophyllum canadense L.	Cryo- and standard SEM	Development	xx-0-BONN-9457
Hydrophyllum fendleri (A. Gray) A. Heller	Cryo- and standard SEM	Anthetic	CA-0-BONN-39162
Hydrophyllum tenuipes A. Heller	Cryo- and standard SEM	Anthetic	US-0-BONN-35287
Hydrophyllum virginianum L.	Cryo- and standard SEM	Anthetic	xx-0-BONN-36861
Nemophila menziesii Hook. & Am.	Cryo- and standard SEM	Development	xx-0-BONN-38177
Phacelia campanularia A. Gray	Cryo- and standard SEM	Development	PE-0-BONN-35820
Phacelia egena (Brand) Greene ex J. T. Howell	Cryo- and standard SEM	Development	US-0-BONN-37009
Phacelia malvifolia Cham.	Cryo- and standard SEM	Development	US-0-BONN-37883
Phacelia secunda J. F. Gmel.	Cryo- and standard SEM	Development	CL-0-BONN-38409

*Flower stages observed for the development of stamen–corolla tube modifications. Nectaries were always studied in anthetic flowers. Development: complete development of the stamen–corolla tube modifications including anthetic stages. Anthetic: only anthetic stages were studied.

prepared for SEM following standard methods: the samples were fixed in FAA, rinsed with ethanol (70%) and dissected under a stereomicroscope. Prior to dehydration, they were transferred back into FAA for at least 1 h, which was subsequently replaced with formaldehyde dimethyl acetal (FDA; 99.0%, Sigma-Aldrich Chemie GmbH, Munich, Germany) and finally stored in acetone (protocol modified after Gerstberger & Leins, 1978). Critical point drying (CPD 020, Balzers Union) followed the standard protocol. Dried specimens were mounted on aluminium stubs using conductive carbon tape and conductive carbon cement followed by the final sample preparation. The mounted specimens were coated with gold or palladium in a sputter coater (SCD 040, Balzers Union) for 1.5–3 min at 30 mA. Images were taken with a Stereoscan 200 scanning electron microscope at 10–15 kV. Contrast and brightness of the images were partially adjusted using standard image editing software.

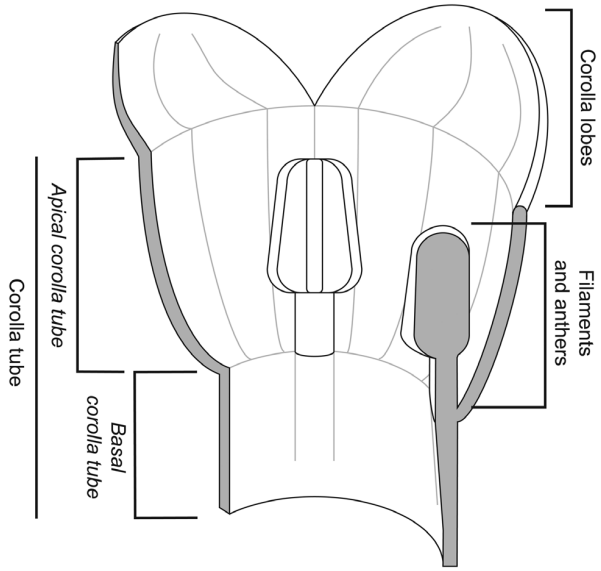

Figure 2. Structure of a typical stamen–corolla tube and terminology applied here. The stamen–corolla tube is divided into three parts: corolla tube, corolla lobes, and filaments and anthers. The corolla tube can be subdivided into two parts: apical part of the corolla tube ranging from the point of filament insertion to the point where the corolla lobes diverge, and basal part of the corolla tube ranging from the base of the corolla tube to the point of filament insertion.

RESULTS

The stamen–corolla tube is composed of the corolla tube, the corolla lobes, and the filaments and anthers. The corolla tube can be subdivided into two parts (Fig. 2): a basal part from the receptacle to the points of filament insertion, and an apical part between the points of filament insertion and where the corolla lobes diverge.

MODIFICATIONS

The development of modifications is initiated at the stage of flower development when both gynoecium and androecium are fully formed, but before filaments, corolla tube and style elongate. The modifications are superimposed onto the adaxial side of the stamen–corolla tube. This pattern is consistent for all species studied. The specific patterns found are as follows.

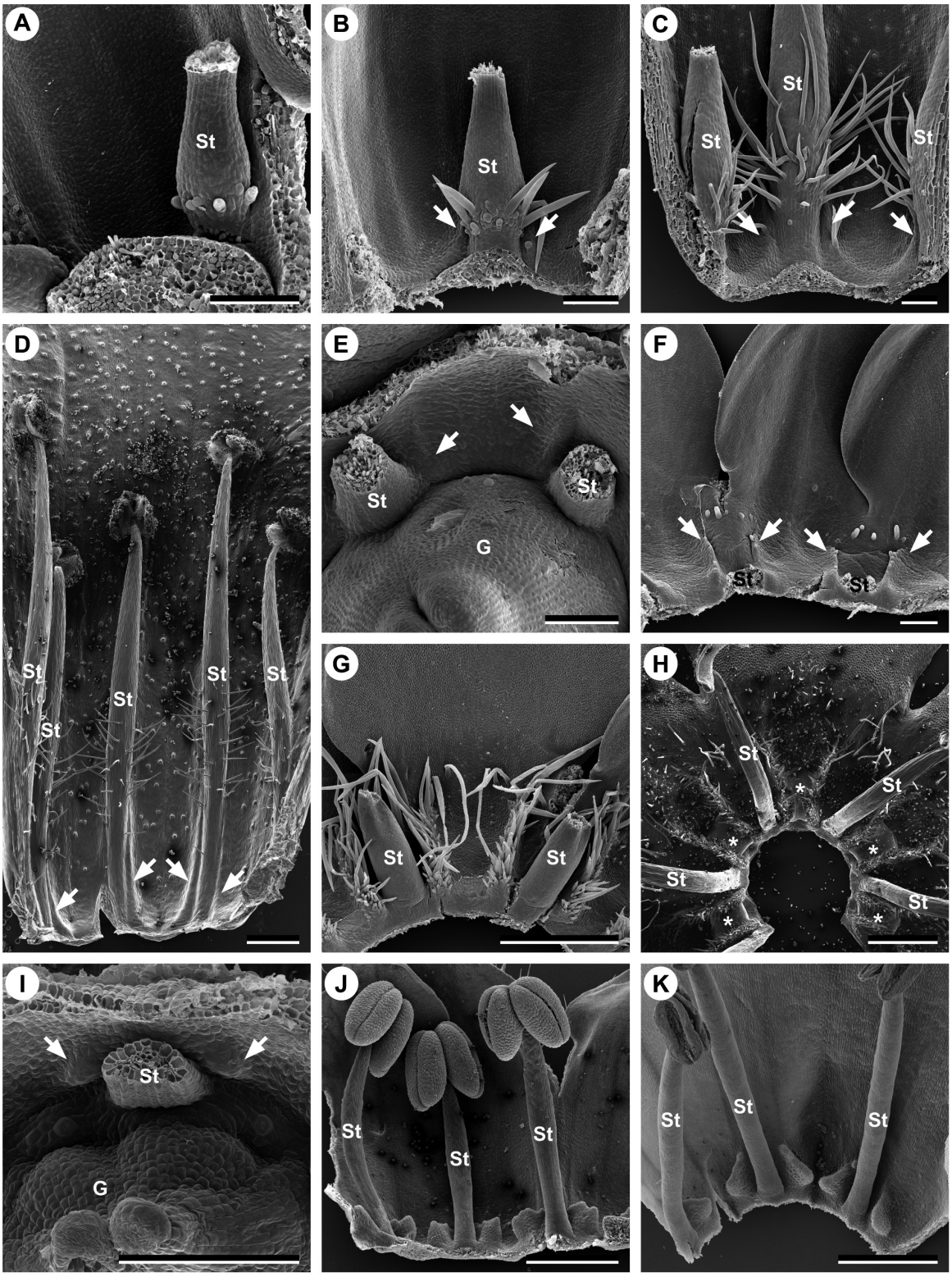

Draperia systyla (Figs 1A, 3A–D)

The modifications start to develop shortly after a ring of trichomes at the insertion point of the filaments is initiated (Fig. 3A). The modifications are initiated as shallow lobes at the level of the insertion point of the filaments and protrude towards the base of the corolla tube from this point (Fig. 3B). On all occasions, two neighbouring modifications originating between two neighbouring filaments form a shallow, upside-down arch at the base of the basal corolla tube (Fig. 3B, C). The modifications become less defined during elongation of the basal corolla tube (Fig. 3C).

The anthetic corolla is tubular to hypocrateriformous (Fig. 1A). The corolla tube is five times as long as the corolla lobes. The filaments are inserted on the base of the corolla tube, but are fused with the tube to different levels. In general, they become free in the lowest quarter of the tube. There is differentiation between a basal and an apical part of the corolla tube. The modifications are shallow protrusions neighbouring the fused part of the filament in the basal part of the tube (Fig. 3D). The length of the modifications correlates with the points where the filaments become free. No independent compartments are enclosed by the modifications. The whole corolla tube and especially the apical part of the tube are covered with wart-like emergences (Fig. 3D).

Nemophila menziesii (Figs 1B, 3E–H)

The modifications develop as elongated ridges neighbouring the base of the filaments (Fig. 3E, F). Their elongation and elaboration continues after the corolla tube reaches its final length (Fig. 3G, H). Just before anthesis the margin of the modifications reaches the sinuses between the corolla lobes. Before anthesis, the apical portion of the corolla tube elongates (Fig. 3G, H). Trichomes are initiated at an early developmental stage. The simple trichomes develop on the proximal ridges of the modifications and between their apices (Fig. 3H).

The anthetic corolla is bowl-shaped with corolla lobes twice as long as the length of the corolla tube (Fig. 1B). The filaments are united with the corolla tube close to its base (Fig. 3H). The modifications are elongated scales densely covered with simple trichomes on their margins (Fig. 3H). Neighbouring modifications form a broad groove which is closed where the modifications touch the nectary disc. The distal end of the ridge is loosely demarcated by simple trichomes (Fig. 3H).

Eucrypta chrysanthemifolia (Figs 1C, 3I–K)

Development of the modifications starts as elongated protrusions above the insertion points of the filaments (Fig. 3I). They broaden and elongate as the corolla tube lengthens (Fig. 3J). Before anthesis they are slightly elevated above the insertion points of the filaments by elongation of the basal part of the corolla tube (Fig. 3K).

The anthetic corolla is campanulate to infundibuliform (Fig. 1C). The tube is twice the length of the free corolla lobes. The filaments are fused with the corolla at the base of the tube (Fig. 3K). The free tip of the triangular modifications faces away from the bases of the filaments, where they are broadly attached to the corolla tube (Fig. 3K). There appears to be no significant connection between filament bases and the modifications (Fig. 3J, K). The margins of the modifications are smooth. Overall, the modifications form five partially closed compartments with broadly triangular openings (Fig. 3K).

Hydrophyllum canadense (Figs 1D, 4A–D)

The modifications are initiated as two elongated protrusions parallel to the midvein of the petals (Fig. 4A). In the earliest stages of their development, they are already visible not only on the short corolla tube, but also extending onto the corolla lobes (Fig. 4A, B). During corolla elongation, the modifications enlarge into scales, and simple papillae-like trichomes differentiate on the margins (Fig. 4B). Subsequently, the modifications increase in size and the margins touch and then overlap (Fig. 4C). At this stage, the modifications are already clearly connected to the filament bases (Fig. 4C, D). At anthesis, while the corolla unfolds, the basal half of

Figure 3. Morphology and development of the modifications in *Draperia systyla*, *Nemophila menziesii* and *Eucrypta chrysanthemifolia*. A–D, *Draperia systyla*. A, onset of trichome development at the point of filament insertion. B, modifications shortly after onset of development. Arrows point at modifications. C, derived state of stamen–corolla tube development. Arrows point at modifications. D, cryo-SEM micrograph of the ventral side of the stamen–corolla tube. Arrows point at modifications. E–H, *Nemophila menziesii*. E, onset of modification development. Arrows point at modifications. F, derived developmental stage, onset of trichome development. Arrows point at modifications. G, modifications of a pre-anthetic stamen–corolla tube. H, cryo-SEM micrograph of the stamen–corolla tube of an anthetic flower. Frozen nectar droplets are visible between the modifications (*). I–K, *Eucrypta chrysanthemifolia*. I, onset of modification development. Arrows point at modifications. J, modifications of the stamen–corolla tube of a pre-anthetic flower. K, modifications of an anthetic flower. St = stamen, G = gynoecium. Scale bars: D, G, H, J, K = 500 μm; A–C, E, F, I = 100 μm.

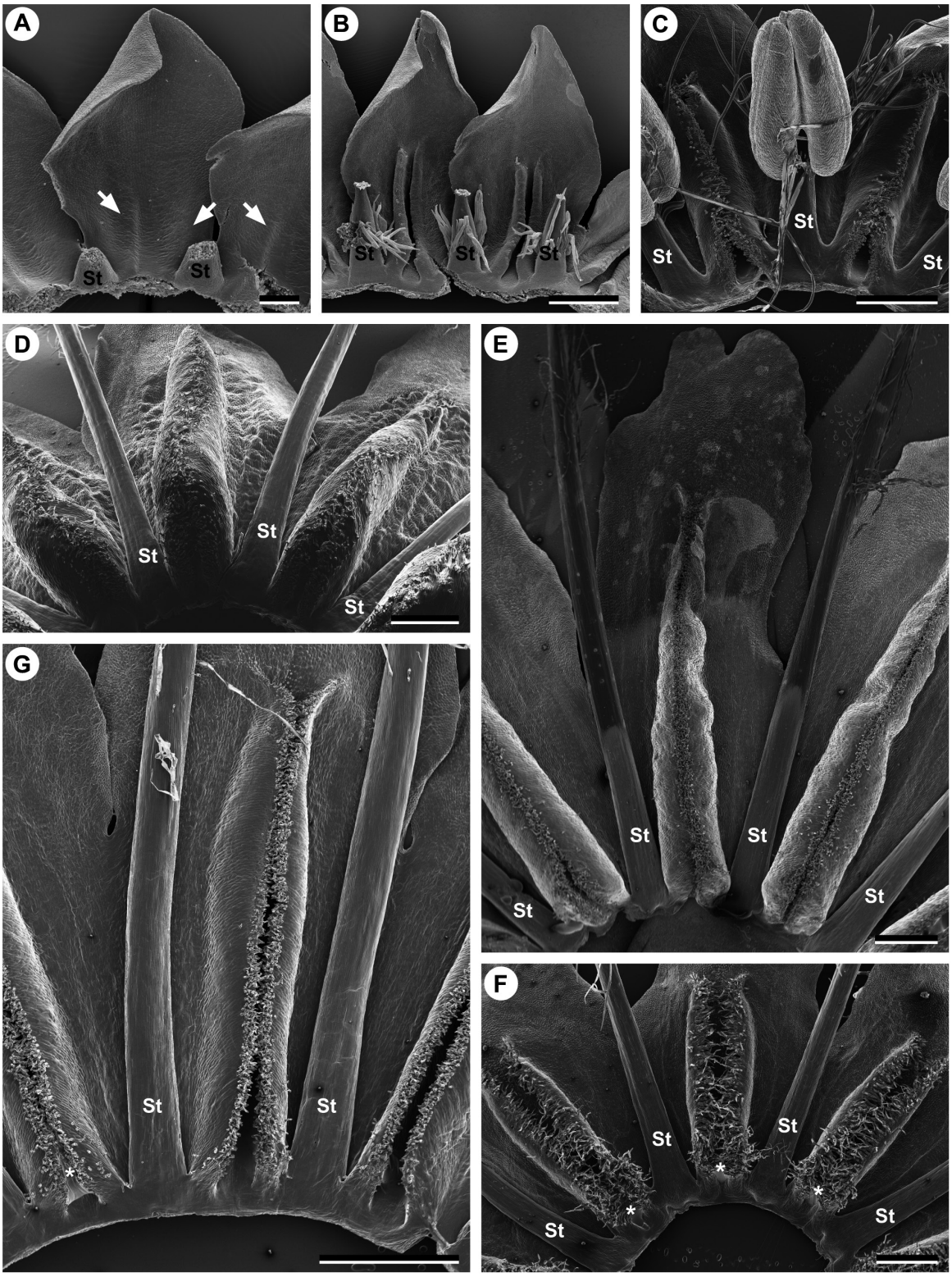

the modification complexes broadens, resulting in a broad base, apically tapering into a tube with an opening towards the centre of the corolla lobes and basally forming the elongated opening towards the nectary gland (Fig. 4D).

The anthetic corolla is campanulate to bowl-shaped (Fig. 1D). The corolla lobes are three times as long as the corolla tube. The filaments are inserted close to the base of the corolla tube. The modifications take the shape of elongate scales (Fig. 4D). Two scales always run parallel from the bases of the filaments up to the middle of the corolla lobes. The margins of the modifications are densely covered with short, almost papillate trichomes (Fig. 4C, D). Two neighbouring scales overlap lengthwise and form a tightly closed compartment. The modifications diverge slightly apically, leaving a trichome-covered opening to the compartment. Basally, the complex is broadened towards the ovary with an elongated opening towards the nectary gland (Fig. 4D).

Hydrophyllum fendleri (Figs 1E, 4E)

The anthetic corolla is narrowly campanulate (Fig. 1E). The corolla lobes are twice as long as the corolla tube. The modifications span from the base of the corolla tube up to the middle of the corolla lobes (Fig. 4E). The modifications are fused with the filament bases. Two neighbouring modifications form a hollow canal tightly closed via capillinection by simple, short trichomes on their margins (Fig. 4E). This canal is open at the base (towards the nectary) and apically near the centre of the corolla lobes. The apical ends of the modifications diverge to form a narrowly triangular, loosely trichome-covered opening.

Hydrophyllum tenuipes (Figs 1F, 4F)

The anthetic corolla is broadly campanulate (Fig. 1F). The corolla lobes are approximately the same length as the corolla tube (Fig. 4F). Filaments insert near the base of the corolla tube. Modifications and filament bases are fused. The modifications take the shape of elongate scales. Two neighbouring modifications always lie parallel to the midveins of the corolla lobes. Their margins are densely covered with simple trichomes (Fig. 4F). Neighbouring modifications enclose a loose compartment. Apically, the modifications widen towards the centre of the corolla lobes and form an opening. At the base another opening with a glabrous margin is formed.

Hydrophyllum virginianum (Fig. 4G)

The anthetic corolla is tubular. Corolla lobes and corolla tube are approximately the same length. The filaments insert slightly above the base of the corolla tube. Modifications and filament bases are fused (Fig. 4G). The modifications are shallow elongate protrusions, ranging from below the points of filament insertion up to the centre of the corolla lobes (Fig. 4G). Two neighbouring modifications form a loosely closed compartment. The margins of the modifications are covered with simple, papillate trichomes. The modifications form an opening towards the centre of the corolla lobe. The margins of the modifications surrounding the opening at the base are glabrous (Fig. 4G).

Phacelia campanularia (Figs 1G, 5A–C)

Development of the modifications starts as irregularly bilobed, slightly double-edged protrusions at the bases of the filaments (Fig. 5A). Parallel to the elongation of the filament bases, the modifications elongate and broaden (Fig. 5B).

The anthetic corolla is campanulate (Fig. 1G). The corolla tube is approximately twice the length of the corolla lobes. Filaments are inserted at the base of the corolla tube (Fig. 5C). The modifications are fused with the filament bases. They are broadened at the ventral side and slightly concave towards the ovary (Fig. 5C). The apical part of the modifications forms an irregularly bilobed, slightly pointed lateral protrusion (Fig. 5C). Apart from their insertion on the corolla tube, there is no connection between corolla tube and modifications and no compartments are formed (Fig. 5C).

Phacelia egena (Fig. 5D–F)

Development of the modifications starts as protrusions close to and already fused with the bases of the filaments (Fig. 5D). The apical part of the modifications

Figure 4. Morphology and development of the modifications in *Hydrophyllum*. A–D, *Hydrophyllum canadense*. A, onset of modification development. Arrows point at modifications. B, derived developmental stage. C, cryo-SEM micrograph of the modifications of a pre-anthetic flower. D, cryo-SEM micrograph of the modifications of an anthetic flower. E, *Hydrophyllum fendleri*; cryo-SEM micrograph of the modifications of an anthetic flower. F, *Hydrophyllum tenuipes*; cryo-SEM micrograph of the modifications of an anthetic flower. Frozen nectar droplets are visible at the basal opening of the modification complexes (*). G, *Hydrophyllum virginianum*; cryo-SEM micrograph of the modifications of an anthetic flower. Frozen nectar droplets are visible at the basal opening of one modification complex (*). St = stamen. Scale bars: A = 100 µm, B = 500 µm, C–J = 1 mm.

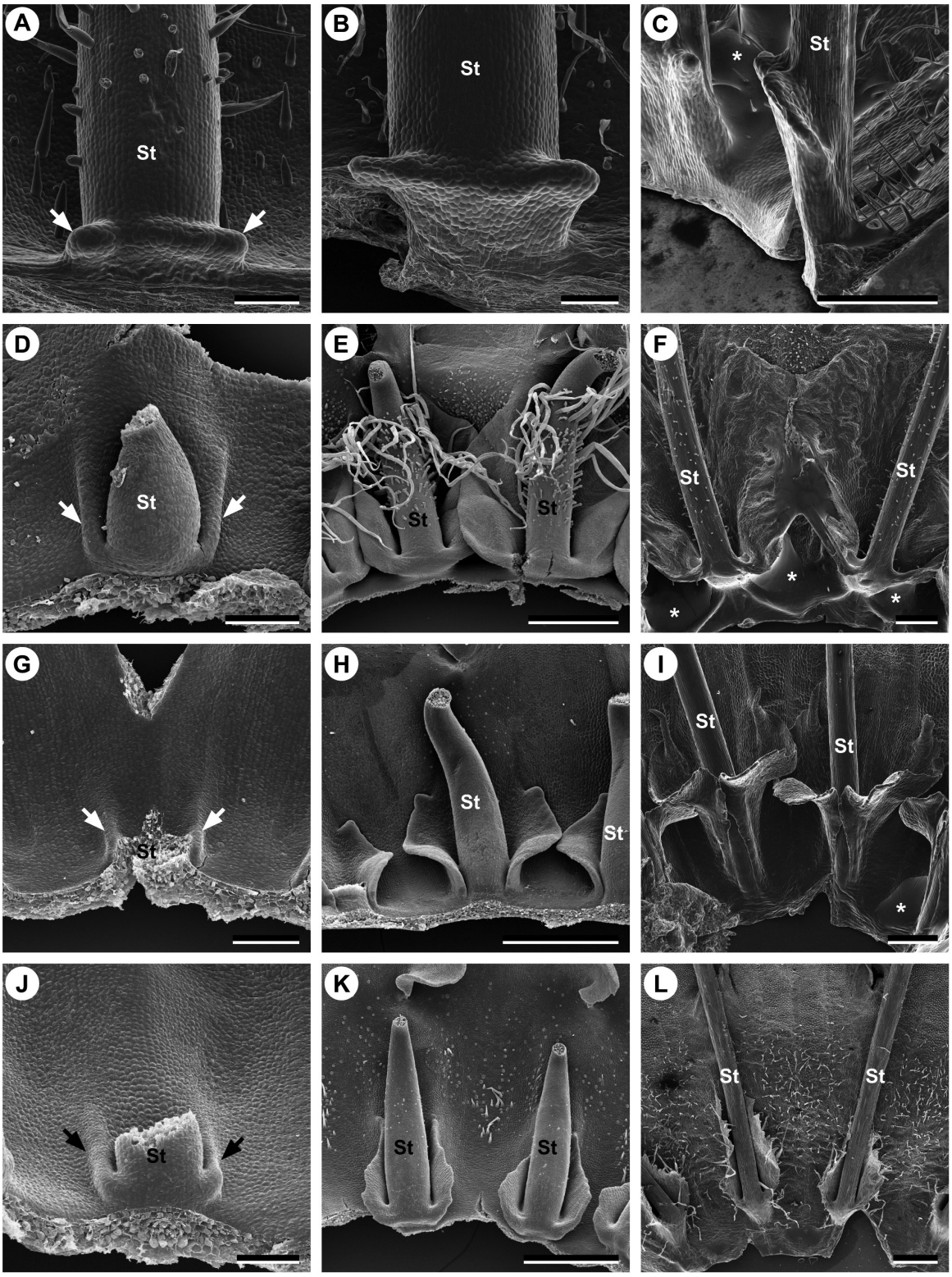

elongates with the corolla tube to which they are fused (Fig. 5D, E). The lateral protrusions of the filaments broaden throughout development of the modifications. Neighbouring modifications meet, continue to grow and consequently overlap (Fig. 5E). As soon as they overlap to large extent, they start to shrivel and interlock (Fig. 5F). The modifications continue to enlarge until anthesis in correlation to corolla tube elongation. Continued shrivelling of the interlocked parts results in clearly defined channels with a broad apical opening (Fig. 5F). Shortly before anthesis, the basal part of the corolla tube elongates.

The anthetic corolla is campanulate, the corolla tube is twice the length of the corolla lobes, and the filaments are inserted on the corolla tube (Fig. 5F). There is clear differentiation between basal and apical corolla tube. The modifications emerge from a broad tissue protrusion from the bases of the filaments (Fig. 5F). These protrusions grow in an ascending curve on both sides of the filament bases until neighbouring modifications meet in an antepetalous position. Where the modifications meet, they overlap and are fused through adhesion-interlocking (Fig. 5F). The modifications are fused with the corolla tube and reach their upper limit close to the level of the divergence points of the corolla lobes (Fig. 5F).

Phacelia malvifolia (Figs 1H, 5G–I)

Development of the modifications starts as elongated protrusions, already fused with the filament bases (Fig. 5G). Their growth parallels the elongation of the basal part of the corolla tube, the fused part of the filaments and the elongation of the apical part of the corolla tube. At intermediate developmental stages, the modifications start to differentiate into a basal part – fused with the filaments – a median part – which starts to develop into a broad scale – and an apical part – which ends in a short, free tip (Fig. 5H). In anthetic flowers, the broad parts of the modifications overlap and enclose a single, common compartment around the ovary and above the nectary disc (Fig. 5I).

The corolla is campanulate with a slight constriction below the diverging corolla lobes (Fig. 1H). The corolla tube is twice as long as the corolla lobes. The filaments are distinguishable from the corolla tube, but remain fused up to one-fifth of its length. The modifications are scale-like. They are fused with the basal part of the free filaments and the corolla tube (Fig. 5I). Above the level where the filaments diverge from the tube the modifications deviate from the filaments, broaden and form large, overlapping appendages. The basal parts of the modifications remain fused with the corolla tube and taper towards the divergence points of the corolla lobes (Fig. 5I). These narrow parts of the modifications each end in a short, free tip and form an opening to the otherwise closed compartment around the nectary formed by the broad, vertical lobes of the modifications (Fig. 5I).

Phacelia secunda (Figs 1I, 5J–L)

Development of the modifications starts as two elongated protrusions, which are already fused with the bases of the filaments (Fig. 5J). Development is correlated with the elongation of the apical part of the corolla tube (Fig. 5J, K). The basal part of the corolla tube elongates shortly before anthesis (Fig. 5L). The trichomes between the modifications are initiated after the onset of modification development (Fig. 5K). The margin beomes more elaborate and the trichomes on the modifications develop shortly before anthesis. In anthetic flowers, the margins of neighbouring modifications bend towards each other and the trichomes become slightly entangled (Fig. 1I).

The corolla is campanulate (Fig. 1I). The corolla tube is three times the length of the corolla lobes. Filaments insert on the corolla tube, demarcating a basal and an apical part of the tube. The filaments are bent towards the centre of the flower. At the point closest to the ovary, the filaments are laterally broadened (Fig. 5L). The modifications are already present on the points of filament insertion. They diverge from the filaments at the level of the lateral broadening but remain fused to the corolla tube. The modifications are broadest in

Figure 5. Morphology and development of the modifications in *Phacelia*. A–C, *Phacelia campanularia*. A, onset of modification development. Arrows point at modifications. B, derived state of modification development. C, cryo-SEM micrograph of the modification of an anthetic flower. Complete corolla tube is covered in frozen nectar (*). D–F, *Phacelia egena*. D, developmental state after onset of modification development. Arrows point at modifications. E, derived state of modification development. Neighbouring modifications overlap. F, cryo-SEM micrograph of the modifications of an anthetic stamen–corolla tube. Huge amounts of frozen nectar are visible at the basal openings of the modifications (*). G–I, *Phacelia malvifolia*. G, onset of modification development. Arrows point at modifications. H, derived state of modification development. I, cryo-SEM micrograph of the modification of the stamen–corolla tube of an anthetic flower. A frozen nectar droplet is visible at the base of the modifications (*). J–L, *Phacelia secunda*. J, developmental state shortly after onset of modification development. Arrows point at modifications. K, derived state of modification development. L, cryo-SEM micrograph of the stamen–corolla tube of an anthetic flower. St = stamen. Scale bars: A, B, D, G, J = 100 μm; C, E, F, H, I, K, L = 500 μm.

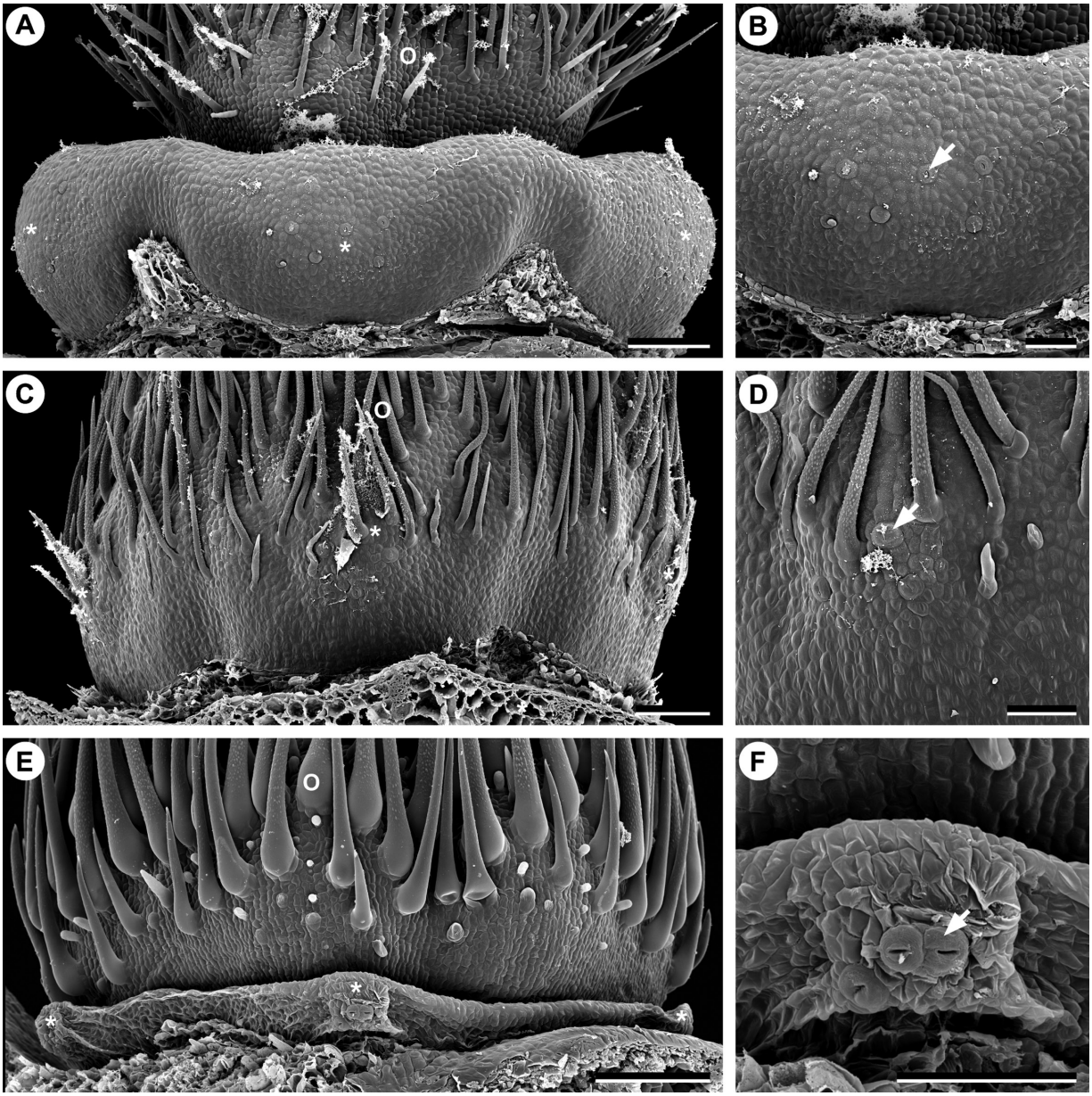

Figure 6. Nectary morphology in *Draperia systyla*, *Nemophila menziesii* and *Eucrypta chrysanthemifolia*. A, B, *Draperia systyla*. A, lobed nectary disc. B, individual lobe of the nectary disc, sparsely covered with nectarostomata. C, D, *Nemophila menziesii*. C, three of the five nectary glands are visible. D, individual nectary gland with nectarostomata. E, F, *Eucrypta chrysanthemifolia*. E, nectary disc. Two of the five glands are visible. F, nectary gland with nectarostomata. O = ovary, arrows point at nectarostomata, asterisks (*) indicate the position of the glands on/lobes of the nectary disc. Scale bars: A, C, E = 100 µm; B, D, F = 50 µm.

their lower third (Fig. 5K, L). They taper towards the sinuses between the corolla lobes, while remaining in close proximity to the filaments. The basal margin of the modifications is irregular and covered with simple trichomes (Fig. 5L). The antepetalous area between two neighbouring modifications is sparsely covered with simple trichomes.

Nectaries

Draperia systyla (Fig. 6A, B)

There is a massive nectary disc present at the base of the ovary. The diameter of the disc exceeds that of the ovary. The disc is slightly lobed, and these lobes are in antepetalous position (Fig. 6A). There are a

few nectarostomata on the central, dorsal parts of the lobes (Fig. 6B). Occasionally, nectarostomata are found on other parts of the disc.

Nemophila menziesii (Fig. 6C, D)

A distinct disc nectary is absent, and there are only five distinct nectary glands consisting of several nectarostomata each (Fig. 6C, D). These glands are localized well above the receptacle at the widest point of the ovary between the glabrous base and the trichomatous upper part of the ovary (Fig. 6D). The glands are slightly raised above the surrounding epidermis.

Eucrypta chrysanthemifolia (Fig. 6E, F)

A distinct nectary disc surrounding the base of the ovary is developed. It is pentagonal, and its diameter equals that of the ovary (Fig. 6E). Two to five nectarostomata are situated in each corner of the pentagonal disc nectary (Fig. 6F). In anthetic flowers, the area with nectarostomata is slightly raised above the disc and the disc tissue itself collapses (Fig. 6E, F).

Hydrophyllum canadense (Fig. 7A, B)

There is no distinct nectary disc, but the base of the ovary is inflated (Fig. 7A). Five nectary glands that are densely covered with nectarostomata emerge from the inflated part (Fig. 7B). Nectarostomata are concentrated on the glands, but some are scattered over the surrounding epidermis (Fig. 7B). The glands are situated above the receptacle at the widest point of the ovary (Fig. 7A). The lower part of the ovary is glabrous; simple trichomes are present at the tip of the ovary where it tapers into the style (not shown).

Hydrophyllum fendleri (Fig. 7C, D)

There is no distinct nectary disc, but the base of the ovary is inflated. Five nectary glands that are densely covered with nectarostomata slightly emerge from the inflated part (Fig. 7C). The lobes are in antepetalous position. There is a nectary gland at the centre of each lobe at the widest diameter of the ovary. The glands are laterally broadened and apically elongated. They are densely covered with nectarostomata (Fig. 7D). The basal part of the ovary is glabrous. Simple trichomes insert above the widest part of the ovary.

Hydrophyllum tenuipes (Fig. 7E, F)

There is no differentiation between ovary and nectary disc. Five separate nectary glands are present at the widest part of the ovary. The ovary is slightly lobed (Fig. 7E), and these lobes are in antepetalous position. The glands are localized at the centre of the lobes. Each gland is densely covered with nectarostomata; the glands are conical protrusions (Fig. 7F). The basal part of the ovary is glabrous. The glands are below the trichomes found in the apical portion of the ovary.

Hydrophyllum virginianum (Fig. 7G, H)

There is no differentiated nectary disc at the base of the ovary. The ovary is shallowly lobed (Fig. 7G), with the lobes in antepetalous position. There are five nectary glands in the centre of each lobe. The glands are laterally broadened protrusions of tissue immediately below the widest point of the ovary. The protrusions are sparsely covered with nectarostomata (Fig 7H). The basal part of the ovary is glabrous.

Phacelia campanularia (Fig. 8A, B)

There is a large, slightly lobed disc at the base of the ovary (Fig. 8A). From this distinct disc, the ovary tapers into the style. There is an increased number of nectarostomata on the dorsal portions of the lobes (Fig. 8B), but otherwise nectarostomata are distributed over the entire disc and even over the basal, glabrous part of the ovary.

Phacelia egena (Fig. 8C, D)

There is a distinct nectary disc at the base of the ovary (Fig. 8C), and it is slightly lobed. Each lobe protrudes into an ascending, laterally broadened tip, which is covered with nectarostomata (Fig. 8C, D). The lobes are in antepetalous position. The disc and the base of the ovary are glabrous.

Phacelia malvifolia (Fig. 8E, F)

There is a nectary disc at the base of the urn-shaped ovary. The nectary disc and lower part of the ovary are glabrous (Fig. 8E). The disc is slightly lobed and roughly pentagonal in shape. The five lobes are in antepetalous position. The upper margins of the lobes exceed the basal margins (Fig. 8E). Nectarostomata are located on the downward-facing parts of the lobes (Fig. 8F). The rest of the disc lacks any nectarostomata.

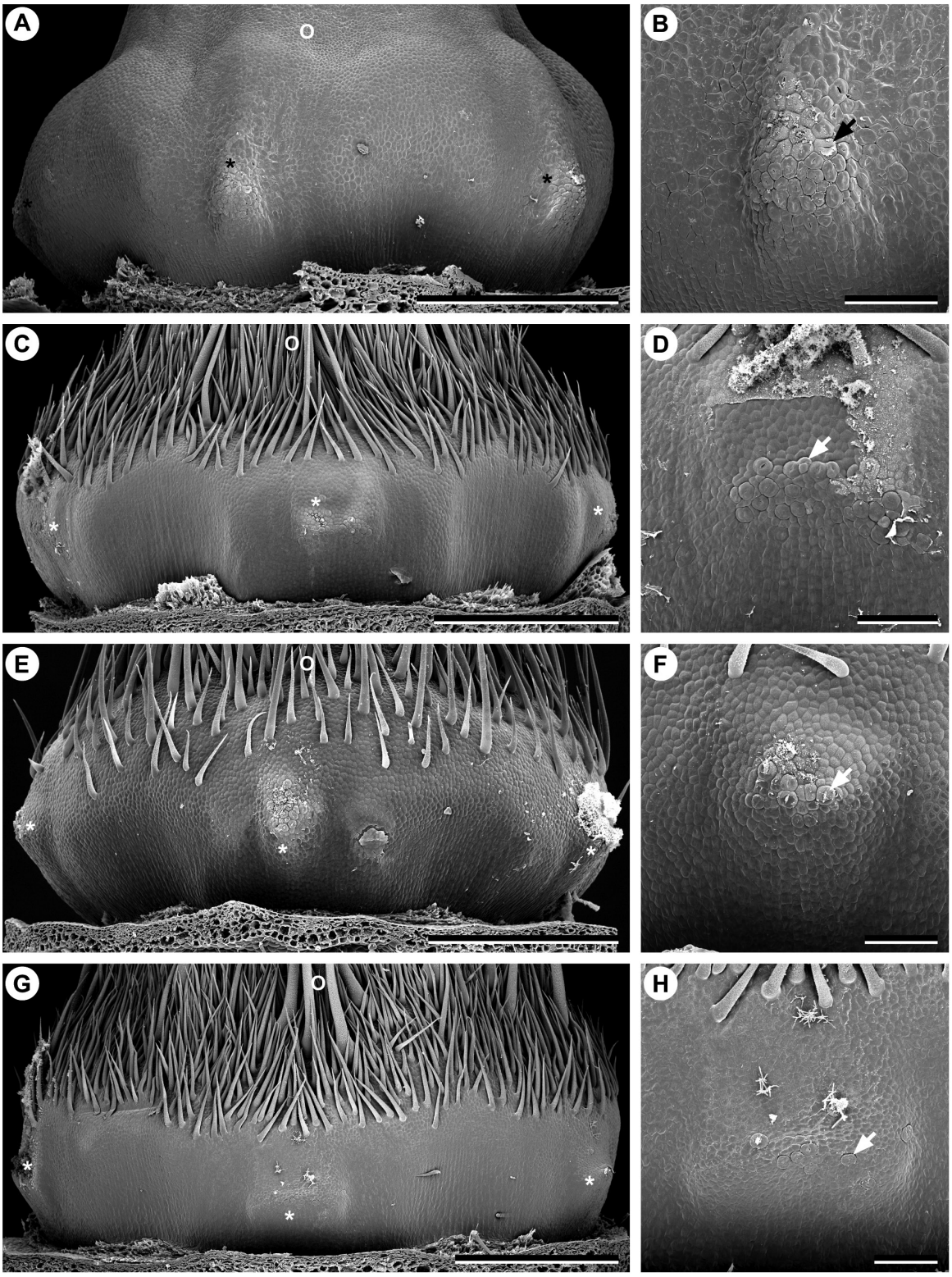

Phacelia secunda (Fig. 8G, H)

There is a flat nectary disc at the base of the urn-shaped ovary. The disc is slightly lobed, with the lobes in antepetalous position (Fig. 8G). Each lobe protrudes into a shallow tip which is covered with nectarostomata (Fig. 8H). The rest of the disc and the base of the ovary lack any nectarostomata and are glabrous.

DISCUSSION

The overall morphology and development of the stamen–corolla tube modifications of the Hydrophyllaceae are remarkably conserved across the family, in spite of superficially divergent flower shape. Development of the modifications universally starts in late flower ontogeny. Their development is tied to the elongation of the corolla tube and the bases of the filaments. Hofmann (1999: p. 208) found the modifications ('corolla scales') to be 'clearly of corolla origin'. However, our results indicate that the modifications are formed by the filament bases and the corolla tube and differentiating between tissues corresponding to these two organs is difficult. We therefore reject an exclusive origin of these modifications from the corolla.

We find that the number of modifications is fixed to ten across the taxa studied, even in species erroneously described as lacking modifications (e.g. *Draperia systyla*, Hofmann *et al.*, 2016). Floral organization is identical across the species and overall corolla shape varies only to a limited degree. The extremes in corolla shape are represented by *Nemophila menziesii* on the one hand (open, bowl-shaped) and *D. systyla* on the other (tubular). The presence of stamen–corolla tube modifications introduces an additional level of complexity into the floral architecture of this family.

Nectaries

The nectaries of the Hydrophyllaceae correspond to the gynoecial nectaries found across Boraginales. Lobed nectary discs are present in *Codon* (Codonaceae: Jeiter *et al.*, 2016), but the nectarostomata are here evenly distributed over the lobed disc. Lobed nectary discs have also been reported in Namaceae (Hofmann *et al.*, 2016), but detailed observations on the distribution of nectarostomata have not been published. The concentration of nectarostomata in specific 'nectary glands', i.e. only on the lobes of the nectary disc, is thus only known from Hydrophyllaceae. The locality of the nectarostomata corresponds to the position of the compartments formed by the modifications. Even in *Draperia* the glands are in antepetalous position, although no separate compartments are formed by the modifications. *Phacelia campanularia* is the only species in our sampling where nectarostomata cover the whole nectary disc and even extend to the glabrous base of the ovary. However, even in this species nectarostomata are concentrated in an antepetalous position. The change in nectarostomata distribution could be of secondary nature and related to the absence of separate compartments.

Function of the stamen–corolla tube modifications

The function of the stamen–corolla tube modifications remains uncertain. One functional aspect is to increase the complexity of the flower, which results in a change in floral architecture, simply through the presence and elaboration of the modifications. A floral architecture, where separate compartments are formed, each holding part of the total nectar reward of the flower, is called revolver architecture. Revolver architecture has been reported from various plant groups (Weigend & Gottschling, 2006; Endress, 2010; Jeiter *et al.*, 2016, 2017a) and is known to influence the pollinator behaviour. To collect the full reward of the flower a pollinator has to probe each compartment separately, rotating its body around the central axis of the flower. Flower complexity and compartmentalization probably increase both handling time and the amount of contact between the pollinator and floral organs, thereby increasing the likelihood of pollen removal and pollen deposition. Handling time has been shown to positively correlate with successful pollination and seed set (e.g. Manetas, 2000), but this aspect would need to be experimentally tested for Hydrophyllaceae, as only a few pollinator observations have been published (Loew, 1891; Merritt, 1897; summarized in Brand, 1913).

Figure 7. Nectary morphology in *Hydrophyllum*. A, B, *Hydrophyllum canadense*. A, three of five glands are visible. B, individual gland densely covered with nectarostomata. C, D, *Hydrophyllum fendleri*. C, three of five glands are visible. D, individual gland densely covered with nectarostomata. E, F, *Hydrophyllum tenuipes*. E, three of five glands are visible. F, individual gland covered with nectarostomata. G, H, *Hydrophyllum virginianum*. G, three of five glands are visible. H, individual gland covered with nectarostomata. O = ovary, arrows point at nectarostomata, and asterisks (*) indicate the position of the nectary glands. Scale bars: A, C, E, G = 500 μm; B, D, F, H = 100 μm.

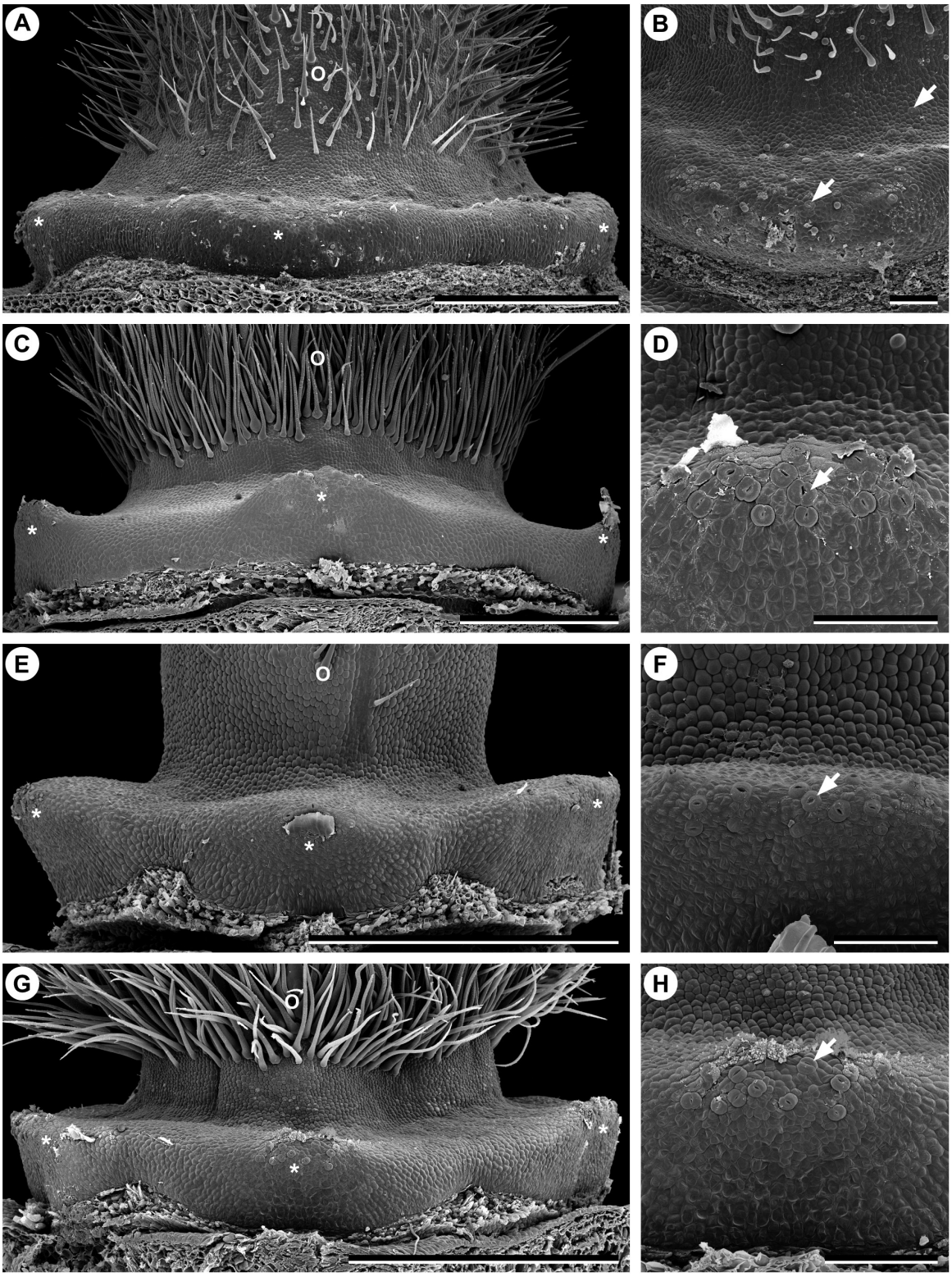

Other possible functions of stamen–corolla tube modifications ('elaborate petals') have been listed by Endress & Matthews (2006). Although each of these functions ideally needs to be tested, there are some functions we believe are more likely to be relevant here. The modifications in Hydrophyllaceae may function as nectar cover and as a protection against illegitimate flower visitors and nectar robbers. They hold the nectar (especially in *Hydrophyllum*; shown for *H. virginianum* by Loew, 1891) and they function as mechanical and possibly also optical nectar guides (e.g. in *P. malvifolia*, Fig. 1H). Simple, water-filled trichomes might additionally serve as nectar decoys (e.g. in *H. tenuipes*, Fig. 1F). The modifications might provide additional mechanical stability to the corolla (e.g. *D. systyla*) and protect important structures such as the ovary from mechanical damage (e.g. in *P. campanularia*). Finally, given our limited knowledge on these modifications in the Hydrophyllaceae, the possibility that the modifications are non-functional in an adaptive context (e.g. in *P. campanularia* or *D. systyla*) cannot be ruled out.

Stamen–corolla tube modifications similar to those described here in the Hydrophyllaceae can be found in several taxa of the Boraginales. Most prominent are faucal and basal scales in the Boraginaceae (Weigend *et al.*, 2016) and the apically broadened septa in *Codon* (Codonaceae: Jeiter *et al.*, 2016). In Namaceae, probably closely related to the Hydrophyllaceae (Weigend *et al.*, 2014; Luebert *et al.*, 2016), some paired modifications at the bases of the filaments have been described for *Nama* (Hitchcock, 1933a, b), but microscopic data and ontogenetic studies have not been published. A detailed comparison of stamen–corolla tube modifications is not the objective of the present study and will require additional observations on other, poorly studied groups based on a broader sampling in Boraginaceae and Namaceae.

Evolution of the stamen–corolla tube modifications

Based on the developmental data provided here, we are able to propose an evolutionary series for stamen–corolla tube modifications in Hydrophyllaceae (Fig. 9). Literature research indicates that our sampling includes all basic types of modifications described in Hydrophyllaceae (Brand, 1913; Hofmann, 1999; Hofmann *et al.*, 2016). Hydrophyllaceae are resolved into three major clades (Luebert *et al.*, 2016): the *Phacelia–Romanzoffia*-clade (Fig. 9, *Phacelia*-clade), the *Hydrophyllum–Pholistoma–Nemophila–Emmenanthe–Ellisia–Eucrypta*-clade (Fig. 9, *Hydrophyllum*-clade), and the *Draperia–Tricardia–Howellanthus–Hesperochiron*-clade (Fig. 9, *Draperia*-clade). Our study includes representatives from all three clades.

The hypothetical last common ancestor of the Hydrophyllaceae (Fig. 9A) likely had a short basal corolla tube and two short and simple modifications, probably similar to those found in *E. chrysanthemifolia* (Fig. 9i). Within the *Hydrophyllum*-clade the relationship between the length of the modifications and the length of the upper part of the corolla tube shifts (Fig. 9ii), finally resulting in modifications extending onto the corolla lobes in *Hydrophyllum* (Fig. 9iii). Elongation of the attached part of the filament with the associated modifications (Fig. 9iv) results in the hypothetical common ancestor of the *Draperia*- and *Phacelia*-clades (Fig. 9B). The modifications are reduced and only basal bulges remain, while the corolla tube is elongated (Fig. 9v). These evolutionary changes result in the floral architecture observed in *Draperia*. The basal bulges are closely associated with the fused part of the filaments (Fig. 9, *Draperia*-clade). Reduction of the elongated part of the filament (fused with the basal corolla tube; Fig. 9vi) results in the pattern observed in most *Phacelia* species (Fig. 9, *Phacelia*-clade). Because our understanding of the phylogeny of *Phacelia* is limited, we are not proposing any evolutionary series within the *Phacelia*-clade (indicated by the circular arrow with question mark in Fig. 9vii). However, the phylogenetic data available (Walden *et al.*, 2014) indicate convergent evolution of similar shapes of stamen–corolla tube modifications, which might either be characteristic for certain clades within *Phacelia* or have evolved more than once independently.

Figure 8. Nectary morphology in *Phacelia*. A, B, *Phacelia campanularia*. A, slightly lobed nectary disc. B, lobe of the nectary disc with nectarostomata present also on the apical part of the disc and on the base of the ovary. C, D, *Phacelia egena*. C, nectary disc with three of the five glandular lobes visible. D, individual glandular lobe. Tip densely covered in nectarostomata. E, F, *Phacelia malvifolia*. E, nectary disc with three of the five glandular lobes visible. F, glandular lobe covered with nectarostomata. G, H, *Phacelia secunda*. G, nectary disc with three of the five glandular lobes visible. H, glandular lobe covered with nectarostomata. O = ovary, arrows point at nectarostomata, and asterisks (*) indicate the position of the lobes of the nectary disc. Scale bars: A, C, E, G = 500 µm; B, D, F, H = 100 µm.

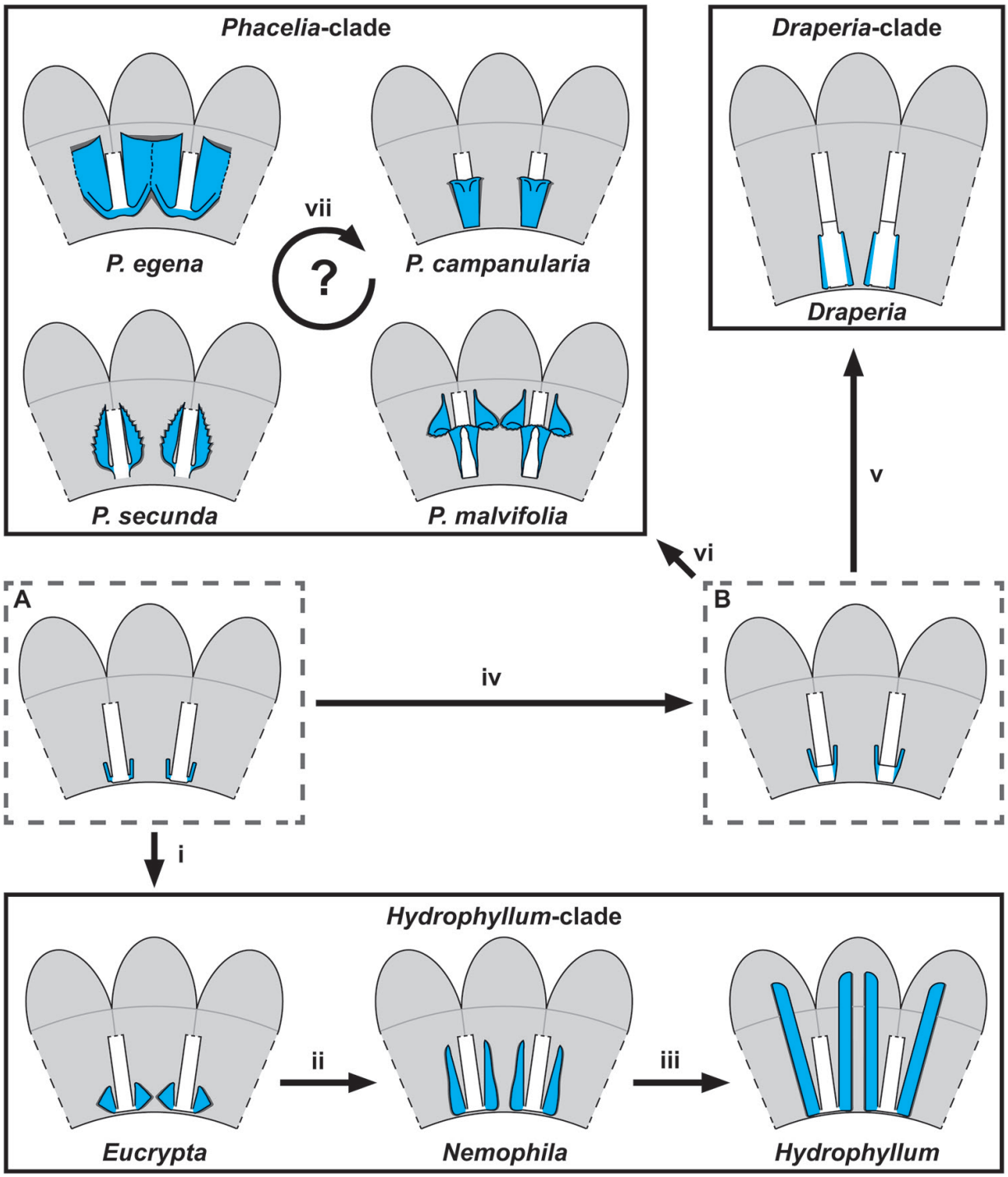

Figure 9. Schematic representation and evolutionary series of stamen–corolla tubes and their modifications in the Hydrophyllaceae. A, hypothetical common ancestor of the Hydrophyllaceae. B, hypothetical common ancestor of the *Draperia*- and *Phacelia*-clades. Refer to the text for further explanation. Dashed-lined grey boxes: reconstructed hypothetical ancestor; grey areas: corolla tube and corolla lobes; white rectangles with black outlines: filaments; blue areas: stamen–corolla tube modifications; dark grey areas: indication of spatial complexity, parts that are free from the corolla tube and/or filament.

CONCLUSIONS

The stamen–corolla tube modifications of the Hydrophyllaceae provide a unique set of characters. The modifications share a more or less uniform developmental trajectory, even in species with weakly developed modifications such as *Draperia systyla*. Relatively minor changes in developmental trajectories (elongation of the basal and/or apical part of the corolla tube) result in changes in position of the modifications in relation to the nectary and ovary and in changes in floral architecture (*sensu* Endress, 1996) and – ultimately – floral function.

However, there are several aspects of the floral architecture in Hydrophyllaceae and the order Boraginales which need to be addressed in further studies. In order to come to a functional understanding of the modifications and how they are integrated into the floral architecture serial sectioning for light microscopy or 3D-imaging techniques, such as high-resolution X-ray computed tomography, need to be employed. This would provide an understanding of the revolver architecture and the formation of separate or connected internal spaces. Functional implications could be studied by an integration of observational studies on flower biology and pollinator behaviour. Furthermore, other factors influencing floral architecture including climatic conditions, and genetic and developmental constraints should be taken into consideration.

This study shows that even simple morphological features can have a major impact on floral morphology and function. Here, we focus on the morphology and development of the stamen–corolla tube modifications in Hydrophyllaceae. Functional aspects will be addressed in future studies.

ACKNOWLEDGMENTS

We thank H.-J. Ensikat for helpful advice regarding cryo-SEM, S. Langecker for technical support and the staff of the Bonn University Botanic Gardens for cultivation of the studied species. We are grateful to G. K. Walden who gave valuable input. We thank E. F. Smets and F. Luebert for enlightening discussions. We also would like to thank L. P. Ronse De Craene and three anonymous reviewers for comments on and improvements to the manuscript. J.J. received funding for his doctoral thesis from the Studienstiftung des deutschen Volkes.

REFERENCES

Arber A. 1939. Studies in flower structure: V. On the interpretation of the petal and 'corona' in *Lychnis*. *Annals of Botany* **3:** 337–346.

Brand A. 1913. Hydrophyllaceae. In: Engler, ed. *Das Pflanzenreich [Heft 59] IV. 251*. Leipzig: Wilhelm Engelmann.

Endress PK. 1996. Homoplasy in angiosperm flowers. In: Sanderson MJ, Hufford L, eds. *Homoplasy – The recurrence of similarity in evolution*. San Diego: Academic Press, 303–325.

Endress PK. 2010. Synorganisation without organ fusion in the flowers of *Geranium robertianum* (Geraniaceae) and its not so trivial obdiplostemony. *Annals of Botany* **106:** 687–695.

Endress PK, Matthews ML. 2006. Elaborate petals and staminodes in eudicots: diversity, function, and evolution. *Organisms Diversity & Evolution* **6:** 257–293.

Gerstberger P, Leins P. 1978. Rasterelektronenmikroskopische Untersuchungen an Blütenknospen von *Physalis philadelphica* (Solanaceae) – Anwendung einer neuen Präparationsmethode. *Berichte der Deutschen Botanischen Gesellschaft* **91:** 381–387.

Gray A. 1875. A conspectus of the North American Hydrophyllaceæ. *Proceedings of the American Academy of Arts and Sciences* **10:** 312–332.

Hitchcock CL. 1933a. A taxonomic study of the genus *Nama*. I. *American Journal of Botany* **20:** 415–430.

Hitchcock CL. 1933b. A taxonomic study of the genus *Nama*. II. *American Journal of Botany* **20:** 518–534.

Hofmann M. 1999. Flower and fruit development in the genus *Phacelia* (Phacelieae, Hydrophyllaceae): characters of systematic value. *Systematics and Geography of Plants* **68:** 203–212.

Hofmann M, Walden GK, Hilger HH, Weigend M. 2016. Hydrophyllaceae. In: Kadereit JW, Bittrich V, eds. *Families and genera of vascular plants XIV*. Heidelberg: Springer, 221–238.

Jeiter J, Danisch F, Hilger HH. 2016. Polymery and nectary chambers in *Codon* (Codonaceae) – flower and fruit development in a small, capsule-bearing family of Boraginales. *Flora* **220:** 94–102.

Jeiter J, Hilger HH, Smets EF, Weigend M. 2017a. The relationship between nectaries and floral architecture: a case study in Geraniaceae and Hypseocharitaceae. *Annals of Botany* **120:** 791–803.

Jeiter J, Weigend M, Hilger HH. 2017b. Geraniales flowers revisited: evolutionary trends in floral nectaries. *Annals of Botany* **119:** 395–408.

Loew E. 1891. Blüthenbiologische Beiträge I. (N Pringsheim, ed.). *Jahrbücher für wissenschaftliche Botanik* **22:** 445–489.

Luebert F, Cecchi L, Frohlich MW, Gottschling M, Guilliams CM, Hasenstab-Lehman KE, Hilger HH, Miller JS, Mittelbach M, Nazaire M, Nepi M, Nocentini D, Ober D, Olmstead RG, Selvi F, Simpson MG, Sutorý K, Valdés B, Walden GK, Weigend M. 2016. Familial classification of the Boraginales. *Taxon* **65:** 502–522.

Manetas Y. 2000. Nectar amount, pollinator visit duration and pollination success in the mediterranean shrub *Cistus creticus*. *Annals of Botany* **86:** 815–820.

Merritt A. 1897. Notes on the pollination of some Californian mountain flowers - IV. *Erythea* **5:** 15–22.

Ronse De Craene LP. 2010. *Floral diagrams: an aid to understanding flower morphology and evolution*. Cambridge: Cambridge University Press.

Smith SD, Kriebel R. 2018. Convergent evolution of floral shape tied to pollinator shifts in *Iochrominae* (Solanaceae). *Evolution* **72:** 688–697.

Vaes E, Vrijdaghs A, Smets EF, Dessein S. 2006. Elaborate petals in Australian *Spermacoce* (Rubiaceae) species: morphology, ontogeny and function. *Annals of Botany* **98:** 1167–1178.

Walden GK, Garrison LM, Spicer GS, Cipriano FW, Patterson R. 2014. Phylogenies and chromosome evolution of *Phacelia* (Boraginaceae: Hydrophylloideae) inferred from nuclear ribosomal and chloroplast sequence data. *Madroño* **61:** 16–47.

Walden GK, Patterson R. 2012. Nomenclature of subdivisions within *Phacelia* (Boraginaceae: Hydrophylloideae). *Madroño* **59:** 211–222.

Weigend M, Gottschling M. 2006. Evolution of funnel-revolver flowers and ornithophily in *Nasa* (Loasaceae). *Plant Biology (Stuttgart, Germany)* **8:** 120–142.

Weigend M, Luebert F, Gottschling M, Couvreur TLP, Hilger HH, Miller JS. 2014. From capsules to nutlets – phylogenetic relationships in the Boraginales. *Cladistics* **30:** 508–518.

Weigend M, Selvi F, Thomas DC, Hilger HH. 2016. Boraginaceae. In: Kadereit JW, Bittrich V, eds. *Families and genera of vascular plants XIV*. Heidelberg: Springer, 41–102.

Whittall JB, Hodges SA. 2007. Pollinator shifts drive increasingly long nectar spurs in columbine flowers. *Nature* **447:** 706–709.

Chapter 6

A hierarchical view of floral architecture in Hydrophyllaceae – a framework for understanding flower evolution

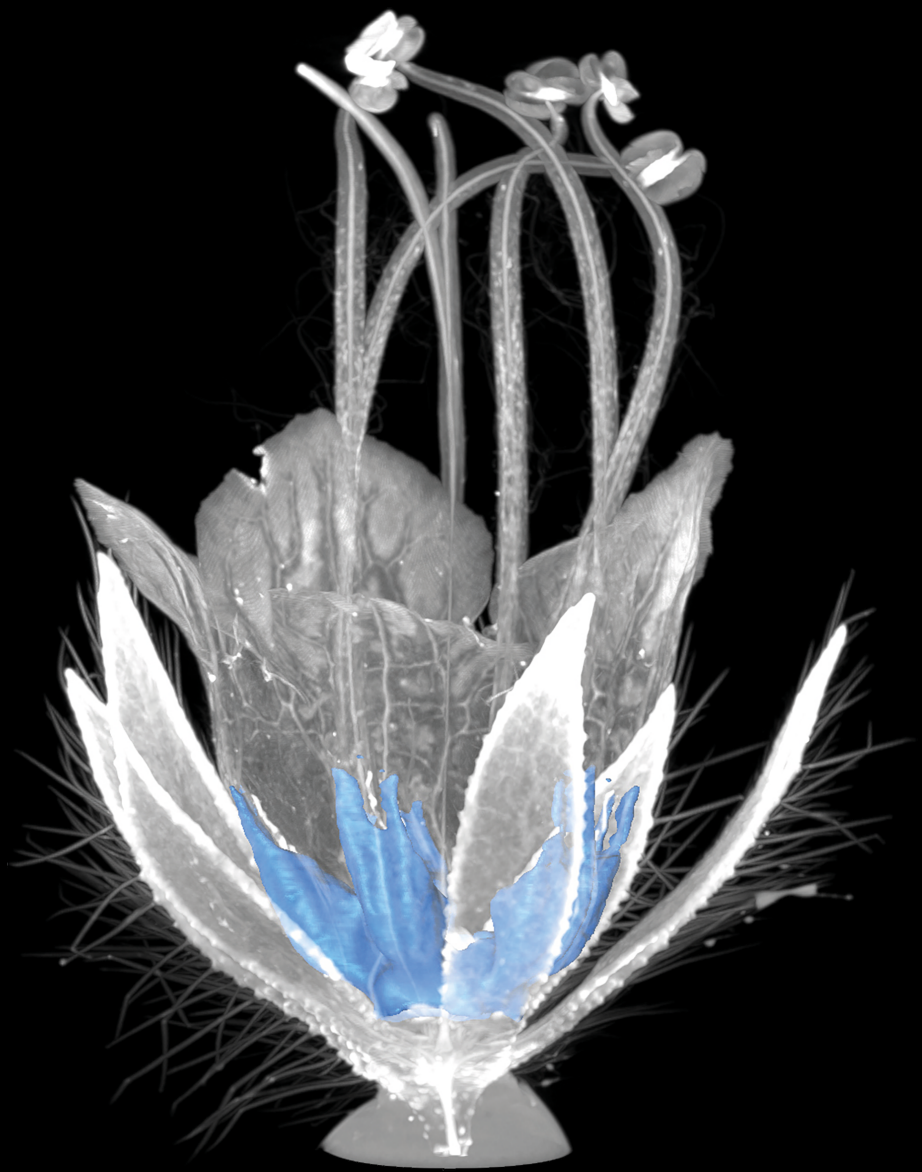

Jeiter J, Staedler YM, Schönenberger J, Luebert F, Weigend M. A hierarchical view of floral architecture in Hydrophyllaceae – a framework for understanding flower evolution. To be submitted.

A hierarchical view of floral architecture in Hydrophyllaceae – a framework for understanding flower evolution

Julius Jeiter[1,*], Yannick M. Staedler[2], Jürg Schönenberger[2], Federico Luebert[1,3], Maximilian Weigend[1]

[1]Nees-Institute for Biodiversity of Plants, University of Bonn, Meckenheimer Allee 170, 53115 Bonn, Germany

[2]Department of Botany and Biodiversity Research, University of Vienna, Rennweg 14, 1030 Vienna, Austria

[3]Departmento de Silvicultura y Conservacíon de la Naturaleza, Universidad de Chile, Santiago, Chile

*Corresponding author: jjeiter@uni-bonn.de

Abstract

Nectar is a common floral reward in angiosperms. Nectar presention varies between taxa and depends on floral architecture. Here, floral architecture and nectar presentation in the Hydrophyllaceae are studied using high-resolution x-ray computed tomography and micro-computed tomography in combination with molecular phylogenetics. Additionally, nectar removal experiments were conducted. 3D-geometric morphometrics were employed based on 3D-landmarking and the results were mapped onto the phylogeny. Furthermore, the air-filled space enclosed by the flowers is visualised. Based on the 3D-visualisation, three types of compartmentalisation are described (completely, incompletely and non-compartmentalised). The nectar removal experiments confirm complete reward partitioning in the flowers with complete compartmentalisation in contrast to flowers with incomplete compartmentalisation, where diverse patterns of nectar presentation were found. Most of the variation in floral architecture was explained by length and position of the stamen-corolla tube modifications and shape and length of the corolla tube. A strong phylogenetic signal for the 3D-landmark configurations was found. The results indicate, that besides floral structure, factors such as nectar amount, viscosity and presentation might influence floral function.

Keywords: flower ecology – flower function – nectar presentation – high-resolution x-ray tomography – micro-computed tomography – 3D-landmarking – 3D-geometric morphometrics

6.1 Introduction

Nectar is the most common reward in angiosperm flowers (Nicolson *et al.*, 2007; Willmer, 2011). The way nectar is presented influences the behaviour of the pollinator on the flower. Nectar is secreted from nectaries, which are integrated into the floral architecture (i.e., synorganisation, fusion, floral organ size differences resulting from differential growth rates and modification of floral organs; Endress, 1994, 1996) and their size and position influence both how and where the nectar can be accessed and thus have a profound effect on floral function. In the simplest case, i.e. in flowers with free access to the

floral centre and its rewards, nectar is presented openly to flower visitors (Endress, 1994). However, in other flowers the nectar is enclosed, e.g. in spurs (Hodges & Arnold, 1995; Whittall & Hodges, 2007) or floral tubes of varying types and depth (Cohen, 2012; Weigend *et al.*, 2016; Nocentini *et al.*, 2012). Here, access is canalized and restricted to certain types of pollinators (Pérez *et al.*, 2006; Cohen, 2016). The depth of flowers measured as the length of tubular structures containing the nectar often varies drastically even among closely related species (Kampny & Dengler, 1997; Weigend *et al.*, 2016), ranging from openly bowl-shaped to narrowly tubular flowers. This, in turn, affects pollinator selection (Muchhala & Thomson, 2009; Smith & Kriebel, 2018). A particularly elaborate and functionally complex type of nectar presentation is its secretion into separate floral compartments resulting in a revolver architecture (Endress, 1994, 1997, 2010; Weigend & Gottschling, 2006; Jeiter *et al.*, 2016, 2017). Prominent examples include *Aquilegia* with five spurred petals (Erbar *et al.*, 1999; Tucker & Hodges, 2005), *Geranium* with five nectar canals formed by sepals, petals and stamens (Endress, 2010; Jeiter *et al.*, 2017), or asclepiads with ten compartments formed by the corona (Endress, 2016).

In this study, we investigate Hydrophyllaceae (Boraginales; Luebert *et al.*, 2016). Floral organisation (i.e., number and insertion of the floral organs; Endress, 1994, 1996) in Hydrophyllaceae is highly conserved: The flowers are tetracyclic and pentamerous with five sepals, five petals, five stamens and two carpels (Hofmann *et al.*, 2016). Their floral architecture is dominated by fusions both within and between organ whorls: the petals are fused with each other and the corolla tube is fused with the filament bases. The resulting structure is called stamen-corolla tube (Fig. 6.1). However, a peculiar feature of Hydrophyllaceae are the usually ten scale-like modifications of the stamen-corolla tube originating from the adaxial surface of the corolla tube and the base of the filaments (Hofmann, 1999; Walden & Patterson, 2012; Hofmann *et al.*, 2016). Their morphology ranges from shallow ridges over various types of simple, trichome covered scales to elaborate scales complexes. Morphology and development of these modifications and their spatial relationships to the nectary disc have recently been studied in detail (Jeiter & Weigend, 2018). Jeiter & Weigend (2018) demonstrate that – despite superficial differences in their morphology – these modifications follow similar developmental trajectories in all species studied. Stamen-corolla tube modifications are initiated late during floral ontogeny, and their elongation and elaboration are correlated with the growth of the corolla tube and the filaments.

We also found that both these modifications and the lobes of the nectary disc where nectar is secreted are both placed in antepetalous position, indicating that these structures are synorganised and functionally integrated (Jeiter & Weigend, 2018). The modifications were shown to form compartments contributing to the formation of a revolver architecture. However, due to the technical limitations of scanning electron microscopy, a detailed three-dimensional characterisation of the floral compartments was impossible, and a functional integration therefore still speculative. The open, bowl-shaped flowers of, e.g. *Nemophila menziesii* would indicate simple nectar harvest, but observations by Brand (1913) documented unexpectedly long handling times of flower visitors and indicated possible hidden complexity.

We here apply high resolution X-ray computed tomography (HRXCT) respectively micro-computed tomography (μCT), 3D-geometric morphometric analyses based on 3D-landmarking and nectar probing experiments to understand the spatial and functional integration of stamen-corolla tube modifications into floral architecture and flower compartmentalisation. This study aims to address the following questions: *i*) What is the actual floral architecture of the different species and how is it influenced by the stamen-corolla tube modifications? *ii*) Are there differences in compartmentalisation of the internal floral space of the flowers? *iii*) How do floral architecture and compartmentalisation influence nectar presentation and removal? *iv*) Are there phylogenetic patterns underlying floral architecture, compartmentalisation and thus nectar presentation?

6.2 Material and methods

Morphology and morphometry

Sample collection and preparation. Anthetic flowers of twelve species from five genera were collected from cultivated plants at the Bonn University Botanic Gardens (Tab. 6.1) and subsequently fixed in formaldehyde-acetic acid-ethanol (FAA; 2% formaldehyde, 2% acetic acid, 70% ethanol). After at least one week in FAA the fixed material was transferred into 70% ethanol in which it was stored. Studied species, voucher numbers and voucher locations are shown in Table 1. The fixed flowers were transferred into an infiltration medium of phosphotungstic acid (PTA, 1%) and ethanol (70%) (Staedler *et al.*, 2013). Flowers were infiltrated for at least 14 days. The infiltration medium was changed every second day. Samples remained in the infiltration medium until preparation for scanning proceeded. The samples were dehydrated using increasing concentrations of ethanol plus PTA (1%) and, finally, acetone plus PTA (1%). The dehydrated samples were critical-point dried in an Autosamdri–3 15 (Series A, Rockville, MD) except for Phacelia tanacetifolia which was critical-point dried in a CPD 020 (Balzers Union, Liechtenstein). The flowers for the reconstruction of the internal space of the flowers were individually mounted on aluminium stubs with two-component epoxy resin (UHU PLUS Sofortfest, UHU, Bühl, Germany). Flowers used solely for landmarking (see below) were mounted in groups of two to eight on plastic plungers with two-component epoxy resin. This mounting technique reduced the final resolution of the scans but allowed for a higher throughput of samples.

Table 6.1: Studied species, IPEN-numbers and voucher placement.

Species	**Number of flowers**	**IPEN-number**	**Herbarium**
Draperia systyla Torr.	13	US-0-BONN-33089	BONN
Eucrypta chrysanthemifolia Greene	2	US-0-BONN-36929	BONN
Hydrophyllum canadense L.	1	xx-0-BONN-9457	BONN
Hydrophyllum fendleri (A. Gray) A. Heller	9	CA-0-BONN-39162	BONN
Hydrophyllum tenuipes A. Heller	11	US-0-BONN-35287	BONN
Hydrophyllum virginianum L.	12	xx-0-BONN-36861	BONN
Nemophila menziesii Hook. & Am.	4	xx-0-BONN-38177	BONN
Phacelia campanularia A. Gray	4	PE-0-BONN-35820	BONN
Phacelia egena (Brand) Greene ex J. T. Howell	12	US-0-BONN-37009	BONN
Phacelia malvifolia Cham.	3	US-0-BONN-37883	BONN
Phacelia secunda J. F. Gmel.	16	CL-0-BONN-38409	BONN
Phacelia tanacetifolia Benth.	5	xx-0-BONN-31966	BONN
Total	**92**		

High-resolution X-ray computed tomography (HRXCT). The scans were performed on a MicroXCT-200 imaging system (Xradia, Pleasanton, CA) with a L9421-02 90kV Microfocus X-ray source (Hamamatsu Photonics, Iwata City, Japan). Scans of *Phacelia tanacetifolia* were performed in a SkyScan 1272 (Bruker Co, Billerica, MA, US) equipped with a HAMAMATSU L11871 20 source (Hamamatsu, Japan) and a Ximea xiRAY16 camera (Ximea GmbH, Münster, Germany). Scan settings are shown in online supplement Table S1. In total, 92 flowers were scanned (Tab. 6.2).

Table 6.2: Number of flowers used for the different parts of this study.

	HRXCT or µCT		
Species	**Landmarking**	**Internal spaces**	**Nectar**
Draperia systyla	13	1	25
Eucrypta chrysanthemifolia	2	1	-
Hydrophyllum canadense	1	1	25
Hydrophyllum fendleri	9	1	25
Hydrophyllum tenuipes	11	1	11
Hydrophyllum virginianum	12	1	25
Nemophila menziesii	4	1	25
Phacelia campanularia	4	1	25
Phacelia egena	12	1	-
Phacelia malvifolia	3	1	19
Phacelia secunda	16	1	25
Phacelia tanacetifolia	5	1	25
Total	**92**	**12**	**230**

Reconstruction, visualisation and segmentation of compartments. 3D reconstruction from the scanning data was either performed using XMReconstructor 8.1.6599 (XRadia, Pleasanton, CA, USA) or InstaRecon Engine v2 (InstaRecon, Champaign, IL, USA). Scans were visualised using AMIRA 5.4.1, 6.4.0 or 6.5.0 (FEI Visualization Sciences Group, Bordeaux, France). The internal floral space is the air-filled volume enclosed in the stamen-corolla tube. Compartments are the portions of the internal spaces that are delimited by two neighbouring modifications of the stamen-corolla tube. Compartments were segmented using the AMIRA segmentation module. The compartments were labelled slice by slice using the magic wand tool of the segmentation module. The magic wand tool was set to the lower end of grey values (0 – ∼7500, 16-bit; 0 – 21, 8-bit) of the histogram which indicate the absence of structure. Where obvious, bright artefacts (ring-, streak artefacts) were corrected manually or otherwise excepted as variation in compartment shape. Deformations of the flowers due to preparation artefacts did not affect the overall configuration of the modifications and compartments.

3D-landmarking. For all 92 flowers 27 homologous landmarks in relation to floral architecture were identified and placed in the digital 3D-model as displayed in AMIRA (Fig. 6.1, Tab. 6.3). Corolla lobes were excluded as prone to preparation artefacts. The landmarks were placed on ideal virtual cross-sections through the model using the Slice function of AMIRA, or directly on the surface of an isosurface rendering set to the minimal value of the histogram used for visualisation of the model.

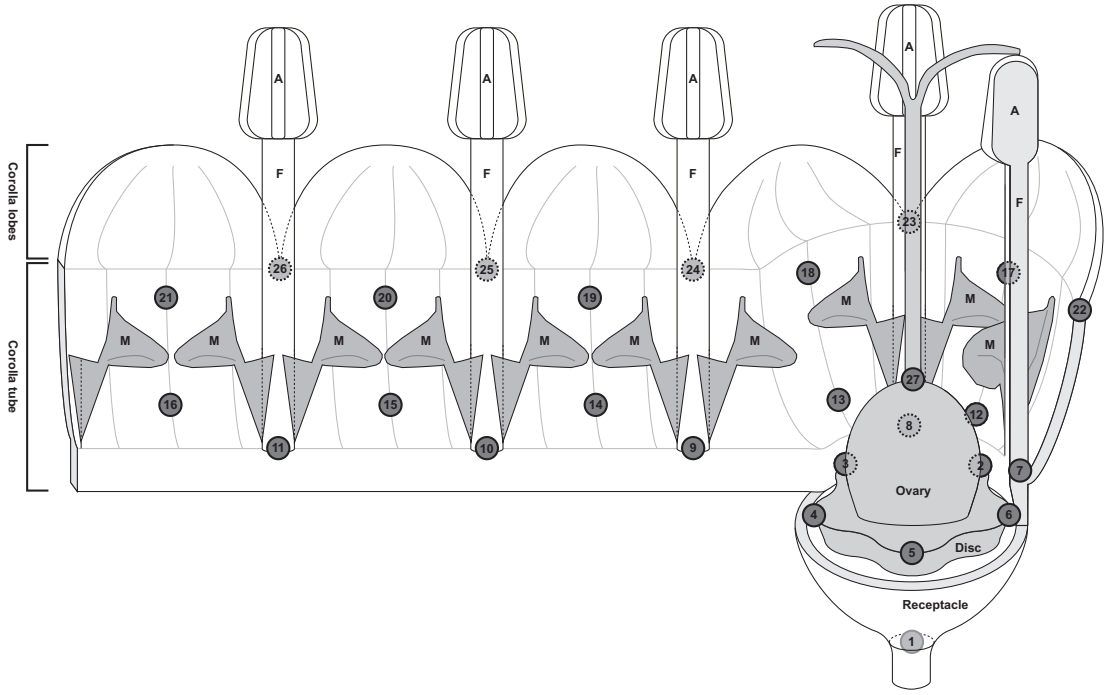

Figure 6.1: Schematical representation of a Hydrophyllaceae flower and landmarks. The modifications (M) resemble those of *Phacelia malvifolia*. Numbers indicate the 3D-landmarks placed for the 3D-geometric morphometric analysis. Dashed lines indicate numbers and structures hidden behind organs in the foreground. Number 1 in a light grey circle is placed inside the receptacle, where the vascular bundles of the petiole diverge. A = anther, F = filament, M = modification.

Nectar measurement

For ten species (Tab. 6.2) nectar volumes were measured. Individual flowers or complete inflorescences were enclosed in fine mesh and the plants were watered to soil capacity the day preceding nectar measurements. Measurements were conducted from June to August 2018 between 8 a.m. and 12 p.m. under comparable weather conditions. For each of the ten species a maximum of 25 flowers from one or two individual plants of the same accession were sampled (Tab. 6.2). Nectar was measured with 0.5 and 5 µl glass capillaries (Minicaps®, Hirschmann Laborgeräte, Eberstadt, Germany). The capillaries were inserted between neighbouring anthers, between neighbouring modifications in antepetalous positions. Each flower was subsimultaneously probed in all five antepetalous positions with five separate capillaries. Disturbance of the flowers was kept to a minimum to avoid coalescence of separate nectar droplets. The nectar column in the capillaries was quantified with a millimetre scale and converted into microlitres.

Statistical analysis

Landmarks were exported as 3D-coordinates and compiled in one file. A generalised Procrustes fit analysis with the raw data was performed and a covariance matrix was generated. The matrix was used in a principal component analysis (PCA). Centroid sizes resulting from the generalised Procrustes analysis as well as the PC-scores resulting from the PCA were pooled by species and mapped onto the phylogeny obtained from Bayesian inference (see below). Centroid sizes as used here can be interpreted as proxy for flower size. The parameters were mapped onto the phylogeny using unweighted squared-change parsimony. The results were weighted by branch length. Mapping was

followed by a permutation test with 1 000 000 random permutations against the Null-hypothesis of no phylogenetic signal (Klingenberg & Gidaszewski, 2010). All analyses of the landmarks were conducted in MorphoJ 1.06d (Klingenberg, 2011).

The centroid sizes per species from the Procrustes fit analysis were exported from MorphoJ and averaged per species and the averages of nectar volume were calculated. The mean values were checked for normal distribution (Shapiro-Wilk-test) followed by a correlation analysis (Pearson-test) in R (Version 3.5.1; R Core Team, 2018). Due to dependence of the five separate nectar measurements per flower, no test was performed to determine the differences in nectar measurements patterns.

Table 6.3: Landmark position and number of landmarks per position and flower.

Landmark position	**N of landmarks**	**Number**
Base of the flower (vascular bundles of the petiole diverge)	1	1
Nectary glands	5	2 – 6
Point where filaments detach from corolla tube	5	7 – 11
Point where modifications detach from filaments	5	12 – 16
Apical limit of the modifications	5	17 – 21
Point where corolla lobes diverge	5	22 – 26
Point where style is inserted on the ovary	1	27
Sum of landmarks per flower	**27**	

Phylogenetic reconstruction

Phylogenetic analyses were based on the data matrix with four plastid loci (ndhF, rbcL, rps16, and trnL-trnF) of Weigend *et al.* (2014), with some additions for Hydrophyllaceae (additional species: *Draperia systyla*, *Hydrophyllum fendleri*, *Hydrophyllum tenuipes*, *Hydrophyllum virginianum Phacelia egena*, *Phacelia malvifolia*, *Phacelia secunda*, *Phacelia tanacetifolia*. All material for DNA extraction was collected from the plants given in table 6.1. GenBank accession numbers will be added once the manuscript is submitted and accepted). Each locus was separately aligned using MAFFT v6.624b (Katoh *et al.*, 2002) and concatenated afterwards. Maximum Likelihood (ML) and Bayesian (BA) analyses were carried out. The ML analysis was conducted using RAxML NG v.0.6.0 BETA over the RAxML BlackBox (Stamatakis, 2006) under the GTR + Γ substitution model (Weigend *et al.*, 2014). ML Bootstrap values were calculated based on 200 replicates. The Bayesian analysis was performed using RevBayes v.1.0.9 (Höhna *et al.*, 2016) under the same substitution model. We ran four independent replicates with 30 000 generations, sampling every 25 generations and with a tuning interval of 200 generations. Convergence was evaluated using Tracer v1.5 (http://tree.bio.ed.ac.uk/software/tracer/, accessed 22 May 2018) and 25% of the trees were discarded as burn-in.

6.3 Results

Compartments

Based on our definition of compartments as portion of the air-filled internal space of the stamen-corolla tube which is enclosed by neighbouring modifications, we found three patterns of compart-

mentalisation: *i*) flowers with five separate compartments (Fig. 6.2 A, B), *ii*) flowers with five basally interconnected compartments (Fig. 6.2 C, D), and *iii*) absence of compartments (Fig. 6.2 E). Flowers with separate compartments are found in *Eucrypta chrysanthemifolia* (Figs. 6.2 A, 6.3 A, A6.1 A–C), *Nemophila menziesii* (Figs. 6.3 B, A6.1 D–F), *Hydrophyllum canadense* (Figs. 6.3 C, A6.1 G–I), *H. fendleri* (Figs. 6.3 D, A6.1 J–L), *H. tenuipes* (Figs. 6.3 E, A6.2 A–C) and *H. virginianum* (Figs. 6.3 F, A6.2 D–F). Flowers with basally interconnected compartments were found in *Phacelia malvifolia* (Figs. 6.2 D, 6.3 G, A6.2 G–I), *P. tanacetifolia* (Figs. 6.3 H, A6.2 J–L), *P. secunda* (Figs. 6.3 I, A6.3 A–C) and *P. egena* (Figs. 6.2 C, 6.3 J, A6.3 D–F). The relative proportions of the compartments and the basal interconnected portion vary between the species. No compartments were found in *Phacelia campanularia* (Figs. 6.3 G, A6.3 G–I) and *Draperia systyla* (Figs. 6.2 E, 6.3 L, A6.3 J–L).

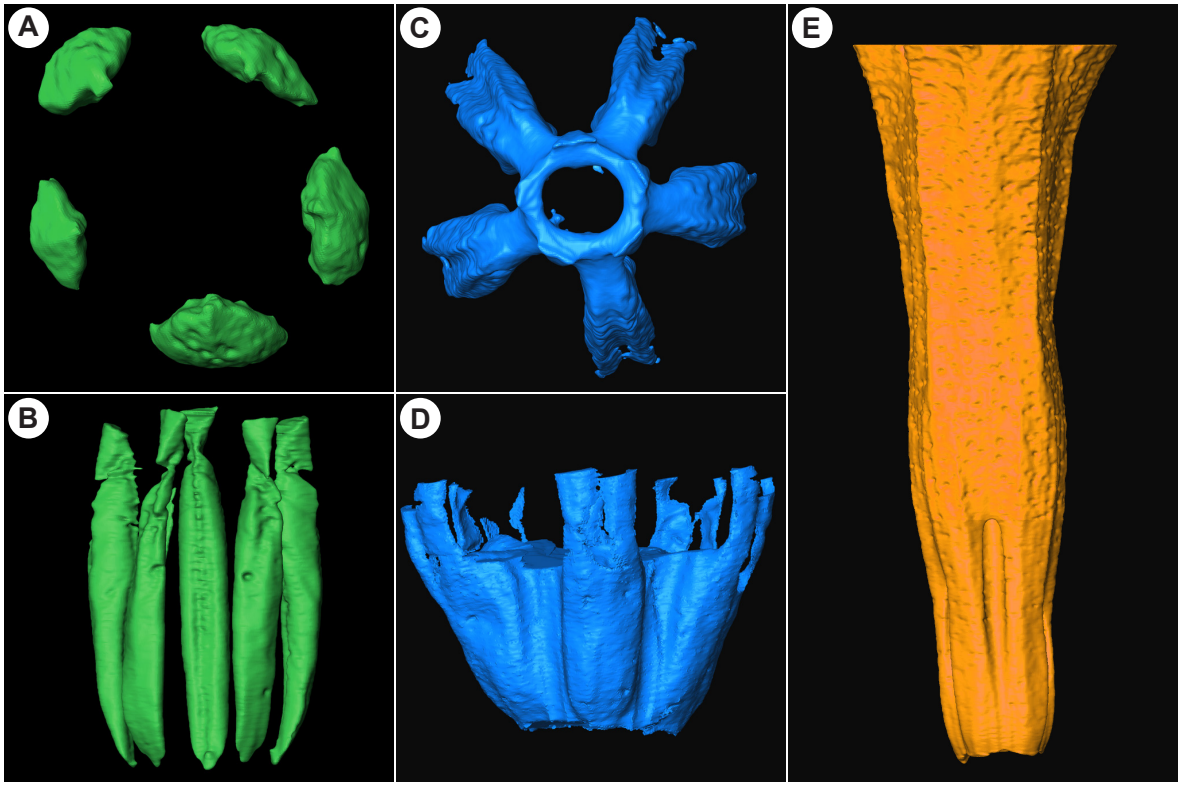

Figure 6.2: Examples of the three types of compartmentalisation found in the Hydrophyllaceae flowers. Shown are 3D-models of the segmented compartments. Segmentation was based on 3D-models from HRXCT-scanning data. A, B, complete compartmentalisation. A, *Eucrypta chrysanthemifolia*, viewed from below. B, *Hydrophyllum virginianum*, in lateral view. C, D, incomplete compartmentalisation. C, *Phacelia egena*, viewed from below. D, *Phacelia malvifolia*, in lateral view. E, absence of compartmentalisation in *Draperia systyla*, in lateral view. The colours represent the three lineages as indicated in figure 6.6 and figure A6.5.

Nectar measurements

The amount of nectar harvested per flower ranged from <0.01 to 8.92 µl. Average amounts of nectar per species are given in table A6.2. The largest amount of nectar was produced by *Hydrophyllum fendleri* (3.89 µl, ± 2.29 µl) and the smallest amount by *Draperia systyla* (<0.01 µl, ± 0.01 µl).

Separate probing of the five compartments resp. nectary glands per flower resulted in widely different removal patterns (Fig. 5). In *Nemophila menziesii* (Fig. 6.4 A), *Hydrophyllum virginianum* (Fig. 6.4 B), *H. canadense* (Fig. 6.4 C), *H. fendleri* (Fig. 6.4 D), *H. tenuipes* (Fig. 6.4 E) and *Phacelia*

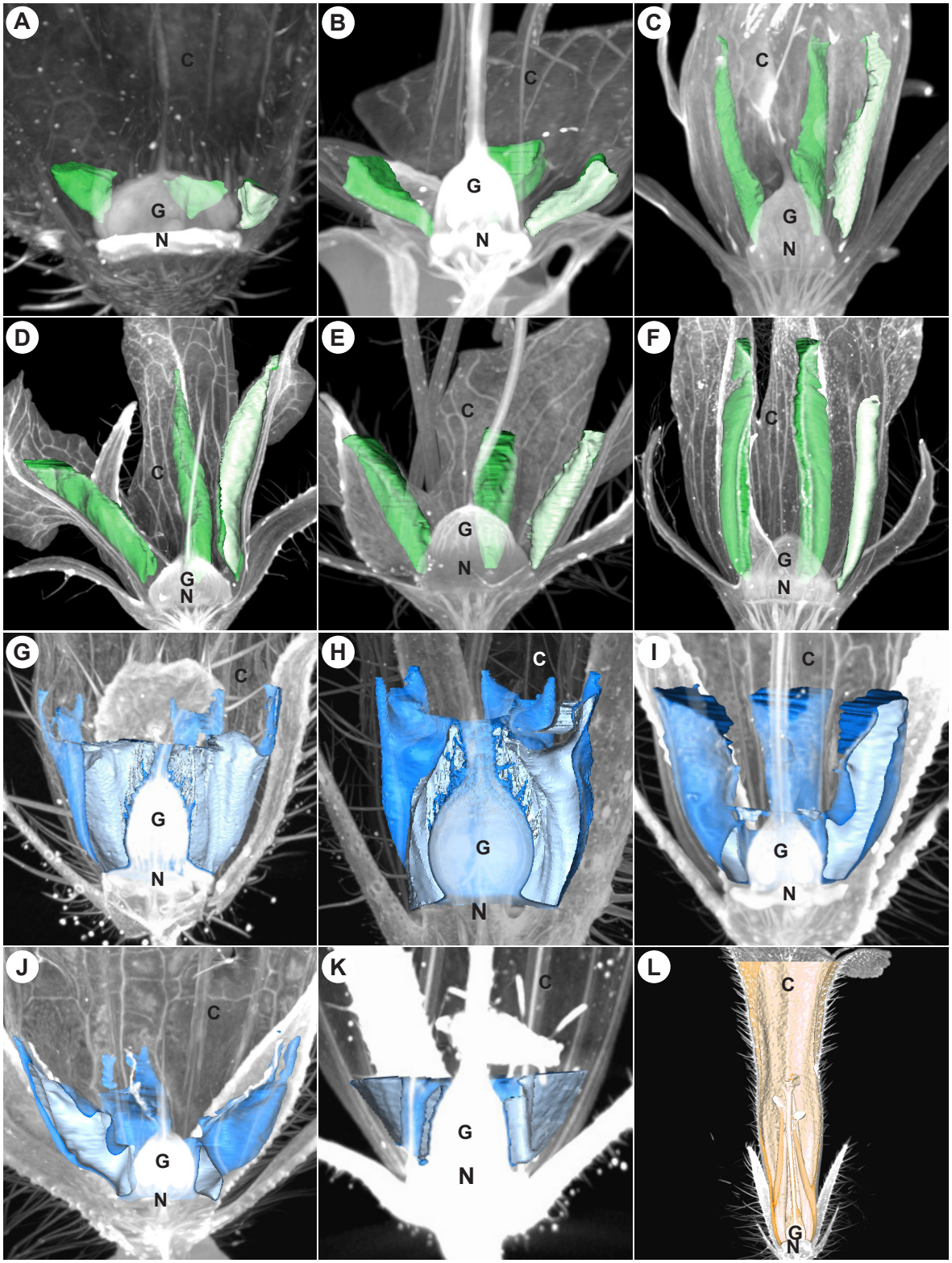

Figure 6.3: 3D-models of the HRXCT-scans with the segmented compartments in colour. An idealized virtual longitudinal section is used to remove one half of the flower to show how the internal spaces are integrated into the floral architecture. A, *Eucrypta chrysanthemifolia*. B, *Nemophila menziesii*. C, *Hydrophyllum canadense*. D, *Hydrophyllum fendleri*. E, *Hydrophyllum tenuipes*. F, *Hydrophyllum virginianum*. G, *Phacelia malvifolia*. H, *Phacelia tanacetifolia*. I, *Phacelia secunda*. J, *Phacelia egena*. K, *Phacelia campanularia*. L, *Draperia systyla*. The colours represent the three lineages as indicated in figure 6.6 and figure A6.5. Strong colours show the outer surface of the internal spaces, light colours show the inner surface where the internal space is cut by the virtual longitudinal section. C = corolla, G = gynoecium, N = nectary disc/ plane of nectary glands.

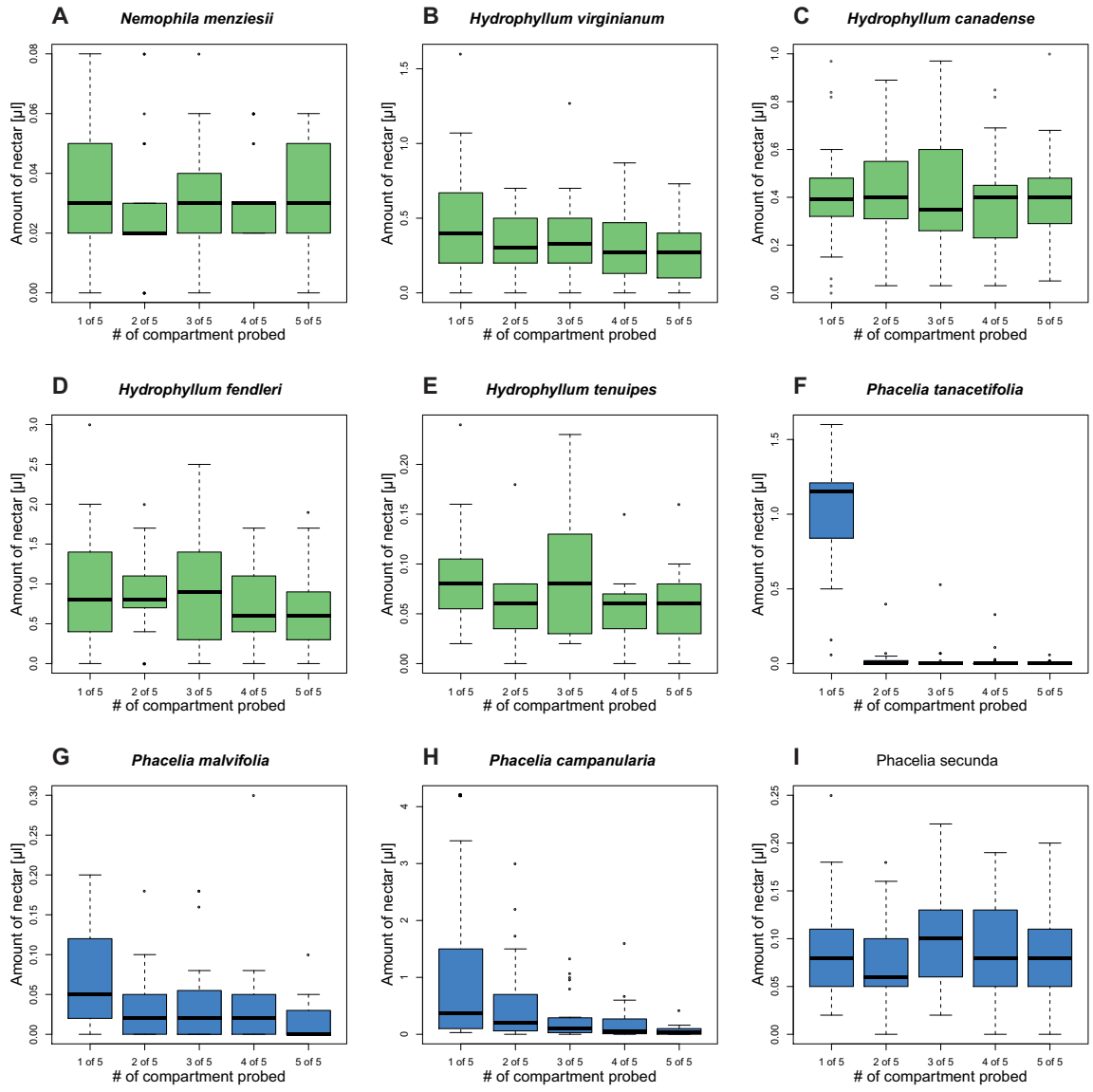

Figure 6.4: Boxplots of the amount of nectar per compartment/consecutive measurement of the flower. A, *Nemophila menziesii*. B, *Hydrophyllum virginianum*. C, *Hydrophyllum canadense*. D, *Hydrophyllum fendleri*. E, *Hydrophyllum tenuipes*. F, *Phacelia tanacetifolia*. G, *Phacelia malvifolia*. H, *Phacelia campanularia*. I, *Phacelia secunda*. Note the differences of scaling between the graphs. Colour coding of this figure follows the colour of the lineages indicated in Figure 6.2 1.

secunda (Fig. 6.4 I) similar amounts of nectar could be extracted from each of the sequentially sampled compartments. From the flowers of *Phacelia tanacetifolia* most of the overall nectar was removed from the first compartment probed (1.02 µl, ± 0.41 µl), while the rest of the compartments only yielded small amounts (0.08 µl, ± 0.20 µl) (Fig. 6.4 F). *Phacelia malvifolia* (Fig. 6.4 G) and *P. campanularia* (Fig. 6.4 H) showed mixed patterns: Most of the nectar was removed from the first compartment probed, decreasing amounts retrieved from the subsequently probed compartments.

Geometric morphometric analysis based on 3D-landmarks

The first two PCs explain 70.39% and 16.12% (total 86.51%) of variation in the principal component analysis of the Procrustes coordinates, respectively (Fig. 6.5 A, Tab. A6.3). The most important

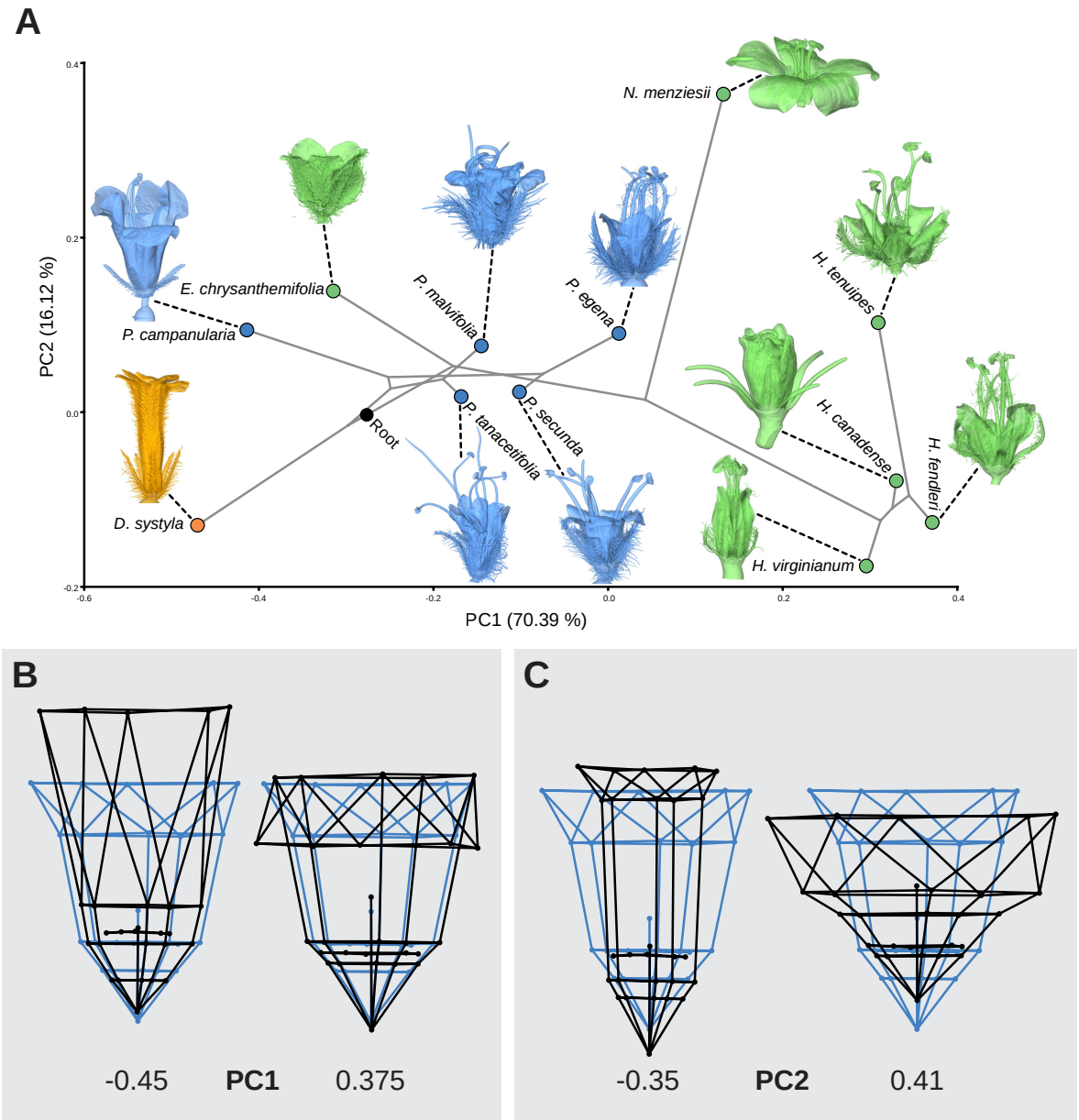

Figure 6.5: PC-scores averaged by species mapped onto the phylogeny and wireframes of the 3D-landmarks. A, results of the PCA plotted by species and mapped onto the phylogeny (grey lines) received from Bayesian inference. For each species a 3D-model from the HRXCT-scanning of the flower is shown (linked by a dashed, black line). B, wireframe visualisation of the shape changes along the PC1-axis. Illustrated is the XY-viewing plane. Blue shows the configuration of the Procrustes landmarks. The black wireframe shows the extremes of the PC1-axis. C, wireframe visualisation of the shape changes along the PC2-axis. Illustrated is the xy-viewing plane. Blue shows the configuration of the Procrustes landmarks. The black wireframe shows the extremes of the PC2-axis. Colour coding in A follows the colour of the lineages as indicated in Figure 6.2.

landmarks for PC1 are the x-coordinates of the sinuses between the corolla lobes (landmarks 22-26; Fig. 6.1) and the x-coordinates of the apical points of the modifications (landmarks 17-21; Fig. 6.1), corresponding to the distance between those two sets of landmarks (Fig. 6.5 A, B) with the longest in *Draperia systyla* and the shortest in *Nemophila menziesii*. In *Hydrophyllum*, the positions of the distal ends of the modifications and the distal end of the corolla tube are switched since the modifications extend onto the corolla lobes. PC2 is influenced by several landmark positions and in contrast to PC1 not just by x-, but also y- and z-coordinates (Fig. 6.5 A, C). It roughly represents corolla tube shape. Flowers with tubular corolla tube shape are present in *Hydrophyllum virginianum*

and *Draperia systyla*. The other extreme is represented by the open, bowl-shaped corolla tube of *Nemophila menziesii*.

The unweighted squared-change parsimony test with 1 000 000 permutations showed no phylogenetic signal for centroid size as a measure of flower size (p = 0.4190, tree length = 208.01; Fig. A6.4), but a significant phylogenetic signal for those PC-scores that are a measure for flower shape (p = 0.0026**, tree length = 0.586, Fig. 6.5). Average centroid sizes are given in table A6.4. No correlation was found between centroid size and the amount of nectar produced (p = 0.4022, r = 0.2985).

Phylogeny

The crown-node of the family is highly supported (BS 100, PP 1, Figs. 6.6, A6.5). *Phacelia* is monophyletic and all nodes show maximum support (100 BS, 1 PP). Within *Phacelia*, *P. malvifolia* and *P. tanacetifolia* form a clade which is sister to the remaining species of *Phacelia*. *Phacelia campanularia* is placed as sister to the clade with *P. egena* and *P. secunda*. *Eucrypta chrysanthemifolia*, *Nemophila menziesii* and *Hydrophyllum* form a fully supported clade (100 BS, 1 PP) and the relations between the genera within this clade are well resolved (100 BS, 1 PP). The relationships among the different species of *Hydrophyllum* are not resolved, nor is the placement of *Draperia systyla*. The phylogenies based on Bayesian inference and Maximum Likelihood (not shown) did not differ in their topology.

6.4 Discussion

The flower morphology of the Hydrophyllaceae is rather simple (Hofmann, 1999; Hofmann *et al.*, 2016; Jeiter & Weigend, 2018), but the stamen-corolla tube modifications and the resulting architecture can be regarded as complex and unique features in this plant family. Both the morphology of the stamen-corolla tube modifications and the resulting compartmentalisation of the internal floral space show a clear phylogenetic pattern (Fig. 6.6), whereas the overall shape of the corolla tube shape and flower size are more plastic. Separate compartments are only found in the clade comprising *Hydrophyllum*, *Nemophila* and *Eucrypta*. Basally interconnected compartments are present in all species studied apart from *Phacelia campanularia*, where it seems to have been secondarily lost (nested in the *Phacelia* clade, Figs. 6.6, A6.5; see also Walden *et al.*, 2014). A PCA based on the 3D-geometric morphometric analysis retrieves two factors as explaining most of the variability between species: *i*) the position and length of stamen-corolla tube modifications relative to the corolla tube and its length, and *ii*) the overall shape of the corolla tube. Corolla tube shape and size appear to be more plastic in Hydrophyllaceae, while the spatial relationship between the stamen-corolla tube modifications and the corolla tube show a clear phylogenetic signal.

Overall architecture appears to represent a crucial functional component in plant-pollinator interaction by modifying nectar access and removal: Corolla tube, modifications and nectary disc are synorganised, and responsible for the formation of specialised compartments of the internal floral space and determine nectar accessibility. Flower and corolla tube shape have been found to influence pollinator flower selection, flower-pollinator interaction and pollination success on micro- and macroevolutionary scales (Galen & Newport, 1987; Galen & Cuba, 2001; Muchhala, 2007; Smith & Kriebel, 2018). However, the shape of the corolla tube tells only part of the story in Hydrophyllaceae. The characteristic stamen-corolla tube modifications form additional tubular structures nested within the corolla tube (Jeiter & Weigend, 2018) as segregated compartments. Especially in the genus Hydrophyllum, pollinator selection through mechanical fit between pollinator mouth parts and flower has evidently

been transferred from the corolla tube itself to the nectar tubes formed by the stamen-corolla tube modifications. The modifications enclose compartments that are either completely separate, or basally connected. In two species, compartments are absent, despite the presence of modifications.

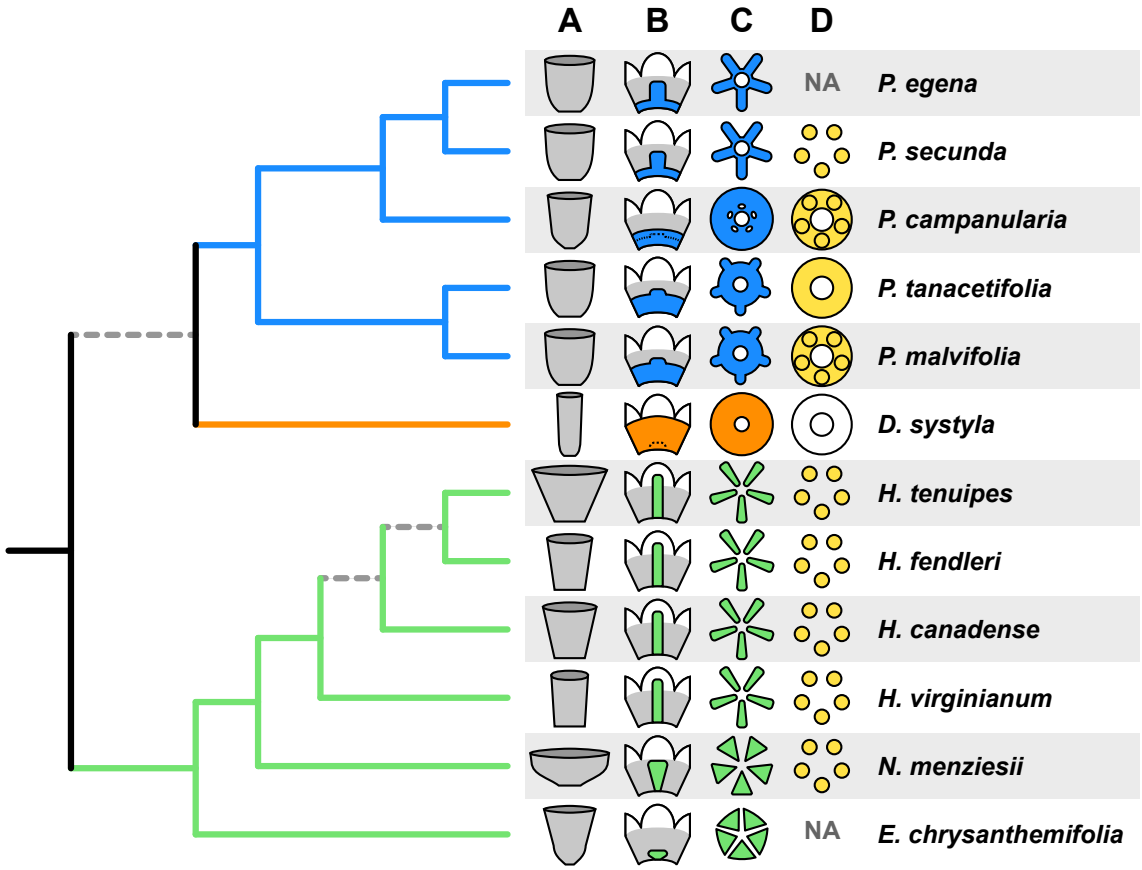

Figure 6.6: Floral architectural characters mapped onto the phylogeny of the Hydrophyllaceae based on four chloroplast markers. Solid lines indicate 100 Bootstrap support and 1 posterior probability. Dashed, grey lines indicate <75 Bootstrap and <0.9 posterior probability. The detailed phylogeny is shown in figure A6.5. A, corolla tube shape. B, internal floral space (grey) and compartments (coloured). C, configuration of the compartments. D, patterns of nectar availability and presentation. Nectar was not measurable in *Draperia systyla*. *Eucrypta chrysanthemifolia* and *Phacelia egena* (NA) were impossible to probe and the plants died before the nectar measurements were conducted for the present study, respectively. The coloured branches represent the three lineages as indicated in figure A6.5.

Endress & Matthews (2006) listed a variety of functions for 'elaborate petals' (including modifications of stamen-corolla tube). In general, Endress & Matthews (2006) list of functions of elaborate petals and stamen-corolla tube modifications can be classified into three types: biotic ecological interactions, abiotic ecological interactions and architectural reinforcements. A range of different pollinators has been documented for Hydrophyllaceae, with hymenoptera such as Andrenid, Megachilid and Halictid bees, but also flower wasps the most commonly reported (Cruden, 1972; Levy, 1988; Eckhart, 1992; Wolfe, 1992; Andersson, 1994; Wroblewska, 2010; McKinney & Goodell, 2011). Oligolectic bees (*Andrena* spec.) have been documented as pollinators for the *Nemophila menziesii*, in our sampling the species with the most open corolla tube and open compartments (Cruden, 1972). However, while we do have reports on pollinator visits, there is no detailed data on pollinator behaviour on the flowers, which should differ depending on the different modalities of nectar access outlined above. Despite revolver architecture reported from numerous plant groups (see e.g., Endress, 1997, 2010, 2016; Tucker & Hodges, 2005; Erbar *et al.*, 1999; Weigend & Gottschling, 2006; Weigend *et al.*, 2010; Jeiter *et al.*, 2016, 2017) there is a general scarcity of documented 'revolver behaviour' of the corresponding polli-

nators, possibly with the sole exception of buzz-pollinated *Dillenia* (Endress, 1997). We argue, that the revolver architecture found in most Hydrophyllaceae enforces increased handling time and the animal has to turn in a circle to access all different access points to the nectar, thus bringing its ventral side into intimate contact with stamens, respectively stigma and increasing the likelihood of pollen transfer. Based on the evidence at hand, functions in abiotic ecological interactions (e.g., nectar cover to reduce evaporation; Naghiloo *et al.*, 2018) or architectural reinforcement have not been tested and multiple functions of the modifications in a single flower are conceivable.

Jeiter & Weigend (2018) hypothesized that the modifications contribute to a revolver architecture in Hydrophyllaceae-flowers, creating internal spaces restricting and modifying access to nectar as floral reward. The data here presented clearly confirm this hypothesis, but provide more far-reaching insights: The modifications partition the reward (usually nectar) of the flower by compartmentalising the internal floral space (Endress, 2010; Jeiter *et al.*, 2016, 2017; Jeiter & Weigend, 2018). The flower visitor has to probe each of the separate compartments to collect the full reward, rotating around the central axis of the flower (Endress, 1994, 1997). This is likely to increase handling time, which has been found to correlate positively with pollen transfer rates and pollination success (e.g., Manetas & Petropoulou, 2000). At the same time, in spite of superficial structural similarity across the family (Jeiter & Weigend, 2018), they are functionally divergent, and compartmentalization is not universally present. We confirmed the effect of architectural differences on reward partitioning directly by simulating nectar harvest. We found that *i*) the species with separate compartments (all four species of *Hydrophyllum*, *Nemophila menziesii*) showed the expected pattern with equal amounts of nectar extracted from each compartment. *ii*) *Phacelia tanacetifolia* showed that the connection of the internal space is fully functional, and the nectar can be reached through five separate entrances between the modifications, but almost all nectar is removed by the first probe. *iii*) in *Phacelia secunda*, on the other hand, equal amounts of nectar are extracted from each compartment, despite their basal connection. The formation of five separate nectar droplets underneath the modifications has been described for *Phacelia mohavensis* (Merritt, 1897) and likely explains this unexpected observation based on architecture. This also indicates that reward (nectar) presentation and access is determined by both the floral architecture and the amount and viscosity of nectar produced. Together, these features determine how and where nectar can be harvested by any given flower visitor.

We here present a hierarchical view of floral architecture in the Hydrophyllaceae which permits a new understanding of floral function well beyond quantitative nectar measurements or simple characterisations of flowers as 'tubular' or 'bowl-shaped'. Complex, compartmentalized internal spaces and the way in which they are filled with nectar are her for the first time demonstrated with the help of 3D-imaging based methods such as HRXCT and μCT. Clearly, future studies should both explore the phylogenetic patterns across a broader sampling of the family and should investigate the actual pollinator selection and behaviour with a view to floral architecture.

6.5 Acknowledgment

We thank S. Sontag, H.-J. Ensikat, J. Nettekoven, D. Straus and S. Langecker for helping with sample preparation for HRXCT. We are also grateful to S. Pamperl and A. Ziegler for scanning and help with data processing. We also acknowledge the help of N. Schmandt who prepared most of the DNA-samples and R.H. Acuña-Castillo for his help with the phylogenetic reconstruction. We thank J. Ruhm for collecting all nectar data and S. Abrahamczyk for his help with the nectar collection and the statistics

applied in this study. All plant species were cultivated by the staff of the University of Bonn Botanic Gardens under the curation of C. Löhne and plants were vouchered by T. Joßberger. The participants of the IV. International Boraginales Working Group Meeting in Florence, Italy 2018 are acknowledged for enlightening discussion on some preliminary data of this study. J.J. received a scholarship for his doctoral thesis and a travel grant to visit the University of Vienna by the Studienstiftung des deutschen Volkes. Funding for the Skyscan 1272 μCT was provided by the Deutsche Forschungsgemeinschaft (INST 217/849-1 FUGG).

6.6 References

Andersson, S. (1994) Floral stability, pollination efficiency, and experimental manipulation of the corolla phenotype in *Nemophila menziesii* (Hydrophyllaceae). *American Journal of Botany* **81**, 1397–1402.

Brand, A. (1913) *Hydrophyllaceae In: Engler, Das Pflanzenreich [Heft 59] IV. 251*, vol. 59 of *Das Pflanzenreich*. Wilhelm Engelmann, Leipzig.

Cohen, J.I. (2012) Continuous characters in phylogenetic analyses: Patterns of corolla tube length evolution in *Lithospermum* L. (Boraginaceae): Evolution of corolla tube length. *Biological Journal of the Linnean Society* **107**, 442–457.

Cohen, J.I. (2016) Floral evolution in *Lithospermum* (Boraginaceae): Independent origins of similar flower types. *Botanical Journal of the Linnean Society* **180**, 213–228.

Cruden, R.W. (1972) Pollination biology of *Nemophila menziesii* (Hydrophyllaceae) with comments on the evolution of oligolectic bees. *Evolution* **26**, 373–389.

Eckhart, V.M. (1992) Spatio-temporal variation in abundance and variation in foraging behavior of the pollinators of gynodioecious *Phacelia linearis* (Hydrophyllaceae). *Oikos* **64**, 573–586.

Endress, P.K. (1994) *Diversity and Evolutionary Biology of Tropical Flowers*. Cambridge Tropical Biology Series, Cambridge University Press, Cambridge.

Endress, P.K. (1996) Homoplasy in angiosperm flowers. *Homoplasy - The Recurrence of Similarity in Evolution* (eds. M.J. Sanderson & L. Hufford), pp. 303–325, Academic Press, San Diego, California, United States.

Endress, P.K. (1997) Relationships between floral organization, architecture, and pollination mode in *Dillenia* (Dilleniaceae). *Plant Systematics and Evolution* **206**, 99–118.

Endress, P.K. (2010) Synorganisation without organ fusion in the flowers of *Geranium robertianum* (Geraniaceae) and its not so trivial obdiplostemony. *Annals of Botany* **106**, 687–695.

Endress, P.K. (2016) Development and evolution of extreme synorganization in angiosperm flowers and diversity: A comparison of Apocynaceae and Orchidaceae. *Annals of Botany* **117**, 749–767.

Endress, P.K. & Matthews, M.L. (2006) Elaborate petals and staminodes in eudicots: Diversity, function, and evolution. *Organisms Diversity & Evolution* **6**, 257–293.

Erbar, C., Kusma, S. & Leins, P. (1999) Development and interpretation of nectary organs in Ranunculaceae. *Flora* **194**, 317–332.

Galen, C. & Cuba, J. (2001) Down the tube: Pollinators, predators, and the evolution of flower shape in the alpine skypilot, *Polemonium viscosum*. *Evolution* **55**, 1963–1971.

Galen, C. & Newport, M.E.A. (1987) Bumble bee behavior and selection on flower size in the sky pilot, *Polemonium viscosum*. *Oecologia* **74**, 20–23.

Hodges, S.A. & Arnold, M.L. (1995) Spurring plant diversification: Are floral nectar spurs a key innovation? *Proceedings of the Royal Society B-Biological Sciences* **262**, 343–348.

Hofmann, M. (1999) Flower and fruit development in the genus *Phacelia* (Phacelieae, Hydrophyllaceae): Characters of systematic value. *Systematics and Geography of Plants* **68**, 203–212.

Hofmann, M., Walden, G.K., Hilger, H.H. & Weigend, M. (2016) Hydrophyllaceae. *Families and Genera of Vascular Plants* (eds. K. Kubitzki, J.W. Kadereit & V. Bittrich), vol. 14, pp. 221–238, Springer, Heidelberg.

Höhna, S., Landis, M.J., Heath, T.A., Boussau, B., Lartillot, N., Moore, B.R., Huelsenbeck, J.P. & Ronquist, F. (2016) RevBayes: Bayesian phylogenetic inference using graphical models and an interactive model-specification language. *Systematic Biology* **65**, 726–736.

Jeiter, J., Danisch, F. & Hilger, H.H. (2016) Polymery and nectary chambers in *Codon* (Codonaceae) – flower and fruit development in a small, capsule-bearing family of Boraginales. *Flora* **220**, 94–102.

Jeiter, J., Hilger, H.H., Smets, E.F. & Weigend, M. (2017) The relationship between nectaries and floral architecture: A case study in Geraniaceae and Hypseocharitaceae. *Annals of Botany* **120**, 791–803.

Jeiter, J. & Weigend, M. (2018) Simple scales make complex compartments – ontogeny and morphology of stamen-corolla tube modifications in Hydrophyllaceae (Boraginales). *Biological Journal of the Linnean Society* **125**, 802–820.

Kampny, C.M. & Dengler, N.G. (1997) Evolution of flower shape in Veroniceae (Scrophulariaceae). *Plant Systematics and Evolution* **205**, 1–25.

Katoh, K., Misawa, K., Kuma, K. & Miyata, T. (2002) MAFFT: A novel method for rapid multiple sequence alignment based on fast Fourier transform. *Nucleic Acids Research* **30**, 3059–3066.

Klingenberg, C.P. (2011) MorphoJ: An integrated software package for geometric morphometrics. *Molecular Ecology Resources* **11**, 353–357.

Klingenberg, C.P. & Gidaszewski, N.A. (2010) Testing and quantifying phylogenetic signals and homoplasy in morphometric data. *Systematic Biology* **59**, 245–261.

Levy, F. (1988) Effects of pollen source and time of pollination on seed production and seed weight in *Phacelia dubia* and *P. maculata* (Hydrophyllaceae). *The American Midland Naturalist* **119**, 193–198.

Luebert, F., Cecchi, L., Frohlich, M.W., Gottschling, M., Guilliams, C.M., Hasenstab-Lehman, K.E., Hilger, H.H., Miller, J.S., Mittelbach, M., Nazaire, M., Nepi, M., Nocentini, D., Ober, D., Olmstead, R.G., Selvi, F., Simpson, M.G., Sutorý, K., Valdés, B., Walden, G.K. & Weigend, M. (2016) Familial classification of the Boraginales. *Taxon* **65**, 502–522.

Manetas, Y. & Petropoulou, Y. (2000) Nectar amount, pollinator visit duration and pollination success in the mediterranean shrub *Cistus creticus*. *Annals of Botany* **86**, 815–820.

McKinney, A.M. & Goodell, K. (2011) Plant–pollinator interactions between an invasive and native plant vary between sites with different flowering phenology. *Plant Ecology* **212**, 1025–1035.

Merritt, A. (1897) Notes on the pollination of some Californian mountain flowers - IV. *Erythea* **5**, 15–22.

Muchhala, N. (2007) Adaptive trade-off in floral morphology mediates specialization for flowers pollinated by bats and hummingbirds. *The American Naturalist* **169**, 494–504.

Muchhala, N. & Thomson, J.D. (2009) Going to great lengths: Selection for long corolla tubes in an extremely specialized bat–flower mutualism. *Proceedings of the Royal Society B: Biological Sciences* **276**, 2147–2152.

Naghiloo, S., Bellstedt, D.U. & Claßen-Bockhoff, R. (2018) Nectar protection in arid-adapted flowers of Zygophyllaceae-Zygophylloideae. *Perspectives in Plant Ecology, Evolution and Systematics* **34**, 37–50.

Nicolson, S.W., Nepi, M. & Pacini, E. (eds.) (2007) *Nectaries and Nectar*. Springer, Dordrecht.

Nocentini, D., Pacini, E., Guarnieri, M. & Nepi, M. (2012) Flower morphology, nectar traits and pollinators of *Cerinthe major* (Boraginaceae-Lithospermeae). *Flora - Morphology, Distribution, Functional Ecology of Plants* **207**, 186–196.

Pérez, F., Arroyo, M.T.K., Medel, R. & Hershkovitz, M.A. (2006) Ancestral reconstruction of flower morphology and pollination systems in *Schizanthus* (Solanaceae). *American Journal of Botany* **93**, 1029–1038.

R Core Team (2018) *R: A Language and Environment for Statistical Computing*, vol. Version 3.5.1. R Foundation for Statistical Computing, Vienna, Austria.

Smith, S.D. & Kriebel, R. (2018) Convergent evolution of floral shape tied to pollinator shifts in Iochrominae (Solanaceae). *Evolution* **72**, 688–697.

Staedler, Y.M., Masson, D. & Schönenberger, J. (2013) Plant tissues in 3D via X-ray tomography: Simple contrasting methods allow high resolution imaging. *PLOS ONE* **8**, e75295.

Stamatakis, A. (2006) RAxML-VI-HPC: Maximum likelihood-based phylogenetic analyses with thousands of taxa and mixed models. *Bioinformatics* **22**, 2688–2690.

Tucker, S.C. & Hodges, S.A. (2005) Floral ontogeny of *Aquilegia*, *Semiaquilegia*, and *Enemion* (Ranunculaceae). *International Journal of Plant Sciences* **166**, 557–574.

Walden, G.K., Garrison, L.M., Spicer, G.S., Cipriano, F.W. & Patterson, R. (2014) Phylogenies and chromosome evolution of *Phacelia* (Boraginaceae: Hydrophylloideae) inferred from nuclear ribosomal and chloroplast sequence data. *Madroño* **61**, 16–47.

Walden, G.K. & Patterson, R. (2012) Nomenclature of subdivisions within *Phacelia* (Boraginaceae: Hydrophylloideae). *Madroño* **59**, 211–222.

Weigend, M., Ackermann, M. & Henning, T. (2010) Reloading the revolver - male fitness as a simple explanation for complex reward partitioning in *Nasa macrothyrsa* (Loasaceae, Cornales). *Biological Journal of the Linnean Society* **100**, 124–131.

Weigend, M. & Gottschling, M. (2006) Evolution of funnel-revolver flowers and ornithophily in *Nasa* (Loasaceae). *Plant Biology* **8**, 120–142.

Weigend, M., Luebert, F., Gottschling, M., Couvreur, T.L., Hilger, H.H. & Miller, J.S. (2014) From capsules to nutlets – phylogenetic relationships in the Boraginales. *Cladistics* **30**, 508–518.

Weigend, M., Selvi, F., Thomas, D.C. & Hilger, H.H. (2016) Boraginaceae. *Families and Genera of Vascular Plants* (eds. K. Kubitzki, J.W. Kadereit & V. Bittrich), vol. 14, pp. 41–102, Springer, Heidelberg.

Whittall, J.B. & Hodges, S.A. (2007) Pollinator shifts drive increasingly long nectar spurs in columbine flowers. *Nature* **447**, 706–709.

Willmer, P. (2011) *Pollination and Floral Ecology*. Princeton University Press, Princeton, N.J.

Wolfe, L.M. (1992) Why does the size of reproductive structures decline through time in *Hydrophyllum appendiculatum* (Hydrophyllaceae)?: Developmental constraints vs. resource limitation. *American Journal of Botany* **79**, 1286–1290.

Wroblewska, A. (2010) Flowering dynamics, nectar secretion and insect visitation of *Phacelia campanularia* A. Gray. *Acta Agrobotanica* **63**, 29–35.

6.7 Appendix

Table A6.1: Scan settings for the HRXCT- and µCT-scans.

Sample	Number of flowers	Acceleration voltage (kV)	Source current (µA)	Exposure time (s)	Pictures per sample	Camera binning	Optical magnification (x)[1]	Pixel size (µm)	Used for [2]
Draperia systyla IV	1	30	200	4	728	2	1	19.94	IS, LM
*Draperia systyla*A1-3	3	23	173	15	1000	2	LFOV	26.46	LM
Draperia systyla B4-7	4	23	173	15	1000	2	LFOV	27.45	LM
Draperia systyla C8-10	3	23	173	15	1000	2	LFOV	27.58	LM
Draperia systyla D11-12	2	23	173	15	1000	2	LFOV	30.14	LM
Eucrypta chrysanthemifolia A1	1	25	197	15	728	2	1	7.99	IS, LM
Eucrypta chrysanthemifolia B2	1	25	197	15	728	2	1	9.16	LM
Hydrophyllum canadense IV	1	30	200	5	728	2	1	22.21	IS, LM
Hydrophyllum fendleri IV	1	30	200	5	728	2	LFOV	22.6	IS, LM
Hydrophyllum fendleri A1-4	4	30	200	40	1000	1	LFOV	16.05	LM
Hydrophyllum fendleri B5-8	4	30	200	40	1000	1	LFOV	16.05	LM
Hydrophyllum tenuipes IV	1	30	200	5	728	2	1	19.83	IS, LM
Hydrophyllum tenuipes A1-4	4	23	173	16	1000	2	LFOV	31.08	LM
Hydrophyllum tenuipes B5-8	4	23	173	16	1000	2	LFOV	31.08	LM
Hydrophyllum tenuipes C9-10	2	23	173	16	1000	2	LFOV	25.43	LM
Hydrophyllum virginianum IV1	1	20	129	30	728	2	LFOV	20.16	IS, LM
Hydrophyllum virginianum IV2	1	30	200	3	728	2	1	17.24	LM
Hydrophyllum virginianum A1-4	4	24	187	18	1000	2	LFOV	29.84	LM
Hydrophyllum virginianum A5-8	4	24	187	18	1000	2	LFOV	38.33	LM
Hydrophyllum virginianum A9-10	2	24	187	18	1000	2	LFOV	29.48	LM
Nemophila menziesii IV	1	30	200	15	728	2	1	23.41	IS, LM
Nemophila menziesii A1	1	23	169	13	728	2	1	18.68	LM
Nemophila menziesii B2	1	23	169	15	728	2	1	20.52	LM
Nemophila menziesii C3	1	23	169	15	728	2	1	20.52	LM
Phacelia campanularia IV	1	37.5	200	2	728	2	LFOV	33.9	IS, LM
Phacelia campanularia A1	1	22	154	30	1000	1	LFOV	25.83	LM
Phacelia campanularia B2	1	22	154	30	1000	1	LFOV	25.83	LM
Phacelia campanularia C3	1	22	154	30	1000	1	LFOV	28.31	LM
Phacelia egena IV1	1	30	200	13	728	2	1	23.99	IS, LM
Phacelia egena IV2	1	40	200	10	728	2	1	24.19	LM
Phacelia egena A1-4	4	22	154	30	1000	1	LFOV	25.83	LM
Phacelia egena A5-8	4	22	154	30	1000	1	LFOV	25.83	LM
Phacelia egena A9-10	2	22	154	30	1000	1	LFOV	25.83	LM
Phacelia malvifolia IV	1	30	200	2	728	2	1	18.35	IS, LM
Phacelia malvifolia A1	1	23	169	13	728	2	1	18.23	LM
Phacelia malvifolia B2	1	23	169	13	728	2	1	18.38	LM
Phacelia secunda IV	1	30	200	3	728	2	1	19.12	IS, LM
Phacelia secunda A1-4	4	23	171	15	1000	2	LFOV	26.53	LM
Phacelia secunda B5-9	5	23	171	15	1000	2	LFOV	26.53	LM
Phacelia secunda C10-13	4	23	171	15	1000	2	LFOV	22.22	LM
Phacelia secunda D14-15	2	23	171	15	1000	2	LFOV	21.44	LM
Phacelia tanacetifolia IV1[3]	1	45	165	0.444 (6x)[4]	1800	2	1	6	IS, LM
Phacelia tanacetifolia A1[3]	1	45	165	0.298 (4x)[4]	900	3	1	8	LM
Phacelia tanacetifolia B2[3]	1	45	165	0.444 (4x)[4]	1800	2	1	7	LM
Phacelia tanacetifolia C3[3]	1	45	165	0.298 (5x)[4]	900	3	1	8	LM
Phacelia tanacetifolia D4[3]	1	45	165	0.298 (5x)[4]	900	3	1	8	LM

[1]LFOV: Large field of view; [2]IS: Internal space; LM: Landmarking; [3]scanned with SkyScan 1272; [4]The number in brackets indicates the number of frames averaged with respective exposure time.

Table A6.2: Nectar measurements. Species and numbers of flowers probed for nectar, average amount of nectar per flower and standard deviation.

Species	N	Average amount of nectar [µl]	Standard deviation
Draperia systyla	25	<0.01	0.01
Eucrypta chrysanthemifolia	-	-	-
Hydrophyllum canadense	25	2.064	1.006
Hydrophyllum fendleri	25	3.888	2.292
Hydrophyllum tenuipes	11	0.168	0.243
Hydrophyllum virginianum	25	1.743	1.042
Nemophila menziesii	25	0.152	0.082
Phacelia campanularia	25	2.074	2.049
Phacelia egena	-	-	-
Phacelia malvifolia	19	0.159	0.182
Phacelia secunda	25	0.417	0.189
Phacelia tanacetifolia	25	1.099	0.431

Table A6.3: PC-scores for shape variation as the result of the PCA based on Procrustes fit 3D-landmarking data.

PC-axis	Eigenvalues	% total variance	Cumulative % variance
PC1	0.08463	70.39	70.39
PC2	0.01938	16.12	86.51
PC3	0.00436	3.62	90.13
PC4	0.00349	2.9	93.03
PC5	0.00126	1.05	94.07
PC6	0.00098	0.81	94.89
PC7	0.00078	0.65	95.54
PC8	0.0007	0.58	96.12
PC9	0.00057	0.48	96.59
PC10	0.00044	0.37	96.96

Table A6.4: Average centroid sizes and standard deviation.

Species	**N**	**Average centroid size**	**Standard deviation**
Draperia systyla	13	20.69	0.94
Eucrypta chrysanthemifolia	2	5.02	0.44
Hydrophyllum canadense	1	10.73	*NA*
Hydrophyllum fendleri	9	14.61	1.51
Hydrophyllum tenuipes	11	9.25	0.26
Hydrophyllum virginianum	12	15.01	0.97
Nemophila menziesii	4	7.41	0.5
Phacelia campanularia	4	21.98	6.21
Phacelia egena	12	13.47	0.52
Phacelia malvifolia	3	10.29	0.07
Phacelia secunda	16	10.46	1.22
Phacelia tanacetifolia	5	8.79	0.35
Total	**92**	**13.31**	**4.65**

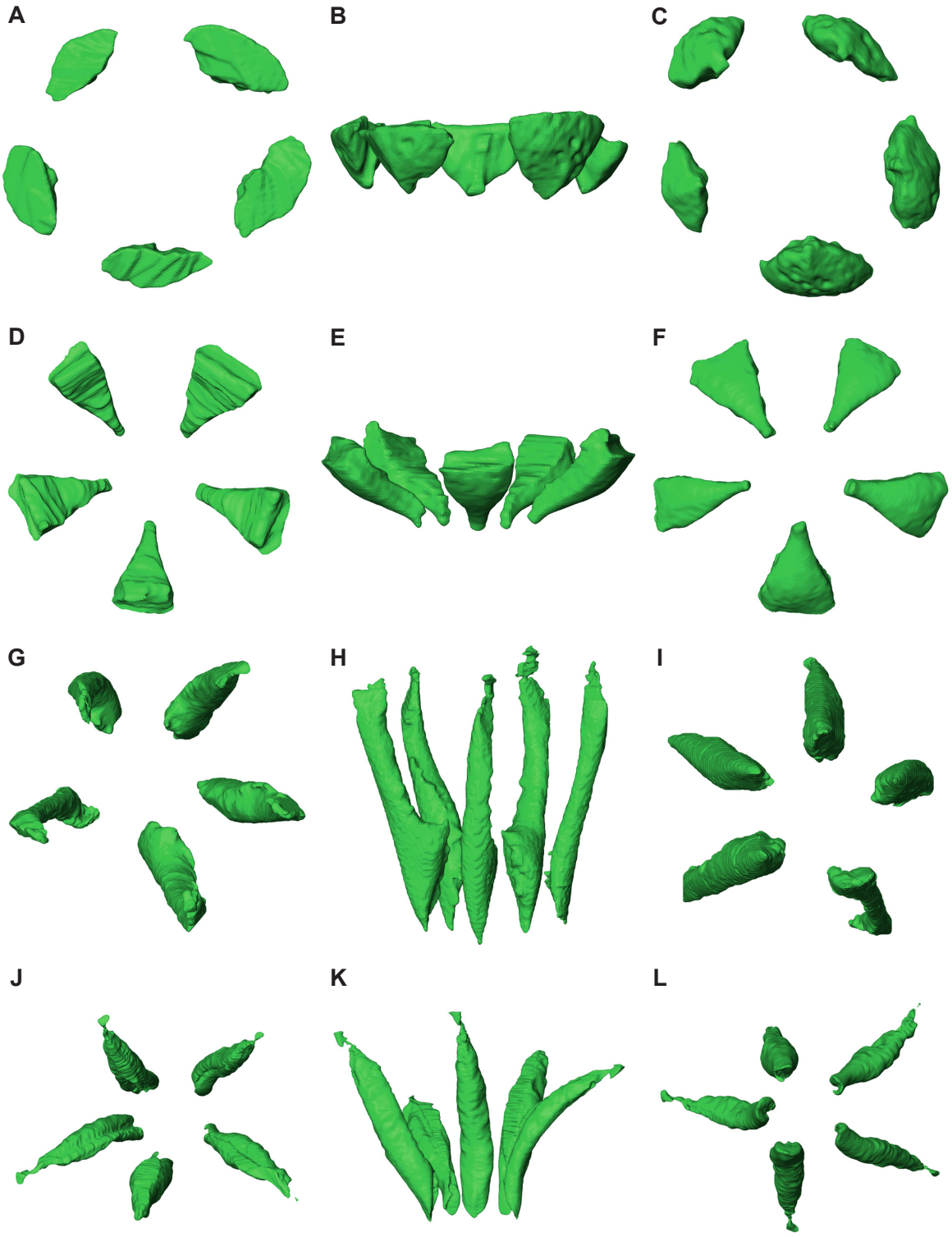

Figure A6.1: Internal spaces of *Nemophila*, *Eucrypta* and *Hydrophyllum* p.p. Internal spaces calculated from the segmented flowers. First column viewed from above, second column viewed from the side, third column viewed from below. A–C, *Eucrypta chrysanthemifolia*. D–F, *Nemophila menziesii*. G–I, *Hydrophyllum canadense*. J–L, *Hydrophyllum fendleri*. The colours represent the three lineages as indicated in figure 6.6 and figure A6.5.

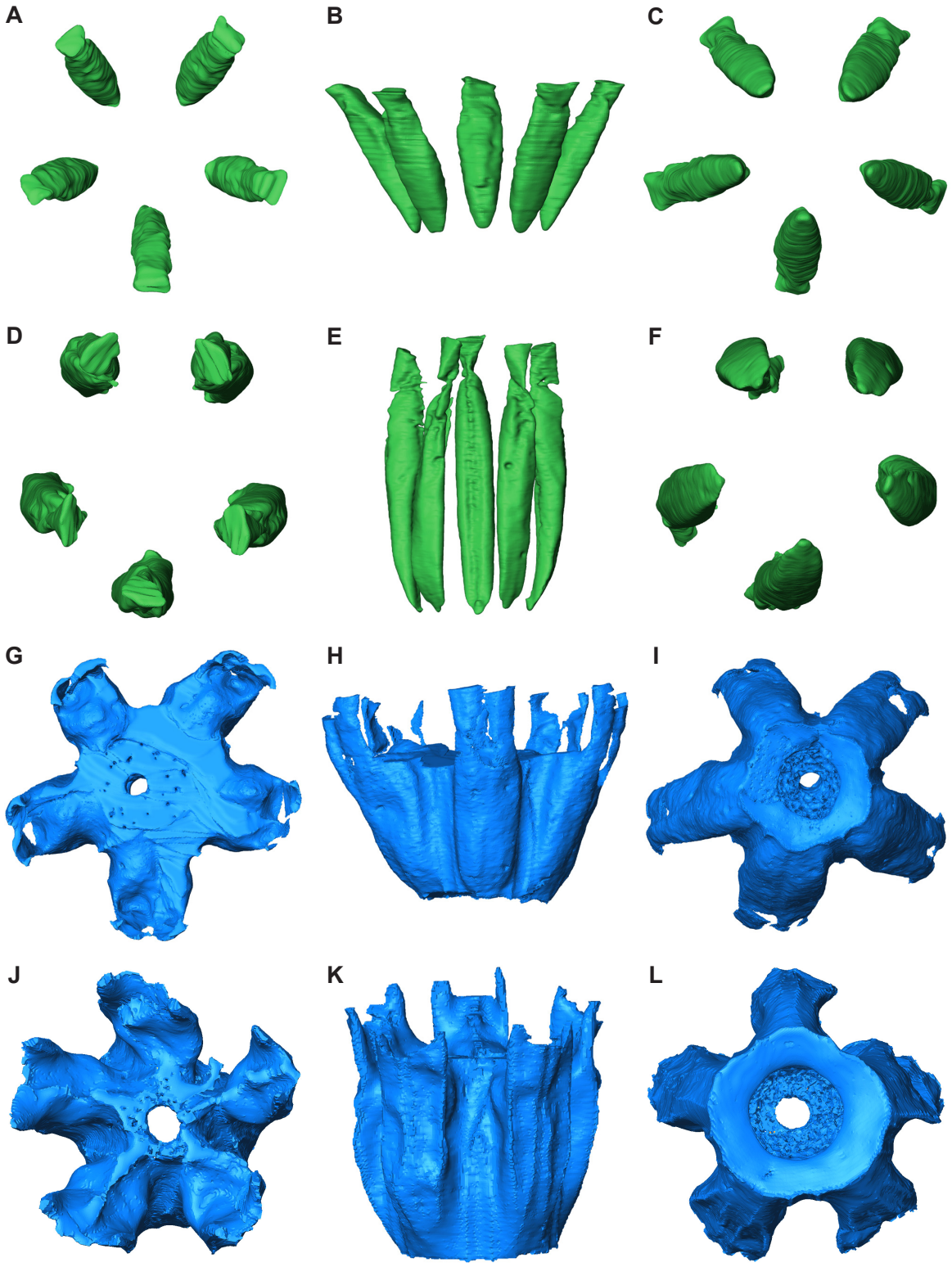

Figure A6.2: Internal spaces of *Hydrophyllum* p.p. and *Phacelia* p.p. Internal spaces calculated from the segmented flowers. First column viewed from above, second column viewed from the side, third column viewed from below. A–C, *Hydrophyllum tenuipes*. D–F, *Hydrophyllum virginianum*. G–I, *Phacelia malvifolia*. J–L, *Phacelia tanacetifolia*. The colours represent the three lineages as indicated in figure 6.6 and figure A6.5.

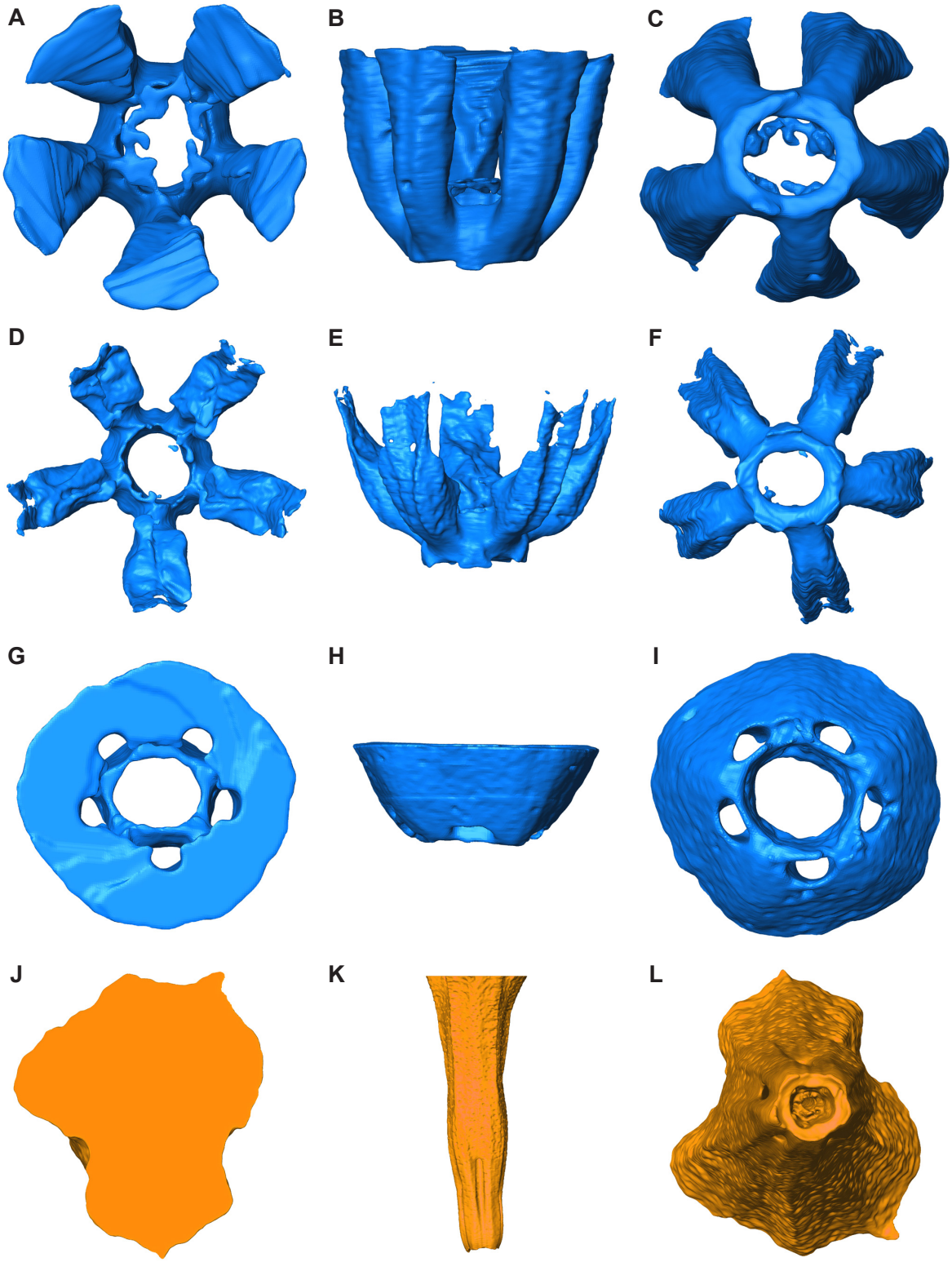

Figure A6.3: Internal spaces of *Phacelia* p.p. and *Draperia*. Internal spaces calculated from the segmented flowers. First column viewed from above, second column viewed from the side, third column viewed from below. A–C, *Phacelia secunda*. D–F, *Phacelia egena*. G–I, *Phacelia campanularia*. J–L, *Draperia systyla*. The colours represent the three lineages as indicated in figure 6.6 and figure A6.5.

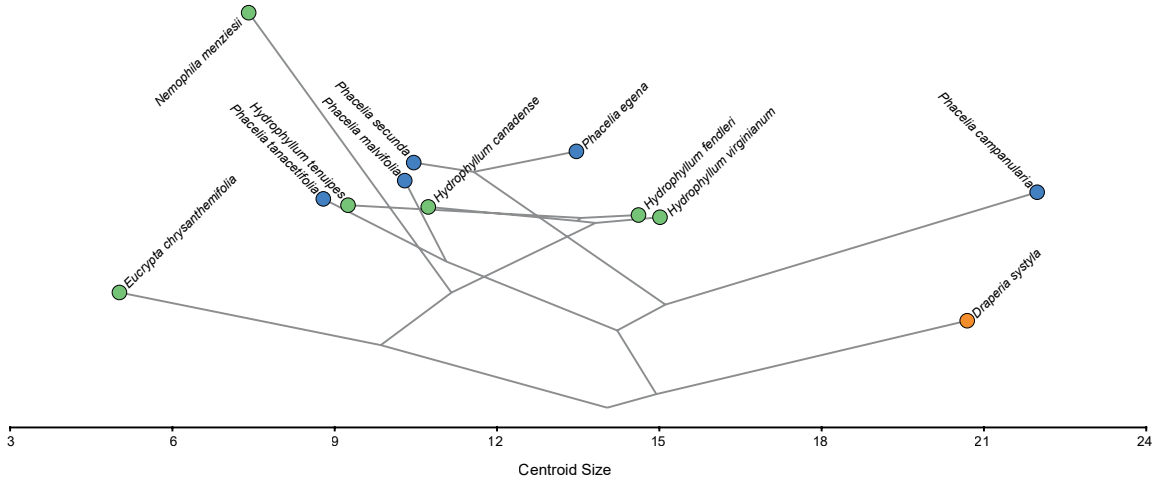

Figure A6.4: Centroid size mapped onto the phylogeny. The axis shows the average relative centroid size. Average centroid size and standard deviation are shown in table A6.4. The colours represent the three lineages as indicated in figure 6.6 and figure A6.5.

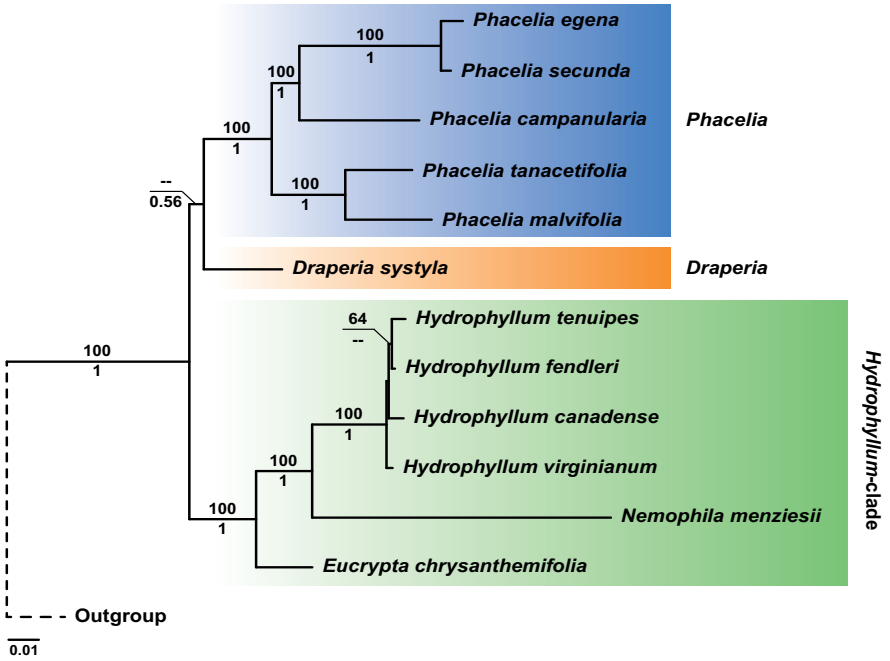

Figure A6.5: Phylogeny of the Hydrophyllaceae species included in this study based on Bayesian inference. Bootstrap support values >50 are shown above the branches. Posterior probability >0.5 is shown below the branches. Blue highlights *Phacelia*, orange *Draperia* and green the *Hydrophyllum*-clade.

Chapter 7

The relationship between nectaries and floral architecture: a case study in Geraniaceae and Hypseocharitaceae

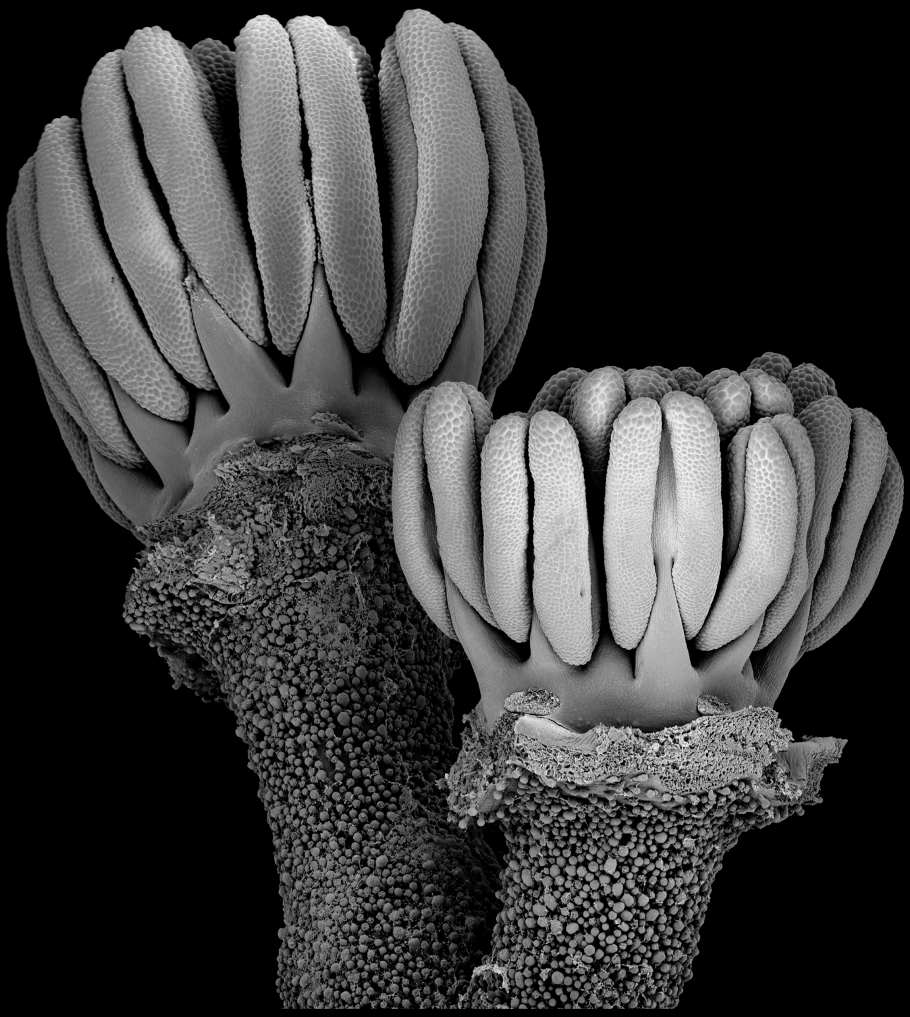

Jeiter J, Hilger HH, Smets EF, Weigend M. 2017. The relationship between nectaries and floral architecture: a case study in Geraniaceae and Hypseocharitaceae. *Annals of Botany* 120: 791–803. https://doi.org/10.1093/aob/mcx101

Annals of Botany **120**: 791–803, 2017
doi:10.1093/aob/mcx101,availableonlineatwww.academic.oup.com/aob

ANNALS OF BOTANY Founded 1887

PART OF A SPECIAL ISSUE ON MORPHOLOGY AND ADAPTATION

The relationship between nectaries and floral architecture: a case study in Geraniaceae and Hypseocharitaceae

Julius Jeiter[1,*], Hartmut H. Hilger[2], Erik F. Smets[3,4] and Maximilian Weigend[1]

[1]Nees-Institut für Biodiversität der Pflanzen, Rheinische Friedrich-Wilhelms-Universität Bonn, Meckenheimer Allee 170, D-53115 Bonn, Germany, [2]Biologie-Botanik, Freie Universität Berlin, Altensteinstraße 6, D-14195 Berlin, Germany, [3]Ecology, Evolution and Biodiversity Conservation, KU Leuven, Kasteelpark Arenberg 31, Box 2437, B-3001 Leuven, Belgium and [4]Naturalis Biodiversity Center, Vondellaan 55, NL-2332 AA Leiden, The Netherlands
**For correspondence. E-mail jjeiter@uni-bonn.de*

Received: 3 May 2017 Returned for revision: 8 June 2017 Editorial decision: 10 July 2017 Accepted: 28 July 2017 Published electronically: 14 September 2017

• **Background and Aims** Flowers of Geraniaceae and Hypseocharitaceae are generally considered as morphologically simple. However, previous studies indicated complex diversity in floral architecture including tendencies towards synorganization. Most of the species have nectar-rewarding flowers which makes the nectaries a key component of floral organization and architecture. Here, the development of the floral nectaries is studied and placed into the context of floral architecture.
• **Methods** Seven species from Geraniaceae and one from Hypseocharitaceae were investigated using scanning electron microscopy and light microscopy. Samples were prepared and processed using standard protocols.
• **Key Results** The development of the nectary glands follows the same trajectory in all species studied. Minor differences occur in the onset of nectarostomata development. The most striking finding is the discovery that a short anthophore develops via intercalary growth at the level of the nectary glands. This anthophore lifts up the entire flower apart from the nectary gland itself and thus plays an important role in floral architecture, especially in the flowers of *Pelargonium*. Here, the zygomorphic flowers show a particularly extensive receptacular growth, resulting in the formation of a spur-like receptacular cavity ('inner spur'). The nectary gland is hidden at the base of the cavity. Various forms of compartmentalization, culminating in the 'revolver flower' of *Geranium maderense*, are described.
• **Conclusions** Despite the superficial similarity of the flowers in Geraniaceae and Hypseocharitaceae, there is broad diversity in floral organization and floral architecture. While the receptacular origin of the spur-like cavity in *Pelargonium* had already been described, anthophore formation via intercalary growth of the receptacle in the other genera had not been previously documented. In the context of the most recent phylogenies of the families, an evolutionary series for the floral architecture is proposed, underscoring the importance of synorganization in these seemingly simple flowers.

Key words: Floral organization, synorganization, flower morphology, nectary development, ontogeny, anthophore, *Geranium*, *Erodium*, *Pelargonium*, *Monsonia*, *Hypseocharis.*

INTRODUCTION

The Geraniaceae comprise about 830 species in five genera (*Erodium*, *Geranium*, *Monsonia*, *Pelargonium* and monotypic *California*) in their most recent circumscription (Albers and van der Walt, 2007). Monotypic *California* was segregated from *Erodium* (Aldasoro *et al.*, 2002). It appears to be the sister group to the remaining *Erodium* species (Fiz *et al.*, 2006). There are two centres of diversity: *Geranium* and *Erodium* are most diverse in the Mediterranean areas of the northern hemisphere, while *Pelargonium* and *Monsonia* are mainly restricted to southern Africa, with only a few species of *Pelargonium* present on Madagascar, the Arabian Peninsula and Australia (Fiz *et al.*, 2008). The phylogenetic sister group to the Geraniaceae are the monogeneric Hypseocharitaceae with 2–6 species. *Hypseocharis* is mainly distributed in the high Andean regions of central South America (Slanis and Grau, 2001). Hypseocharitaceae are often included in the family Geraniaceae (Albers and van der Walt, 2007; APG IV, 2016).

Various aspects of the flowers of these two families have been studied (e.g. Brunies, 1900; Narayana and Arora, 1963; Labbe, 1964; Kumar, 1976; Link, 1989, 1994; Devi, 1991; Struck, 1997; Aldasoro *et al.*, 2001). Several authors investigated the ontogeny, anatomy and morphology of the floral nectaries in the Geraniaceae and related families and genera (e.g. Link, 1989, 1994; Vogel, 1998; Ronse Decraene and Smets, 1999; Jeiter *et al.*, 2017). Flowers of species from both families are shown in Fig. 1.

All five genera of the Geraniaceae and the one of Hypseocharitaceae have flowers that reward nectar. The position of the nectaries at the base of the antesepalous filaments between the bases of the neighbouring petals is conserved within both families (Jeiter *et al.*, 2017). The only apparent exception is found in *Pelargonium*, where the nectar is hidden in a spur-like cavity on the adaxial side of the flower.

The morphology of this spur-like cavity is often described as 'fused sepal spur' or 'hypanthium with adnate spur' (e.g.

FIG. 1. Floral organization and architecture of some of the species studied in Geraniaceae and Hypseocharitaceae. (A–E) Geraniaceae: (A) *Geranium pratense* (*BONN-3785*); (B) *Geranium maderense* (*GHB 49664*); (C) *Erodium manescavi* (*BONN-3787*); (D) *Monsonia emarginata* (*GHB 44182*); and (E) *Pelargonium australe* (*GHB 36554*). (F) Hypseocharitaceae: *Hypseocharis bilobata* (*Ortuño 2361*).

Sauer, 1933; Röschenbleck *et al.*, 2014), a 'spur formed half by the receptacle and half by the adaxial sepal' (Payer, 1857), 'receptacular spur' or 'receptacular tube' (Japp, 1909; Labbe, 1964; Link, 1989, 1994; Tsai, 2016), or – with no interpretation – simply as 'spur' (e.g. Price and Palmer, 1993; Struck, 1997). Similar structures are present in some species of *Monsonia* (Kers, 1971; Link, 1989, 1994). Unlike the single 'spur' in *Pelargonium*, the actinomorphic flowers of *Monsonia* have five spur-like cavities which are shorter compared with those present in most species of *Pelargonium*.

Apart from nectary development, floral architecture and synorganization are poorly studied in Geraniaceae and Hypseocharitaceae, and incompletely understood in angiosperms in general. There are several misconceptions regarding terms such as 'floral architecture', 'floral structure', 'floral organization' and 'synorganization'. Often these are even used as synonyms, which makes it difficult to pinpoint a clear definition.

The clearest definitions and relationships between those terms have been given by Endress (1994, 1996). According to him, floral structure can be approached on different levels: floral organization, floral architecture and floral mode. 'Floral organization' may be synonymized with floral morphology. Independent organs may be synorganized. 'Synorganization' is the 'spatial and functional connection between organs of the same or different kind leading to homogeneous functional structures' (Ronse De Craene, 2010, p. 412). Common examples of synorganization are fusions between organs of the same or different whorls as in most asterids. Synorganization, fusions and differential growth rates lead to structures of higher order which are described as 'floral architecture'. Structures of higher order exceed the function of the individual or collective of floral organs of which they are composed, and introduce new or modified functions. Finally, the interactions of flowers, for example during pollination, constitute the 'floral mode'.

Synorganization is well known for asterids, where it is usually represented by the fusion of various floral organs (e.g. sympetalous corolla fused with androecium), without explicitly mentioning it under this term [e.g. Asterales (Leins and Erbar, 2006); but see Endress, 2016]. Conversely, synorganization has been rarely studied in rosids, which usually have free petals and separate stamens.

The most detailed study on floral architecture in Geraniaceae was provided by Endress (2010). He described the synorganization in the flowers of *Geranium robertianum* and found a 'revolver architecture' (formation of regular and independent nectary compartments without strict fusion). His study focused on floral organization and floral architecture. Similar studies are available especially for *Pelargonium* (e.g. McDonald and van der Walt, 1992; Struck and van der Walt, 1996; Struck, 1997) but, in contrast to the study by Endress (2010), these focus mainly on the length and shape of the entrance of the spur-like cavity and its relationship to flower–pollinator interaction. The emphasis of these studies is on floral organization and floral mode. A particularly nice example where minute changes in organ shape have major consequences for the organization

and floral mode is found in *Erodium* where zygomorphy arose several times independently (Fiz *et al.*, 2006). These changes towards zygomorphy are mainly due to the presence of glandular trichomes or coloured spots on individual petals, or slight changes in the size relationship between the petals and/or nectary glands of the flower.

We hypothesize that the flowers of Geraniaceae and Hypseocharitaceae, although superficially similar in organization, show divergent architectures, which are the result of various levels of synorganization. Since the presentation of nectar is strongly related to floral mode, which results from changes in floral architecture, we follow a two-step approach: (1) we study the development of the nectary glands in Geraniaceae and Hypseocharitaceae; and (2) we combine our developmental data with detailed observations of the anthetic functional unit.

MATERIALS AND METHODS

Flowers in various developmental stages, including anthetic flowers, of five genera from the Geraniaceae (*Erodium*, *Geranium*, *Monsonia* and *Pelargonium*) and Hypseocharitaceae (*Hypseocharis*) (Table 1) were collected in the Botanical Garden Berlin, Germany and the Botanical Gardens of the University of Bonn, Germany. The material was fixed in formaldehyde–acetic acid–ethanol (FAA; 2 % formaldehyde, 2 % acetic acid, 70 % ethanol) for at least 1 week.

For electron microscopy, the samples were rinsed with ethanol (70 %) and dissected under a stereomicroscope. They were then transferred into FAA for at least 1 h and afterwards dehydrated using formaldehyde dimethyl acetal (FDA; 99.0 %, Sigma-Aldrich Chemie GmbH, Munich, Germany) and finally stored in acetone (protocol modified after Gerstberger and Leins, 1978). Critical point drying (CPD 020, Balzers Union, Liechtenstein) followed the standard protocol. Dried specimens were mounted on aluminium stubs using conductive carbon cement (Leit-C, PLANO GmbH, Wetzlar, Germany) and final preparations were conducted. The mounted specimens were coated with gold or palladium in a sputter coater (SCD 040, Balzers Union) for 1.5 min up to 3 min (depending on the structural complexity of the specimen) at 30 mA. Images were taken in a Stereoscan 200 electron microscope (Cambridge, UK) at 10–15 kV. Contrast and brightness of the images were partially improved using standard image editing software.

For light microscopy, the material was dehydrated using an increasing ethanol to isopropanol to butanol dehydration series. The butanol was gradually replaced with Paraplast© (Leica Biosystems Nussloch GmbH, Nussloch, Germany) and finally stored at 60 °C for at least 2 weeks. The samples were then moulded in blocks, which were trimmed and mounted on wooden blocks. The sectioning was performed using a rotary microtome (Rotationsmikrotom 1515, Leitz, Wetzlar, Germany). The sections were stained in Safranin red and Astra blue. Sections were documented using a light microscope (Axio Scope.A1, Carl Zeiss microscopy GmbH, Jena, Germany) with a digital camera (AxioCam ERc5s, Carl Zeiss microscopy GmbH). Images were partially improved using standard image editing software.

Table 1. *Species studied, vouchers and voucher locations*

Species	Family	Voucher*	Herbarium
Hypseocharis bilobata Killip	Hypseocharitaceae	*Ortuño 2361*	BONN
Erodium manescavi Coss.	Geraniaceae	*BONN-3787*	BONN
Geranium maderense Yeo	Geraniaceae	*GHB 49664*	B
Geranium pratense L.	Geraniaceae	*BONN-3785*	BONN
Monsonia brevirostrata Knuth	Geraniaceae	*GHB 44350*	B
Monsonia emarginata L'Hér.	Geraniaceae	*GHB 44182*	B
Pelargonium australe Willd.	Geraniaceae	*GHB 36554*	B
Pelargonium reniforme (Andrews) Curtis	Geraniaceae	*GHB 8138*	B

*GHB, Garten Herbar Beleg.

RESULTS

Nectary gland development

The development of the nectary glands in the five species studied is shown in Figs 2–6. In all species studied, gland development starts at late stages of floral development, as is common for nectarial tissues. At the onset of nectary gland development, the anthers and ovary are already differentiated. The ovary is still open and a common style is not yet developed.

Geranium pratense (Fig. 2). The development of the nectary gland starts from small, shallowly bilobed bulges below the base of the antesepalous stamen (Fig. 2A–C). The development of the nectary glands is strongly linked with the development of the receptacle below all floral organs except the calyx (Fig. 2C–I). The glands start to develop at the same level as the petals (Fig. 2B, C). Below this region, a circular constriction forms (Fig. 2C, D, I). The resulting column elongates, forming a short anthophore ('extension of the receptacle between the calyx and the rest of the organs in a flower', Ronse De Craene, 2010, p. 404; Fig. 2E, F). The nectarostomata (open, nectar-secreting stomata; nectary-modified stomata; Smets, 1988) are mainly localized at the portion of the gland which faces the base of the flower (Fig. 2D, E). At the final stages of development, shortly before anthesis, the anthophore broadens, shifting the zone with nectarostomata towards a distal position (Fig. 2F). The formation of the nectarostomata happens simultaneously with the development of simple trichomes which arise at the apical and apicolateral area of the gland (Fig. 2C–F).

Erodium manescavi (Fig. 3). The nectary gland initiates its development as a small bulge of tissue at the base of the antesepalous stamen and between the antepetalous stamens (Fig. 3A, B). In later stages, this bulge forms a clear edge at its base, separating it from the base of the sepal and receptacle (Fig. 3C, D). With continuing development, the gland first broadens and finally grows apically (Fig. 3C–F). The five nectary glands vary in size: the most prominent gland is that in the adaxial position (Fig. 3F), and the smallest are on the abaxial side. The adaxial gland shows a strong apical growth. While growing, it covers parts of the base of the adaxial, antesepalous filament. Besides the growth of the glands, the receptacle lifts the inner floral organs only slightly, forming a very short undifferentiated anthophore. The petals stay at the same level during the entire development of the flower (Fig. 2A–E). The glands are glabrous (Fig. 3F). Nectarostomata become visible shortly before

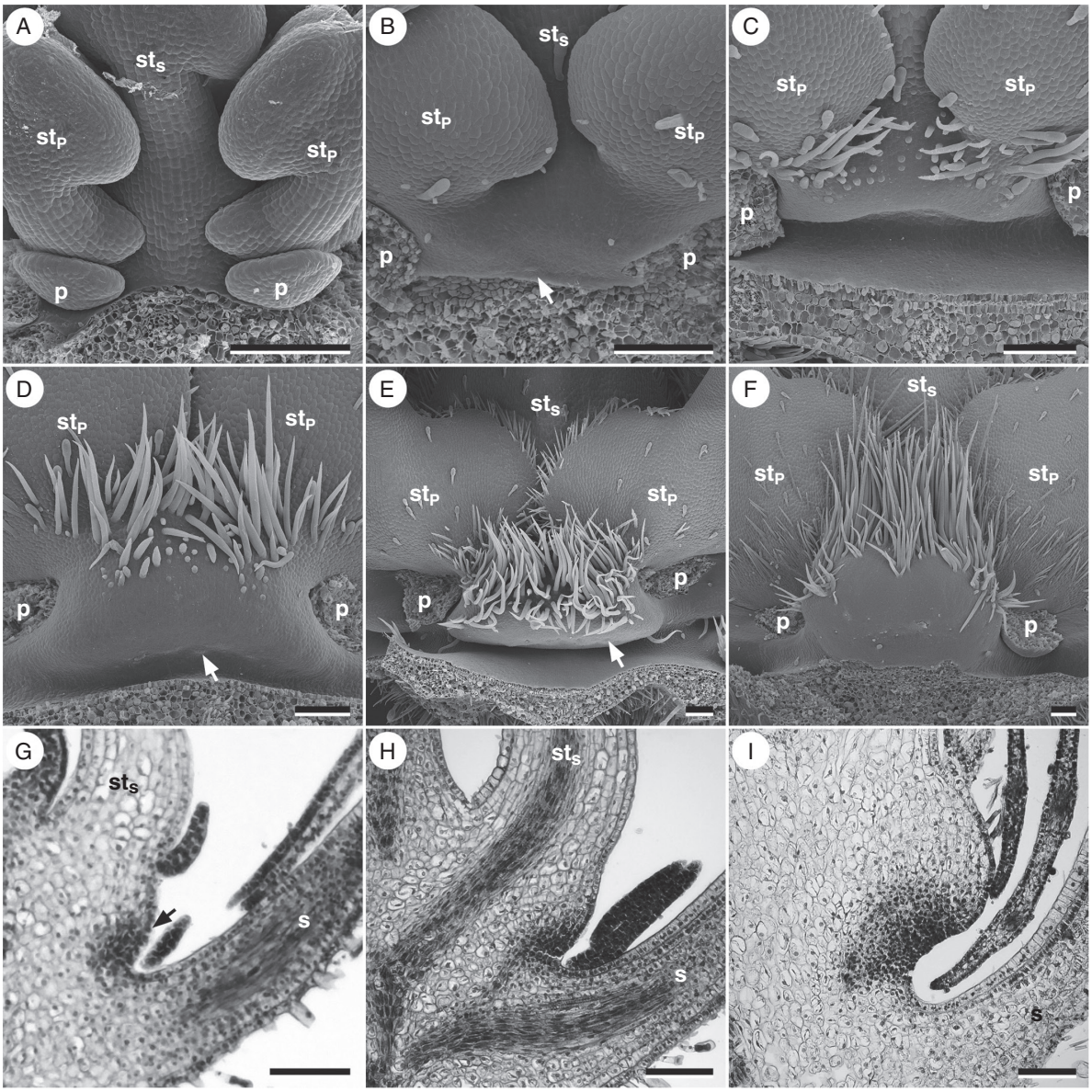

FIG. 2. Nectary gland development in *Geranium pratense*. (A–F) Micrographs obtained using scanning electron microscopy. (G–I) Longitudinal sections. (A) Base of the antesepalous stamen before insertion of the nectary gland. (B) First bulging of the developing gland. The arrow indicates the first bulging of nectary gland tissue. (C) Formation of the anthophore and onset of trichome development. (D) Onset of nectarostomata development. The arrow is pointing to one nectarostoma. (E) Onset of development of circular constriction of the anthophore. The arrow is pointing to one nectarostoma. (F) Nectary gland at anthesis. (G) Longitudinal section through the state corresponding to (B). The arrow indicates developing glandular tissue. (H) Longitudinal section through the state corresponding to (C). (I) Section through an almost anthetic flower. Perianth organs removed. p, petal; s, sepal; st_p, antepetalous stamen; st_s, antesepalous stamen. Scale bars in (A–I) = 100 μm.

anthesis. They are slightly immersed into the epidermis of the glands (Fig. 3F).

Pelargonium australe (Fig. 4). The single nectary gland in *P. australe* also develops late, but along a different trajectory compared with the other Geraniaceae. The distance between the adaxial petals as well as the size of the adaxial sepal is significantly larger than the distances between the other petals and sepals, respectively (Fig. 4A, D). In the space between the adaxial sepal and the adaxial antesepalous stamen, a small number of nectarostomata develops. While the number of nectarostomata increases, a bulge of tissue is formed. At this point, intercalary growth of the surrounding tissue now overtops the nectary, which thus 'sinks' into a tube-like structure (Fig. 4B, E, F). In longitudinal section, a secondary meristem at the base of all floral organs (including the sepals) becomes

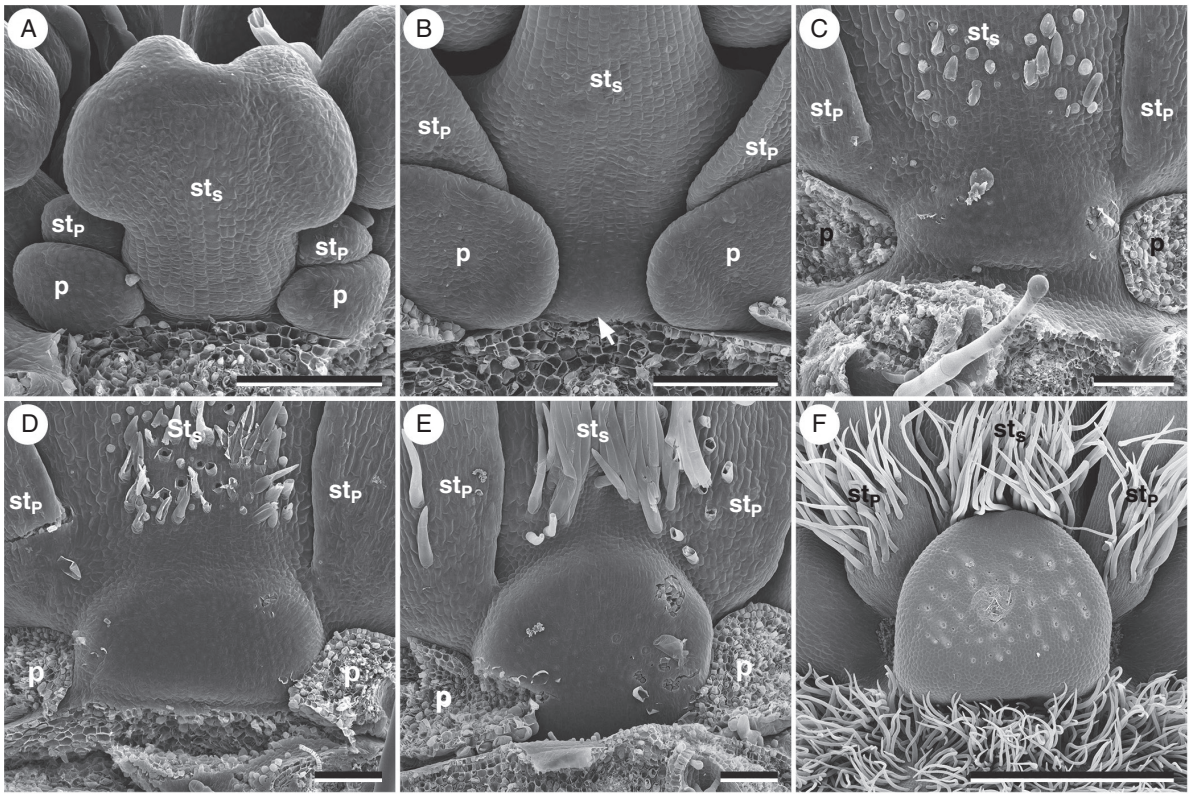

FIG. 3. Nectary gland development in *Erodium manescavi*. (A) Antesepalous stamen before the onset of nectary gland development. (B) Onset of nectary gland development. The arrow indicates the earliest observed stage of nectary gland development. (C) The gland broadens laterally, and trichomes begin to develop. (D) Gland and trichome development progresses. (E) First nectarostomata develop. (F) Adaxial nectary gland in the anthetic flower. Perianth organs removed. p, petal; s, sepal; st_p, antepetalous stamen; st_s, antesepalous stamen. Scale bars in (A–E) = 100 µm, (F) = 1 mm.

visible. This meristem produces regularly shaped cells which elongate subsequently or after a short delay. This elongation process occurs at late stages of floral development, right before anthesis. No secondary meristem is initiated under the nectary gland, so this is the only area retaining its original level (Fig. 4E, F). The gland at the base of this tube-like structure develops a conical shape (Fig. 4C, F). The nectarostomata are located on the ventral (proximal) surface of the gland. The 'sinking' of the nectary gland is thus actually an overtopping of the gland by the surrounding tissue. The entrance of the tube-like structure and the base where the gland is located enlarge during the final stages of development (Fig. 4C, F).

Monsonia brevirostrata (Fig. 5). In the early developmental stages, the glands of *M. brevirostrata* develop similarly to those of *G. pratense*; below the base of the glands and all other floral organs (except for the sepals), a short anthophore is formed (Fig. 5E). After onset of development, the glands become increasingly bilobed (Fig. 5D–F). Nectarostomata develop late and are at first restricted to the part of the gland above the anthophore (Fig. 5A–D, G, H). Shortly before anthesis, the basal part of the gland emerges from the anthophore (Fig. 5E, F). At anthesis the nectary gland shrinks and the zone of nectarostomata becomes enclosed by the basal and apical parts of the nectary gland, while the anthophore is not involved in this shrinking process (Fig. 5E, F). At the same time, the triplet of stamens is tilted distally (Fig. 5I).

Hypseocharis bilobata (Fig. 6). The formation of the nectary glands in *H. bilobata* starts with the emergence of nectarostomata at the base of the triplet of antesepalous and antepetalous stamens (Fig. 6A). After development of several nectarostomata, the upper part of this zone bulges, so that a cleft between the base of the sepal and the nectary gland is formed (Fig. 6B, C). The growth of the upper part of the gland continues and at anthesis the zone of nectarostomata is almost completely hidden between the rest of the gland, the receptacle and the sepal bases, respectively (Fig. 6–F). Nectary glands and the other floral organs are slightly lifted by receptacular growth. The sepal bases form shallow pockets into which the nectary glands protrude (Fig. 6F).

Floral architecture and synorganization

Floral organization is similar amongst Geraniaceae and Hypseocharitaceae (Fig. 1). Apart from changes in symmetry, which are related to receptacle and nectary gland development, variation occurs almost exclusively within the androecium. The number of stamens is usually ten (*Geranium*, *Erodium* and *Pelargonium*) or 15 (*Hypseocharis* and *Monsonia*). Fertile stamens range between five and 15.

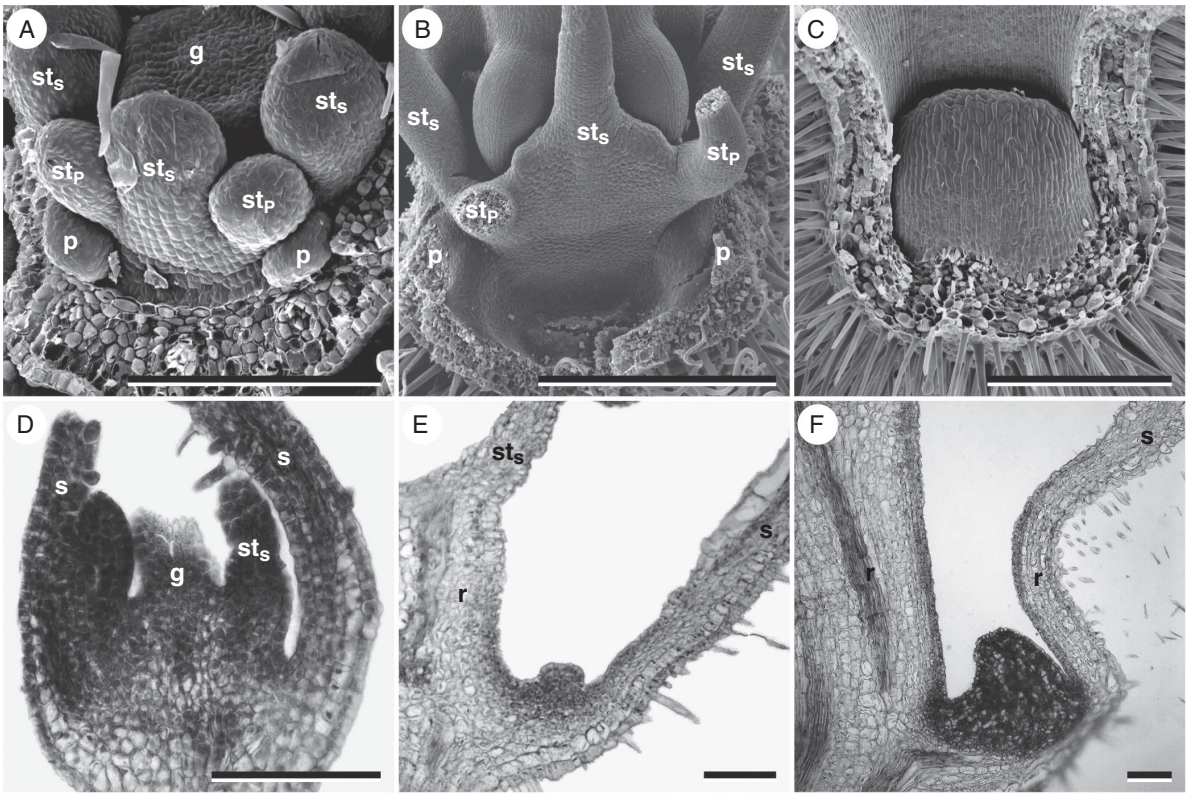

FIG. 4. Nectary gland development in *Pelargonium australe*. (A–C) Micrographs obtained using scanning electron microscopy. (D–F) Longitudinal sections. (A) Adaxial side of the flower before onset of nectary gland development. (B) Tube formation by growth of the receptacle. (C) Nectary gland at the base of the tube of an anthetic flower. (D) Longitudinal section through the developmental state similar to (A). (E) Developmental state similar to (B). (F) Anthetic flower. Perianth organs and wall of the tube in (C) removed. g, gynoecium; p, petal; r, receptacle; s, sepal; st_P; antepetalous stamen; st_S, antesepalous stamen. Scale bars in (A, D–F) = 100 μm, (B, C) = 500 μm.

Geranium pratense (Fig. 1A). The flowers are bowl-shaped. The bases of the filaments, the apical parts of the glands and the bases of the petals are covered with simple trichomes (Fig. 2C–F). Nectar is secreted through nectarostomata at the lower part of the gland (Fig. 2F). A common inner space is formed through the circular constriction of the anthophore and above the bases of the sepals (Figs 1F and 6A). This space may function as a nectarotheca (nectar holder). It is only compartmentalized above the anthophore by the bases of the petals (Fig. 7B, C).

Geranium maderense (Figs 1B and 7D–F). The bases ('claws') of the petals form two ridged, longitudinal protrusions which fit around the central part of the filaments of the antepetalous stamens (Fig. 7F). Additional to the central protrusions of the petal bases, recurved lobes are present, which enclose the glands (Fig. 7E). Below the points of petal attachment to the receptacle, the petals form a distinct tip which fits into the circular constriction of the anthophore. This elaboration of the petals leads to the compartmentalization of the flower. Apart from paired petals, the flattened filaments of three stamens and one sepal are involved in the formation of a compartment (Fig. 7F). Each of these compartments contains one nectary gland. A short anthophore is formed and a circular constriction is present, but the basolateral lobes of the petals prevent the formation of a common space. The inside of the flower is completely glabrous (with the exception of the gynoecium, which is not directly involved in the formation of the compartments).

Erodium manescavi (Fig. 1C). The slightly zygomorphic flower of *E. manescavi* is bowl-shaped. The sizes of the nectary glands differ between small on the abaxial side to two to four times larger on the adaxial side. The petals show distinct, almost claw-like bases. The distance between the adaxial petals is significantly larger compared with the distances to and between the other three petals. Additionally, they show white nectar guides with dark purple veins. The formation of a short anthophore leads to a common space between the insertion of the floral organs and the bases of the sepals. This space is densely filled with simple trichomes emerging from the surrounding organs (Fig. 2F). Above the point of petal and nectary gland insertion, trichomes are present on the filaments. These trichomes form a 'zone' above the glabrous nectary glands (Fig. 2F). The petal bases are covered with the same type of trichomes as present on the filaments. The staminodes are variable in their appearance. In many flowers, only a few staminodes were present.

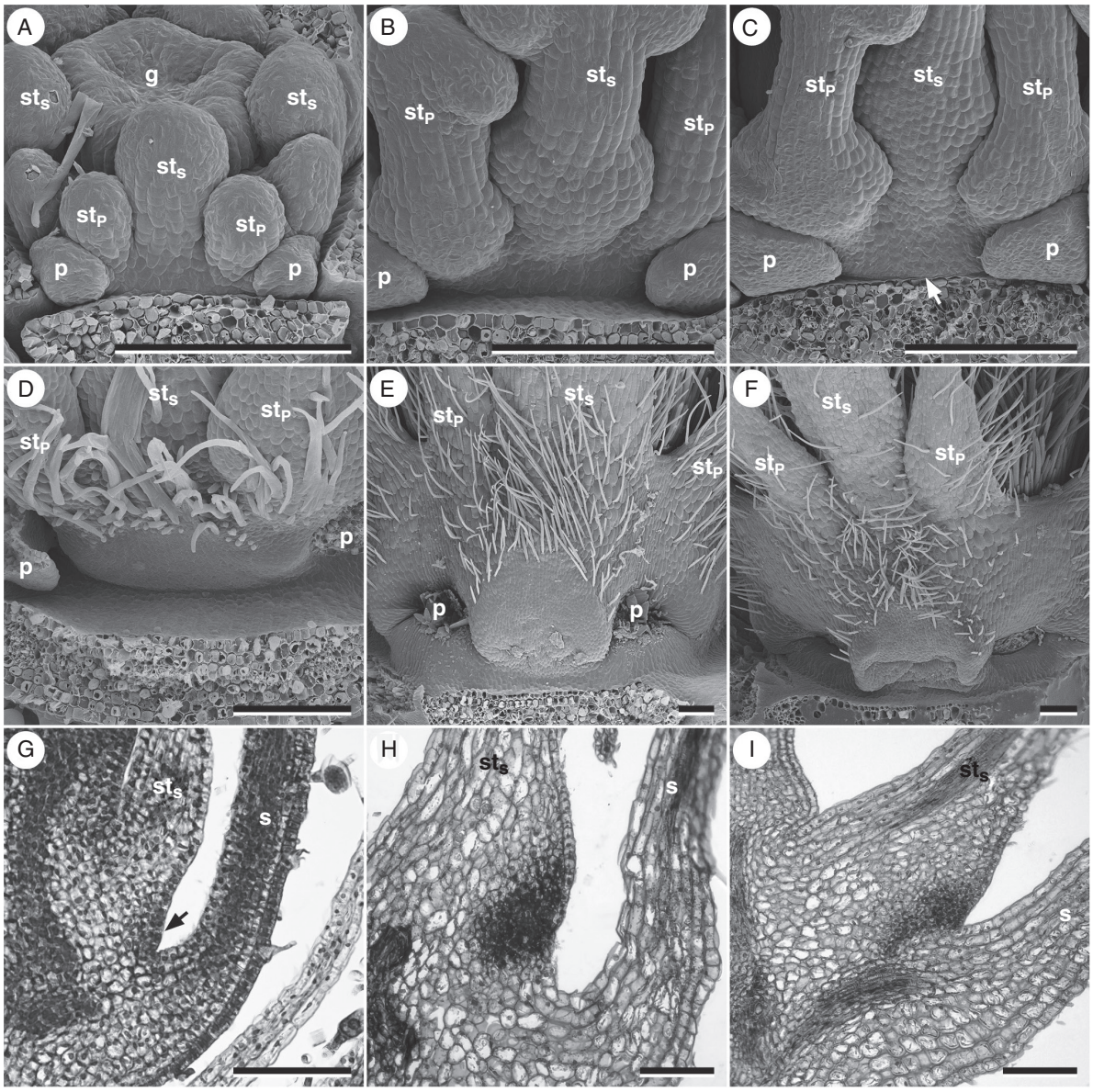

FIG. 5. Nectary gland development in *Monsonia brevirostrata*. (A–F) Micrographs obtained using scanning electron microscopy. (G–I) Longitudinal sections. (A) Young flower showing the early formation of stamen triplets. (B) Stamen base before the onset of nectary gland development. (C) Onset of nectary gland development. (D) Slightly bilobed young nectary gland and onset of anthophore development. (E) Gland shortly before anthesis. (F) Partially collapsed nectary gland and anthophore of an anthetic flower. (G) Longitudinal section through a nectary gland in a corresponding stage to (C). (H) Similar stage to (E). (I) Gland in an anthetic flower. Arrows indicate the earliest observed stage of nectary gland development. Perianth organs removed. g, gynoecium; p, petal; S, sepal; st_p, antepetalous stamen; st_s, antesepalous stamen. Scale bars in (A–I) = 100 μm.

Monsonia emarginata (Fig. 1D) and *M. brevirostrata*. In *Monsonia*, the antepetalous staminal whorl has ten stamens, while the antesepalous whorl has only five. All filaments are basally fused, and those of the antesepalous stamens are longer than those of the antepetalous stamens. The antesepalous stamens form triplets with the adjacent antesepalous stamens. These triplets are fused up to half of their length. Each petal base has two lateral lobes which partially enclose the neighbouring nectary glands. The sepals bend upwards slightly, while the petals and stamen triplets bend outwards through the partial shrinking of the nectary glands and anthophore. This bending leads to an increased distance between the entry zones and the nectary glands. The apicolateral parts of the glands, the petal bases and the filaments are scarcely covered with simple trichomes.

Pelargonium australe (Fig. 1E). The single nectary gland is hidden in a tube-like cavity on the adaxial side of the flower

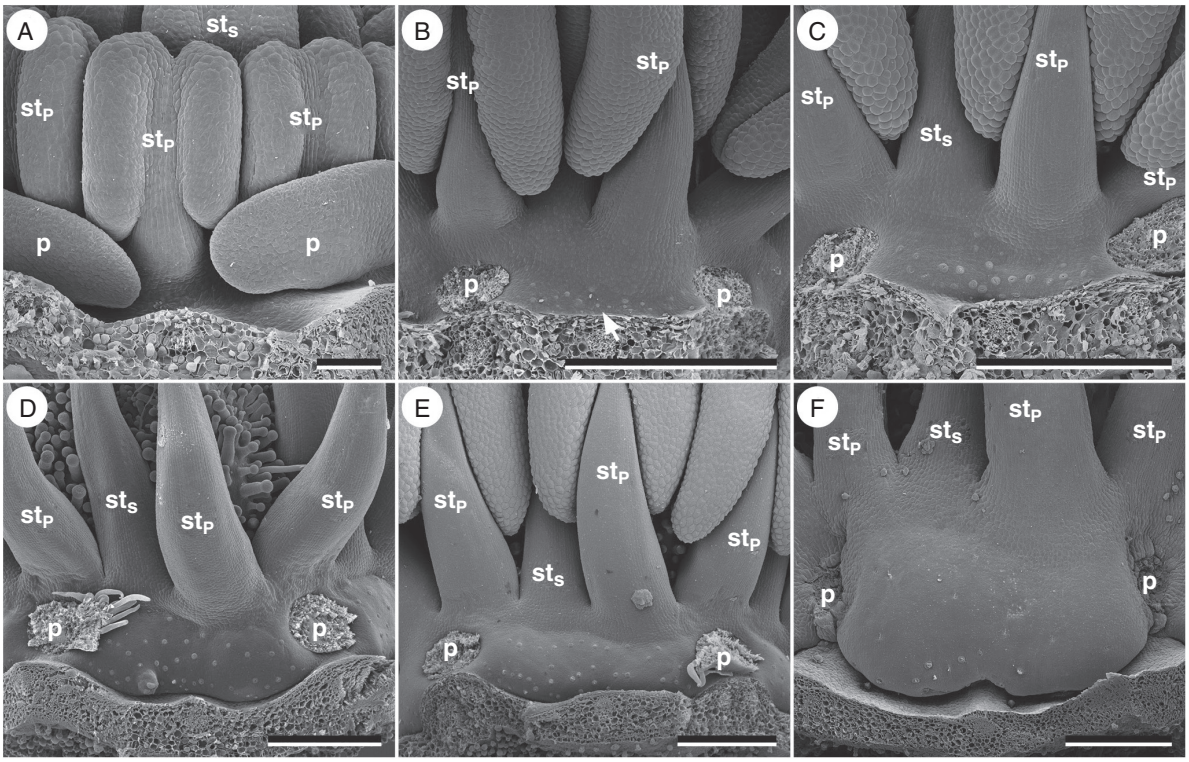

FIG. 6. Nectary gland development in *Hypseocharis bilobata*. Micrographs obtained using scanning electron microscopy. (A) Androecium before onset of nectary gland development. (B) Onset of nectary gland development as a field of nectarostomata. (C) First bulging of the nectary gland. (D) Growth of the nectary gland and the neighbouring receptacle. (E) Continuing growth of the nectary gland. The field of nectarostomata is shifted towards its basipetal position. (F) Nectary gland of an anthetic flower. Arrows indicate the earliest observed stage of nectary gland development. Perianth organs removed. p, petal; s, sepal; st_p, antepetalous stamen; st_s, antesepalous stamen. Scale bars in (A) = 100 μm, (B–F) = 500 μm.

(Fig. 4C, F). The broad opening tapers gradually into a constricted part before it widens again and forms a basal, almost globular compartment in which the nectary gland is localized (Fig. 4F). All floral organs, with the exception of the gynoecium, are glabrous. The abaxial and the lateral antesepalous stamens are staminodial. Their shape ranges from filament-like to triangular with a single large trichome emerging from the tip. All stamens and staminodes are basally fused. The two fertile antepetalous stamens on the adaxial side form a triplet with the adaxial antesepalous stamen. The filament of the latter stamen abruptly broadens towards the fused part of the androecium, forming two 'shoulders' (Fig. 4B). The receptacle below the insertion point of the adaxial petals forms a ring, which constricts the entrance of the cavity (Fig. 4F). In longitudinal sections, a clear difference between the ventral epidermis of the adaxial sepal and the inner epidermis of the cavity is visible (Fig. 4F).

Pelargonium reniforme. The development is similar to that of *P. australe*. The entrance to the spur-like receptacular cavity is surrounded by the partially fused stamen triplet on the proximal side, the erect adaxial sepal on the distal side and the bases of the adaxial petals, demarcating the entrance laterally (Fig. 7H, I). The massive nectary gland is present at the base of the cavity (Fig. 7G).

Hypseocharis bilobata (Fig. 1F). The flowers are bowl-shaped. The nectary glands in *H. bilobata* are located at the bases of 3–4 stamens (Fig. 6). The antepetalous staminal whorl has ten stamens, while the antesepalous has only five. One of the antepetalous stamens is in the antepetalous position, and the second one is shifted towards one of the neighbouring nectary glands. The antesepalous stamens are positioned closer to the centre of the flower. The zone of the nectary glands which is covered with nectarostomata faces towards the base of the sepals (Fig. 6F). The sepals form shallow basipetal protrusions, right in front of the nectary glands (Figs. 6F, 7J). The floral organs are glabrous, possessing simple trichomes only laterally at the bases of the petal (Fig. 7J, K).

DISCUSSION

The study of nectary development adds important information for our understanding of floral organization and floral architecture. The present study of nectary ontogeny in Geraniaceae and Hypseocharitaceae shows that the overall nectary development and floral organization is similar across the taxa studied. They are classified as axial (receptacular) nectaries (Smets, 1988; Smets and Cresens, 1988; Jeiter *et al.*, 2017). Apart from differences in shape and size, major differences occur in the timing of the development of the nectarostomata, through which nectar is

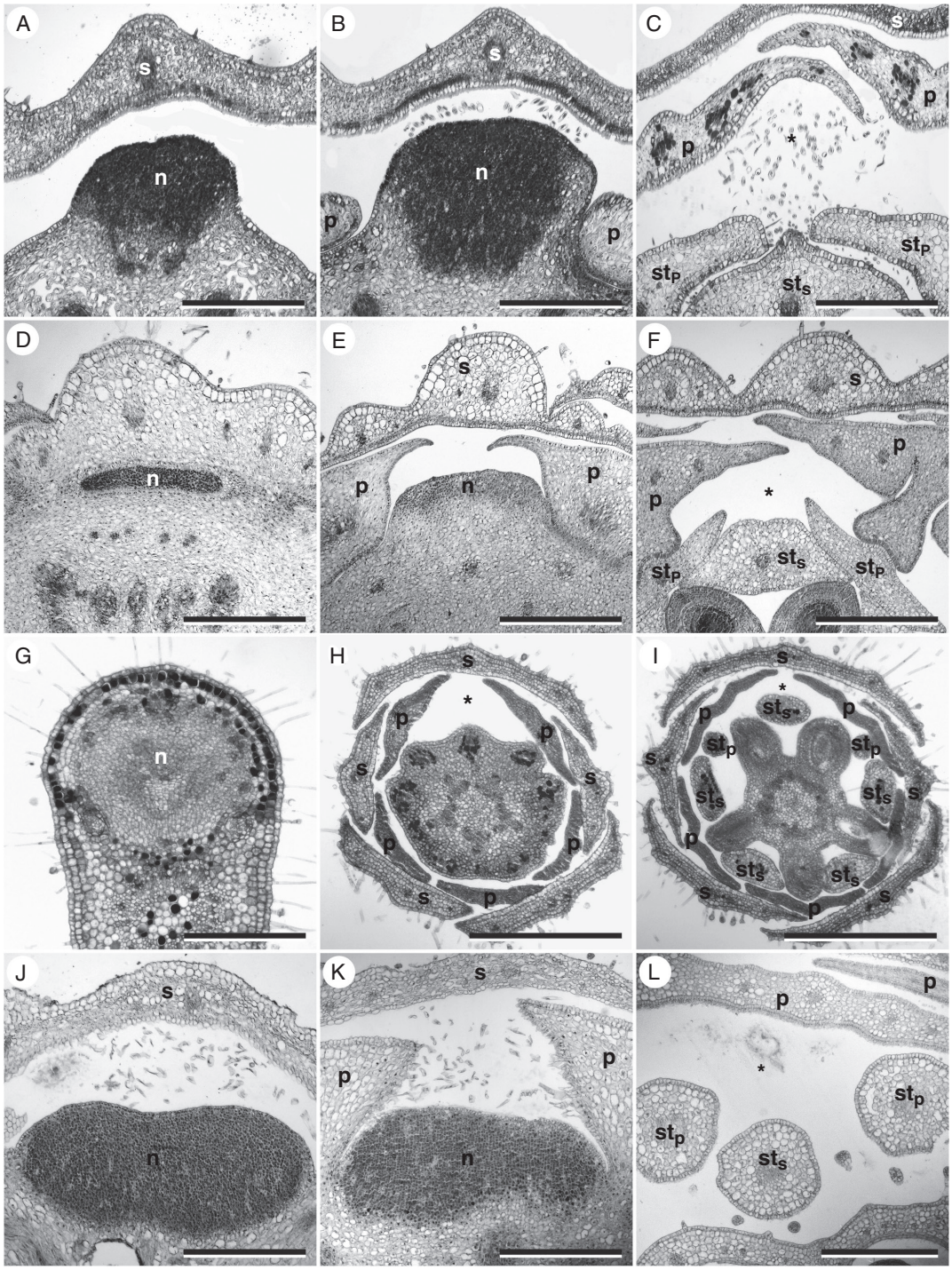

FIG. 7. Floral architecture: cross-sections through mature flowers. (A–C) *Geranium pratense*. (A) Level of circular constriction below petal. (B) Level of petal insertion. (C) Level above nectary gland. (D–F) *Geranium maderense*. (D) Base of the flower and insertion of the nectary gland. (E) Level of petal insertion. (F) Level above the nectary gland. (G–I) *Pelargonium reniforme* (pre-anthetic flower). (G) Level at the base of the receptacular cavity and the base of the gland. (H) Level above the entrance of the cavity. (I) Level of the ovaries. (J–L) *Hypseocharis bilobata*. (J) Level below petal insertion. (K) Level at petal insertion. (L) Level above the nectary gland. n, nectary gland; p, petal; s, sepal; st_p, antepetalous stamens; st_s, antesepalous stamens, *Position of the nectary gland in lower levels. Scale bars in (A–I, K, L) = 500 μm, (J) = 250 μm.

exudated (early in *Hypseocharis*, *Geranium* and *Pelargonium*, and late in *Erodium* and *Monsonia*).

Possibly the most surprising discovery of this study is the presence of a non-nectariferous receptacular structure below the level of petal and anther insertion. This is an anthophore similar to what is found in Caryophyllaceae (e.g. *Lychnis flos-jovis*; Weberling, 1981, p. 30). Anthophore development is the result of intercalary growth of the receptacle and it has two consequences: (1) the size of the nectary glands increases; and (2) the inner volume of the flower increases. Both changes may result in a higher amount of nectar produced and held by the flower. A higher inner volume of the flower may be especially relevant in *G. pratense*, where the anthophore shows a circular constriction. A floral organization and floral architecture similar to that of *G. pratense* have been beautifully illustrated for *G. sylvaticum* (Nilsson, 1984).

Some studies found a positive correlation between the amount of nectariferous tissue and the volume of nectar exudated (e.g. Petanidou *et al.*, 2000). The amount of nectar held by a flower has been found to correlate with the duration of pollinator visit and ultimately with pollination success and seed set (e.g. Manetas, 2000). Increasing the amount of nectar offered is one possible strategy to prolong the time a pollinator spends on a flower. An alternative way to prolong handling time could be compartmentalization of the flower. We found an increased floral complexity in *G. maderense* with five separate nectary compartments formed by a total of six organs from four different whorls. A pollinator would have to probe all five compartments to collect the complete reward of the flower. This form of floral architecture, called 'revolver flower', has been previously described for *G. robertianum* (Endress, 2010). Compartmentalization of the flower is realized through two longitudinal ridges on the base of the petals. This kind of modification appears to be systematically relevant as we confirmed its presence in other species of *Geranium* section *Robertium* (Picard) Rouy & Fouc. (Yeo, 1984), such as *G. reuteri*. This floral architecture is striking because it represents an extreme degree of synorganization in the absence of organ fusion.

Flower compartmentalization is known from several other plant groups either with [e.g. *Brugmansia sanguinea*, Solanaceae (Endress, 1994); Codonaceae (Jeiter *et al.*, 2016)] or without fused organs (e.g. *Aquilegia*; Willmer, 2011), or with a combination of free and fused organs (e.g. Loasaceae; Weigend and Gottschling, 2006). In the case of *Aquilegia*, compartmentalization is realized by individual nectary organs ('Honigblätter'). In the Geraniaceae and Hypseocharitaceae studied, we found a tendency towards the formation of stamen triplets around the nectary gland. Our findings concur with those of Endress (2010), who demonstrated that the formation of (nectar) guide rails in *G. robertianum* is facilitated by the obdiplostemonous organization of the androecium and the formation of stamen triplets. We propose an evolutionary series for the floral architecture (and synorganization) focusing on the occurrence of stamen triplets and nectary position in the Geraniaceae and Hypseocharitaceae (Fig. 8). Selected morphological features are presented in the context of our current understanding of Geraniales phylogeny (Fig. 9). The phylogeny of the Geraniaceae is fully resolved, and the sister group relationships between Hypseocharitaceae and Geraniaceae and to the rest of Geraniales are well supported (Fiz *et al.*, 2008; Palazzesi *et al.*, 2012). Sister to these two families is a well-supported clade comprising the three families Melianthaceae, Francoaceae and Vivianiaceae (Palazzesi *et al.*, 2012). The relationships amongst these three families remain uncertain (Palazzesi *et al.*, 2012), but phylogenies are present for each genus of the Geraniaceae [e.g. *Erodium* (Fiz *et al.*, 2006); *Monsonia* (Touloumenidou *et al.*, 2007); *Pelargonium* (Röschenbleck *et al.*, 2014); *Geranium* (Marcussen and Meseguer, 2017)]. According to APG IV (2016), Myrtales is the sister group of Geraniales, but the relationships between the orders of the rosids remain poorly resolved.

Our results show two character sets which are partially correlated: (1) the androecium and (2) the receptacle including the nectary glands. Within Geraniaceae and Hypseocharitaceae there appears to be a high degree of plasticity in the number of fertile and sterile stamens. The numbers range from five fertile stamens in *California macrophylla* (Aldasoro *et al.*, 2002), to 15 in *Hypseocharis* and *Monsonia*. Additionally, there is variation within genera. In *Pelargonium*, the number of fertile stamens ranges from two to seven while in *Hypseocharis tridentata* only five fertile stamens are present. Considering the common number of ten stamens in Geraniaceae and other genera of the Geraniales (Jeiter *et al.*, 2017), a hypothetical common ancestor with a pentacyclic flower seems to be more likely than one with a tetracyclic flower with one whorl of five stamens as proposed by Ronse De Craene and Bull-Hereñu (2016).

Surprisingly, the seemingly derived receptacular cavity found in *Pelargonium* is linked to several taxa with depressions or cavities formed by the receptacle. Apart from the receptacular cavity in *Pelargonium*, there are depressions in *Hypseocharis*, and the basal clade of *Monsonia* shows several species with tubular receptacular/axial structures (Kers, 1971; Link, 1989; Touloumenidou *et al.*, 2007). We propose a hypothetical ancestor with similar depressions in the receptacle.

Most of the species in this study across *Geranium*, *Erodium* and *Monsonia* show different levels of complexity of floral architecture, synorganization and compartmentalization, but *Pelargonium* represents an entirely different type of floral organization. In the zygomorphic flowers of *Pelargonium*, four of the five nectary glands, present in the other genera, have been lost (Jeiter *et al.*, 2017). The intercalary growth of the receptacle here also includes the bases of the sepals. The only organ that 'remains' in its original position is the nectary gland on the adaxial side of the flower. The intercalary growth results from cell division and subsequent cell elongation (Tsai, 2016). There is considerable variation in the spur length amongst the *Pelargonium* species, ranging from 1 to 100 mm (Bakker *et al.*, 2004). Differences in length appear to be the result of differences in duration of activity of the intercalary meristem; however, the spur-like receptacular cavity growth has so far only been studied in two *Pelargonium* species (Tsai, 2016). In comparison with the often bowl-shaped (and rarely hypocrateriform) flowers of the other genera of the Geraniaceae and Hypseocharitaceae, most *Pelargonium* species show a tubular overall architecture. A similar mechanism of receptacular cavity formation can be assumed for some species of *Monsonia*. The actinomorphic flowers have five independent receptacular cavities, each with one nectary gland (Kers, 1971; Link, 1989). The formation of a tube via intercalary growth of almost the complete receptacle is a rare phenomenon. Endress (1994, p. 115) reports only a few cases where

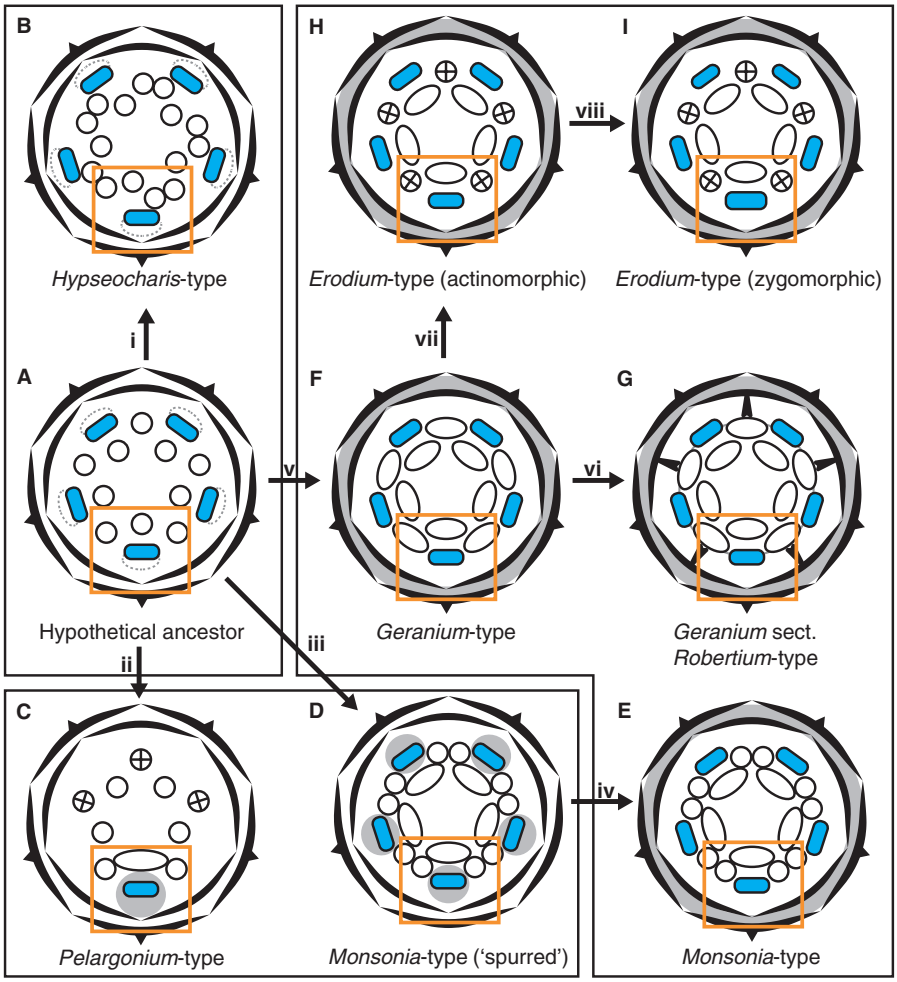

Fig. 8. Schematic representation of the assumed evolutionary series of androecial floral organization in Geraniaceae and Hypseocharitaceae. (A) Type of organization as assumed for the hypothetical ancestor. Nectaries are slightly sunken into the receptacle. (i) Dédoublement in the antepetalous whorl of stamens. (B) *Hypseocharis*-type. (ii) Reduction of four nectary glands and three anthers and the formation of a receptacular cavity through intercalary growth. (C) *Pelargonium*-type. (iii) Dédoublement in the antepetalous androecial whorl and formation of receptacular cavities. (D) *Monsonia*-type with five receptacular cavities ('spurred'). (iv) Reduction of receptacular cavities. (E) *Monsonia*-type. (v) Lateral broadening of the filaments and formation of an elaborate anthophore. (F) *Geranium*-type. (vi) Formation of basal outgrowth of the petals and elaborate synorganization and compartmentalization of the flower. (G) *Geranium* sect. *Robertium*-type. (vii) Reduction of the anthers of the antepetalous stamens. (H) Actinomorphic *Erodium*-type. (viii) Elaboration of the adaxial side of the flower. (I) Slightly zygomorphic *Erodium*-type. Black structures, perianth organs; white circles/ellipses, stamens; crossed circles, staminodes; blue rectangles, nectar glands; small grey circles with dashed line around nectary glands, slightly sunken nectary glands; grey areas, areas which are not affected by intercalary growth of the receptacle; orange boxes, functional unit formed around the nectary gland; black boxes, denote types with similar morphological configuration of the receptacle. Gynoecium not shown.

such 'inner spurs' occur. A 'free receptacular spur' has been described for *Tropaeolum* (Ronse Decraene and Smets, 2001). Tubular structures as such are, of course, common in angiosperm flowers and can be formed by individual organs (usually referred to as 'spurs', e.g. *Aquilegia*; Tucker and Hodges, 2005), by the formation of a hypanthial (receptacular) tube (e.g. *Oenothera*; De Vos, 1981) or by fused sepals or petals (e.g. *Lithospermum*; Cohen, 2016). Variations in length and concomitant shifts in pollinators seem to represent parallel ecological adaptations (Bakker *et al.*, 2004; Whittall and Hodges, 2007; Cohen, 2012).

Interestingly, the function of the unique spur-like receptacular cavity in *Pelargonium* as a key innovation has been rejected (Hodges and Arnold, 1995; Hodges, 1997). The main reason is that a key innovations test is based exclusively on species numbers of sister groups (Slowinski and Guyer, 1993). Considering the number of species present in the sister group, the simplistic view of their diversity in floral architecture, the divergence of dispersal modes, vegetative morphology and the vastly different geographical range of the sister taxa, there may be several 'hidden key innovations' masking the importance of the spur-like receptacular cavity in *Pelargonium*. Comparing the number of species per unit area and coexisting species, *Pelargonium* far exceeds those of the sister group (especially those of *Geranium*). Considering the broad range of pollination

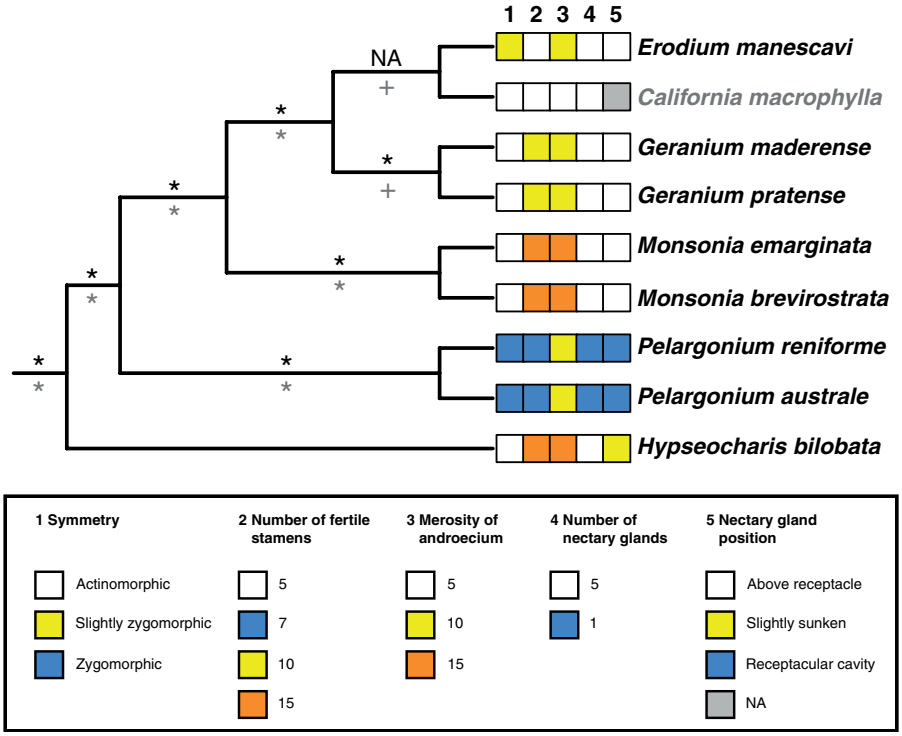

FIG. 9. Phylogenetic relationships and selected character states of the species studied. The topology is based on Palazzesi *et al.* (2012) and Fiz *et al.* (2008). Black labels above the branches refer to support values from Palazzesi *et al.* (2012). Grey labels below the branches refer to support values from Fiz *et al.* (2008). Asterisks (*) indicate bootstrap support values of 100 % and a posterior probability of 1. Pluses (+) indicate a bootstrap support between 50 and 75 % and a posterior probability of 1. *California macrophylla* was not included in the sampling of Palazzesi *et al.* (2012) which is why there are no support values given (NA). The morphological data for *California macrophylla* come from Aldasoro *et al.* (2002) and personal observations. For character coding, please refer to the key.

syndromes documented for *Pelargonium* – vs. a relatively small range in the sister taxa – the specific functional divergence facilitated by the 'inner spur' may well be a key innovation.

Erbar and Leins (1996) underscore the evolutionary significance of sympetaly based on intercalary growth of the stamen–corolla tube. We here demonstrate that part of the floral diversification of Geraniaceae, particularly in the species-rich genus *Pelargonium*, goes back to the hitherto overlooked form of anthophore formation via receptacular, intercalary growth. This expands our appreciation for the importance of intercalary growth contributing to floral architecture and thereby floral mode in highly diversified plant groups.

We further demonstrate that the complex floral synorganization first reported for *G. robertianum* by Endress (2010) is not unique to that species, and a superficial survey indicates that functional floral morphology in *Geranium* may actually be more complex and diverse than generally assumed. A broader sampling of the genus *Geranium* would be particularly interesting for understanding its evolutionary success with >460 species and a sub-cosmopolitan distribution. Jeiter *et al.* (2017) could demonstrate the morphological coherence of flowers across the superficially very different genera of the order Geraniales. The present study illustrates the degrees of freedom obtained by relatively minor changes as a result of intercalary growth or displacement within the rigid constraints of a fairly conserved floral organization.

ACKNOWLEDGEMENTS

We thank the staff of the botanical gardens at Berlin and Bonn for the cultivation of the plant material used in this study. We also gratefully acknowledge the technical support by Ch. Dietrich and H.-J. Ensikat. We are grateful for valuable comments and suggestions by two anonymous reviewers and the handling editor J. Harrison. Cross-sections of *Pelargonium reniforme* are from the B.Ed. thesis of C. Rixen (Freie Universität Berlin, 2014). J.J. receives a scholarship from the Studienstiftung des deutschen Volkes.

LITERATURE CITED

Albers F, **van der Walt JJA. 2007**. Geraniaceae. In: Kubitzki K, ed. *The families and genera of vascular plants IX*. Heidelberg: Springer, 157–167.

Aldasoro JJ, **Navarro C**, **Vargas P**, **Aedo C. 2001**. Anatomy, morphology, and cladistic analysis of *Monsonia* L. (Geraniaceae). *Anales del Jardín Botánico de Madrid* **59**: 75–100.

Aldasoro JJ, **Navarro C**, **Vargas P**, **Sáez L**, **Aedo C. 2002**. *California*, a new genus of Geraniaceae endemic to the southwest of North America. *Anales del Jardín Botánico de Madrid* **59**: 209–216.

APG IV. 2016. An update of the Angiosperm Phylogeny Group classification for the orders and families of flowering plants: APG IV. *Botanical Journal of the Linnean Society* **181**: 1–20.

Bakker F, **Culham A**, **Hettiarachi P**, **Touloumenidou T**, **Gibby M. 2004**. Phylogeny of *Pelargonium* (Geraniaceae) based on DNA sequences from three genomes. *Taxon* **53**: 17–28.

Brunies S. 1900. *Anatomie der Geraniaceenblätter in Beziehung zur Systematik der Familie*. Inauguraldissertation, Universität Breslau, now Wrocław, Poland.

Cohen JI. 2012. Continuous characters in phylogenetic analyses: patterns of corolla tube length evolution in *Lithospermum* L. (Boraginaceae): evolution of corolla tube length. *Biological Journal of the Linnean Society* **107**: 442–457.

Cohen JI. 2016. Floral evolution in *Lithospermum* (Boraginaceae): independent origins of similar flower types. *Botanical Journal of the Linnean Society* **180**: 213–228.

Devi DR. 1991. Floral anatomy of *Hypseocharis* (Oxalidaceae) with a discussion on its systematic position. *Plant Systematics and Evolution* **177**: 161–164.

De Vos OC. 1981. Ontogeny and vascularisation of the flower of *Oenothera* (Onagraceae). *Acta Botanica Neerlandica* **30**: 219–229.

Endress PK. 1994. *Diversity and evolutionary biology of tropical flowers*. Cambridge: Cambridge University Press.

Endress PK. 1996. Homoplasy in angiosperm flowers. In: Sanderson MJ, Hufford L, eds. *Homoplasy – the recurrence of similarity in evolution*. San Diego, CA: Academic Press, 303–325.

Endress PK. 2010. Synorganisation without organ fusion in the flowers of *Geranium robertianum* (Geraniaceae) and its not so trivial obdiplostemony. *Annals of Botany* **106**: 687–695.

Endress PK. 2016. Development and evolution of extreme synorganization in angiosperm flowers and diversity: a comparison of Apocynaceae and Orchidaceae. *Annals of Botany* **117**: 749–767.

Erbar C, **Leins P. 1996**. Distribution of the character states 'Early Sympetaly' and 'Late Sympetaly' within the 'Sympetalae Tetracyclicae' and presumably allied groups. *Botanica Acta* **109**: 427–440.

Fiz O, **Vargas P**, **Alarcón M**, **Aldasoro JJ. 2006**. Phylogenetic relationships and evolution in *Erodium* (Geraniaceae) based on trnL–trnF sequences. *Systematic Botany* **31**: 739–763.

Fiz O, **Vargas P**, **Alarcón M**, **Aedo C**, **Garcia JL**, **Aldasoro JJ. 2008**. Phylogeny and historical biogeography of Geraniaceae in relation to climate changes and pollination ecology. *Systematic Botany* **33**: 326–342.

Gerstberger P, **Leins P. 1978**. Rasterelektronenmikroskopische Untersuchungen an Blütenknospen von *Physalis philadelphica* (Solanaceae) Anwendung einer neuen Präparationsmethode. *Berichte der Deutschen Botanischen Gesellschaft* **91**: 381–387.

Hodges SA. 1997. Floral nectar spurs and diversification. *International Journal of Plant Sciences* **158**: S81–S88.

Hodges SA, **Arnold ML. 1995**. Spurring plant diversification: are floral nectar spurs a key innovation? *Proceedings of the Royal Society B: Biological Sciences* **262**: 343–348.

Japp G. 1909. Über die morphologische Wertigkeit des Nektariums der Blüten des *Pelargonium zonale*. *Verhandlungen des Naturforschenden Vereines Brünn* **47**: 201–216.

Jeiter J, **Danisch F**, **Hilger HH. 2016**. Polymery and nectary chambers in *Codon* (Codonaceae) – flower and fruit development in a small, capsule-bearing family of Boraginales. *Flora* **220**: 94–102.

Jeiter J, **Weigend M**, **Hilger HH. 2017**. Geraniales flowers revisited: evolutionary trends in floral nectaries. *Annals of Botany* **119**: 395–408.

Kers LE. 1971. *Monsonia parvifolia* Schinz (Geraniaceae), a species with concealed spurs. *Botaniska Notiser* **124**: 208–212.

Kumar A. 1976. Studies in Geraniales II. The floral anatomy. *Journal of the Indian Botanical Society* **55**: 233–253.

Labbe A. 1964. On the spur of the flower of *Pelargonium*. *Bulletin de la Société Botanique de France* **8**: 321–324.

Leins P, **Erbar C. 2006**. Secondary pollen presentation syndromes of the Asterales – a phylogenetic perspective. *Botanische Jahrbücher* **127**: 83–103.

Link DA. 1989. *Die Nektarien der Geraniales – Morphologie, Anatomie, Histologie, Blütenökologische Bedeutung und Konsequenzen für die Systematik*. Dissertation, Universität Mainz, Germany.

Link DA. 1994. The nectaries of Geraniaceae. In: Vorster P, ed. *Proceedings of the international Geraniaceae Symposium*. South Africa: Stellenbosch University, 215–225.

Manetas Y. 2000. Nectar amount, pollinator visit duration and pollination success in the mediterranean shrub *Cistus creticus*. *Annals of Botany* **86**: 815–820.

Marcussen T, **Meseguer AS. 2017**. Species-level phylogeny, fruit evolution and diversification history of *Geranium* (Geraniaceae). *Molecular Phylogenetics and Evolution* **110**: 134–149.

McDonald DJ, **van der Walt JJA. 1992**. Observations on the pollination of *Pelargonium tricolor*, section *Campylia* (Geraniaceae). *South African Journal of Botany* **58**: 386–392.

Narayana HS, **Arora PK. 1963**. Floral anatomy of *Monsonia senegalensis* Guill. and Perr. *Current Science* **32**: 184–185.

Nilsson L. 1984. *Nature magnified*. London: Macdonald & Co. Ltd.

Palazzesi L, **Gottschling M**, **Barreda V**, **Weigend M. 2012**. First Miocene fossils of Vivianiaceae shed new light on phylogeny, divergence times, and historical biogeography of Geraniales. *Biological Journal of the Linnean Society* **107**: 67–85.

Payer J-B. 1857. *Traité d'organogénie comparée de la fleur*. Paris: V. Masson.

Petanidou T, **Goethals V**, **Smets E. 2000**. Nectary structure of Labiatae in relation to their nectar secretion and characteristics in a Mediterranean shrub community: does flowering time matter? *Plant Systematics and Evolution* **225**: 103–118.

Price RA, **Palmer JD. 1993**. Phylogenetic relationships of the Geraniaceae and Geraniales from rbcL sequence comparisons. *Annals of the Missouri Botanical Garden* **80**: 661–671.

Ronse De Craene LP. 2010. *Floral diagrams: an aid to understanding flower morphology and evolution*. Cambridge: Cambridge University Press.

Ronse De Craene LP, **Bull-Hereñu K. 2016**. Obdiplostemony: the occurrence of a transitional stage linking robust flower configurations. *Annals of Botany* **117**: 709–724.

Ronse Decraene LP, **Smets EF. 1999**. Similarities in floral ontogeny and anatomy between the genera *Francoa* (Francoaceae) and *Greyia* (Greyiaceae). *International Journal of Plant Sciences* **160**: 377–393.

Ronse Decraene LP, **Smets EF. 2001**. Floral developmental evidence for the systematic relationships of *Tropaeolum* (Tropaeolaceae). *Annals of Botany* **88**: 879–892.

Röschenbleck J, **Albers F**, **Müller K**, **Weinl S**, **Kudla J. 2014**. Phylogenetics, character evolution and a subgeneric revision of the genus *Pelargonium* (Geraniaceae). *Phytotaxa* **159**: 31–76.

Sauer H. 1933. Blüte und Frucht der Oxalidaceen, Linaceen, Geraniaceen, Tropaeolaceen und Balsaminaceen. Vergleichend-entwicklungsgeschichtliche Untersuchungen. *Planta* **19**: 417–481.

Slanis AC, **Grau A. 2001**. El género *Hypseocharis* (Oxalidaceae) en la Argentina. *Darwiniana* **39**: 343–352.

Slowinski JB, **Guyer C. 1993**. Testing whether certain traits have caused amplified diversification: an improved method based on a model of random speciation and extinction. *American Naturalist* **142**: 1019–1024.

Smets EF. 1988. La présence des 'nectaria persistentia' chez les Magnoliophytina (Angiospermes). *Candollea* **43**: 709–716.

Smets EF, **Cresens EM. 1988**. Types of floral nectaries and the concepts 'character' and 'character-state' – a reconsideration. *Acta Botanica Neerlandica* **37**: 121–128.

Struck M. 1997. Floral divergence and convergence in the genus *Pelargonium* (Geraniaceae) in southern Africa: ecological and evolutionary considerations. *Plant Systematics and Evolution* **208**: 71–97.

Struck M, **van der Walt JJA. 1996**. Floral structure and pollination in *Pelargonium*. In: van der Maesen LJG, van der Burgt XM, van Medenbach de Rooy JM, eds. *The biodiversity of African plants*. Dordrecht: Kluwer Academic Publishers, 631–638.

Touloumenidou T, **Bakker FT**, **Albers F. 2007**. The phylogeny of *Monsonia* L. (Geraniaceae). *Plan Systematics and Evolution* **264**: 1–14.

Tsai T. 2016. *The receptacular nectar tubes of Pelargonium (Geraniaceae): a study of development, length variation, and histology*. Paper 950. Master's theses, University of Connecticut. http://digitalcommons.uconn.edu/gs_theses/950

Tucker SC, **Hodges SA. 2005**. Floral ontogeny of *Aquilegia*, *Semiaquilegia*, and *Enemion* (Ranunculaceae). *International Journal of Plant Sciences* **166**: 557–574.

Vogel S. 1998. Remarkable nectaries: structure, ecology, organophyletic perspectives IV. Miscellaneous cases. *Flora* **193**: 225–248.

Weberling F. 1981. *Morphologie der Blüten und der Blütenstände*. Stuttgart: Ulmer.

Weigend M, **Gottschling M. 2006**. Evolution of funnel-revolver flowers and ornithophily in *Nasa* (Loasaceae). *Plant Biology* **8**: 120–142.

Whittall JB, **Hodges SA. 2007**. Pollinator shifts drive increasingly long nectar spurs in columbine flowers. *Nature* **447**: 706–709.

Willmer P. 2011. *Pollination and floral ecology*. Princeton, NJ: Princeton University Press.

Yeo PF. 1984. Fruit-discharge-type in *Geranium* (Geraniaceae): its use in classification and its evolutionary implications. *Botanical Journal of the Linnean Society* **89**: 1–36.

Chapter 8

Internal floral spaces provide three-dimensional insights into angiosperm ecology and evolution

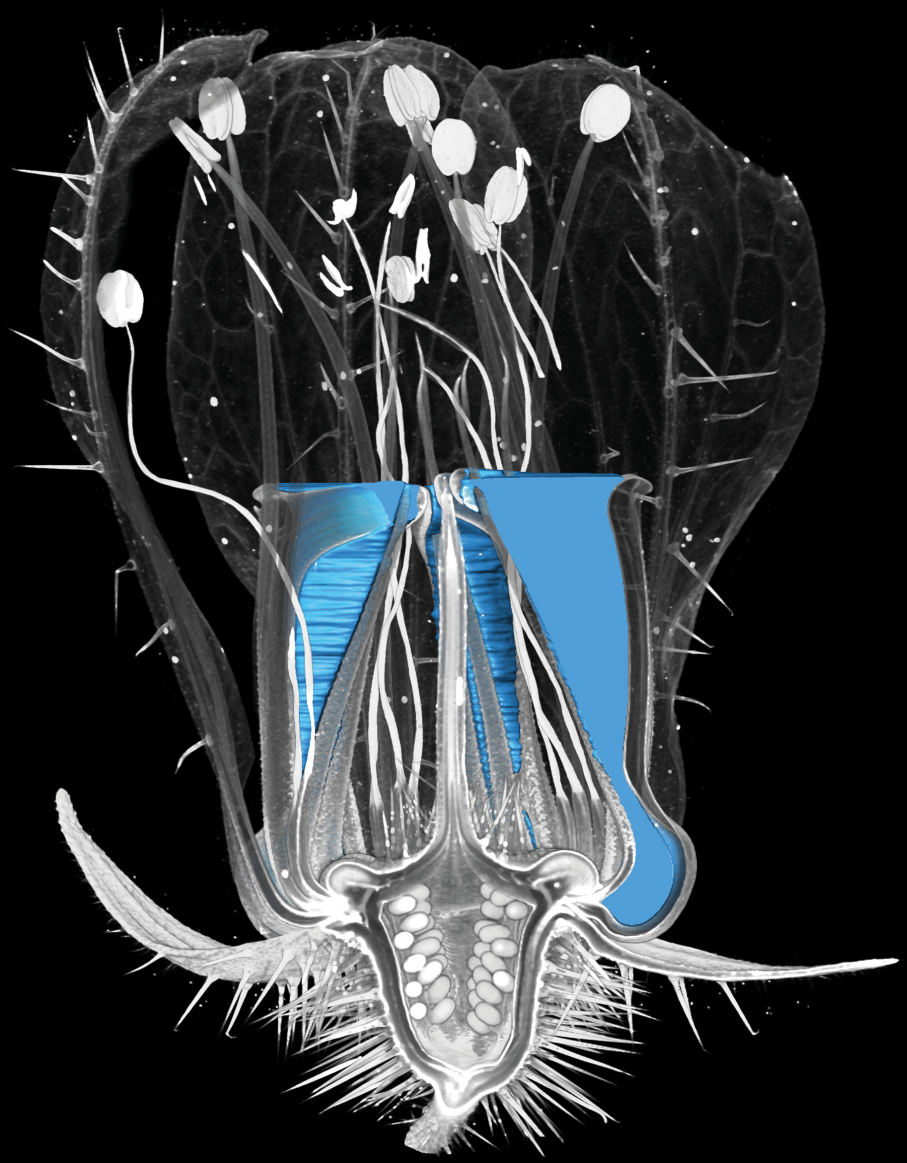

Jeiter J, Ziegler A, Weigend M. Internal floral spaces provide three-dimensional insights into angiosperm ecology and evolution. To be submitted.

Internal floral spaces provide three-dimensional insights into angiosperm ecology and evolution

Julius Jeiter[1,*], Alexander Ziegler[2], Maximilian Weigend[1]

[1]Nees-Institut für Biodiversität der Pflanzen, Rheinische Friedrich-Wilhelms-Universität, Meckenheimer Allee 170, 53115 Bonn, Germany

[2]Institut für Evolutionsbiologie und Ökologie, Rheinische Friedrich-Wilhelms-Universität, An der Immenburg 1, 53121 Bonn, Germany

*Corresponding author Email: jjeiter@uni-bonn.de

Abstract

Flowers as complex three-dimensional (3D) structures are composed of organs and spaces enclosed by the organs, the internal floral space (IFS). The study of IFS has recently become possible due to advances in 3D imaging techniques such as micro-computed tomography. Here, we highlight the importance of the IFS for a more detailed understanding of floral function and are providing a novel set of characters for evolutionary, systematic and functional inferences. We demonstrate the relevance of the IFS for a variety of plant species in Geraniaceae, Hydrophyllaceae and Loasaceae.

Keywords: Micro-computed tomography – volumetrics – morphology – compartmentalisation

8.1 Introduction

Angiosperm flowers are complex three-dimensional structures that are the result of evolutionary history, recent adaptations, and developmental constraints. Most angiosperm species rely on animal vectors for transfer of pollen and these organisms have to interact with the flower in a particular way to pick up pollen from the anther of one flower and later deposit it on a receptive stigma of a different flower. Beyond pollen transfer, the legitimate pollinator has to be able to locate and access the floral reward, commonly nectar, while potential nectar thieves preferably should not be able to do so.

There are thus a range of variables in flower function and accordingly there are complex patterns of co-evolution and co-adaptation between flowers and pollinators (Ollerton *et al.*, 2011). Co-adaptation from the floral perspective often includes synorganisation between floral organs in adaptation to a guild of pollinators with specific requirements and abilities or even a more or less specialised group of pollinators.

Apart from the floral signal (optical, olfactory) and the quality and quantity of the floral reward one very important aspect of floral architecture is the enclosure of a space or spaces in the flower. Part of these spaces if often filled with nectar as the rewards, other parts of these spaces determine the way the different floral organs are accessed by the visitors, e.g., because all or part of the pollinator has to enter them. These spaces are from here onward called the internal floral space (IFS).

Although the IFS is a ubiquitous feature of floral architecture, it has so far not been addressed as a discrete entity, possibly because of methodological limitations. Flowers are complex, three-dimensional (3D), and often delicate objects, therefore visualising their IFS is not a simple feat. The traditional approach is serial sectioning and subsequent reconstruction of the three-dimensional shape. However, this technique is extremely time-consuming, leads to a plethora of artefacts and is strongly size-limited, dramatically limiting its usefulness.

8.2 Results and discussion

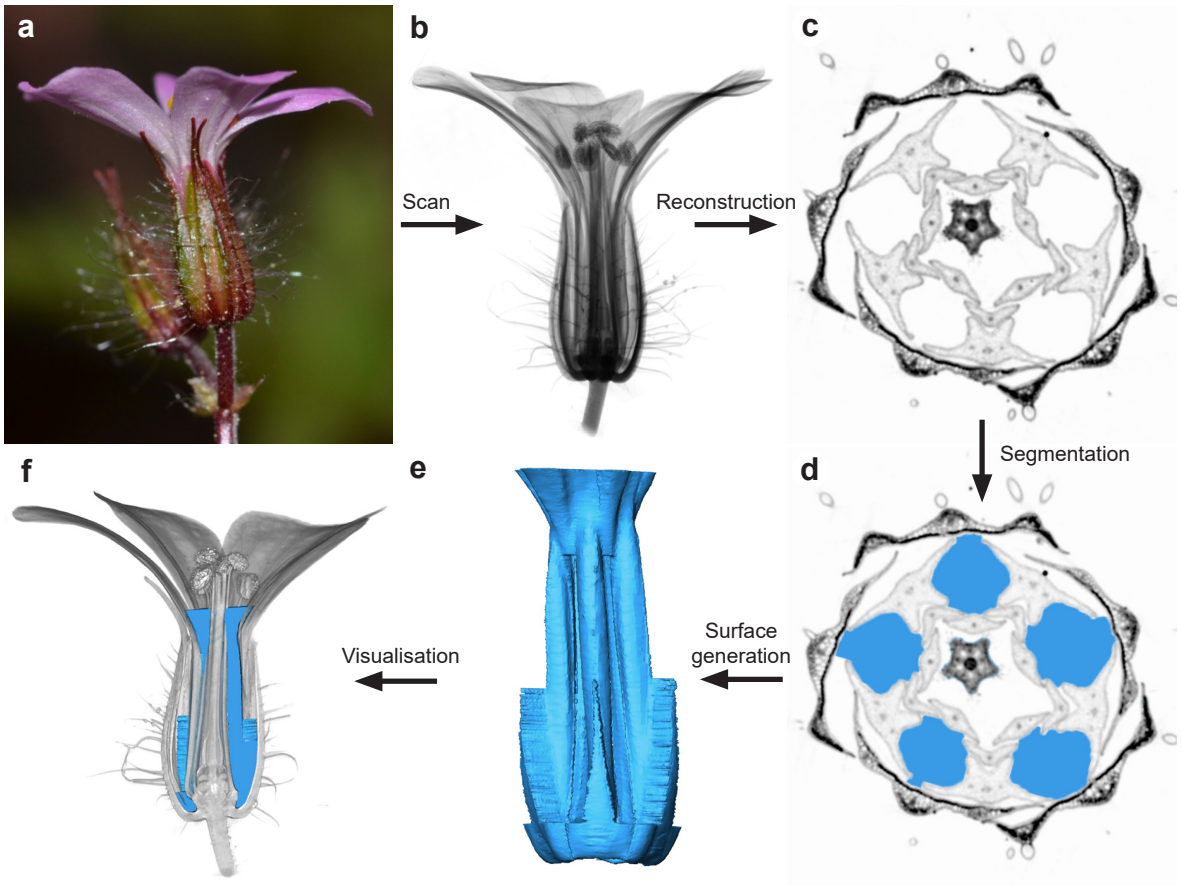

Figure 8.1: From flower to internal floral space in *Geranium robertianum* (Geraniaceae). a, photograph of a fresh flower of *Geranium robertianum*. b, simulated radiography of a fresh flower. c, virtual cross-section through as the result of reconstruction from µCT-data. d, segmented compartments of the IFS. e, IFS after surface generation f, ideal virtual cross-section through the three-dimensional-model of the fresh flower with the surface of the IFS placed inside. Refer to the text for explanations.

Recent advances in 3D imaging techniques (Stuppy *et al.*, 2003; Ledford, 2018) now permit the direct, non-invasive investigation and visualisation of all floral structural elements. To illustrate the methodological steps required to visualise the IFS, the flower of *Geranium robertianum* (Geraniaceae) is here used as an example (Fig. 8.1). A fresh flower of this species is collected (Fig. 8.1 a) and scanned using micro-computed tomography (µCT). A stack of virtual cross-sections is reconstructed (Fig. 8.1 c) from the preliminary X-ray images (Fig. 8.1 b). This stack is subsequently analysed, and the IFS is manually segmented (Fig. 8.1 d). Finally, the segmented parts are used to generate a rendered surface (Fig. 8.1 e), which may then be visualized inside a 3D volume rendering of the flower (Fig. 8.1 f), combining the presentation of structure and enclosed space in a single image. Previous studies of

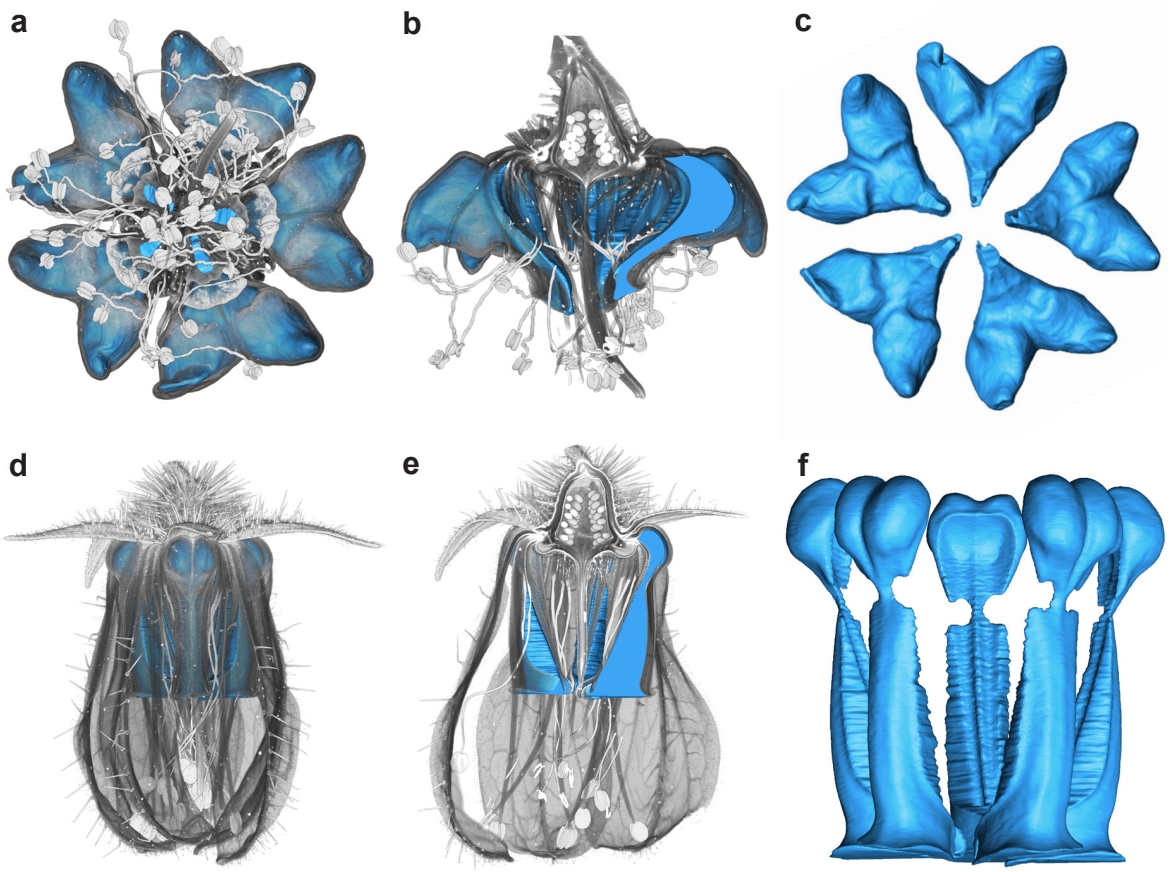

Figure 8.2: Internal floral spaces of two species of the genus *Nasa* (Loasaceae). a-c, *Nasa poissoniana*. a, 3D-model of the nectar scales with surfaces of the IFS placed inside. b, virtual cross-section through the 3D-model with the IFS placed inside. c, isolated IFS surfaces viewed from above. d-f, *Nasa amaluzensis*. d, 3D-model of the flower with enclosed nectar scales and surfaces of the IFS placed inside. e, virtual cross-section through the 3D-model with the IFS placed inside. f, isolated IFS surfaces viewed from lateral.

the IFS in *G. robertianum* were carried out with scanning electron microscopy and light microscopy (Endress, 2010). The present approach provides a much more comprehensive visualization of the IFS, including the distal widening of the IFS (pollinator access) and the relatively large volume hidden deep in the flower (hidden nectar). In angiosperms, the IFS are as divergent in shape, structure and volume as flower morphology and are moreover often compartmentalised, i.e. separate spaces can be identified within the individual flower. These compartments can either be equal or unequal, both in shape and function.

A common example for typically equal compartments are flowers with a revolver architecture. Here, the IFS is subdivided into separate compartments, each holding part of the overall reward of the flower. The organs involved in formation of these compartments vary widely. Common examples are spurs in *Aquilegia* (Ranunculaceae, Tucker & Hodges, 2005), the four synorganised organ whorls in *G. robertianum* (Fig. 8.1, Endress, 2010) and *G. maderense* (Geraniaceae, Jeiter *et al.*, 2017), the septa between filament bases and corolla tube in *Codon* (Codonaceae, Jeiter *et al.*, 2016), or the staminodial nectar scales in the Loasaceae (Weigend *et al.*, 2004; Weigend & Gottschling, 2006, e.g., *Nasa poissoniana*, Fig. 8.2 a-c; and *N. amaluzensis*, Fig. 8.2 d-f). Certainly the most prominent examples of unequal compartmentalisation are represented by trapping flowers, which are subdivided into a tube and an utricle (e.g. *Aristolochia*, Aristolochiaceae, Oelschlägel *et al.*, 2009 and *Ceropegia*, Apocynaceae, Ollerton *et al.*, 2009).

A 3D visualisation of the IFS as such provides a completely new perspective on pattern formation in floral form and function on micro- and macroevolutionary scales, independent from differences in floral organ composition. So far, there is only one example where visualisation of compartmentalised IFS has been used in an evolutionary study: The Hydrophyllaceae have scale-like modifications of the stamen-corolla tube (Jeiter & Weigend, 2018), which in some species enclose compartments (Chapter 6, Fig. 8.3). These compartments are of variable complexity and their conformation shows a phylogenetic signal (Fig. 8.3 a). In some species the IFS lacks compartmentalisation (Fig. 8.3 b, c), in others five basally interconnected compartments represent an imperfect revolver architecture (Fig. 8.3 d, e), or five separate compartments constitute a perfect revolver architecture (Fig. 8.3 f, g). These results are promising, and could be profitably employed to come to an in-depth understanding of complex floral conformations such as found in Geraniaceae (Jeiter *et al.*, 2017).

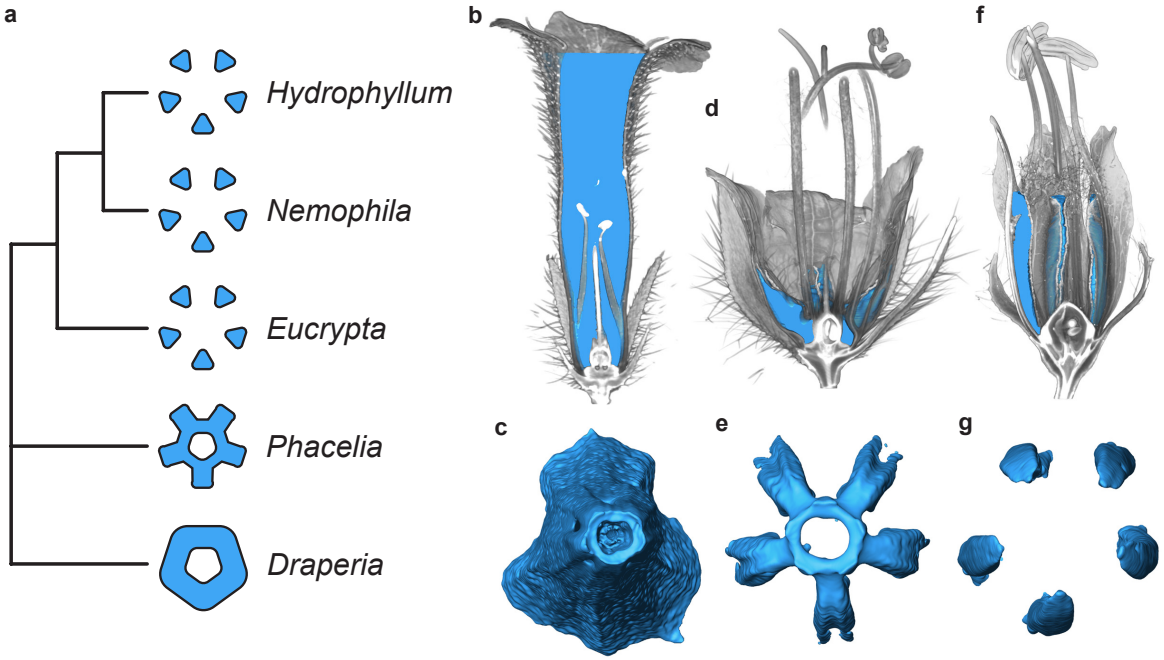

Figure 8.3: Evolution of IFS in the Hydrophyllaceae. a, reduced phylogeny of the five genera included in chapter 8. Resolved nodes have 100% Bootstrap support and 1.0 posterior probability in the Bayesian analysis. In *Draperia* separate compartments are absent and the whole flower encloses the IFS. *Phacelia* shows incomplete compartmentalisation with five basally interconnected compartments. *Hydrophyllum*, *Nemophila* and *Eucrypta* show complete compartmentalisation with five separate compartments. b, c, *Draperia systyla*. b, virtual cross-section through the 3D-flower model with the surface generated from the segmented IFS placed inside. c, isolated IFS surface viewed from below. d, e, *Phacelia egena*. d, virtual cross-section through the 3D-flower model with the surface generated from the segmented IFS placed inside. e, isolated IFS surface viewed from below. f, g, *Hydrophyllum virginianum*. f, virtual cross-section through the 3D-flower model with the surface generated from the segmented IFS placed inside. g, isolated IFS surface viewed from below.

Segmentation and visualisation of the IFS also helps to improve our understanding of flower-pollinator interactions. For successful pollen transfer, most flowers rely on a lock-key type of interaction (Minnaar *et al.*, 2019). This principle has been suggested for a variety of flower-pollinator interactions (e.g., Ollerton *et al.*, 2011; Newman *et al.*, 2015; Pauw *et al.*, 2009), however, so far relatively simple measurements of length or width for both pollinator and flower have been used to simplify these complex interactions and reduce them to one or two dimensions. Flower volume has only been used in two studies dealing with flower choice (Galen & Newport, 1987) and the correlation between flower and pollinator volume (Blionis & Vokou, 2001), respectively. In both studies, a simple geometrical proxy is used for flower (and pollinator) volume, grossly underrepresenting the complexity of the IFS. Both flowers and their pollinators are 3D objects and looking at actual shapes and spaces is a much

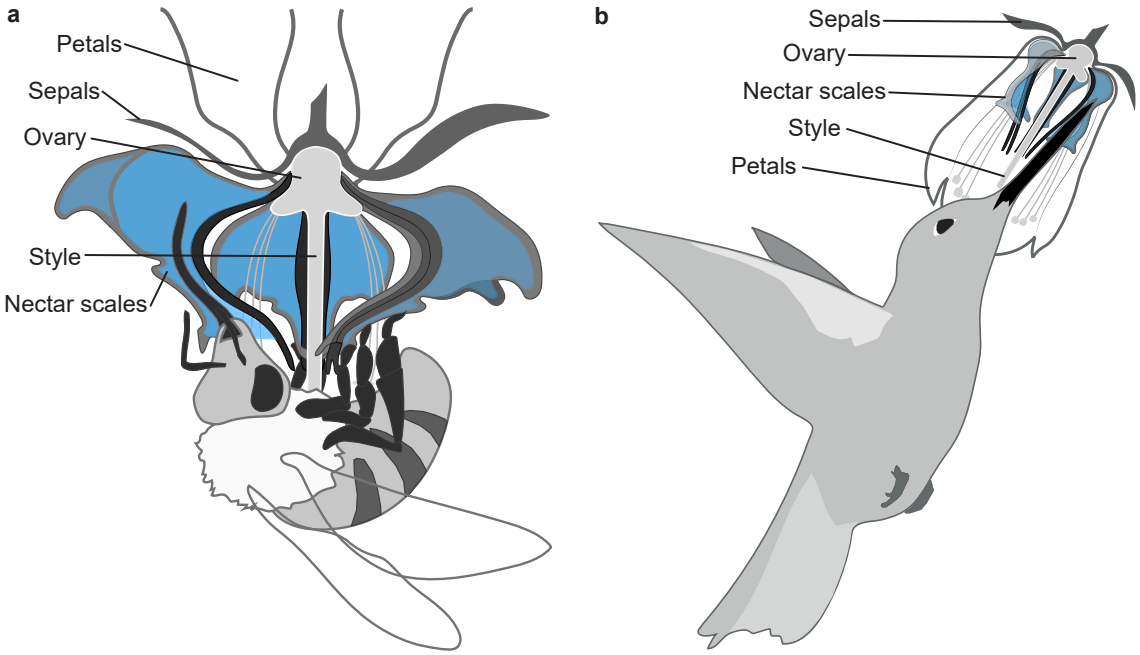

Figure 8.4: Illustration of interactions between pollinators and the IFS of two species of *Nasa* (Loasaceae). a, bee interacting with the nectar scale and the enclosed IFS of *Nasa poissoniana*. Note the reversible change in IFS shape during the interaction. b, hummingbird interacting with the nectar scale and the enclosed IFS of *Nasa amaluzensis*.

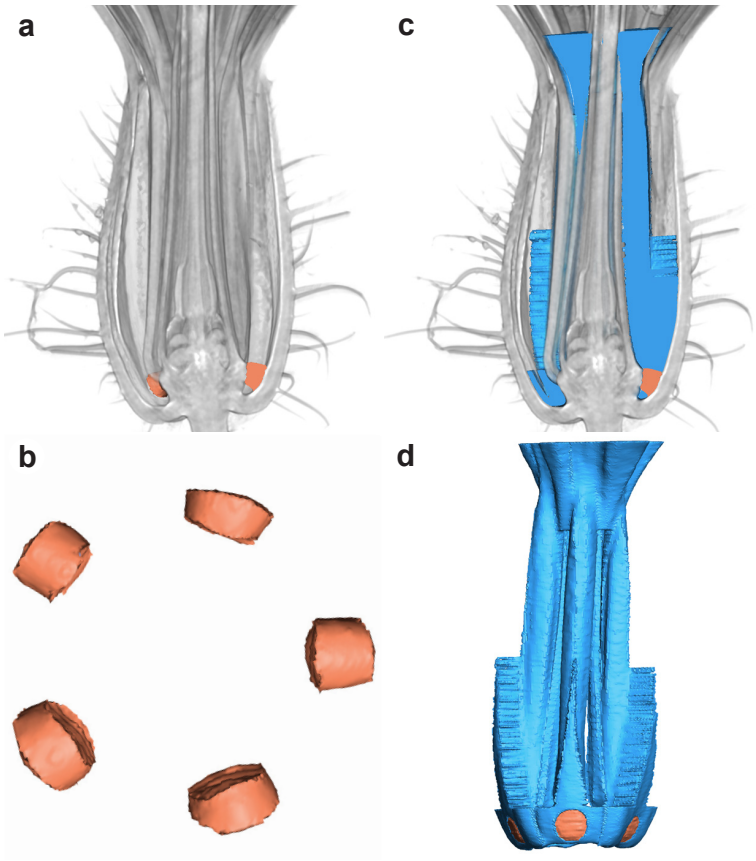

Figure 8.5: Nectar droplets in relation to the compartmentalised IFS in *Geranium robertianum* (Geraniaceae). a, segmented nectar droplets inside the three-dimensional flower model. b, surface of the nectar droplets. c, nectar in relation to the compartmentalised IFS. d, surface of the compartmentalised IFS and nectar.

more natural way of investigating interactions.

Published studies on the length or depth of flowers in relation to the amount of reward (nectar) offered found a clear correlation between those two traits (e.g., Johnson *et al.*, 2017; Tavares *et al.*, 2016). However, using segmented 3D IFS permits a direct comparison of the amount of reward offered to the IFS, e.g. in plant groups where shifts between pollinators have taken place. This is the case in the genus *Nasa* (Loasaceae), where several shifts from insect to bird pollination occurred (Weigend *et al.*, 2004; Weigend & Gottschling, 2006, Fig. 8.4). Preliminary results of bee-pollinated *N. poissoniana* and hummingbird-pollinated *N. amaluzensis* indicate that the amount of nectar and size of the IFS compartments are decoupled. While the volume per IFS-compartment is similar in both species (*N. poissoniana*: 12.89 mm^3/scale, N=1; *N. amaluzensis*: 11.23 mm^3/scale, N=1), the amount of nectar differs by more than a factor of three (*N. poissoniana*: 0.69 µl/scale, N=25; *N. amaluzensis*: 2.39 µl/scale, N=25; T. Joßberger, unpublished data). This underscores the multifunctionality of the floral scales enclosing these compartments, which are also believed to play a crucial role in pollinator attraction and in – hummingbird-pollinated flowers – physically guiding the pollinators to the nectar, which requires a disproportionate increase in size and volume (Weigend & Gottschling, 2006).

If fresh flowers are used for scanning, the localization of the nectar in the flower can be observed and visualized directly. Scans of a fresh flower of *G. robertianum* (Fig. 8.1 a) reveal five separate nectar droplets (Fig. 8.5) at the base of its five separate IFS-channels. Apart from the shape and position of the nectar droplets, this approach allows an accurate determination of the nectar volume, an option worth considering in flowers with very small nectar amounts. The aspect of nectar localization in relation to IFS configuration is a grossly understudied aspect of floral functional morphology. The previously cited study on the Hydrophyllaceae (Chapter 6) documented that spatial relationships may be complex (Chapter 6). Usually, nectar presentation and IFS configuration show a similar pattern, i.e. presence of separate compartments and reward partitioning, or no compartments and no reward partitioning. However, in *Phacelia*, flowers with near-identically shaped IFS either presented their nectar as five separate droplets accessible through the IFS, while others filled up all five basally interconnected compartments with nectar.

The selection of research topics mentioned above covers only a selection of the research areas that might benefit from the use of 3D segmentation and visualisation of IFS in the study of floral evolution and function. Overall or partial surface areas can be easily derived from the rendered surfaces and might be an important variable in, e.g., floral microbiology and nectar yeasts. With the constant improvements in imaging technology increasingly complex questions in flower form and function can be addressed, which previously eluded direct analysis (Ledford, 2018).

8.3 Material and methods

Plant material

Plant material was collected from cultivation at the Botanic Gardens of the University of Bonn. Voucher information is given below (Tab. 8.1).

Photography

Macro images were taken with a Nikon D3100 camera (Tokyo, Japan) equipped with a Sigma DG Macro 105 mm (Ronkonkoma, NY, US). Contrast and brightness of the images were adjusted using Photoshop CC 2015 and CC 2019 (Adobe, San Jose, CA, USA).

Table 8.1: Plant species used in this study. Vouchers are placed in the herbarium of the Nees-Institut für Biodiversität der Pflanzen (BONN), Rheinische Friedrich-Wilhelms-Universität, Bonn.

Species	Family	Order	IPEN-number
Geranium robertianum L.	Geraniaceae	Geraniales	DE-0-BONN-14522
Nasa amaluzensis (Weigend) Weigend	Loasaceae	Cornales	EC-0-BONN-39275
Nasa poissoniana (Urb. & Gilg) Weigend	Loasaceae	Cornales	PE-0-BONN-37093

Flower preparation

Flowers were fixed in formaldehyde-acetic acid-ethanol (4% formaldehyde, 4% acetic acid, 70% ethanol) for approximately one week. Followed by infiltration in 1% phosphotungstic acid dissolved in 70% ethanol for approximately two weeks. The infiltration medium was exchanged every second day. Infiltrated samples were dehydrated using an increasing ethanol series and finally 100% acetone. Each dehydration step contained 1% PTA. Dehydrated samples were critical point dried in a CPD 020 critical point dryer (Balzers Union, Liechtenstein).

Each dried flower was mounted on a round aluminium pole (6 mm in diameter, 30 mm long) using two-component epoxy resin adhesive (UHU plus Sofortfest, UHU GmbH & Co. KG, Bühl, Germany) (modified after Staedler *et al.*, 2013).

The fresh flower of *Geranium robertianum* was kept in a saturated water atmosphere and scanned within 30 min after collection. No liquid water was used to avoid diluting or disturbing the nectar inside the flower. For scanning it was put into a 5 ml pipet tip with moist absorbent cotton at the base. The tip was sealed with PARAFILM® M (Bemis Company, Inc, Neenah, WI, US).

Micro-computed tomography

Scans were conducted in a SkyScan 1272 (Bruker Co, Billerica, MA, US) with a Hamamatsu L11871 20 source (Hamamatsu, Japan) and a Ximea xiRAY16 camera (Ximea GmbH, Münster, Germany). Scan settings are shown in table 8.2.

Table 8.2: Scan settings used for the samples in the SkyScan 1272 µCT.

Species	Object to source [mm]	Camera to source [mm]	Source voltage [kV]	Source current [µA]	Image pixel size [µm]	Rotation	Rotation steps	Camera binning	Exposure [ms]	Number of images
Geranium robertianum (dried)	59	174.64	45	165	5	360°	0.2°	2 x 2	444	1800
Geranium robertianum (fresh)	94.4	174.64	45	165	16	193.2°	0.6°	4 x 4	254	322
Nasa amaluzensis	136.61	224.64	50	200	9	360°	0.2°	2 x 2	569	1800
Nasa poissoniana	82.6	174.64	50	200	7	360°	0.2°	2 x 2	305	1800

Three-dimensional visualisation

Scans were reconstructed using InstaRecon Engine v2 (InstaRecon, Champaign, IL, US). Down sampling of high resolution 16-bit reconstructed slice and adjusting of slice orientation, contrast and brightness was done in Fiji (ImageJ 1.52a distribution, National Institutes of Health, US). Samples were visualised in AMIRA 5.3.0 and 6.5.0 (FEI, France), where also segmentation of the functional floral spaces, and surface rendering and processing were conducted. Segmentation was done manually in the segmentation module of AMIRA. Inner volumes were selected using either the magic wand tool set to background grey values (0 – 30 in 8 bit or 0 – 4000 in 16 bit) or labelling the sections through floral organs and then using the magic wand tool exploiting the whole spectrum of the grey values. More complex inner volumes were segmented using the brush tool in combination with the latter segmentation method, as this was faster and more precise in these cases.

From the created labels, surfaces were generated using the AMIRA 'Surface Generation' function with smoothing set to constrained and the option 'compactify' selected. Both options had only minor effects on the quality of the surfaces generated, but noticeably increased computational speed and final appearance. The function 'Surface Area' allowed to calculate the area and the volume of the generated surface. In combination with the pixel size the inner volume was calculated.

8.4 Acknowledgements

The material used in this study was kindly provided by the Botanical Gardens of the University of Bonn. We thank T. Joßberger for providing the nectar measurement data. We are grateful for the drawings in figure 4 by S. Langecker. The drawing of the hummingbird was based on a field observation of R. Acuña, whom we also thank for insight in the biology of the genus *Nasa*. We thank T. Joßberger for providing nectar data of the *Nasa* species. We like to thank F. Luebert for valuable input on the idea of this paper. Funding for the µCT used in this study was provided by the Deutsche Forschungsgemeinschaft (INST 217/849-1 FUGG). JJ received a scholarship from the Studienstiftung des deutschen Volkes.

8.5 References

Blionis, G.J. & Vokou, D. (2001) Pollination ecology of *Campanula* species on Mt Olympos, Greece. *Ecography* **24**, 287–297.

Endress, P.K. (2010) Synorganisation without organ fusion in the flowers of *Geranium robertianum* (Geraniaceae) and its not so trivial obdiplostemony. *Annals of Botany* **106**, 687–695.

Galen, C. & Newport, M.E.A. (1987) Bumble bee behavior and selection on flower size in the sky pilot, *Polemonium viscosum*. *Oecologia* **74**, 20–23.

Jeiter, J., Danisch, F. & Hilger, H.H. (2016) Polymery and nectary chambers in *Codon* (Codonaceae) – flower and fruit development in a small, capsule-bearing family of Boraginales. *Flora* **220**, 94–102.

Jeiter, J., Hilger, H.H., Smets, E.F. & Weigend, M. (2017) The relationship between nectaries and floral architecture: A case study in Geraniaceae and Hypseocharitaceae. *Annals of Botany* **120**, 791–803.

Jeiter, J. & Weigend, M. (2018) Simple scales make complex compartments – ontogeny and morphology of stamen-corolla tube modifications in Hydrophyllaceae (Boraginales). *Biological Journal of the Linnean Society* **125**, 802–820.

Johnson, S.D., Moré, M., Amorim, F.W., Haber, W.A., Frankie, G.W., Stanley, D.A., Cocucci, A.A. & Raguso, R.A. (2017) The long and the short of it: A global analysis of hawkmoth pollination niches and interaction networks. *Functional Ecology* **31**, 101–115.

Ledford, H. (2018) The lost art of looking at plants. *Nature* **553**, 396–398.

Minnaar, C., Anderson, B., de Jager, M.L. & Karron, J.D. (2019) Plant–pollinator interactions along the pathway to paternity. *Annals of Botany* **123**, 225–245.

Newman, E., Manning, J. & Anderson, B. (2015) Local adaptation: Mechanical fit between floral ecotypes of *Nerine humilis* (Amaryllidaceae) and pollinator communities. *Evolution* **69**, 2262–2275.

Oelschlägel, B., Gorb, S., Wanke, S. & Neinhuis, C. (2009) Structure and biomechanics of trapping flower trichomes and their role in the pollination biology of *Aristolochia* plants (Aristolochiaceae). *New Phytologist* **184**, 988–1002.

Ollerton, J., Masinde, S., Meve, U., Picker, M. & Whittington, A. (2009) Fly pollination in *Ceropegia* (Apocynaceae: Asclepiadoideae): Biogeographic and phylogenetic perspectives. *Annals of Botany* **103**, 1501–1514.

Ollerton, J., Winfree, R. & Tarrant, S. (2011) How many flowering plants are pollinated by animals? *Oikos* **120**, 321–326.

Pauw, A., Stofberg, J. & Waterman, R.J. (2009) Flies and flowers in Darwin's race. *Evolution* **63**, 268–279.

Staedler, Y.M., Masson, D. & Schönenberger, J. (2013) Plant tissues in 3D via X-ray tomography: Simple contrasting methods allow high resolution imaging. *PLOS ONE* **8**, e75295.

Stuppy, W.H., Maisano, J.A., Colbert, M.W., Rudall, P.J. & Rowe, T.B. (2003) Three-dimensional analysis of plant structure using high-resolution X-ray computed tomography. *Trends in Plant Science* **8**, 2–6.

Tavares, D.C., Freitas, L. & Gaglianone, M.C. (2016) Nectar volume is positively correlated with flower size in hummingbird-visited flowers in the Brazilian Atlantic Forest. *Journal of Tropical Ecology* **32**, 335–339.

Tucker, S.C. & Hodges, S.A. (2005) Floral ontogeny of *Aquilegia*, *Semiaquilegia*, and *Enemion* (Ranunculaceae). *International Journal of Plant Sciences* **166**, 557–574.

Weigend, M. & Gottschling, M. (2006) Evolution of funnel-revolver flowers and ornithophily in *Nasa* (Loasaceae). *Plant Biology* **8**, 120–142.

Weigend, M., Gottschling, M., Hoot, S. & Ackermann, M. (2004) A preliminary phylogeny of Loasaceae subfam. Loasoideae (Angiospermae: Cornales) based on trnL(UAA) sequence data, with consequences for systematics and historical biogeography. *Organisms Diversity & Evolution* **4**, 73–90.

Chapter 9

General conclusions

9 General conclusions

The two major threads of this thesis are *i*) the interpretation of detailed morphological observations and descriptions in the context of recent phylogenetic studies, and *ii*) the integration of structures into floral architecture. The following discussion attempts to address these two aspects across the different papers presented in chapters 2, 3, 4, 5, 6, 7 and 8. The first aspect is treated in sections 1 and 4. Sections 2–6 deal with various aspects of flower evolution and floral architecture, and section 7 gives an overview of future research questions that arose from this work.

9.1 Floral structure in a phylogenetic context

In the last few decades, molecular phylogenies have changed our understanding of angiosperm systematics which was primarily based on morphological, anatomical, developmental and chemical characters (e.g., Cronquist, 1981; Takhtajan, 1997). The majority of studies were conducted by comparing these characters under the assumption of their homology to infer phylogenetic relations. This worked surprisingly well for some groups, but failed for others (e.g., compare Geraniales *sensu* Takhtajan, 1997 to the classification presented by Palazzesi *et al.*, 2012). With the growing importance of molecular phylogenies and their increasing availability, morphological and anatomical studies switched from formulating phylogenetic hypotheses to utilising molecular phylogenetic hypotheses to understand structural evolution.

In this thesis molecular phylogenies provide the basis for studies of floral structure in chapters 2, 4, 5, 6 and 7. In chapters 4, 5, 6 and 7 existing phylogenetic hypotheses are used to describe and understand the evolution of specific morphological characters and to formulate phylogeny-based hypotheses for structural evolution. Stamen-corolla tube modifications evolution and their integration into floral architecture were assessed on the basis of recent phylogenetic studies in Boraginaceae (chapter 4; Weigend *et al.*, 2009; Cohen, 2014; Chacón *et al.*, 2016) and Hydrophyllaceae (chapters 5 and 6; Walden *et al.*, 2014; Weigend *et al.*, 2014; Ferguson, 1999). In Hydrophyllaceae (chapter 5) an evolutionary series of stamen-corolla tube modification evolution was proposed. Similarly, an evolutionary series for floral architecture in Geraniaceae and Hypseocharitaceae was proposed on the basis of recent phylogenetic studies (chapter 7; Fiz *et al.*, 2006, 2008; Palazzesi *et al.*, 2012; Röschenbleck *et al.*, 2014; Marcussen & Meseguer, 2017).

The study of gynoecium and fruit development in *Heliotropium* sect. *Heliothamnus* (chapter 2) does not use a phylogeny to reconstruct the evolution of a morphological character. Instead, based on previously published phylogenetic hypotheses (Diane *et al.*, 2002; Luebert *et al.*, 2011) and resulting changes in our understanding of the evolution of gynoecium and fruit characters in the Boraginales (Weigend *et al.*, 2014), development and morphology were reassessed. The columella, a structure at the base of the style and the four mericarps of the boraginaceous gynoecium was proposed as present in *Heliotropium* sect. *Heliothamnus* (Hilger, 1992). Since homology between those structures (*sensu* Stevens, 1984; de Pinna, 1991; Scotland, 2011) was rejected *a priori*, this study investigated if the proposed columella in *Heliotropium* sect. *Heliothamnus* is actually present. The goal was to assess if this structure in *Heliotropium* sect. *Heliothamnus* and the columella of the Boraginaceae are structural correspondent, thus, convergent (*sensu* Scotland, 2011). The result of this study showed that the columella of the Boraginaceae and the newly reported 'disrupting tissue' of the fruits of *Heliotropium* sect. *Heliothamnus* are not structurally correspondent and therefore analogous structures. Chapter 2

is an example for challenging long-standing structural questions after recent molecular phylogenetic approaches changed the understanding of relations between taxonomic groups.

In general, structural studies placed in a phylogenetic context harbour great potential for our understanding of evolutionary processes and structural evolution. A major benefit of detailed structural studies as opposed to studies mining taxonomic (and structural) literature, is that the (re-)investigation of structural characters often highlights similarities or differences that have been overlooked previously. Simple literature mining introduces these imprecise or wrong observations into studies exploring structural evolution and underlying evolutionary mechanisms. Especially taxonomic studies often turn out to be unreliable sources of structural information, as these tend to focus on structural differences and not similarities and usually take only macroscopic observations of anthetic flowers and mature fruits into consideration. Additionally, herbarium specimens are often the major source of information and some structural characters and especially spatial integration is usually lost through the preservation process and cannot be considered.

Several examples of imprecise observations and descriptions were found in the course of this thesis: for example the presence of modifications in *Draperia systyla* (Hydrophyllaceae, chapter 5) and several new observations of faucal and basal scales in Boraginaceae flowers (chapter 4). *Draperia systyla* (Hydrophyllaceae) and *Rindera lanata* (Boraginaceae) are examples showing that the modifications are easily overlooked in the anthetic flower, although they are clearly visible during development and similar to the structures found in related species. Observations in the context of taxonomy and classification serve the purpose of distinguishing species, however, evolutionary studies try to identify underlying mechanisms and processes. In these types of studies, imprecise observations might lead to misleading conclusions of structural character evolution in particular and underlying evolutionary mechanisms and processes in general.

9.2 Floral nectaries

Floral nectaries are variable floral structures and probably best characterised as specialised, secretory tissues (Ronse De Craene, 2010). These tissues can arise in different positions in the flower. In many cases, they are an outgrowth of the receptacle or the gynoecium, or they are appendages of other basic floral organs or modifications of them (e.g., staminodes or carpelodes). Several classifications of floral nectaries have been proposed. Vogel (1977) distinguished between three types of nectaries based on their anatomy: mesenchymatic, ephithelial and trichomatous nectaries. This classification emphasises superficial anatomical similarities and does not take into account convergent evolution of identical types. Thus, this descriptive classification is of limited use for understanding underlying evolutionary processes. Most commonly nectaries are assigned to the organs to which they are spatially related (e.g., gynoecial nectary, sepal nectary, staminodial nectary; summarised in Nicolson *et al.*, 2007). Smets (1986, 1988) and Smets & Cresens (1988) proposed a classification with two basic categories: nectaries on falling floral organs (*nectaria caduca*) and nectaries on persisting floral parts (*nectaria persistentia).* Two subtypes can be distinguished for the nectaries on persisting floral parts: *i*) nectaries formed by sepals, gynoecium and the receptacle, and *ii*) septal nectaries. This approach of classification allowed for a direct comparison of nectaries and was a first attempt to explain nectary evolution across angiosperms (Smets, 1986).

In some plant taxa floral nectaries are quite variable in shape, size and position within the flower (e.g., Saxifragales, Nicolson *et al.*, 2007), while for several – especially larger – taxonomic groups

certain types of nectaries are predominant (e.g., septal nectaries in monocots, Smets *et al.*, 2000; Rudall, 2002, gynoecial nectaries in the asterids, Nicolson *et al.*, 2007, or receptacular nectaries in the Geraniales, Jeiter *et al.*, 2017). Floral nectaries are one of the main sources of floral reward and essential in mediating flower-pollinator interaction and thus their integration is an important part of floral architecture.

Floral nectaries have been studied in this thesis in chapters 2, 3, 4, 5 and 7. Boraginales (chapters 2, 3, 4 and 5) have a variably shaped gynoecial disc nectary at the base of the ovary. In *Heliotropium* sect. *Heliothamnus* (chapter 2), Codonaceae (chapter 3), and Boraginaceae (chapter 4) the nectary disc is rather simple, either round or slightly lobed with nectarostomata distributed more or less evenly. In Hydrophyllaceae the nectary disc is similar, however, nectar is not secreted from the entire disc surface, but from highly localised patches of nectarostomata ('glands') located at the apices of the nectary disc lobes in antepetalous position. Nectary development in the Boraginales has been studied in *Heliotropium* sect. *Heliothamnus* (chapter 2) and *Codon* (chapter 3). Their development is similar. Nectaries arise late in floral ontogeny. With the onset of nectary development, the first nectarostomata appear on the surface. Nectarostomata development continues until anthesis.

The morphology and development of nectaries in Geraniaceae and Hypseocharitaceae were studied in chapter 7. The nectaries are receptacular. In contrast to gynoecial nectaries, receptacular nectaries are usually extrastaminal. Nectar is secreted through nectarostomata. The onset of nectary development occurs in late stages of floral ontogeny. The nature of the nectaries of the Geraniales has been subject to debate. Many authors proposed a staminodial origin of the nectary glands (e.g., Lefor, 1975; Steyn *et al.*, 1987). However, there are numerous studies suggesting a receptacular origin of the nectary glands in various Geraniales families (e.g., Ronse Decraene & Smets, 1999; Ronse Decraene *et al.*, 2001; Endress, 2010; Jeiter *et al.*, 2017), which is confirmed in the current study.

There is only little variation in nectary morphology within Geraniaceae and Hypseocharitaceae, and within Boraginales, however, the architecture of the flower, in which the nectaries are integrated, shows more plasticity. This aspect will be addressed in the following sections.

9.3 Modifications of floral organs

A major focus of this work is on modifications of the corolla and the stamen-corolla tube, respectively. These modifications can be found in various angiosperm taxa. A detailed review of modifications ('elaborate petals', including modifications of the stamen-corolla tube) is presented by Endress & Matthews (2006). Apart from this overview, detailed studies of modifications are scarce and modifications are often treated only briefly in the context of general floral ontogeny (e.g., *Phacelia*, Hydrophyllaceae, Boraginales, Hofmann, 1999). Examples of detailed studies on modifications can be found for Boraginceae (Arber, 1939; Schaefer, 1942), Apocynaceae (Kunze, 2005) and *Spermacoce* (Rubiaceae, Vaes *et al.*, 2006; Vrijdaghs *et al.*, 2015). Not only is the understanding of the structure of modifications limited, but also descriptions of their function are often anecdotal. One of the few exceptions is an experimental study of staminal scales in flowers of drought-adapted Zygophyllaceae, where the modifications have been found to reduce water evaporation from the nectar held by the flower (Naghiloo *et al.*, 2018).

Modifications of the corolla and the stamen-corolla tube have been studied in chapters 3, 4 and 5 in the Boraginales and they are described for *Geranium maderense* in chapter 7. Stamen-corolla tube modifications of the Boraginales and their evolution will be discussed in section 4.

In Geraniaceae modifications can be found on the petals of species belonging to *Geranium* subgen. *Robertium*. The modifications are elongate ridges on the lower parts of the petals, which – depending in overall corolla shape – are either shallow (e.g., *Geranium robertianum*, Endress, 2010), or arise from short septa (*Geranium maderense*, chapter 7). The modifications are rather simple. However, in combination with an obdiplostemonous androecium, they contribute to a specific type of floral architecture, as will be discussed later.

9.4 Evolution of the stamen-corolla tube modifications in Boraginales

Stamen-corolla tube modifications of Boraginales have been studied in chapters 3, 4 and 5. Each chapter deals with one of the eleven families of Boraginales following the classification by Luebert *et al.* (2016). Morphology and development of stamen-corolla tube modifications are studied in Codonaceae (chapter 3), Boraginaceae (chapter 4), and Hydrophyllaceae (chapter 5). At first sight, the morphology of the modifications appears to be rather different among the three families. Apically broadened septa below the filament bases are present in Codonaceae. In the Boraginaceae two different types of modifications can be found: faucal scales, usually five invaginations of the apical part of corolla tube, and basal scales, usually ten protuberances of the basal part of the corolla tube. The ten basal scales can be fused into an annulus, reduced to five or completely reduced. In Hydrophyllaceae, there are usually ten elongate scales, connected at the bases of the filaments, diverse in appearance and synorganisation with neighbouring scales.

The developmental data presented in chapters 3, 4, and 5 shows similarities between the developing stamen-corolla tube modifications in those three families. The late onset of modification development indicates that they are peramorphoses. There is always a set of five antesepalous modifications inserted below the points of filament insertion. The modifications are usually broader than the filament bases. Faucal scales of Boraginaceae differ in morphology and development from the basal scales and the modifications found in the other two families. Their uniqueness indicates that they are apomorphies of the Boraginaceae and therefore not considered in the discussion of the evolution of stamen-corolla tube modifications in Boraginales.

Modifications of the stamen-corolla tube have been reported for other families of Boraginales (Fig. 9.1). In Boraginales I, four scales on the basal part of the corolla tube have been described in monogeneric Wellstediaceae. Detailed morphological observations of these scales are wanting, however, the illustrations and descriptions available (Hunt, 1969; Hunt & Lebrun, 1975; Thulin & Johansson, 1996; Hilger & Weigend, 2016) indicate a certain similarity with the basal scales found in Boraginaceae.

Within Boraginales II, modifications of the stamen-corolla tube have been described and used for taxonomy and classification in the Namaceae (Hitchcock, 1933b,a; Di Fulvio *et al.*, 1997; Hofmann *et al.*, 2016), but detailed observations are lacking. Other families of Boraginales II seem to lack any comparable modifications of the stamen-corolla tube with some notable exceptions: modifications of the apical part of the corolla tube are found in some Heliotropiaceae species (e.g., *Euploca pottii*, de Melo & Semir, 2010; *Heliotropium hirsutissimum*, *H. arbainense*, Diane *et al.*, 2016). Observations of trichome tufts, bulges and small scales at and below the points where the filaments are inserted have been made for some *Cordia* (Cordiaceae, Gottschling *et al.*, 2016), and *Bourreria* and *Tiquilia* species (Ehretiaceae, Gottschling, 2004; Gottschling *et al.*, 2014, 2016), respectively.

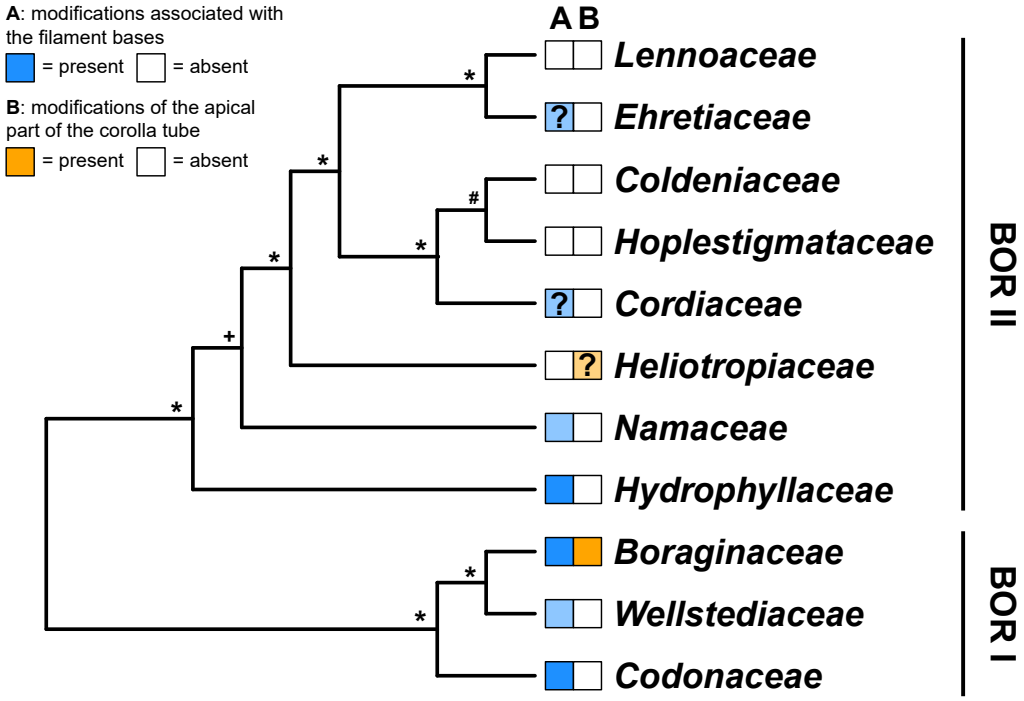

Figure 9.1: Overview of the main types of stamen-corolla tube modifications found in the Boraginales. The phylogenetic tree and familial classification is based on Luebert *et al.* (2016). It is a combination of three recent phylogenetic studies on the order (Weigend *et al.*, 2014; Refulio-Rodriguez & Olmstead, 2014; Stull *et al.*, 2015). Asterisks (*) indicate supported nodes (Bayesian posterior probability > 0.95, maximum likelihood bootstrap values > 80. Plus (+) indicates a node with high support only in the studies by Refulio-Rodriguez & Olmstead (2014) and Stull *et al.* (2015). The node indicated with hash (#) is moderately supported (Bayesian posterior probability = 0.9, maximum likelihood bootstrap value = 60). Boxes with lighter colours indicate that stamen-corolla tube modifications have been reported, but no detailed study has been conducted. Boxes with question marks indicate an even more limited knowledge about the reported modifications. BOR I = Boraginales I; BOR II = Boraginales II.

The distribution of stamen-corolla tube modifications on the phylogeny of Boraginales and the morphological and developmental similarities of the modifications studied in chapters 3, 4 and 5 suggest their homology. In the following, an evolutionary series for stamen-corolla tube modifications will be proposed (Fig. 9.2). In the reconstruction of the evolution of stamen-corolla tube modifications in Boraginales, two issues remain: *i*) the phylogeny is not fully resolved and there are incongruities between nuclear and plastid markers and *ii*) it remains uncertain which taxon is sister to the Boraginales. The first issue results in problems in the reconstruction of the evolution of scales especially within Boraginales II, where the relationships between and within Hydrophyllaceae, Namaceae and the remaining Boraginales II families are not fully resolved (Ferguson, 1999; Taylor, 2012; Walden *et al.*, 2014; Weigend *et al.*, 2014; Refulio-Rodriguez & Olmstead, 2014; Stull *et al.*, 2015; Luebert *et al.*, 2016). The second issue affects the reconstruction of the directionality of evolution of stamen-corolla tube modifications. Did the most recent common ancestor of the Boraginales have complex modifications, which were variously modified and reduced in the separate lineages, or were they simple and evolved to more complex modifications before they were reduced in several lineages? These questions cannot be addressed without extensive morphological and phylogenetic studies within the Boraginales and the lamiid-clade of the angiosperms. This study proposes a potential evolutionary series taking into account the various independent simplifications and complete reductions of stamen-corolla tube modifications in several lineages of the Boraginales, assuming evolution can be explained by parsimony.

Assuming the most recent common ancestor of the Boraginales had elongated bulges below the insertion points of the filaments and two appendages per bulge protruding onto the apical part of the corolla tube (Fig. 9.2, node A), the reduction of the appendages (Fig. 9.2, i) resulted in the most recent common ancestor of Boraginales I (Fig. 9.2, node B). Further elongation of the basal part of the corolla tube and their radial elongation coupled with a shift of the filaments towards the centre of the flower (Fig. 9.2, ii) resulted in the modifications observed in Codonaceae. Decoupling of the modifications from the filament bases and a reduction of the basal bulges (Fig. 9.2, iii) resulted in the most recent common ancestor of Wellstediaceae and Boraginaceae (Fig. 9.2, node C). Further broadening of the modifications (Fig. 9.2, iv) led to the morphology reported for Wellstediaceae (Hunt, 1969; Hunt & Lebrun, 1975; Thulin & Johansson, 1996; Hilger & Weigend, 2016). The shift of the modifications to the base of the basal part of the corolla tube and a second set of basal scales in antepetalous position led to the morphology observed Boraginaceae (Fig. 9.2, v). Within Boraginaceae, modifications are sometimes fused to an annulus, reduced to five scales or completely reduced.

In Boraginales II, the appendages protruding from the bulging below the point of filament insertion onto the apical part of the corolla tube were further promoted (Fig. 9.2, vi) resulting in the most recent common ancestor of Boraginales II (Fig. 9.2, node D). Further reduction of the modifications below filament insertion and the promotion of the two appendages per filament (Fig. 9.2, vii) led to the morphology of the most recent common ancestor of the Hydrophyllaceae. Within Hydrophyllaceae, reduction of the basal part of the corolla tube and successive elongation of the appendages happened in the *Hydrophyllum*-clade, while in *Phacelia*, the bulge on the basal part of the corolla tube was mostly reduced. In *Draperia*, the modifications are mostly reduced and restricted to the basal part of the corolla tube. Reduction of the appendages protruding onto the apical part of the corolla tube (Fig. 9.2, viii) resulted in the morphology of the most recent common ancestor of Namaceae and the remaining families of the Boraginales II (Fig. 9.2, node E). The full diversity of stamen-corolla tube modifications in Namaceae is poorly known. Various types of winged bulges below the points of filament insertion have been described (Hitchcock, 1933b,a; Di Fulvio *et al.*, 1997), indicating that such winged bulges might have been present in the most recent common ancestor of the Namaceae (Fig. 9.2, ix).

As shown above, there are reports of bulged and even winged filament bases in a number of genera in Boraginales II. However, they are scattered across the phylogeny. The most parsimonious explanation for this pattern might be a complete reduction of stamen-corolla tube modifications (Fig. 9.2, x) and independent regains in those genera. Further research on that topic is needed to fully understand and reconstruct the evolution of stamen-corolla tube modifications in Boraginales.

One aspect that shall only briefly be mentioned in this thesis are the changes in the proportions of the three parts of the stamen-corolla tube (basal and apical part and corolla lobes). Similar observations have been made in the Swertiinae (Gentianaceae, Gentianales, von Hagen & Kadereit, 2002), where the change in proportions was not unidirectional but shifted repeatedly within the Swertiinae-clade. Similar assumptions can be made for Boraginales, especially since tube length and proportions are rather variable, even between closely related species for instance within Boraginaceae (chapter 4). Since the length of the modifications especially in the Hydrophyllaceae has been found to correlate to corolla tube length, this character should not be overemphasised considering its assumed plasticity.

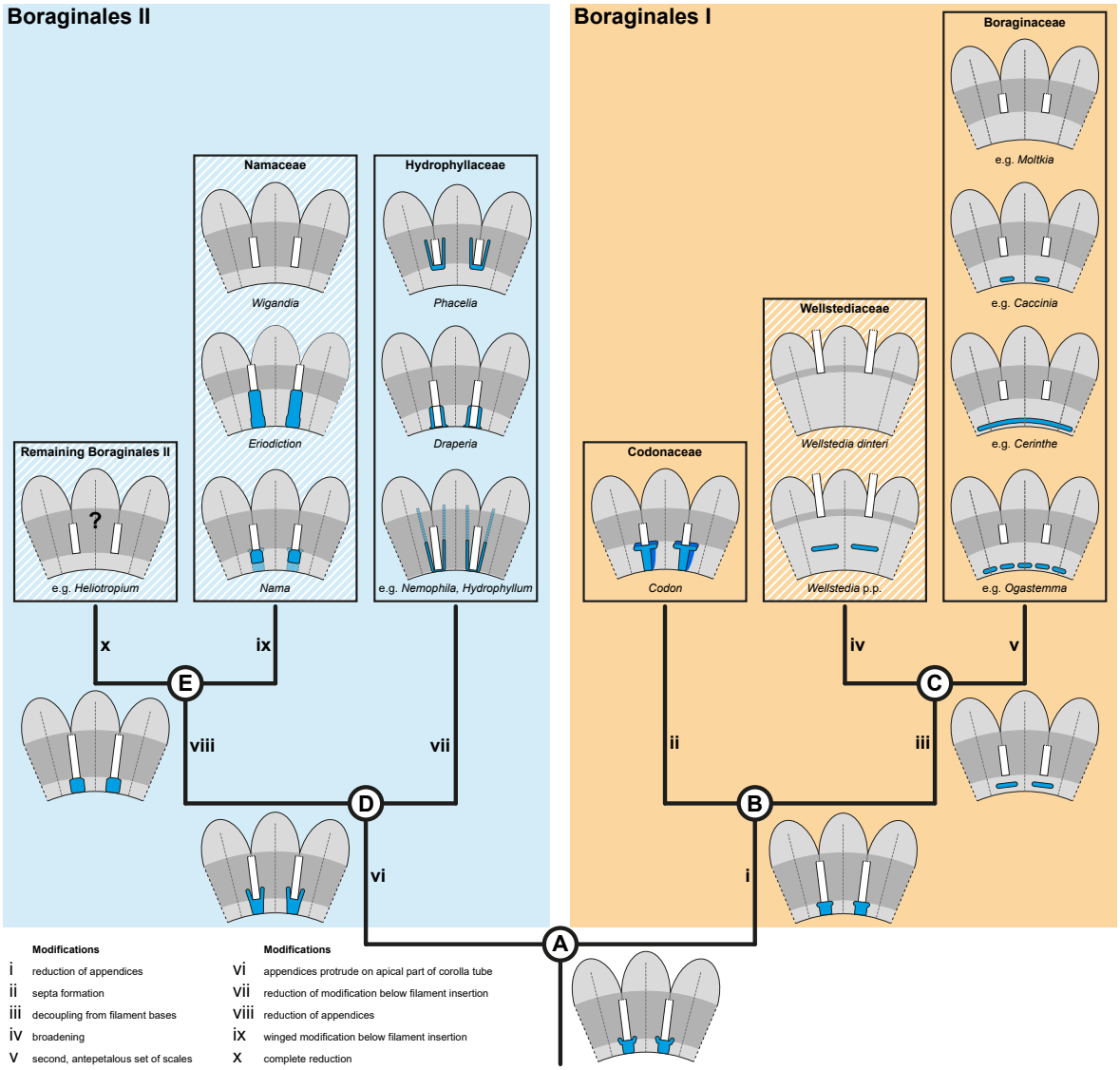

Figure 9.2: Evolutionary series of stamen-corolla tube modifications associated with the filaments on the basal part of the corolla tube. The phylogenetic reconstruction is based on Weigend *et al.* (2014), Refulio-Rodriguez & Olmstead (2014) and Stull *et al.* (2015). Node A, last common ancestor of all Boraginales. Node B, last common ancestor of all Boraginales I. Node C, last common ancestor of Wellstediaceae and Boraginaceae. Node D, last common ancestor of all Boraginales II. Node E, last common ancestor of the Namaceae and the remaining Boraginales II. Modifications (blue), filament bases (white), basal part of the corolla tube and corolla lobes (light grey), apical part of the corolla tube (dark grey). Dashed grey lines show the positions of the petal vascular bundles. White shaded boxes indicate families with limited information on stamen-corolla tube modification morphology and development and most information is taken from the literature. Please refer to the text for additional information.

9.5 Floral architecture, modifications and nectaries

Modifications of basal floral organs and nectaries are of particular importance in floral architecture and function. It should be noted that floral architecture does not only depend on specialised structures, such as nectaries and modifications, but also on the interplay of all floral organs. The reason why modifications and nectaries are in the focus of this thesis, is that these structures are commonly overlooked and often neglected in the context of morphological and/or ontogenetic studies.

Within Geraniaceae and Hypseocharitaceae (chapter 7), modifications only play a role in floral architecture in *Geranium* subgen. *Robertium*. In these cases, elongated ridges on the petal bases lead

to the formation of separate compartments, each with a nectary gland at the base. In all investigated species, obdiplostemony in combination with stamen triplets were involved in the formation of guide rails towards the nectary glands. Only *Pelargonium* differs noticeably in floral organisation and floral architecture: four of the five glands are reduced and the remaining gland is hidden inside a receptacular cavity, which is the result of the formation of a secondary meristem below all floral organs except the remaining gland. The formation of an anthophore as a results of similar activity in the receptacle was observed in other species of Geraniaceae and Hypseocharitaceae. In combination with trichomes on the petal bases and an anthophore lifting gynoecium, androecium, nectary glands and corolla, variable types of revolver architecture were described (chapter 7). Revolver architecture is the formation of separate compartments in actinomorphic flowers (Endress 1994). As shown for Geraniaceae and Hypseocharitaceae, this type of floral architecture can either be strict (i.e. complete separation of compartments by structures such as septa or scales) or relatively lax (i.e. incomplete separation of compartments without completely separating structures).

Revolver architecture in Boraginales was described for *Codon* (chapter 3) and Hydrophyllaceae (chapters 5 and 6). The modifications and septa in *Codon* are pressed against the ovary, forming separate compartments. Each compartment encloses a lobe of the nectary disc. Similarly, in the *Hydrophyllum*-clade of Hydrophyllaceae, two neighbouring modifications form separate compartments with each pair enclosing one nectary gland. In *Phacelia*, despite the formation of five separate access points, all channels converge into a common volume around the ovary and above the nectary disc. The nectary disc is lobed and nectarostomata are highly localised on the tips of the lobes in antepetalous positions, where the access points are located as well. The exact configuration of stamen-corolla tube modifications, the size of the common basal volume and the amount of nectar produced result in lax revolver architecture in some *Phacelia* species, as shown through nectar removal experiments. This complex pattern of floral architecture in *Phacelia* is similar to the patterns observed in Geraniaceae and Hypseocharitaceae.

In Boraginaceae (chapter 4) no revolver architecture was observed. However, one of the most striking features of the Boraginaceae flowers are the faucal scales. Faucal scales influence floral architecture. They can narrow the entrance to the reward of the flower or contribute to the formation of anther cones. Their presence often has the effect of enclosing a compartment similar to the common basal volume observed in several *Phacelia*-species (chapter 6). The function of the basal scales in Boraginaceae, on the other hand, remains uncertain. In contrast to the modifications of the other Boraginales taxa studied (chapters 3, 5 and 6), the basal scales are deeply hidden inside the corolla tube and direct interaction between pollinators and these scales appear to be improbable. However, a common feature that all modifications share is their spatial relation to the nectary disc. In Boraginaceae they might function as an additional protective layer covering the nectary disc and the ovary protecting them from mechanical damage.

The function of revolver architecture as observed in *Codon* (chapter 3) and Hydrophyllaceae (chapters 5 and 6) is likely to be an adaptation to pollination. Each of the separate compartments holds part of the total reward of the flower. A pollinator collecting nectar has to probe each of the separate compartments (usually by rotating around the central axis) to get the full reward of the flower. This manipulation of the pollinators behaviour by the flower increases the time the pollinator stays on the flower. Pollinator visitation duration and pollination success have been found to be positively correlated (e.g., Manetas & Petropoulou, 2000).

Revolver architecture can be found in a number of taxa across the angiosperms (e.g., *Aquilegia*, Ranunculaceae, Tucker & Hodges, 2005; *Nasa*, Loasaceae, Weigend & Gottschling, 2006; *Geranium*

robertianum, Geraniaceae, Endress, 2010, asclepiads, Apocynaceae, Endress, 2016). The structures involved in revolver architecture formation are similarly diverse (e.g., nectar leaves in *Aquilegia*, nectar scales derived from staminodes in *Nasa* or modifications of the stamen-corolla tube in Boraginales; chapter 3, 5 and 6). Surprisingly few studies have looked at the functional consequences of the presence of revolver architecture (e.g., Endress, 1997; Weigend *et al.*, 2010). The present study contributes to a broader understanding of revolver architecture. Structurally separate compartments as in *Geranium* subgen. *Robertium*, *Codon* and the *Hydrophyllum*-clade of the Hydrophyllaceae are one way of creating revolver flowers. On the one hand, increased distance and other architectural constraints might have similar architectural consequences as structural separation. On the other hand, flowers which appear to have separate compartments, such as many *Phacelia* species, are in fact architecturally more variable. This variability depends on other factors, such as nectar volume and presumably nectar viscosity. In the following, compartmentalisation of the flower and resulting revolver architecture will be discussed.

9.6 Compartmentalisation, the internal floral space and 3D-visualisation

The studies on Geraniaceae (*Geranium* subgen. *Robertium*), Codonaceae, Boraginaceae and Hydrophyllaceae show how floral architecture results in the formation of spaces within flowers. The spaces are elaborated on in chapter 8. The entire air filled space enclosed by the flower is the internal floral space (IFS). As shown for flowers with revolver architecture, the IFS can be compartmentalised. Compartments can be differentiated in *i*) those involved in holding the reward of the flower (e.g., nectar), *ii*) those enclosed by structures guiding the pollinator towards the reward and *iii*) those without any apparent function, possibly the result of developmental constraints. Furthermore, compartments can be equal or unequal. The flowers of *Codon schenckii* have ten to twenty separate compartments, each holding part of the total reward of the flower. The entire IFS is made up by the separate compartments and all compartments are more or less identical in shape and function. An example of unequal compartments is *Geranium robertianum* (chapter 8). Five separate channels converge into a common space at the base of the flower, where the nectar is held as separate droplets. Aside from these functional spaces, there is a space around the gynoecium enclosed by the broadened filaments and five separate spaces formed between neighbouring petals and sepals. These spaces probably have no function and can be considered as an outcome of developmental constraints. Similarly, unequal compartments can be observed in several *Phacelia* species, where a single compartment is enclosed by the modifications and another compartment is located above the modifications. Although the latter compartment can be viewed as the outcome of developmental constraints, pollinators interact with them while collecting nectar, thus a function of these compartments cannot be ruled out.

The visualisation of IFS has not been conducted so far, although there are some hints towards the role of flower volume in ecological and evolutionary contexts. One study on bumble bee selection of *Polemonium* flowers found a negative correlation between flower volume and pollination success (Galen & Newport, 1987). Another study found a correlation between the flower volume in *Campanula* and the visiting pollinators body volume (Blionis & Vokou, 2001). Both studies used rough geometric approximation of flower volumes. A more accurate measurement of volumes is more difficult to obtain. Serial sections and 3D-reconstruction from those sections would be a possible approach to get a more precise understanding of the flower volume. However, this approach is size limited and prone to preparation artefacts. Recent advances in 3D-visualisation techniques (e.g., μCT, Stuppy *et al.*,

2003; summarised in Ledford, 2018) hold a comparatively easy way to visualise IFS and allow precise 3D-visualisations.

Internal floral spaces can be used in a variety of studies: *i*) They allow for an accurate volume measurement of the flower and its compartments, *ii*) the visualised IFS can be used as an additional set of morphological characters for comparative studies, and *iii*) they allow the visualisation of complex spatial relations which are difficult to reproduce without a 3D-approach.

Apart from the IFS approach formally introduced in chapter 8 and applied in chapter 6, 3D-visualisation of flowers has been used in chapter 4 to understand integration of the stamen-corolla tube modifications into floral architecture in Boraginaceae. Further, micro-computed tomography has been used for visualisation of the internal organisation of the gynoecium and fruit in *Heliotropium* sect. *Heliothamnus* (chapter 2) and for 3D-geometric morphometrics of Hydrophyllaceae in chapter 6. Micro-computed tomography and subsequent data processing produces 3D-models of the scanned objects. These models are accurate representations of the object and allow precise measurements and the application of other morphometric approaches such as 3D-landmarking. Through 3D-landmarking floral architecture can be quantified and the morphospace of the study group can be explored (van der Niet *et al.*, 2010). In Hydrophyllaceae (chapter 6) this approach was used to compare floral architecture and the integration of stamen-corolla tube modifications between the sampled species and to test for a phylogenetic signal in floral architecture configuration.

Since the first recommendation of the application of µCT in botany (Stuppy *et al.*, 2003), there is an increasing number of in studies applying µCT to address a variety of research questions (e.g., Milien *et al.*, 2012; Staedler *et al.*, 2013; Wason *et al.*, 2017; Chomicki *et al.*, 2018). New 3D-approaches including µCT have recently been highlighted as part of the 'botanical renaissance' (Ledford, 2018). However, 3D-approaches only deploy their full strength if combined with other 'classical' approaches, such as ontogenetic, anatomical and morphological studies in the context of a phylogenetic framework as shown in this thesis (chapter 2, 4, 6 and 8).

9.7 Future research in the context of this thesis

The evolution of stamen-corolla tube modifications in Boraginales is a field that requires additional studies. As pointed out in section 4, there are still considerable gaps in our understanding of flower development and morphology of Wellstediaceae and Namaceae. Additionally, several reported modifications in families of Boraginales II still need to be critically examined. Chapter 4 gives a first overview of stamen-corolla tube modifications in Boraginaceae, however, an improved sampling might allow for identification of phylogenetic patterns in development and morphology of modifications. Furthermore, a refined understanding of the phylogeny of Boraginales II in general and Hydrophyllaceae and Namaceae in particular is required regarding the topic of evolution of stamen-corolla tube modification in Boraginales.

The studies on the integration of stamen-corolla tube modifications and nectaries into floral architecture represent only a first step towards a functional understanding of these structures. Further morphometric studies combined with field observations of pollinator behaviour might help to understand how these structures function.

Another topic in Boraginales is fruit evolution. This has briefly been addressed in chapters 2 and 3. A highly interesting aspect about fruit evolution in Boraginales is that capsular fruits can be found

in the consecutive sister taxa of both Boraginales I (Wellstediaceae, Codonaceae) and Boraginales II (Namaceae, Hydrophyllaceae), while the remaining families either have four single-seeded nutlets or four-seeded drupes (with the derived, parasitic family Lennoaceae being the only exception; Weigend *et al.*, 2014; Bittrich, 2016; Luebert *et al.*, 2016) . Chapters 2 and 3 combine developmental, morphological and anatomical data to understand fruit formation in *Heliotropium* sect. *Heliothamnus*, sister to the remaining *Heliotropium* species (Diane *et al.*, 2002; Luebert *et al.*, 2011) and Codonaceae, sister to the rest of Boraginales I, respectively. Similar studies should be conducted in Wellstediaceae, Hydrophyllaceae and Namaceae as the accessible information on these three families is sparse.

Within the Geraniales, nectary evolution has been studied (chapter 7, Jeiter *et al.*, 2017). However, the evolution of integration of nectaries into floral architecture is an exciting topic. Especially, the species-rich genera *Geranium* and *Pelargonium* show a large variety in floral architectures on the basis of largely similar floral organisation. Floral architectural studies might benefit from the application of 3D-geometric morphometrics and the quantification of architectural traits.

Internal floral spaces are introduced in this study (chapter 8) and have so far only been applied in Hydrophyllaceae (chapter 6). Application of this approach in a wider taxonomic context and its use in volumetric, as well as morphological and functional studies should be brought forward in further studies.

This thesis shows the importance of a combination of different approaches, combining 'classical' with 3D-approaches, and analysis and discussion of the data produced by these approaches in the context of recent phylogenies. This multimethodological approach should be combined with ecological studies, which might harbour insights into evolutionary mechanisms that resulted in the diversity of flowers we can observe today.

9.8 References

Arber, A. (1939) Studies in flower structure: V. On the interpretation of the petal and 'corona' in *Lychnis*. *Annals of Botany* **3**, 337–346.

Bittrich, V. (2016) Lennoaceae. *Families and Genera of Vascular Plants* (eds. K. Kubitzki, J.W. Kadereit & V. Bittrich), vol. 14, pp. 257–261, Springer, Heidelberg.

Blionis, G.J. & Vokou, D. (2001) Pollination ecology of *Campanula* species on Mt Olympos, Greece. *Ecography* **24**, 287–297.

Chacón, J., Luebert, F., Hilger, H.H., Ovchinnikova, S., Selvi, F., Cecchi, L., Guilliams, C.M., Hasenstab-Lehman, K., Sutorý, K., Simpson, M.G. & Weigend, M. (2016) The borage family (Boraginaceae s.str.): A revised infrafamilial classification based on new phylogenetic evidence, with emphasis on the placement of some enigmatic genera. *Taxon* **65**, 523–546.

Chomicki, G., Staedler, Y.M., Bidel, L.P.R., Jay-Allemand, C., Schönenberger, J. & Renner, S.S. (2018) Deciphering the complex architecture of an herb using micro-computed X-ray tomography, with an illustrated discussion on architectural diversity of herbs. *Botanical Journal of the Linnean Society* **186**, 145–157.

Cohen, J.I. (2014) A phylogenetic analysis of morphological and molecular characters of Boraginaceae: Evolutionary relationships, taxonomy, and patterns of character evolution. *Cladistics* **30**, 139–169.

Cronquist, A. (1981) *An Integrated System of Classification of Flowering Plants*. Columbia University Press, New York.

de Melo, J.I.M. & Semir, J. (2010) Taxonomy of the genus *Euploca* Nutt. [Heliotropiaceae] in Brazil. *Acta Botanica Brasilica* **24**, 111–132.

de Pinna, M.G.G. (1991) Concepts and tests of homology in the cladistic paradigm. *Cladistics* **7**, 367–394.

Di Fulvio, T.E., Cosa, M.T. & Dottori, N. (1997) Morfologia y vascularizacion floral en *Turricula*, *Eriodictyon* y *Wigandia* (Phacelieae; Hydrophyllaceae) con relacion a la taxonomia. *Kurtziana* **25**, 47–66.

Diane, N., Förther, H. & Hilger, H.H. (2002) A systematic analysis of *Heliotropium*, *Tournefortia*, and allied taxa of the Heliotropiaceae (Boraginales) based on ITS1 sequences and morphological data. *American Journal of Botany* **89**, 287–295.

Diane, N., Hilger, H.H., Förther, H., Weigend, M. & Luebert, F. (2016) Heliotropiaceae. *Families and Genera of Vascular Plants* (eds. K. Kubitzki, J.W. Kadereit & V. Bittrich), vol. 14, pp. 203–211, Springer, Heidelberg.

Endress, P.K. (1997) Relationships between floral organization, architecture, and pollination mode in *Dillenia* (Dilleniaceae). *Plant Systematics and Evolution* **206**, 99–118.

Endress, P.K. (2010) Synorganisation without organ fusion in the flowers of *Geranium robertianum* (Geraniaceae) and its not so trivial obdiplostemony. *Annals of Botany* **106**, 687–695.

Endress, P.K. (2016) Development and evolution of extreme synorganization in angiosperm flowers and diversity: A comparison of Apocynaceae and Orchidaceae. *Annals of Botany* **117**, 749–767.

Endress, P.K. & Matthews, M.L. (2006) Elaborate petals and staminodes in eudicots: Diversity, function, and evolution. *Organisms Diversity & Evolution* **6**, 257–293.

Ferguson, D.M. (1999) Phylogenetic analysis and relationships in Hydrophyllaceae based on ndhF sequence data. *Systematic Botany* **23**, 253–268.

Fiz, O., Vargas, P., Alarcón, M., Aedo, C., Garcia, J.L. & Aldasoro, J.J. (2008) Phylogeny and historical biogeography of Geraniaceae in relation to climate changes and pollination ecology. *Systematic Botany* **33**, 326–342.

Fiz, O., Vargas, P., Alarcón, M. & Aldasoro, J.J. (2006) Phylogenetic relationships and evolution in *Erodium* (Geraniaceae) based on trnL-trnF sequences. *Systematic Botany* **31**, 739–763.

Galen, C. & Newport, M.E.A. (1987) Bumble bee behavior and selection on flower size in the sky pilot, *Polemonium viscosum*. *Oecologia* **74**, 20–23.

Gottschling, M. (2004) Floral ontogeny in *Bourreria* (Ehretiaceae, Boraginales). *Flora* **199**, 409–423.

Gottschling, M., Nagelmüller, S. & Hilger, H.H. (2014) Generative ontogeny in *Tiquilia* (Ehretiaceae: Boraginales) and phylogenetic implications. *Biological Journal of the Linnean Society* **112**, 520–534.

Gottschling, M., Weigend, M. & Hilger, H.H. (2016) Ehretiaceae. *Families and Genera of Vascular Plants* (eds. K. Kubitzki, J.W. Kadereit & V. Bittrich), vol. 14, pp. 165–178, Springer, Heidelberg.

Hilger, H.H. (1992) Morphology of *Heliotropium* (Boraginaceae) dispersal units. *Botanica Acta* **105**, 387–393.

Hilger, H.H. & Weigend, M. (2016) Wellstediaceae. *Families and Genera of Vascular Plants* (eds. K. Kubitzki, J.W. Kadereit & V. Bittrich), vol. 14, pp. 403–406, Springer, Heidelberg.

Hitchcock, C.L. (1933a) A taxonomic study of the genus *Nama*. I. *American Journal of Botany* **20**, 415–430.

Hitchcock, C.L. (1933b) A taxonomic study of the genus *Nama*. II. *American Journal of Botany* **20**, 518–534.

Hofmann, M. (1999) Flower and fruit development in the genus *Phacelia* (Phacelieae, Hydrophyllaceae): Characters of systematic value. *Systematics and Geography of Plants* **68**, 203–212.

Hofmann, M., Walden, G.K., Hilger, H.H. & Weigend, M. (2016) Hydrophyllaceae. *Families and Genera of Vascular Plants* (eds. K. Kubitzki, J.W. Kadereit & V. Bittrich), vol. 14, pp. 221–238, Springer, Heidelberg.

Hunt, D.R. (1969) *Wellstedia*. *Hooker´s Icones Plantarum* **37**, 3665–3667.

Hunt, D.R. & Lebrun, J.P. (1975) A new *Wellstedia* (Boraginaceae) from Ethiopia. *Kew Bulletin* **30**, 222–222.

Jeiter, J., Weigend, M. & Hilger, H.H. (2017) Geraniales flowers revisited: Evolutionary trends in floral nectaries. *Annals of Botany* **119**, 395–408.

Kunze, H. (2005) Morphology and evolution of the corolla and corona in the Apocynaceae s.l. *Botanische Jahrbücher für Systematik* **126**, 347–383.

Ledford, H. (2018) The lost art of looking at plants. *Nature* **553**, 396–398.

Lefor, M.W.M. (1975) A taxonomic revision of the Vivianiaceae. *University of Connecticut Occasional Papers, Biological Science Series* **2**, 225–255.

Luebert, F., Brokamp, G., Wen, J., Weigend, M. & Hilger, H.H. (2011) Phylogenetic relationships and morphological diversity in Neotropical *Heliotropium* (Heliotropiaceae). *Taxon* **60**, 663–680.

Luebert, F., Cecchi, L., Frohlich, M.W., Gottschling, M., Guilliams, C.M., Hasenstab-Lehman, K.E., Hilger, H.H., Miller, J.S., Mittelbach, M., Nazaire, M., Nepi, M., Nocentini, D., Ober, D., Olmstead, R.G., Selvi, F., Simpson, M.G., Sutorý, K., Valdés, B., Walden, G.K. & Weigend, M. (2016) Familial classification of the Boraginales. *Taxon* **65**, 502–522.

Manetas, Y. & Petropoulou, Y. (2000) Nectar amount, pollinator visit duration and pollination success in the mediterranean shrub *Cistus creticus*. *Annals of Botany* **86**, 815–820.

Marcussen, T. & Meseguer, A.S. (2017) Species-level phylogeny, fruit evolution and diversification history of *Geranium* (Geraniaceae). *Molecular Phylogenetics and Evolution* **110**, 134–149.

Milien, M., Renault-Spilmont, A.S., Cookson, S.J., Sarrazin, A. & Verdeil, J.L. (2012) Visualization of the 3D structure of the graft union of grapevine using X-ray tomography. *Scientia Horticulturae* **144**, 130–140.

Naghiloo, S., Bellstedt, D.U. & Claßen-Bockhoff, R. (2018) Nectar protection in arid-adapted flowers of Zygophyllaceae-Zygophylloideae. *Perspectives in Plant Ecology, Evolution and Systematics* **34**, 37–50.

Nicolson, S.W., Nepi, M. & Pacini, E. (eds.) (2007) *Nectaries and Nectar*. Springer, Dordrecht.

Palazzesi, L., Gottschling, M., Barreda, V. & Weigend, M. (2012) First Miocene fossils of Vivianiaceae shed new light on phylogeny, divergence times, and historical biogeography of Geraniales. *Biological Journal of the Linnean Society* **107**, 67–85.

Refulio-Rodriguez, N.F. & Olmstead, R.G. (2014) Phylogeny of Lamiidae. *American Journal of Botany* **101**, 287–299.

Ronse De Craene, L.P. (2010) *Floral Diagrams: An Aid to Understanding Flower Morphology and Evolution*. Cambridge University Press, Cambridge ; New York.

Ronse Decraene, L.P., Linder, H.P., Dlamini, T. & Smets, E.F. (2001) Evolution and development of floral diversity of Melianthaceae, an enigmatic southern African family. *International Journal of Plant Sciences* **162**, 59–82.

Ronse Decraene, L.P. & Smets, E.F. (1999) Similarities in floral ontogeny and anatomy between the genera *Francoa* (Francoaceae) and *Greyia* (Greyiaceae). *International Journal of Plant Sciences* **160**, 377–393.

Röschenbleck, J., Albers, F., Müller, K., Weinl, S. & Kudla, J. (2014) Phylogenetics, character evolution and a subgeneric revision of the genus *Pelargonium* (Geraniaceae). *Phytotaxa* **159**, 31–76.

Rudall, P. (2002) Homologies of inferior ovaries and septal nectaries in Monocotyledons. *International Journal of Plant Sciences* **163**, 261–276.

Schaefer, H. (1942) Die Hohlschuppen der Boraginaceen. *Botanische Jahrbücher für Systematik, Pflanzengeschichte und Pflanzengeographie* **72**, 304–346.

Scotland, R.W. (2011) What is parallelism? *Evolution & Development* **13**, 214–227.

Smets, E. & Cresens, E. (1988) Types of floral nectaries and the concepts 'character' and 'character-state' - a reconsideration. *Acta Botanica Neerlandica* **37**, 121–128.

Smets, E.F. (1986) Localization and systematic importance of the floral nectaries in the Magnoliatae (Dicotyledons). *Bulletin du Jardin botanique national de Belgique / Bulletin van de National Plantentuin van België* **56**, 51–76.

Smets, E.F. (1988) La présence des 'nectaria persistentia' chez les Magnoliophytina (Angiospermes). *Candollea* **43**, 709–716.

Smets, E.F., Ronse Decraene, L.F., Caris, P. & Rudall, P.J. (2000) Floral nectaries in Monocotyledons: Distribution and evolution. *Monocots: Systematics and Evolution* (eds. K.L. Wilson & D.A. Morrison), pp. 230–240, CSIRO, Melbourne, Australia.

Staedler, Y.M., Masson, D. & Schönenberger, J. (2013) Plant tissues in 3D via X-ray tomography: Simple contrasting methods allow high resolution imaging. *PLOS ONE* **8**, e75295.

Stevens, P.F. (1984) Homology and Phylogeny: Morphology and Systematics. *Systematic Botany* **9**, 395–409.

Steyn, E.M.A., Robbertse, P.J. & van Wyk, A.E. (1987) Floral development in *Greyia flanaganii* with notes on inflorescence initiation and sympodial branching. *South African Journal of Botany* **53**, 194–201.

Stull, G.W., de Stefano, R.D., Soltis, D.E. & Soltis, P.S. (2015) Resolving basal lamiid phylogeny and the circumscription of Icacinaceae with a plastome-scale data set. *American Journal of Botany* **102**, 1794–1813.

Stuppy, W.H., Maisano, J.A., Colbert, M.W., Rudall, P.J. & Rowe, T.B. (2003) Three-dimensional analysis of plant structure using high-resolution X-ray computed tomography. *Trends in Plant Science* **8**, 2–6.

Takhtajan, A.L. (1997) *Diversity and Classification of Flowering Plants*. Columbia University Press, New York.

Taylor, S.E. (2012) *Molecular Systematics and the Origins of Gypsophily in* Nama *L. (Boraginaceae)*. Thesis.

Thulin, M. & Johansson, N.B. (1996) Taxonomy and biogeography of the anomalous genus *Wellstedia*. *The Biodiversity of African Plants* (eds. L.J.G. van der Maesen, X.M. van der Burgt & J.M. van Madenbach de Rooy), pp. 73–86, Kluwer Academic Publishers, Dordrecht.

Tucker, S.C. & Hodges, S.A. (2005) Floral ontogeny of *Aquilegia*, *Semiaquilegia*, and *Enemion* (Ranunculaceae). *International Journal of Plant Sciences* **166**, 557–574.

Vaes, E., Vrijdaghs, A., Smets, E.F. & Dessein, S. (2006) Elaborate petals in Australian *Spermacoce* (Rubiaceae) species: Morphology, ontogeny and function. *Annals of Botany* **98**, 1167–1178.

van der Niet, T., Zollikofer, C.P., de León, M.S.P., Johnson, S.D. & Linder, H.P. (2010) Three-dimensional geometric morphometrics for studying floral shape variation. *Trends in Plant Science* **15**, 423–426.

Vogel, S. (1977) Nektarien und ihre ökologische Bedeutung. *Apidologie* **8**, 321–335.

von Hagen, K.B. & Kadereit, J.W. (2002) Phylogeny and flower evolution of the Swertiinae (Gentianaceae-Gentianeae): Homoplasy and the principle of variable proportions **27**, 548–572.

Vrijdaghs, A., De Block, P., Brecht, V., Groeninckx, I., Smets, E. & Dessein, S. (2015) A developmental model for the corolla in Rubiaceae. Cryptic character states in corollas of the Spermacoceae alliance. *Plant Ecology and Evolution* **148**, 237–255.

Walden, G.K., Garrison, L.M., Spicer, G.S., Cipriano, F.W. & Patterson, R. (2014) Phylogenies and chromosome evolution of *Phacelia* (Boraginaceae: Hydrophylloideae) inferred from nuclear ribosomal and chloroplast sequence data. *Madroño* **61**, 16–47.

Wason, J.W., Huggett, B.A. & Brodersen, C.R. (2017) MicroCT imaging as a tool to study vessel endings in situ. *American Journal of Botany* **104**, 1424–1430.

Weigend, M., Ackermann, M. & Henning, T. (2010) Reloading the revolver - male fitness as a simple explanation for complex reward partitioning in *Nasa macrothyrsa* (Loasaceae, Cornales). *Biological Journal of the Linnean Society* **100**, 124–131.

Weigend, M. & Gottschling, M. (2006) Evolution of funnel-revolver flowers and ornithophily in *Nasa* (Loasaceae). *Plant Biology* **8**, 120–142.

Weigend, M., Gottschling, M., Selvi, F. & Hilger, H.H. (2009) Marbleseeds are gromwells – Systematics and evolution of *Lithospermum* and allies (Boraginaceae tribe Lithospermeae) based on molecular and morphological data. *Molecular Phylogenetics and Evolution* **52**, 755–768.

Weigend, M., Luebert, F., Gottschling, M., Couvreur, T.L., Hilger, H.H. & Miller, J.S. (2014) From capsules to nutlets – phylogenetic relationships in the Boraginales. *Cladistics* **30**, 508–518.

Summary

Jeiter, Julius. 2019. Evolution of floral organisation and architecture in Boraginales and Geraniales. Doctoral thesis, Mathematisch-Naturwissenschaftliche Fakultät, Rheinische Friedrich-Wilhelms-Universität Bonn, Germany.

In this thesis, development, morphology and anatomy of structures from selected taxa from the Geraniales and Boraginales are studied. Furthermore, the integration of structures such as stamen-corolla tube modifications and nectaries into floral architecture is investigated. The results of the investigations are interpreted in the context of the current phylogenetic understanding of the study groups.

The following questions are addressed in this thesis:

1. Are the gynoecium and fruit of *Heliotropium* sect. *Heliothamnus* structurally correspondent to those of the Boraginaceae?
2. How does the flower of *Codon* develop?
3. How do the stamen-corolla tube modifications of Boraginaceae develop, how are they integrated into floral architecture and is there a phylogenetic pattern?
4. How do the stamen-corolla tube modifications of Hydrophyllaceae develop, how are they integrated into floral architecture and is there a phylogenetic pattern underlying these structures?
5. How are the internal floral spaces, enclosed by stamen-corolla tube modifications, in Hydrophyllaceae configured and how are the modifications contributing to the floral architecture?
6. What is the relationship between floral nectaries and floral architecture in Geraniaceae and Hypseocharitaceae?
7. What is the internal floral space and how does it contribute to our understanding of floral ecology and evolution?
8. Can the various stamen-corolla tube modifications found in different Boraginales families be homologise and if so, is it possible to propose an evolutionary series?

To address these questions, the following approaches and methods were used: floral morphology, anatomy and development based on scanning electron microscopy, serial sectioning and light microscopy, and high-resolution x-ray computed tomography (HRXCT) respective micro-computed tomography (µCT). Based on 3D-HRXCT- and µCT-scans, segmentation of the floral surfaces and internal spaces was conducted. Furthermore, 3D-landmarking based 3D-geometric morphometric analyses were employed. The phylogenetic signal in the 3D-landmarks was tested for on the basis of phylogenetic reconstruction.

This is a cumulative thesis. Chapters 2, 3, 5 and 7 are published and chapter 4 is submitted. Chapters 6 and 8 follow the structure of scientific articles and are in preparation for submission.

Chapter 1 is the general introduction. It introduces the two main research topics: *i*) study of floral structure in the context of phylogeny and *ii*) floral architecture. Furthermore, hypotheses, research questions and objectives are formulated and an overview of the thesis is given.

In **chapter 2**, gynoecium and fruit development in *Heliotropium* sect. *Heliothamnus* is investigated using an ontogenetic approach based on scanning electron microscopy, light microscopy and HRXCT. The columella, a structure between the nutlets on which the style is inserted, similar to that found in all Boraginaceae species, was proposed for this section, based on light microscopic observations. We found that a columella is absent and instead a disrupting tissue within the ovary can be observed. Based on phylogenetic evidence, homology of columella and disrupting tissue was rejected *a priori*, the morphological and developmental evidence presented here, further indicates that structural correspondence can be rejected as well.

In **chapter 3**, flower and fruit development of *Codon* from monogeneric Codonaceae is studied using scanning electron microscopy and light microscopy. Codonaceae are sister to Wellstediaceae and Boraginaceae on the Boraginales I clade. They have polymerous flowers with a 10- to 20-merous calyx, corolla and androecium. The bicarpellate gynoecium has a lobed nectary disc at the base and develops into a capsule. Between filament bases and corolla tube apically broadened septa are formed in late floral developmental stages. The septa compartmentalise the flower which results in revolver architecture.

Chapter 4 is the first systematic study of faucal and basal scales of Boraginaceae. Based on a systematic sampling, their development and morphology are investigated using scanning electron microscopy. Furthermore, the scales integration into floral architecture is visualised using µCT-data and the results are mapped onto a recent phylogeny of the family. Faucal scales were present in 18 and basal scales in 27 out of 29 species. Their development in late floral ontogeny indicates that they are peramorphoses. Faucal scales might have a function in pollination and other ecological interactions, as they tend to narrow the entrance to the corolla tube, are in close proximity to the anthers and, in some species, are involved in anther cone formation. The role of basal scales remains unknown. However, they are fairly conserved in their position within the flower and usually cover either the nectary disc or the entire ovary. Both types of scales can be found in all clades of Boraginaceae. No phylogenetic patterns in presence or absence of faucal and basal scales or in their combinations with other floral architectural characters are found. Only anther cone formation is commonly either associated with faucal scales, or the anthers themselves are modified. Basal scales are probably homologous to stamen-corolla tube modifications found in other Boraginales families. Faucal scales, on the other hand, appear to be an apomorphy of Boraginaceae.

In **chapter 5**, the development and morphology of stamen-corolla tube modifications and nectaries of Hydrophyllaceae are described using scanning electron microscopy. All Hydrophyllaceae species have ten modifications in antepetalous position. Each filament is basally connected to two adjacent modifications. The development of the modifications starts in late stages of floral development and is correlated to the differential elongation of the three parts of the stamen-corolla tube. The nectary is a gynoecial nectary disc at the base of the ovary. The disc is lobed and in the majority of species, nectarostomata are restricted to the tips of the lobes in antepetalous position. Always two modifications are synorganised with the nectary glands and form different types of pockets or tubes, which compartmentalise the flower resulting in revolver architecture. The position of the modifications in relation to the basal part of the corolla tube indicates variability in revolver architecture. An evolutionary series of the stamen-corolla tube modifications is proposed.

Chapter 6 explores floral architecture and the integration of stamen-corolla tube modifications into floral architecture in Hydrophyllaceae. The study is based on HRXCT- and µCT-scans and molecular phylogenetics. The scans are used for a 3D-landmarking based 3D-geometric morphometric approach. Furthermore, the spaces enclosed by the modifications are visualised through segmentation in the

3D-models. Three types of spatial configurations are described: completely, incompletely and non-compartmentalised flowers. The 3D-geometric morphometric analysis reveals that modification length and position as well as the corolla tube shape have the greatest effect on floral architecture. Both the compartment configuration and the 3D-geometric morphometric analysis show a clear phylogenetic pattern and a test indicates phylogenetic signal. To test the influence of the different compartment configurations on floral function, a nectar removal experiment was conducted by probing each of the five compartments of the flower separately. In the completely compartmentalised flowers, each compartment holds a similar amount of nectar. In incompletely compartmentalised flowers, the results are more variable. In some species, the first probe removed the majority of nectar. In other species, the results are similar to the completely compartmentalised flowers. In non-compartmentalised flowers, the results were similarly variable. The results indicate that not just the configuration of the stamen-corolla tube modifications and the spaces they enclose, but also nectar amount and viscosity have an effect on floral architecture and function.

In **chapter 7**, the relationship between nectaries and floral architecture in Hypseocharitaceae and Geraniaceae is explored using an ontogenetic approach based on scanning electron microscopy and light microscopy. The receptacular nectaries are in antesepalous position and are initiated in late stages of flower development. Nectar is secreted through nectarostomata. The development of the nectary glands is correlated with the receptacle development, which elongates in most species and forms a short anthophore. In *Pelargonium* a secondary meristem forms at the level of the single nectary gland lifting up the entire flower, except for the nectary gland. As a result, a receptacular cavity is formed around the gland. The nectary is integrated into floral architecture. Besides the anthophore and the receptacular cavity, the formation of stamen triplets is one of the key features of floral architecture in both families. In some *Geranium* species, the petal bases are modified, resulting in an elaborate revolver architecture. In the other species, stamen triplets, petal bases and sepals result in a lax revolver architecture. The functionality of these revolver architectures might depend on nectar properties. An evolutionary series of floral architecture in Hypseocharitaceae and Geraniaceae is proposed.

Chapter 8 introduces the concept of the internal floral space. The internal floral space is the air-filled volume of a flower. It can be visualised using 3D-visualisation methods, segmentation and surface rendering. The internal floral space can be equally or unequally compartmentalised. An application of this concept is demonstrated for two *Nasa* species (Loasaceae), *Geranium robertianum* (Geraniaceae) and Hydrophyllaceae based on the results of chapter 6. The internal floral space harbours great potential for ecological and evolutionary studies. It can be used for *i*) comparative morphological approaches, *ii*) to visualise complex spatial relations, and *iii*) in volumetric studies.

Chapter 9 are the general conclusions of this thesis. Here, the results of the individual chapters are discussed in the light of the main topics of this thesis and are put into a larger context. Furthermore, an evolutionary series for the stamen-corolla tube modifications of the Boraginales is proposed, taking into account the results of chapters 3, 4 and 5 as well as the information available from the literature. Finally, future research questions, which are related to this thesis, are discussed.

Zusammenfassung

Jeiter, Julius. 2019. Evolution von Blütenorganisation und -architektur in den Boraginales und Geraniales. Dissertation, Mathematisch-Naturwissenschaftliche Fakultät, Rheinische Friedrich-Wilhelms-Universität Bonn, Deutschland.

In dieser Dissertationsschrift werden die Entwicklung, Morphologie und Anatomie bestimmter Strukturen ausgewählter Taxa aus den Ordnungen Boraginales und Geraniales untersucht. Des Weiteren wird die Integration von Strukturen, wie etwa der Stamen-Corollen Tubus Modifikationen und Nektarien in die Blütenarchitektur erarbeitet. Die Ergebnisse dieser Untersuchungen werden im Kontext des aktuellen Verständnisses der Phylogenie der beforschten Pflanzengruppen interpretiert.

Es werden folgende Fragen adressiert:

1. Sind Gynoeceum und Frucht von *Heliotropium* sect. *Heliothamnus* und Boraginaceae strukturell korrespondierend?
2. Wie entwickelt sich die Blüte von *Codon*?
3. Wie entwickeln sich die Stamen-Corollen Tubus Modifikationen der Boraginaceae, wie sind diese in die Blütenarchitektur integriert und zeigen sie ein phylogenetisches Muster?
4. Wie entwickeln sich die Stamen-Corollen Tubus Modifikationen der Hydrophyllaceae, wie sind diese in die Blütenarchitektur integriert und gibt es ein diesen Strukturen zugrunde liegendes phylogenetisches Muster?
5. Wie sind die inneren Blütenräume, welche von den Stamen-Corollen Tubus Modifikationen eingeschlossen werden, in den Hydrophyllaceae konfiguriert und wie tragen die Modifikationen zur Blütenarchitektur bei?
6. Wie lässt sich die Beziehung zwischen Blütennektarien und Blütenarchitektur in den Geraniaceae und Hypseocharitaceae beschreiben?
7. Was ist der innere Blütenraum und wie trägt er zum Verständnis von Blütenökologie und Blütenevolution bei?
8. Können die unterschiedlichen Stamen-Corollen Tubus Modifikationen der verschiedenen Boraginales Familien homologisiert werden? Ist es möglich eine evolutionäre Serie abzuleiten?

Um diese Fragen zu adressieren, wurden folgende Ansätze und Methoden angewandt: Blütenmorphologie, -anatomie und -entwicklung wurden mittels Rasterelektronenmikroskopie, Serienschnitten und Lichtmikroskopie, sowie hochauflösender Röntgen Computer Tomographie (HRXCT), beziehungsweise Mikro-Computer Tomographie (µCT) untersucht. Basierend auf den HRXCT- und µCT-Scans wurden Blütenoberflächen und die inneren Blütenräume segmentiert. Des Weiteren wurden basierend auf 3D-Landmarking 3D-geometrisch-morphometrische Analysen durchgeführt. Die 3D-Landmarks wurden auf Grundlage einer phylogenetischen Rekonstruktion auf ein phylogenetisches Signal hin getestet.

Dies ist eine kumulative Dissertationsschrift. Die Kapitel 2, 3, 5 und 7 sind bereits publiziert und Kapitel 4 ist eingereicht. Die Kapitel 6 und 8 sind wie wissenschaftliche Artikel aufgebaut und werden zum Einreichen vorbereitet.

Kapitel 1 lässt sich als allgemeine Einleitung der Dissertationsschrift lesen. Hier werden die zwei Hauptforschungsschwerpunkte der Arbeit eingeführt: *i*) die Untersuchung der Blütenstruktur im Kontext phylogenetischer Rekonstruktionen und *ii*) Blütenarchitektur. Des Weiteren werden die Hypothesen, Forschungsfragen und -vorhaben formuliert und eine Übersicht des Inhalts der Dissertationsschrift gegeben.

In **Kapitel 2** wird die Gynoeceum- und Fruchtentwicklung von *Heliotropium* sect. *Heliothamnus* mittels Rasterelektronenmikroskopie, Lichtmikroskopie und HRXCT untersucht. Eine Columella, als Struktur zwischen den Klausen und unterhalb des Stylus, ähnlich der Columella der Boraginaceae, wurde basierend auf Lichtmikroskopie für diese Sektion beschrieben. Hier zeigen wir, dass es in dieser Sektion keine Columella gibt und stattdessen ein zerreißendes Gewebe im Fruchtknoten beobachtet werden kann. Basierend auf phylogenetischen Anhaltspunkten wurden eine Homologie der Columella und des zerreißenden Gewebes *a priori* ausgeschlossen. Hinweise aus Morphologie und Entwicklung, welche hier präsentiert werden, deuten darauf hin, dass auch eine strukturelle Korrespondenz ausgeschlossen werden kann.

In **Kapitel 3** wird die Blüten- und Fruchtentwicklung der Gattung *Codon* aus der monogenerischen Familie Codonaceae mittels Rasterelektronenmikroskopie und Lichtmikroskopie beschrieben. Die Codonaceae sind die Schwestergruppe zu den Wellstediaceae und Boraginaceae in den Boraginales I. Sie haben vielteilige Blüten mit 10- bis 20-zähligem Kelch, Krone und Androeceum. Das zweikarpellige Gynoeceum hat einen gelappten Nektardiskus an der Basis des Fruchtknotens. Das Gynoeceum entwickelt sich zu einer Kapsel. Zwischen den Filamentbasen und dem Corollen Tubus entwickeln sich apikal verbreiterte Septen in einem späten Stadium der Blütenentwicklung. Die Septen teilen die Blüte in Kompartimente ein, die in einer Revolverarchitektur resultieren.

Kapitel 4 stellt die erste systematische Studie der Schlund- und Basalschuppen der Boraginaceae dar. Basierend auf einer systematischen Beprobung wird deren Entwicklung und Morphologie mit Hilfe von Rasterelektronenmikroskopie untersucht. Des Weiteren wird die Integration der Schuppen in die Blütenarchitektur mit Hilfe von µCT visualisiert, sowie die Ergebnisse der Untersuchung auf die Phylogenie aufgebracht. Schlundschuppen waren in 18 und Basalschuppen in 27 von 29 Arten vorhanden. Die Entwicklung der Schuppen in späten Stadien der Blütenentwicklung deutet darauf hin, dass es sich um Peramorphosen handelt. Schlundschuppen könnten eine Funktion in der Bestäubung oder anderen ökologischen Interaktionen haben, da sie den Eingang des Corollen Tubus einengen, in räumlicher Nähe zu den Antheren stehen und häufig in der Formierung von Antherenkoni beteiligt sind. Die Rolle der Basalschuppen bleibt unbekannt, allerdings sind sie in ihrer Position konserviert und bedecken gewöhnlich den Nektardiskus oder den gesamten Fruchtknoten. Beide Schuppentypen sind in allen Kladen der Boraginaceae vertreten. Es wurden keine phylogenetischen Muster in der An- und Abwesenheit der Schuppen oder in deren Kombination mit anderen blütenarchitektonischen Merkmalen gefunden. Nur die Formierung von Antherenkoni ist häufig mit Schlundschuppen assoziiert. In Abwesenheit von Schlundschuppen sind häufig die Antheren selbst modifiziert. Die Basalschuppen sind vermutlich homolog zu Stamen-Corollen Tubus Modifikationen in anderen Familien der Boraginales. Schlundschuppen scheinen eine Apomorphie der Boraginaceae zu sein.

In **Kapitel 5** wird die Entwicklung und Morphologie der Stamen-Corollen Tubus Modifikationen und Nektarien der Hydrophyllaceae mit Hilfe von Rasterelektronenmikroskopie beschrieben. Alle Arten in den Hydrophyllaceae haben zehn antepetale Modifikationen. Jedes Filament ist an seiner Basis mit zwei benachbarten Modifikationen verbunden. Die Entwicklung der Modifikationen startet in späten Phasen der Blütenentwicklung und korreliert mit dem differentiellen Längenwachstum der unterschiedlichen Teile des Stamen-Corollen Tubus. Das Nektarium ist ein gynoecialer Nektardiskus and

der Basis des Fruchtknotens. Der Nektardiskus der meisten Arten ist gelappt und die Nectarostomata sind hauptsächlich auf den Loben zu finden. Jeweils zwei benachbarte Modifikationen in antepetaler Position sind mit den Nektardrüsen synorganisiert und bilden verschiedene Formen von Taschen oder Röhren, die die Blüten in Kompartimente unterteilen wodurch eine Revolverarchitektur gebildet wird. Die Stellung der Modifikationen in Relation zum basalen Teil des Corollen Tubus deutet auf Variabilität in der Ausprägung der Revolverarchitektur hin. Eine Evolutionsserie der Stamen-Corollen Tubus Modifikationen wird vorgeschlagen.

Kapitel 6 erforscht die Blütenarchitektur und die Integration von Stamen-Corollen Tubus Modifikationen in die Blütenarchitektur in den Hydrophyllaceae. Die Studie basiert auf HRXCT- und µCT-Scans sowie molekularer Phylogenetik. Die Scans werden für 3D-Landmarking und 3D-geometrische Morphometrie verwendet. Des Weiteren werden die Räume, welche von den Modifikationen eingeschlossen werden mittels Segmentierung der 3D-Modelle sichtbar gemacht. Drei räumliche Konfigurationen werden beschrieben: vollständige, unvollständige und unkompartimentierte Blüten. Die 3D-geometrische Analyse zeigt, dass die Länge und Position der Modifikationen, sowie die Form des Corollen Tubus den größten Effekt auf die Blütenarchitektur haben. Sowohl Kompartimentkonfiguration, als auch die 3D-geometrisch morphometrischen Analysen zeigen ein klares phylogenetisches Muster und der Test auf phylogenetisches Signal ist positiv. Um den Einfluss der Kompartimentierunskonfigurationen zu testen, wurde ein Experiment durchgeführt, bei dem der Nektar aus den Blüten entfernt wurde, indem jedes Kompartiment einer Blüte separat beprobt wurde. Jedes Kompartiment in den vollständig kompartimentierten Blüten hält etwa die gleiche Menge an Nektar. In den unvollständig kompartimentierten Blüten sind die Ergebnisse variabel. In manchen Arten wurde fast der gesamte Nektar der Blüte bei der ersten Beprobung entnommen. Andere Arten zeigten ein ähnliches Muster wie die vollständig kompartimentierten Blüten. Auch in den unkompartimentierten Blüten war das Ergebnis variabel. Die Ergebnisse deuten darauf hin, dass nicht nur die Konfiguration der Stamen-Corollen Tubus Modifikationen und der Kompartimente, die sie einschließen, sondern auch die Menge und Viskosität des Nektar einen Einfluss auf die Blütenarchitektur und -funktion hat.

In **Kapitel 7** wird die Beziehung zwischen Nektarien und Blütenarchitektur in den Hypseocharitaceae und Geraniaceae mittels Rasterelektronenmikroskopie und Lichtmikroskopie anhand eines ontogenetischen Ansatzes erforscht. Die rezeptakulären Nektarien befinden sich in antesepaler Position und werden in späten Blütenentwicklungsstadien initiiert. Nektar wird durch Nectarostomata sekretiert. Die Entwicklung der Nektardrüsen korreliert mit der Entwicklung des Blütenbodens, der sich in den meisten Arten zu einem kurzen Anthophor ausbildet. In *Pelargonium* bildet sich ein sekundäres Meristem, das die gesamte Blüte, bis auf die einzige Nektardrüse emporhebt. Hierdurch bildet sich eine rezeptakuläre Höhle aus, an deren Grund sich die Nektardrüse befindet. Die Nektarien sind in die Blütenarchitektur integriert. Neben den Ausbildungen des Rezeptakulums ist die Ausbildung von Stamendrillingen eines der Schlüsselelemente der Blütenarchitektur der Geraniaceae und Hypseocharitaceae. In einigen *Geranium* Arten sind die Basen der Petalen modifiziert, was eine elaborierte Revolverarchitektur zur Folge hat. In anderen Arten resultieren die Anwesenheit von Stamendrillingen, die Position der nicht-modifizierten Petalbasen und die Position der Kelchblätter zu einer einfacheren Form von Revolverarchitektur. Es ist anzunehmen, dass eine Funktion dieser Revolverarchitektur von Nektareigenschaften abhängt. Eine Evolutionsserie der Blütenarchitektur in den Hypseocharitaceae und Geraniaceae wird vorgeschlagen.

Kapitel 8 führt das Konzept des inneren Blütenraumes ein. Der innere Blütenraum ist das mit Luft gefüllte Volumen der Blüte. Es kann durch 3D-Visualisierungsmethoden, Segmentierung und Oberflächenrendering sichtbar gemacht werden. Der innere Blütenraum kann gleich oder ungle-

ich kompartimentiert sein. Die Anwendung des Konzepts wird für zwei Arten der Gattung *Nasa* (Loasaceae), *Geranium robertianum* (Geraniaceae) und, basierend auf den Ergebnissen aus Kapitel 6, für die Hydrophyllaceae demonstriert. Der innere Blütenraum hat großes Potential für blütenökologische und -evolutionäre Studien. Er kann für *i*) für komparativ morphologische Ansätze, *ii*) zur Visualisierung komplexer räumlicher Beziehungen und *iii*) in volumetrischen Studien verwendet werden.

Kapitel 9 besteht aus den Schlussfolgerungen der Dissertationsschrift. Hier werden die Ergebnisse der einzelnen Kapitel im Lichte der zwei Hauptaspekte der Arbeit diskutiert und in einen größeren Zusammenhang gestellt. Des Weiteren wird eine evolutionäre Serie für die Stamen-Corollen Tubus Modifikationen in den Boraginales vorgeschlagen, wobei die Ergebnisse aus den Kapiteln 3, 4 und 5 und weitere Informationen aus der Literatur herangezogen werden. Zuletzt werden weitere Forschungsfragen angeführt, die sich aus dieser Dissertationsschrift auftun.

Publication List

Peer-Reviewed Publications

***Jeiter J, Weigend M. 2018**. Simple scales make complex compartments – ontogeny and morphology of stamen-corolla tube modifications in Hydrophyllaceae (Boraginales). *Biological Journal of the Linnean Society* **125**: 802–820. https://doi.org/10.1093/biolinnean/bly167

***Jeiter J, Staedler YM, Schönenberger J, Weigend M, Luebert F. 2018**. Gynoecium and fruit development in *Heliotropium* sect. *Heliothamnus* (Heliotropiaceae). *International Journal of Plant Sciences* **179**: 275–286. https://doi.org/10.1086/696219

***Jeiter J, Hilger HH, Smets EF, Weigend M. 2017**. The relationship between nectaries and floral architecture: a case study in Geraniaceae and Hypseocharitaceae. *Annals of Botany* **120**: 791–803. https://doi.org/10.1093/aob/mcx101

Jeiter J, Weigend M, Hilger HH. 2017. Geraniales flowers revisited: evolutionary trends in floral nectaries. *Annals of Botany* **119**: 395–408. https://doi.org/10.1093/aob/mcw230

***Jeiter J, Danisch F, Hilger HH. 2016**. Polymery and nectary chambers in *Codon* (Codonaceae) – flower and fruit development in a small, capsule-bearing family of Boraginales. *Flora* **220**: 94–102. https://doi.org/10.1016/j.flora.2016.02.010

Non-Peer-Reviewed Publications

Jeiter J, Cole TCH, Hilger HH. 2017. Geraniales phylogeny poster (GPP). *PeerJ Preprints* **5:e3127v1**. https://doi.org/10.7287/peerj.preprints.3127v1

Jeiter J, Cole TCH, Hilger HH. 2016. Geraniales – Phylogeny of the order, families, genera with characteristics.

Conference Contributions

Talks

***Jeiter J.* 2018**. Stamen-corolla tube modifications in the Boraginales. *IV. International Boraginales Meeting*, Natural History Museum, Botanical section "Filippo Parlatore", Università degli studi Firenze, Florence, Italy.

***Weigend M*, Jeiter J, Mustafa A, Ensikat H.-J, Luebert F, Chacón J. 2017**. Evolutionary trends in Boraginales. *IBC 2017 - XIX International Botanical Congress*, Shenzhen, China.

***Jeiter J.* 2016**. Polymery and nectary chamber formation in *Codon* (Codonaceae). *III. International Boraginales Meeting*, Nees-Institute for Biodiversity of Plants, University of Bonn, Germany.

Posters

Jeiter J, Weigend M. 2016. Corolla modifications in Hydrophyllaceae and Namaceae. *III. International Boraginales Meeting*, Nees-Institute for Biodiversity of Plants, University of Bonn, Germany.